Synthesis and Kinetic Studies on Palladium Hydride-Initiated Vinyl Polymerisation of Functionalised Norbornenes

LYNN DONLON

Synthesis and Kinetic Studies on Palladium Hydride-Initiated Vinyl Polymerisation of Functionalised Norbornenes

Lynn Donlon

A thesis submitted in partial fulfilment for the degree of Ph.D

Department of Chemistry
University of Durham
November 2010

Abstract

Chapter I provides a summary of the vinyl polymerisation of norbornenes and their functionalised derivatives, using palladium-based initiators. The concept of photolithography is introduced along with discussion of hexafluoropropanol-(HFP) functionalised norbornene derivatives that provide the basis for the work described in this thesis.

In Chapter II, the synthesis of a series of HFP-functionalised monomers of the type $NB(CH_2)_nC(CF_3)_2OH$ (n = 1-2) and $NB(CH_2)_nOCH_2C(CF_3)_2OH$ (n = 0-6) is described. The monomers prepared differ in the number of methylene units (n) separating the HFP-functionality from the norbornene skeleton, which has previously been shown to have an influence upon polymerisation rate. The series of palladium hydride initiator complexes $[Pd(H)(MeCN)(PCy_3)_2][X]$ (anion X = BF_4, PF_6, SbF_6, I and $B(C_6F_5)_4$) were also prepared with a view to determining the effect of the anion on polymerisation rate.

The in-depth study of the stability and reactivity of the discrete complex $[PdH(MeCN)(PCy_3)_2][B(C_6F_5)_4]$ (**Pd1388**) is examined in Chapter III. The complex **Pd1388** is shown to decompose in chlorinated solvents at 70 °C to form $PdCl_2(PCy_3)_2$ and two further species, **b** and **c** that, despite extensive efforts, could not be identified. Both **Pd1388** itself and **Pd1388** in its decomposed form (*i.e.* the mixture of $PdCl_2(PCy_3)_2$, **b** and **c**) are able to act as pro-initiator systems in the polymerisation of *exo*-$NBCH_2OCH_2C(CF_3)_2OH$ (**SX1**). The kinetics of these polymerisation reactions are explored in detail and a kinetic model is proposed, which accurately describes the overall observed polymerisation rate.

In Chapter IV the kinetic model was extended to the study of pure *exo*- and pure *endo*-HFP-functionalised norbornenes, with the model proving to be an excellent fit to experimental data for monomer consumption. An increase in the value of n is shown to produce a corresponding enhancement of polymerisation rate. An examination of the polymerisation of HFP-functionalised norbornenes using GPC as function of time is also described. High molecular weight material is formed at low conversion (<35%) with a reduction in molecular weight observed during the first 30 minutes of the reaction to yield a polymer of peak average molecular weight ~20,000 Daltons and low PDI (<1.4).

In Chapter V, the kinetic model is further extended to the study of mixtures of *endo*- and *exo*-HFP-functionalised norbornenes (n = 0-6). As in the case of pure isomers, an increase in the value of n leads to an enhancement in overall polymerisation rate. Finally, the polymerisation of *endo*-/*exo*-$NBCH_2C(CF_3)_2OH$ (**SXN4**) is explored using initiators containing different counter anions (prepared in Chapter II) in order to determine the effect of the anion on polymerisation rate.

Memorandum

This thesis is based on work conducted by the author, in the Department of Chemistry at Durham University, during the period October 2006 – October 2009.
All work described in this thesis is original unless otherwise acknowledged in the text or in the references. None of this work has been submitted for another degree in this or any other university.

Signed_____ Date_____

Financial Support

This project would not have been possible without the generous financial support of Promerus LLC. Promerus are also gratefully acknowledged for the supply of norbornene monomers and catalysts.

Acknowledgements

First and foremost I would like to thank my supervisors, Drs Phil Dyer and Ezat Khosravi for their enthusiasm, advice, support and patience over the past few years. It has been a pleasure to work with you both, honestly ☺. I would also like to thank my industrial supervisor, Dr Andrew Bell for his helpful advice.

NMR spectroscopy makes up a large majority of this thesis and my deepest thanks go to Ian McKeag for teaching me the finer points of the NMR spectrometers, putting up with endless days of kinetic experiments and supplying me with coffee. Dr Alan Kenwright and Catherine Heffernan are also gratefully acknowledged for their help in the assignment and acquisition of NMR spectra, respectively.

As a synthetic chemist, Dr Ilya Kuprov and Prof. Nigel Clarke are gratefully acknowledged for their help with all things mathematical and the finer points of non-linear curve fitting in Origin. In no particular order, the contributions of Dr Andrei Batsanov (X-ray Crystallography), Dave Hunter (High Pressure Lab), Doug Carswell (DSC and fixing my vac pumps), Dr Jackie Mosely (Mass Spectrometry), Lenny Lauchran (GC) and Judith Magee (Elemental Analysis) during the course of this project are gratefully acknowledged. Particular thanks also go to Dr Lian Hutchings for his help with GPC analysis.

The group you work with makes a massive difference to the Ph.D experience and I was lucky enough to work with one of the best. In particular, thanks to Ahmed Eissa, Barry Dean, Iain Johnson, Yulia Rogan, Mariusz Majchrzak and Solomon Kimani – you have been invaluable friends and a pleasure to work with. Thanks also to the Dyer group past and present, in particular to Pippa Monks and Ben Coombs and for their help at the 11th hour. The members of the IRC past and present are gratefully acknowledged for their helpful advice and some brilliant nights out.

I've been lucky enough to make some fantastic friends whilst in Durham. In no particular order: Adam Todd, Lisa Murphy, Alisdair Wallis, Peter Duncan and Cat Pridmore. Thanks for being great coffee (and cake) break companions and for keeping me sane (well almost!) when the going got tough.

Finally, and most importantly, I'd like to thank my family for their support and encouragement throughout my time in Durham, even though none of you still have a clue what I do! To Mum, for making sure Max didn't starve when things went wrong, Dave, Nanna and Granddad – you're the best family I could wish for. Finally, and saving the best for last, thanks to Mark for providing chocolate, wine and sympathy after a hard day - your support means everything to me. This one's for you!

Contents

Chapter I

Chapter II

2 Preparation of hexafluoropropanol-functionalised norbornene monomers and palladium hydride initiators

Chapter IV

Chapter V

5 Polymerisation of mixtures of *endo*- and *exo*- hexafluoropropanol-functionalised norbornenes

Appendices

Abbreviations

Bu:	butyl
COD:	cyclooctadiene
COSY:	correlation spectroscopy
CP:	cyclopentadiene
Cp:	cyclopentyl
Cy:	cyclohexyl
Δ:	heat
d:	deuterated unless specified otherwise
2D:	2-dimensional
DANFABA:	$[HNMe_2Ph][B(C_6F_5)_4]$
DCM:	dichloromethane
Dec:	decyl
DMF:	dimethylfomamide
DMSO:	dimethyl sulfoxife
ES:	electrospray
Ether:	diethyl ether
Et:	ethyl
ΔG_p:	Gibbs free energy of polymerisation
GC:	gas chromatography
GCMS:	gas chromatography mass spectrometry
GPC:	gel permeation chromatography
h:	hours unless specified otherwise

ΔH_p:	enthalpy of polymerisation
hex:	hexyl
HFANB:	$NBCH_2C(CF_3)_2OH$
HFIBO:	2,2-bis(trifluoromethyl)oxirane
HFP:	hexafluoropropanol functionality
HMBC:	heteronuclear multiple bond correlation
HSQC:	heteronuclaer single quantum correlation
Hz:	Hertz
^{i}-Bu:	*iso*-butyl
^{i}-Pr:	*iso*-propyl
IR:	infrared
J:	coupling constant
k:	rate constant
L:	generic ligand
LIFABA:	$[Li(Et_2O)_{2.5}][B(C_6F_5)_4]$
M:	generic metal centre
MAO:	methyl aluminiunoxide
Me:	methyl
M_n:	number average molecular weight
M_p:	peak average molecular weight
M_w:	weight average molecular weight
n:	nano unless specified otherwise
NB:	norbornene, bicyclo[2.2.1]hept-2-ene
NMR:	nuclear magnetic resonance
NOESY:	nuclear overhauser effect spectroscopy
OAc:	acetate
OMs:	mesylate
OTf:	triflate
PAG:	photoacid generator
Pd-H:	palladium hydride species
PDI:	polydispersity index
Pd1388:	$[Pd(H)(MeCN)(PCy_3)_2][B(C_6F_5)_4]$
ppb:	parts per billion
ppm:	parts per million
psi:	pounds per square inch

RT:	retention time unless specified otherwise
R:	alkyl unless specified otherwise
ROMP:	ring opening metathesis polymerisation
ΔS_p:	entropy of polymerisation
^{t}Bu:	tertiary butyl
T_c:	ceiling temperature
TCE:	1,1,2,2-tetrachloroethane
T_g:	glass transition temperature
THF:	tetrahydrofuran
TMAOH:	tetramethyl ammonium hydroxide
TMEDA:	tetramethylethylenediame
TMS:	trimethylsilyl
Ts:	tosyl
UV:	ultra-violet
UV/vis:	ultra-violet and visible light
WCA:	weakly coordinating anion

NMR Abbreviations

δ:	chemical shift (in ppm)
(s):	singlet
(d):	doublet
(t):	triplet
(q):	quartet
(quin):	quintet
(sept):	septet
(m):	complex multiplet
(br):	broad
(ur):	unresolved

Palladium Hydride Complexes

Pd1388: $[Pd(H)(MeCN)(PCy_3)_2][B(C_6F_5)_4]$

Pd945: $[Pd(H)(MeCN)(PCy_3)_2][SbF_6]$

Pd854: $[Pd(H)(MeCN)(PCy_3)_2][PF_6]$

Pd836: $[Pd(H)(MeCN)(PCy_3)_2]I$

Pd796: $[Pd(H)(MeCN)(PCy_3)_2][BF_4]$

Pd817: $[Pd(H)(OTf)(PCy_3)_2]$

Pd 795: $[Pd(H)(I)(PCy_3)_2]$

Pd 704: $[Pd(Cl)(H)(PCy_3)_2]$

Coding System for Norbornene Monomers (e.g. ZXN1 etc.)

The first letter in the code refers to the number of methylene (CH_2) groups separating the functionality from the norbornene skeleton, n. The second set of letters refers to the stereo chemistry of the functional group whilst the final number is arbitrary and used to differentiate between monomers with the same number methylene units but different functional groups.

Z: n = 0 (zero-spaced)

S: n = 1 (single-spaced)

D: n = 2 (double-spaced)

T: n = 3 (triple-spaced)

Q: n = 4 (quad-spaced)

H: n = 6 (hexa-spaced)

X: *exo*

N: *endo*

XN: unseparated mixture of *endo* and *exo* isomers

Hexafluoropropanol-functionalised Norbornene Monomers

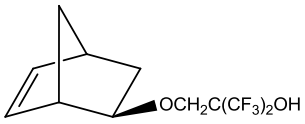

ZX3

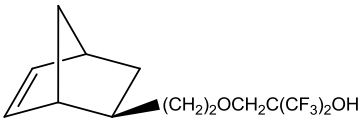

DX2

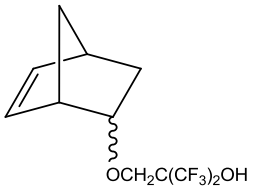

ZXN2

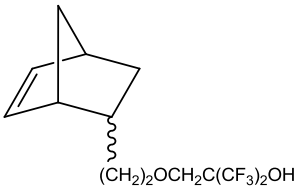

DXN2

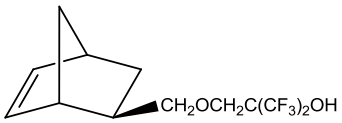

SX1

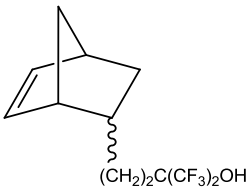

DXN5

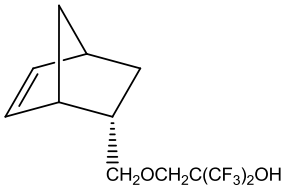

SN2

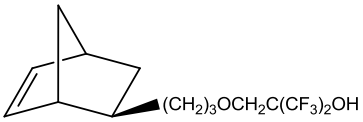

TX2

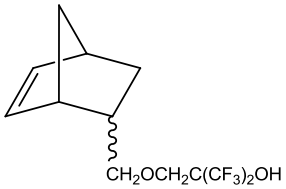

SXN3

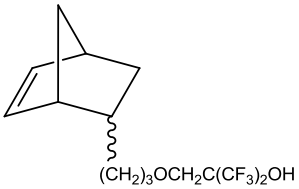

TXN3

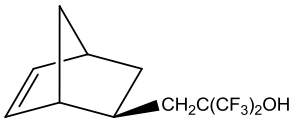

SX2

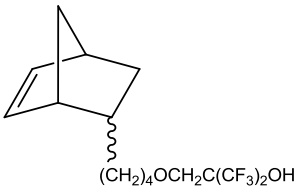

QXN1

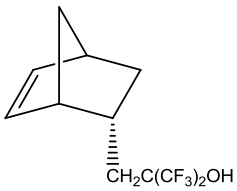

SN3

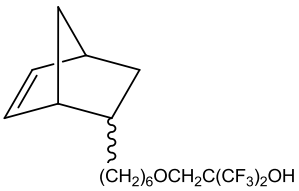

HXN1

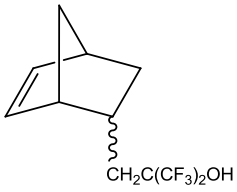

SXN4

Chapter I

Introduction and Literature Review

Chapter I

Introduction and Literature Review

1.1 Introduction to norbornene polymerisation

The polymerisation of cyclic olefins has attracted a great deal of interest over the past two decades, primarily due to the attractive properties of the resulting polymeric materials. Of particular interest is the polymerisation of bicyclo[2.2.1]hept-2-ene (also known by the trivial name norbornene, NB), from which different classes of polymers may be obtained by suitable choice of a polymerisation catalyst (Scheme 1.1).[1]

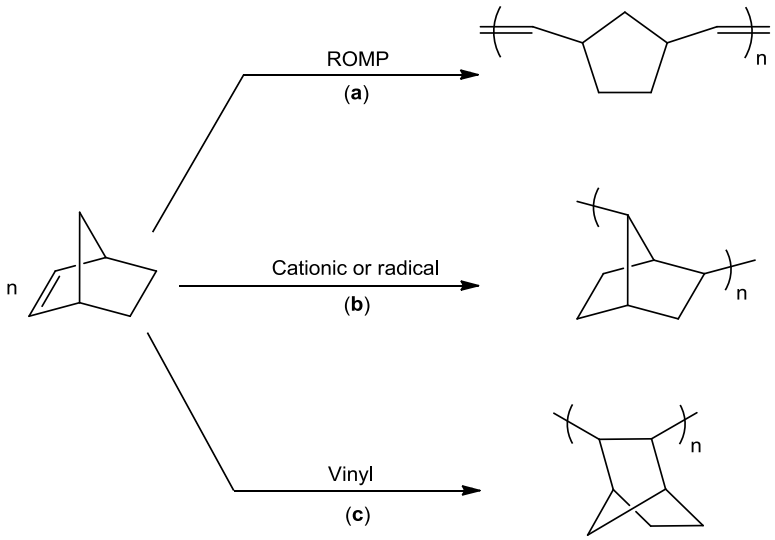

Scheme 1.1 Schematic representation of the three different types of norbornene polymerisation reaction. (**a**) Ring opening metathesis polymerisation (ROMP), (**b**), Cationic or radical polymerisation and (**c**) vinyl polymerisation.[1]

Taking each polymerisation mechanism in turn, ring opening metathesis polymerisation (ROMP) (**a**) yields poly(1,3-cyclopentylenevinylene)-type materials that retain double bond functionality in the backbone chain. ROMP is achieved using mid-to-late transition metal alkylidine initiators, such as those developed by Schrock and Grubbs.[2-3] The reaction proceeds *via* the formation of a strained 4-membered metallacyclobutane, as illustrated in Scheme 1.2.

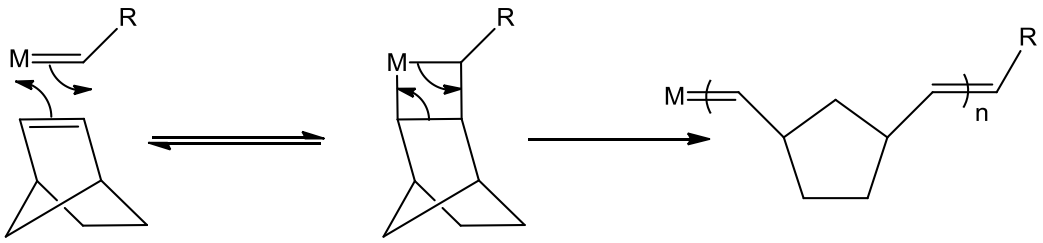

Scheme 1.2 Schematic representation of the mechanism of ring opening metathesis polymerisation of a strained olefin

The ring opening metathesis polymerisation of norbornenes has been studied extensively. However detailed discussion of ROMP goes beyond the scope of this review.[4] In contrast to ROMP, comparatively little is known about the polymerisation of norbornene by cationic and radical pathways (Figure 1.1, **b**). Radical polymerisation of norbornene has been achieved using azoisobutyronitrile (AIBN) as a radical initiator whilst $EtAlCl_2$ has been shown to be an effective initiator for the polymerisation of norbornene by a cationic pathway. [5-8] However, the materials resulting from both radical and cationic polymerisation processes are low molecular weight oligomers with 2,7-connectivity, achieved *via* rearrangement of the norbornene framework. [5-8]

Vinyl addition polymerisation normally involves the insertion of norbornene monomers into a metal-carbon or metal-hydride bond and yields saturated poly(2,3-bicyclo[2.2.1]hept-2-ene) species (Figure 1.1, **c**), which retain the rigid fused ring system within the backbone chain. Vinyl-type norbornene polymers display a number of advantageous properties, which include excellent thermal stability (T_g > 370 ºC), high optical transparency, low dielectric constant, low birefringence and excellent etch resistance. Such properties make vinyl poly(norbornenes), and in particular their functionalised derivatives, ideal candidates for use in demanding optical and optoelectronic applications.[9-16] Judicious choice of norbornene monomers, in combination with the development of effective polymerisation initiators, has allowed the commercial exploitation of functionalised vinyl poly(norbornenes) by Promerus LLC (formerly B.F. Goodrich electronics division), for use in deep UV photolithography.[9-16]

Over the past two decades the vinyl polymerisation of norbornene and its functionalised derivatives has been studied in detail, using a multitude of transition metal-based initiators which have been reviewed elsewhere.[1,17-18] The main focus of this review will be in the area of late-transition metal-based initiators, used to prepare commercially relevant poly(norbornenes) of interest in photolithography

1.2 Introduction to functionalised norbornene monomers

Un-substituted poly(norbornene) is characterised by excellent thermal stability and optical transparency, however these advantageous physical properties are offset by the mechanical brittleness of the polymer and poor adhesion to common surfaces.[1] These drawbacks are easily overcome by the preparation of norbornenes bearing pendant functional groups, in particular the introduction of polar, oxygen- or nitrogen-containing substituents which enhance solubility and surface adhesion.[1]

Functionalised norbornene derivatives are readily synthesised *via* Diels-Alder addition of cyclopentadiene to a dienophile bearing a pendant functionality (Scheme 1.3). The resulting norbornene monomers are particularly versatile as their properties may be tailored to suit a wide range of applications. The desired functionality may be introduced directly during the Diels-Alder synthesis or *via* functional-group modification of a precursor norbornene monomer such as an alcohol or ester.

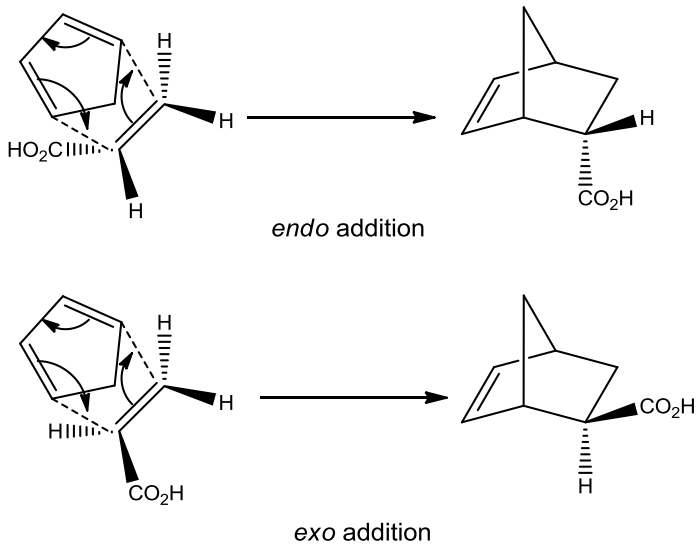

Scheme 1.3 Formation of *endo*- and *exo*-substituted norbornene monomers *via* the Diels-Alder reaction

Reaction of a cyclic diene with an asymmetric dieneophile leads to two isomeric products, referred to as *endo* (Scheme 2.2, **a**) and *exo* compounds (Scheme 2.2, **b**).[19] The ratio of *endo*:*exo* isomers obtained depends strongly upon the reaction conditions used. Addition of the sterically bulky side of the dieneophile under the ring leads to the *endo* isomer, which is the kinetically-favoured product obtained under moderate reaction temperature conditions. The thermodynamically favoured *exo* isomer is achieved *via* addition of the less sterically bulky side of the dieneophile (hydrogen in Scheme 1.3) underneath the ring. High temperatures and long reaction times are required to promote formation of this *exo* isomer, however neither the pure *exo* nor the pure *endo* isomer is usually formed *via* the initial Diels-Alder reaction. Instead, approximately an 80:20 mixture of *endo*:*exo* isomers is obtained which are usually impossible to separate.[20] Mixtures of *endo*:*exo* norbornene isomers occasionally differ sufficiently in their boiling point to permit separation by distillation (for example, the cyano-functionalised norbornene derivative, *endo*-/*exo*-norbornenecarbonitrile, NB-CN),[21] however typically this is not the case. Separation of a mixture of *endo*-/*exo*-isomers is also occasionally possible chromatographically (*e.g.* *endo*-/*exo*-$NBCO_2H$), however for the majority of functionalised monomers, the R_f values of the two isomers are too similar to permit separation.[22]

Work by a large number of research groups, including our own, has demonstrated that *endo* norbornene monomers polymerise much more slowly than their *exo* counterparts.[23-36] This difference in polymerisation rate can be problematic, as during the polymerisation of mixtures of *endo*/*exo* isomers, overall polymerisation rates are greatly reduced and a homogeneous distribution of monomer units throughout the backbone chain is not achieved. Many research groups have tried to understand this phenomenon, particularly in the case of the palladium-catalysed polymerisation of oxygen-containing norbornene monomers and a number of theories have been suggested.[23-36] The subject of *endo*-/*exo*-substituted monomers will be discussed in section 1.6 and in more detail in Chapters IV and V.

1.3 Vinyl addition polymerisation of norbornenes

A wide variety of transition metal-based initiators for both the vinyl homopolymerisation and ROMP of norbornenes have been described in the literature, which are summarised in Scheme 1.4.[1] Vinyl and ROMP polymerisations are usually catalysed by different transition metal centres, due to the mechanistic differences between the two polymerisation processes. However, certain cases provide exceptions to this rule. For example, titanium- and cobalt-based systems may initiate either polymerisation route depending upon the reaction conditions used.[37-40]

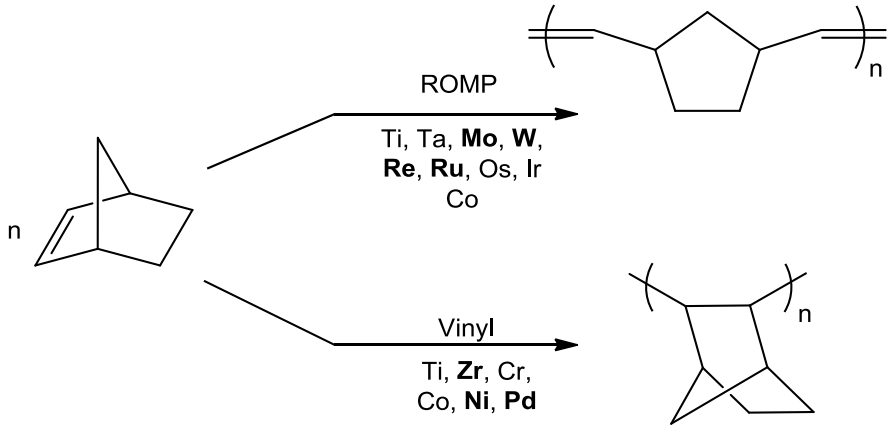

Scheme 1.4 Transition metal centres used in the polymerisation of norbornenes (key metal centres are given in bold)

Species that initiate the vinyl polymerisation of norbornene may be broadly classified into three types depending on the central metal ion: (i) early transition metals (Ti, Zr), (ii) mid-transition metals (Cr, Mn, Fe, Co), and (iii) late transition metals (Ni, Pd). Early work on the vinyl polymerisation of norbornene focused on the use of group IV metallocenes, species that have found widespread use in the polymerisation of olefins.[41-47] More recently, the use of initiators based upon the central transition metals (V, Cr, Mn, Fe and Co) has been demonstrated.[48-57] However, a major drawback of both early- and mid-transition metal-based systems is that in almost all cases, these initiators require activation with a large excess of methylaluminoxane (MAO) (one possible representation of which is given in Figure 1.1) or an alternative Lewis acidic co-catalyst, which can prove to be expensive.[1,56-58] The exceptions to this rule are based on group X metals, in particular cationic palladium complexes, such as $[Pd(MeCN)_4][BF_4]_2$ or $[Pd(H)(MeCN)(PCy_3)_2][B(C_6F_5)_4]$.[1,59-60] Another drawback of early and mid-transition metal-based initiators is their low tolerance to the presence of functional

groups, which are key to the studies conducted in this thesis. For this reason, the remainder of this review will focus on initiators based on the group X metals palladium and nickel, in particular those which do not require a co-catalyst, and their use in the polymerisation of functionalised norbornene derivatives. For further reference, excellent reviews on the topic of metal-catalysed norbornene polymerisation are given by Janiak and Lassahn (2001), Blank and Janiak (2009) and Ma and co-workers (2009).[1,17-18]

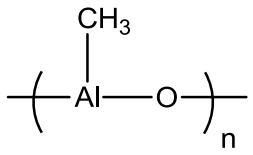

Figure 1.1 One possible representation of the structure of MAO

1.4 Late transition metal-based initiators for the polymerisation of norbornenes

The vinyl polymerisation of norbornene using late transition metal-based initiators was first achieved in 1966 using $PdCl_2$ and then again in the late 1970s when $PdCl_2(C_5H_5CN)_2$ and $PdCl_2(Ph_3P)_2$ were shown to be active.[5-6,61-63] The major breakthrough in this area was achieved by Sen and co-workers in 1981.[64] They introduced the cationic palladium(II) system $[Pd(CH_3CN)_4][BF_4]_2$ (**1**) for the polymerisation of olefins.

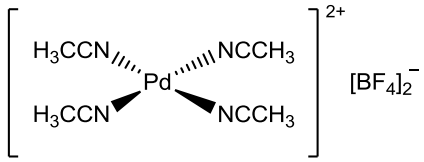

1

Further investigation revealed that complex **1** also catalysed the polymerisation of a wide range of other species including acetylenes, α-methyl styrene, 1,3-cyclohexadiene, norbornene, and norbornadiene.[65] Polymerisation of norbornene under an inert atmosphere ([norbornene]:[initiator] = 100:1) in CH_3NO_2 was found to proceed at room temperature to give >90% conversion after only 5 minutes, however characterisation of the resulting polymer was not possible due to its insolubility in THF, $CHCl_3$, CH_2Cl_2 and C_6H_6.[64-66]

The analogous Ni(II) and Co(II) $[M(CH_3CN)_6](BF_4)_2$ (M = Ni (**2**); M = Co (**3**)) systems were also investigated, however they were found to be inactive under the same conditions employed for the Pd system.[23] Consideration of charge/radius ratios could suggest that Ni^{2+} and Co^{2+} may be more electrophilic than Pd(II), however direct comparison between the three systems is complicated by the fact that **1** is diamagnetic whilst **2** and **3** are paramagnetic. It has also been suggested that the inactivity of **2** and **3** may be due to the stronger interaction between the acetonitrile ligands and the metal centre. It has been shown that the coordinated acetonitrile in **1** will exchange 'instantaneously' with solvent when dissolved in CD_3CN at ambient temperature, whilst no exchange is observed for the nickel complex **2**, even after heating to 60 °C for 8 hours.[67-69] This observation would suggest that displacement of acetonitrile by olefin in the coordination sphere of the metal is a vital precursor to polymerisation.

For many years, little interest was taken in the vinyl polymerisation of norbornene initiated by late transition metal-based initiators and it was not until 1991 that Risse began to reinvestigate palladium(II) systems.[37,70] The resulting vinyl polymers were found to have relatively good solubility in solvents such as tetrachloroethane and chlorinated aromatics and the ensuing characterisation by size exclusion chromatography (SEC, GPC) indicated molecular weights in excess of 100,000 g mol^{-1} and high glass transition temperatures (>300 °C).

Risse also studied the polymerisation of *exo*- and *endo*-substituted norbornene derivatives. These included polycyclic norbornenes and more relevantly those with pendant ester functionalities.[23-25,71] Unlike early transition metals, palladium species such as $[(\eta^3\text{-allyl})Pd^{(II)}(SbF_6)]$ (**4**) as well as **1** were found to be tolerant of the ester functionality (due to the preference of late transition metals for soft ligands).[72] However, the rate of polymerisation of ester-functionalised norbornenes initiated using **4** was low in comparison to non-oxygen containing monomers.[24] This study indicated that such cationic palladium species may also tolerate other oxygen-containing functionalities (such as carboxylic acids and ethers), and facilitate the homo- and co-polymerisation of substituted norbornene derivatives to yield a series of novel polymers.[23]

Complex **1** provided a platform from which many other systems were developed and subsequently investigated. Heitz and co-workers considered the effect of the nitrile residues in the system $[Pd(RCN)_4]^{2+}$.[73] Replacement of the acetonitrile ligands with 2-cyanonorbornane, complex **14**, overcame the ongoing problem that whilst many poly(norbornenes) were soluble in chlorobenzene, the $[Pd(CH_3CN)_4][BF_4]_2$ initiator (**1**),

developed by Sen, was not, resulting in a heterogeneous reaction system. The percentage conversions of norbornene observed using initiators **5-14** were found to be very similar irrespective of the nature of R, the only exception being complex **1** in which R = methyl. The polydispersities of the resultant polynorbornenes, prepared using **5-14** were also relatively low (1.3 – 1.5).[73]

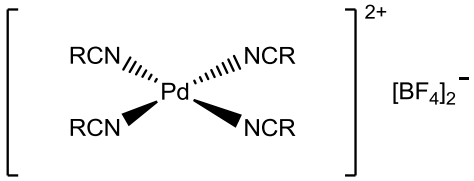

1: R = CH_3
5: R = $CH_3(CH_2)_2$
6: R = $CH_3(CH_3)_2$
7: R = $(CH_3)_2CH$
8: R = $(CH_3)_3C$
9: R = C_6H_5
10: R =

11: R =
12: R =
13: R =
14: R =

Another study, also by Heitz, investigated the effect of the weakly coordinating counter anion in the system $[Pd(CH_3CN)_4][X]_n$.[74] The counter ions X studied included $[BF_4]^-$, $[OSO_2CF_3]^-$, $[SbCl_6]^-$ and $[SnCl_6]^{2-}$ with the smallest counter ion $[BF_4]^-$ being found to produce polynorbornene with significantly higher molar mass than that from the other initiators studied (1 hour, room temperature, [norbornene]:[initiator] = 500:1).

Building upon the early work of Sen and Risse, in 1995, Safir and Novak introduced a new series of highly active σ-, π-bicyclic palladium(II) initiators **15-19** capable of quantitative polymerisation of norbornene in <15 minutes, without the need for anhydrous conditions.[75-77] Addition of MAO to initiator **17** served to substantially increase the activity. Although a related system to initiator **17** had been prepared for the polymerisation of olefins, including norbornene, *via* addition of β-pinene to $[PdCl_2(C_6H_5CN)_2]$ as early as the 1970s, this system had never previously been fully understood.[78] Copolymerisation of norbornene and 7-oxanorbornadiene dicarboxylic acid dimethyl ester was achieved using complex **17** and in this instance, the polymerisation was found to be living.

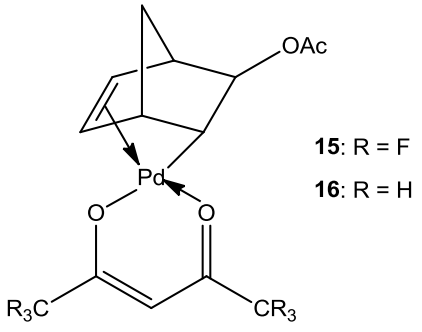

15: R = F
16: R = H

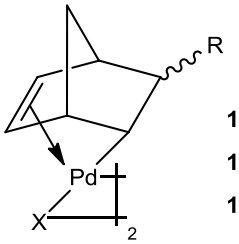

17: R = OMe X = Cl
18: R = OMe X = Br
19: R = Ph X = I

Initiator systems with coordinated cyclooctadiene (COD) ligands were also developed and subsequently patented by Goodall.[79] The most successful of these was the "naked nickel" system[(η^3-allyl)Ni(1,5-cyclooctadiene)]$^+$ (**20**), so called due to the lability of both the COD and allyl ligands. However, the palladium analogues **21** and **22** were found to be surprisingly less active in comparison to both **20** and **1**.[79]

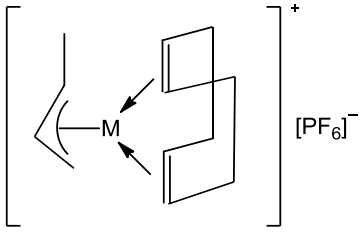

20: M = Ni

21: M = Pd

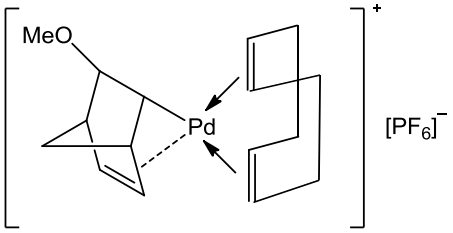

22

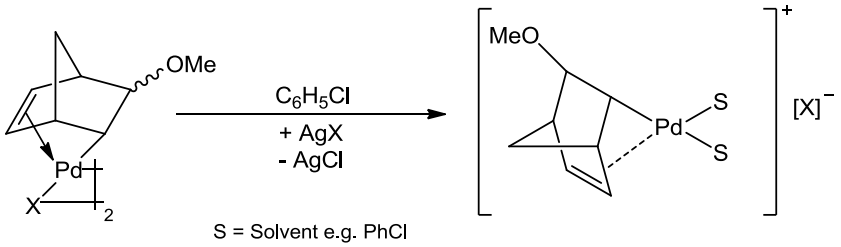

17

23: X = $[BF_4]^-$

24: X = $[SbF_6]^-$

The observed lower activity of **21** and **22** led to the development of several higher activity derivatives such as **23** and **24** reported by Heitz, prepared *via* reaction of **17** with silver tetrafluoroborate or silver hexafluoroantimonate in chlorobenzene, respectively.[25,80] Complex **22** was found to react sixty times faster than **17** (although 1700 times slower than **17** with MAO as a co-initiator) and unlike $[Pd(CH_3CN)_4][BF_4]_2$ (**1**), **23** was readily soluble in chlorobenzene. The resulting amorphous polymer obtained using complex **22** was also found to be soluble in chlorobenzene, unlike the material obtained using **17** and MAO, which proved to be insoluble.

Initiator system **24** in which the counter anion is the larger (and less strongly coordinating) $[SbF_6]$ was shown to be even more active, particularly in the polymerisation of mixtures of *endo*-/*exo*-functionalised norbornene derivatives such as esters.[25] Polymerisation of *endo*-/*exo*-carboxylic acid ester-functionalised monomers in >70% yield had previously only been possible at elevated temperature (>100 ^oC) with Pd(II) halide complexes. For polymerisation at ambient temperatures using Pd(II) allyl

complexes or $[Pd(CH_3CN)_4][BF_4]_2$ to be successful, pure *exo* monomers were required.[1]

Risse also studied the polymerisation of norbornene carboxylic acid esters with the related and highly active allyl systems $[(\eta^3\text{-allyl})Pd][SbF_6]$ (**25**) and $[(\eta^3\text{-allyl})Pd][BF_4]$ (**26**) obtained *in situ via* reaction of $[(\eta^3\text{-allyl})PdCl]_2$ with 2 equivalents of $AgSbF_6$ and $AgBF_4$ (in chlorobenzene), respectively.[26-27] Interestingly, the addition of four equivalents of acetonitrile to the reaction with $AgBF_4$ leads to the formation of complex **27** upon reaction with norbornene (rather than the expected polymerisation) *via* a single insertion of norbornene into the palladium-allyl bond.

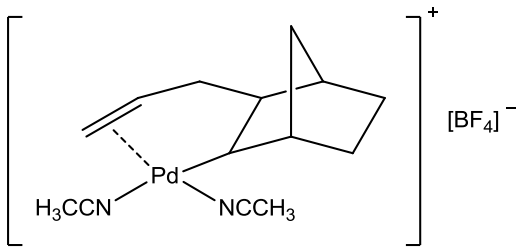

27

The formation of complex **27** indicates that electron donating ligands such as acetonitrile will reduce the activity of group X norbornene polymerisation catalysts, hence the high activity observed for the initiators **25** and **26**, which do not possess nitrile ligands. In the case of systems based on **25** and **26** it is suggested that an equilibrium exists between the species in Scheme 1.5 in solvents such as CH_2Cl_2 and chlorobenzene.[26-27] Although there is no conclusive evidence to support this, others have reported systems in which solvents such as CH_2Cl_2 can act as ligands.[81] Decomposition of **25** and **26** to black palladium particles upon attempted removal of solvent also serves to suggest that the solvent may have a stabilising effect.

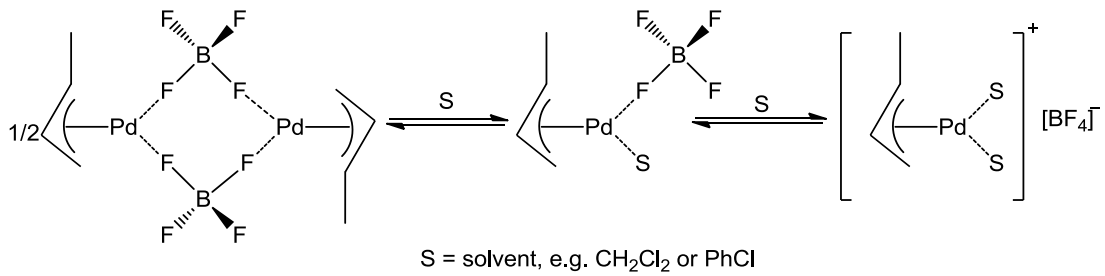

Scheme 1.5 Proposed equilibrium between weakly coordinated solvent and tetrafluoroborate palladium species

Reaction of complex **25** with the monomer *endo*-/*exo*-5-norbornene-2-methylester (*endo*-/*exo*-$NBCO_2Me$, [monomer]:[initiator] = 50:1) produced a 68% yield of polymer {M_n (GPC) = 7100 Daltons; PDI = 1.7} after 90 hours at 20 °C. In contrast, polymerisation with **26** led to a lower yield (59%), and molecular weight {M_n (GPC) = 4600 Daltons}, and higher polydispersity (PDI = 2.2). $[Pd(CH_3CN)_4][BF_4]_2$ (**1**), was insufficiently active to promote polymerisation of *endo*-/*exo*-$NBCO_2Me$ under these conditions.[26-27]

More recently, research in the area of vinyl polymerisation of norbornenes has been extended to palladium phosphine systems. Sen showed that cationic palladium methyl species were effective in the polymerisation of oxygen-functionalised norbornene derivatives.[28] Reaction of [PdCl(Me)(COD)] with one equivalent of a monodentate phosphine ligand generates the known bridged dimer $[Pd(\mu\text{-}Cl)(PR_3)]_2$. Addition of 1 equivalent of $Na[B(3,5\text{-}(CF_3)_2C_6H_3)_4]$ to [PdCl(Me)(COD)] in the presence of norbornene monomer is believed to generate the highly active solvent/monomer-coordinated cationic species $[PdMe(L)][B(3,5\text{-}(CF_3)_2C_6H_3]_4]$ (**28**), where L is a generic ligand, most likely coordinated solvent. Species **28** is unstable in the absence of monomer and decomposes to metallic palladium over time.

In 1996 Brookhart demonstrated the synthesis of $[(\eta^3\text{-allyl})Pd(PCy_3)_2(ether)][B(3,5\text{-}(CF_3)_2C_6H_3)_4]$, (**32**), (Scheme 1.6).[82] Reaction of the dimeric complex $[(\eta^3\text{-allyl})PdCl]_2$ (**29**) with tricyclohexylphosphine *via* chloride bridge splitting yields the monomeric complex $[(\eta^3\text{-allyl})PdCl(PCy_3)]$ (**30**).[83-84] Subsequent reaction of **30** with CH_3MgBr yields the corresponding palladium methyl complex $[(\eta^3\text{-allyl})Pd(CH_3)(PCy_3)]$ (**31**). Finally, protonation of **31** with $[H(OEt)_2][B(3,5\text{-}(CF_3)_2C_6H_3)_4]$ gives the cationic palladium complex $[(\eta^3\text{-allyl})Pd(PCy_3)(OEt)][B(3,5\text{-}(CF_3)_2C_6H_3)_4]$, (**32**).

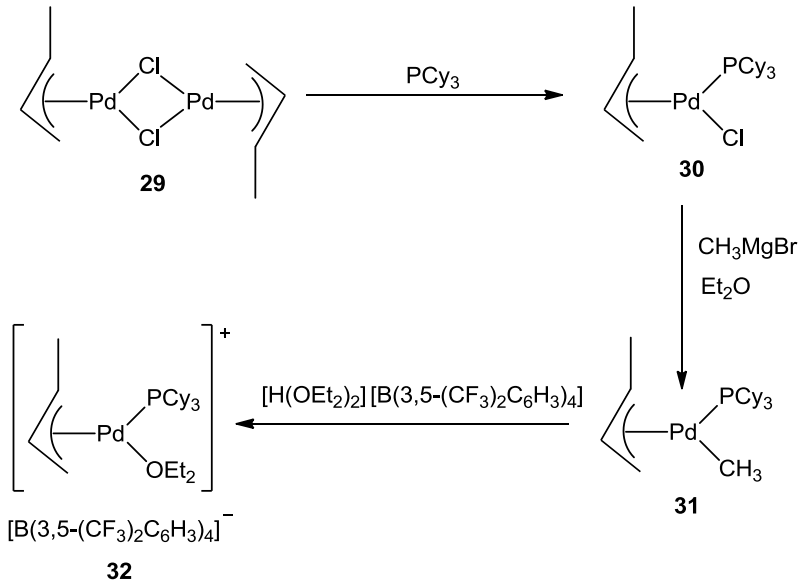

Scheme 1.6 Synthesis of the pre-catalyst $[(\eta^3\text{-allyl})Pd(PCy_3)_2(ether)][B(3,5\text{-}(CF_3)_2C_6H_3)_4]$, (**32**) [82]

Promerus LLC examined the use of **32** in the polymerisation of norbornene derivatives.[85] Copolymerisation of 5-butylnorbornene and 5-triethoxylsilylnorbornene (95:5 molar ratio) with **32** was extremely efficient the catalyst producing more than a metric tonne of copolymer per mole Pd per hour. Once the high activity of **32** had been established, further research concentrated on the production of η^3-allylpalladium phosphine pro-initiators containing anionic ligands which could act as leaving groups in the presence of salts of weakly coordinating anions. Scheme 1.7 indicates the simple, one pot synthetic route to pro-initiator **30**, which can be further reacted with silver salts to yield complexes **33**-**37**.

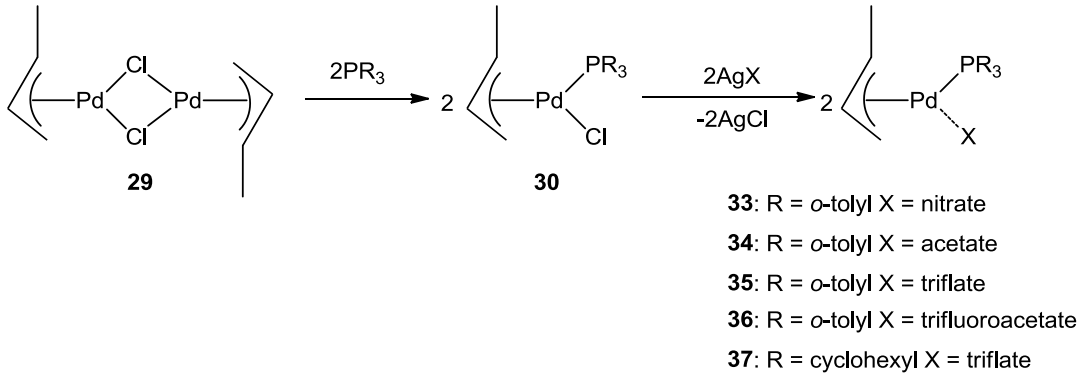

Scheme 1.7 Synthesis of $(\eta^3\text{-allyl})PdX(PR_3)$ systems for the polymerisation of norbornene monomers

In order to establish the essential features for high catalytic activity, Lipian and co-workers examined the polymerisation of 5-butylnorbornene and 5-triethoxylsilylnorbornene (95:5 molar ratio) using various combinations of complex **29**, PCy_3 and $[Li(Et_2O)_{2.5}][B(C_6F_5)_4]$.[85] Reaction of $[(\eta^3\text{-allyl})Pd(Cl)]_2$ (**29**) with PCy_3 yields the monomeric complex $[(\eta^3\text{-allyl})Pd(Cl)(PCy_3)]$ (**30**), however complex **30** is inactive in the polymerisation of the butyl-/triethyoxysilyl-monomer mixture, even after heating for 4 hours at 65 °C. Reaction of complex **29** with the lithium salt, $[Li(Et_2O)_{2.5}][B(C_6F_5)_4]$ in the presence of the monomer was also carried out., however the resulting complex is also inactive in the polymerisation of the butyl-/triethyoxysilyl-monomer mixture. Finally, reaction of the monomer mixture with all three catalyst components (complex **29**, phosphine and the lithium salt) was carried out and in this instance, high conversion of monomer to polymer (~85%) was observed. The observed polymerisation in the presence of the three component system is strong evidence that a palladium cation containing an initiating metal carbon σ-bond, a neutral, two-electron-donor phosphine ligand and a weakly coordinating counter ion are necessary attributes for a high activity polymerisation catalyst.[85]

The effect of variation of the phosphine component of the systems described in Scheme 1.7 was also investigated. Phosphine ligands of the type PR_3 are extremely important as they constitute one of the few series of ligands in which electronic and steric properties may be tailored in a systematic and predictable way over wide range, simply by varying R.[86] The steric and electronic properties of phosphines were further collated by Tolman, who proposed a model which serves as a basis to rationalise the effect of phosphine ligands in chemical reactions.[87]

In order to understand the influence of the steric and electronic properties of the phosphine ligand in the copolymerisation of 5-butylnorbornene and 5-triethoxylsilylnorbornene (95:5 molar ratio, toluene, 4h, 65 °C, [monomers] = 2.0 M, [Pd] = 0.042 mM, [Li] = 0.20 mM), a range of initiators were generated *via* addition of PR_3 to $[(\eta^3\text{-allyl})Pd(Cl)]_2$ in the presence of $[Li(Et_2O)_{2.5}][B(C_6F_5)_4]$. It was found that in general, bulky phosphines, with large cone angles, yield polymers with lower molecular weights than their less sterically demanding counterparts.[85]

The effect of the leaving group, X, in the copolymerisation of 5-butylnorbornene and 5-triethoxylsilylnorbornene (95:5 molar ratio, toluene, 4h, 65 °C, [monomers] = 1.0 M, [Pd] = 0.026 mM, [Li] = 0.13 mM) was also studied for the series of complexes **30** and **33-37** (Scheme 1.7). Active polymerisation initiators were generated *in situ via* reaction of each complex with $[Li(Et_2O)_{2.5}][B(C_6F_5)_4]$. Systems **35** and **36**, in which X =

triflate and trifluoroacetate, respectively, led to 100% conversion of monomer, whilst the nitrate (**33**), acetate (**34**), and chloride (**30**) systems gave 70, 80 and 84% conversion, respectively. This variation can be explained in terms of the lability of anionic ligand, with the more labile groups generating the most active catalysts.[85] The nature of the group X appears to have little influence on the molecular weight of the polymer produced, which was found to vary between 187 and 238 x 10^3 g mol^{-1} for the systems studied.

Related work by BF Goodrich/Promerus LLC and others, demonstrated the ability of mixtures of $[Pd(O_2CCH_3)_2(R_3P)_2]$ (R = ^{i}Pr, Cy) with $[Li(Et_2O)_{2.5}][B(C_6F_5)_4]$, $[(HNMe_2Ph)][B(C_6F_5)_4]$ or alternative Lewis acid activators to promote the polymerisation of norbornene upon thermal activation.[59-60,88-89] In an attempt to understand this behaviour, a large number of novel cationic palladium acetate species were synthesised and subsequently characterised.[59-60,88] The thermolytic behaviour of these species was also examined, as unlike the initiators discussed previously (such as allyl systems), they lack the presence of a Pd-H or Pd-C bond into which olefin insertion may take place (Scheme 1.8).[60]

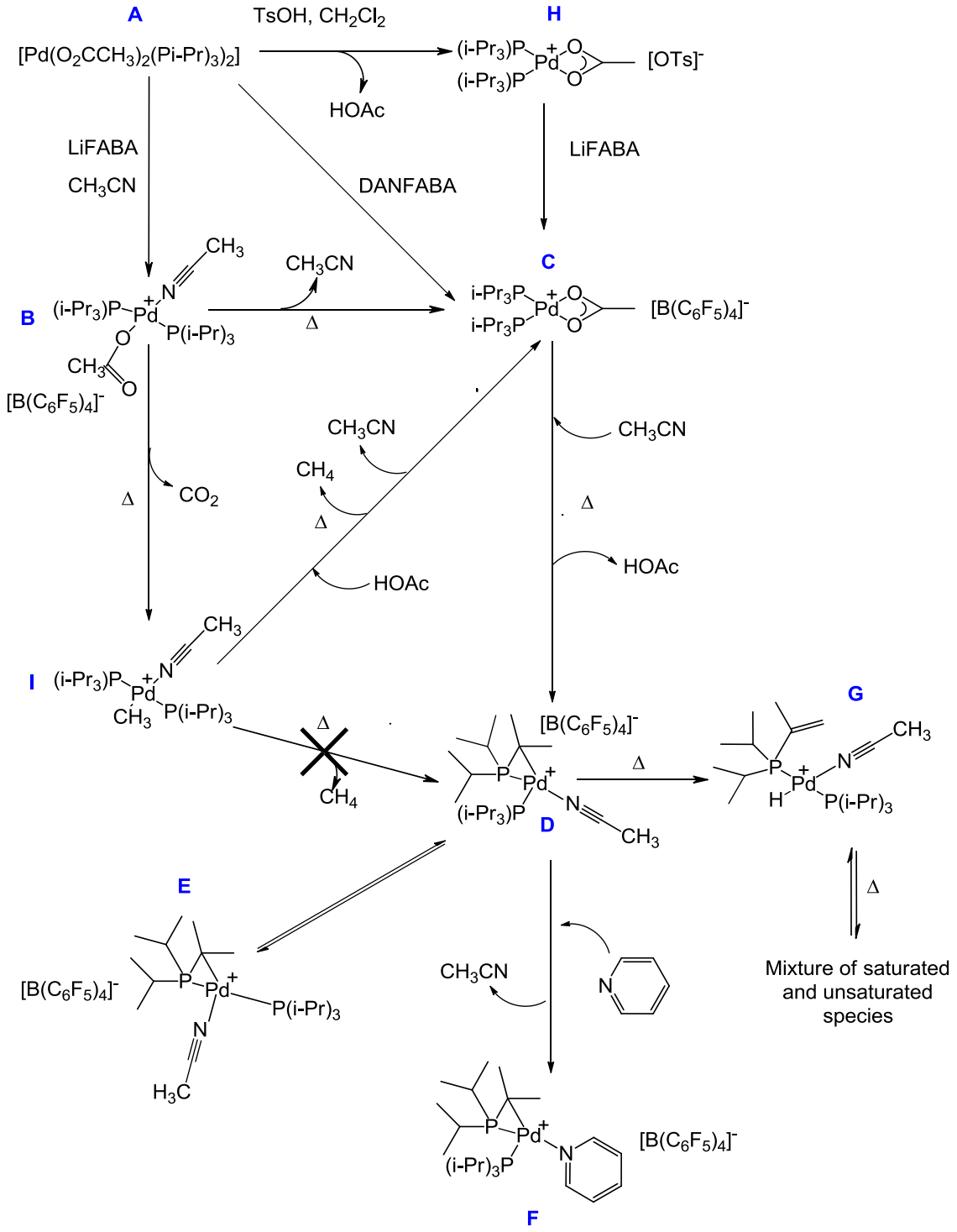

LIFABA = $[Li(OEt_2)_{2.5}][B(C_6F_5)_4]$

DANFABA = $[HNMe_2Ph][B(C_6F_5)_4]$

Scheme 1.8 Transformations of palladium acetate to yield highly active palladium pro-initiator and initiator species for the polymerisation of norbornenes [60]

Reaction of $[Pd(OAc)_2(R_3P)_2]$ (R=Cy, ^{i}Pr) (Scheme 1.8, **A**) with either $[Li(Et_2O)_{2.5}][B(C_6F_5)_4]$ (LiFABA) or $[HNMe_2Ph][B(C_6F_5)_4]$ (DANFABA) in acetonitrile led to acetate loss and the selective formation of *trans*-$[Pd(OAc)(R_3P)_2(MeCN)][B(C_6F_5)_4]$ (**B**). Crystallographic analysis confirmed the monodentate acetate binding mode and showed the palladium centre to have square planar geometry.

Generation of the species $[Pd(\kappa^2\text{-O,O'-OAc})(R_3P)_2][B(C_6F_5)_4]$ (**C**) with chelation of the acetate ligand was achieved *via* two alternative routes. Initial reaction of $[Pd(OAc)_2(R_3P)_2]$ (**A**) with *p*-toluene sulfonic acid in dichloromethane gave the species $[Pd(OAc)(OTs)(R_3P)_2]$ (**H**) in which one of the acetate ligands was replaced by the tosylate anion, and subsequent reaction with $[Li(Et_2O)_{2.5}][B(C_6F_5)_4]$ gave complex **C**. An alternative route to **C** is *via* direct reaction of $[Pd(OAc)_2(R_3P)_2]$ (**A**) with $[HNMe_2Ph][B(C_6F_5)_4]$ again in CH_2Cl_2, however higher yields were obtained using the former process.[59]

Addition of acetonitrile to $[Pd(\kappa^2\text{-O,O'-OAc})(^iPr_3P)_2][B(C_6F_5)_4]$ (**C**) does not promote formation of the monodentate acetate species $[Pd(OAc)(MeCN)(R_3P)_2][B(C_6F_5)_4]$. Instead, the reversible formation of a *cis*-three-membered palladacycle, (Scheme 1.8, **D**) is observed *via* loss of acetate as acetic acid, followed by β-hydride abstraction from one of the isopropyl groups of the phosphine ligands. The yield of species **D** was improved in the presence of sodium carbonate, however the waxy nature of the product meant that a clean sample of **D** was not obtained.

Treatment of **D** with 2 equivalents of pyridine led to the selective formation of the closely related complex **F**. The small $^2J_{PP}$ coupling constants for **D** and **F** (29 and 30 Hz, respectively) are consistent with the *cis* arrangement of phosphines, which was confirmed by crystallographic analysis of complex **F**.

The thermolytic behaviour of species **B**-**D** was also investigated.[60] Under appropriate conditions, the thermolysis of **C** led to the formation of the cationic palladium hydride **G** as the major product with palladacycle **D** as an intermediate. Subsequent ^{13}C NMR and deuterium labelling studies confirmed the origin of the hydride as being from the trialkylphosphine ligand. Further heating of the palladium hydride complex **G** led to scrambling of the saturated and unsaturated phosphine species to yield a mixture of products. It is suggested that thermolysis of **B** leads to formation of the palladium methyl species **I** *via* loss of CO_2, although no concrete evidence is presented for the

formation of this species. It is also suggested that **I** can be readily reconverted to **C** *via* addition of acetic acid and loss of methane and acetonitrile.[60]

The reactions outlined in Scheme 1.8 suggest that the cationic palladium hydride $[Pd(H)(MeCN)(R_3P)_2][B(C_6F_5)_4]$ (**G**) may be the active species in the polymerisation of norbornene and this observation sparked interest in the development of both new palladium hydride initiators and alternative routes for their formation.[60] The syntheses of $[Pd(H)(L)(PCy_3)_2]X$ (in which R = ^{t}Bu or Cy and L = OH_2 or CH_3CN, X = BF_3OH, BF_4 or BPh_4) are described in the early literature,[90-91] *via* oxidative addition of acids such as $[H_3O][X]$ to *bis*-phosphine palladium(0) complexes. A closely related synthesis in which treatment of $Pd(PCy_3)_2$ with $[HNMe_2Ph][B(C_6F_5)_4]$ in acetonitrile yields $[Pd(H)(Me_2NPh)(PCy_3)_2][B(C_6F_5)_4]$ (**38**), which is readily converted to $[Pd(H)(MeCN)(PCy_3)_2][B(C_6F_5)_4]$ (known as **Pd1388**) *via* sonication to eliminate dimethylaniline, was developed by Promerus LLC (Scheme 1.9).[59]

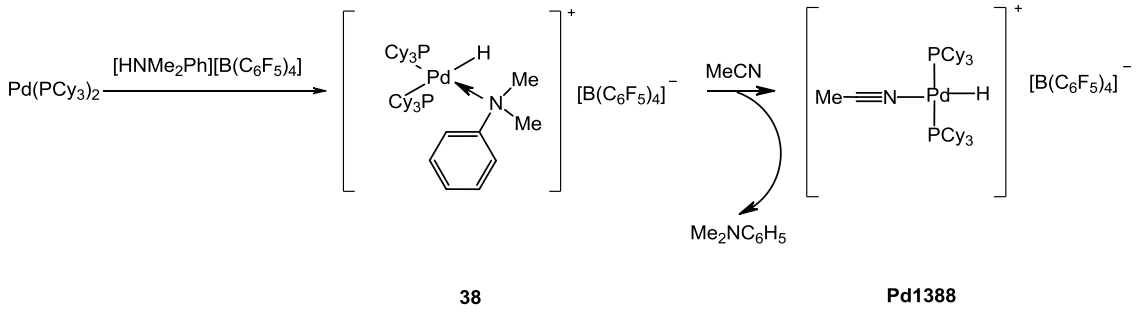

Scheme 1.9 Generation of palladium hydride complexes **38** and **Pd1388** species using dimethylanilinium reagents

An alternative synthetic route to palladium hydride complexes such as **Pd1388** goes *via* formation of $[PdCl(H)(^iPr_3P)_2]$ (**39**) followed by abstraction of chloride to yield the hydride product (Scheme 1.10).[34,92-93] The generation of the corresponding palladium methyl complex, $[Pd(Me)MeCN(^iPr_3P)_2][B(C_6F_5)_4]$ (**40**) is achieved in an analogous manner to that for palladium hydride formation.

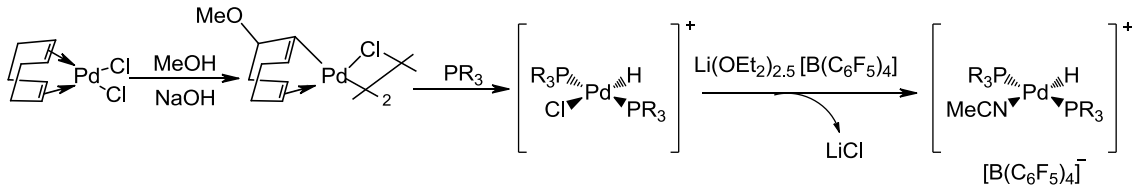

39 **Pd1388**

Scheme 1.10 Generation of cationic palladium hydride species *via* chloride abstraction from $[PdCl(H)(^{i}PrP_3)_2]$

In 2006, Nozaki investigated the activity of bulky monophosphine-ligated methylpalladium complexes in the polymerisation of norbornenes.[94] Prepared *via* reaction of [PdCl(Me)(COD)] with bulky phosphines $P^{t}Bu_3$ and P(*o*-tol)$_3$, the structures of the resulting palladium complexes were found to depend upon the nature of the ligand; the mononuclear structure $[PdCl(Me)\{P(^{t}Bu)_3\}]$ (**41**) was observed with $P^{t}Bu_3$ however the chloride-bridged dimeric complex $[PdCl(Me)\{P(o\text{-tol})_3\}]_2$ (**42**) was observed when the phosphine was P(*o*-tol)$_3$. An X-ray molecular structure determination confirmed the three-coordinate T-shape structure of complex **41**, which is stabilised *via* a weak agostic interaction between the palladium atom and one of the ^{t}butyl groups of the phosphine. Complex **41** is reported as the first example of a three-coordinate alkyl-palladium complex. Reaction of **41** and **42** with silver triflate led to chloride abstraction and the formation of the corresponding mononuclear and bridged triflate analogues **43** and **44**, the structures of which were confirmed by X-ray crystallographic analysis.[94]

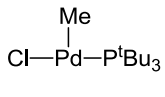

41

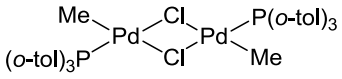

42

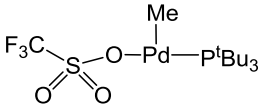

43

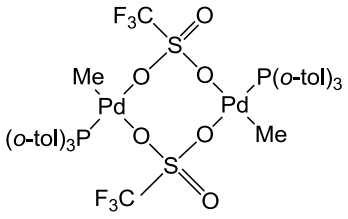

44

Combination of complexes **41-44** with Na[B(3,5-$(CF_3)_2C_6H_3)_4$] leads to the formation of active initiators for the homopolymerisation of norbornene. Complex **44** was shown to be active, even in the absence of Na[B(3,5-$(CF_3)_2C_6H_3)_4$], however the catalytic activity was found to be lower than that of the activated system **41**. Furthermore, **41** in combination with Na[B(3,5-$(CF_3)_2C_6H_3)_4$], was shown to initiate the homopolymerisation of methoxycarbonylnorbornene and also its copolymerisation with norbornene. Reaction of **41** with Na[B(3,5-$(CF_3)_2C_6H_3)_4$] yields the binuclear-bridged complex **45** (Scheme 1.11) Structures similar to that of **45** had previously been reported in the literature.[95] Complex **45** was shown to be in equilibrium with the coordinatively unsaturated palladium species **46**, and in the presence of norbornene monomer, complex **47** (Scheme 1.12).

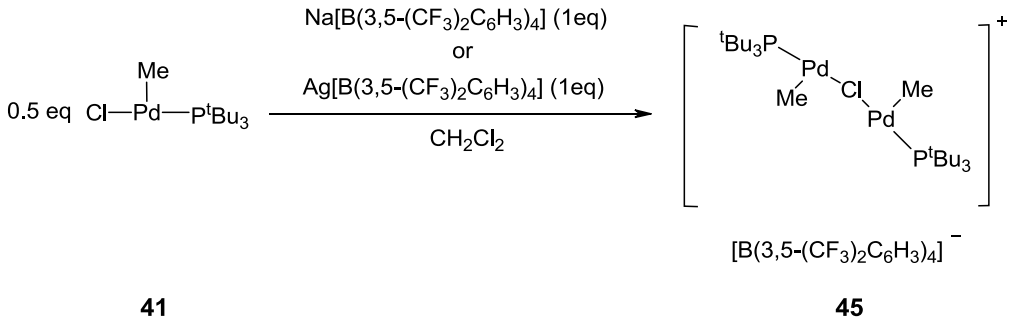

Scheme 1.11 Formation of the binuclear-bridged complex, [PdMe(^{t}Bu$_3$P)}$_2$Cl][B(3,5-$(CF_3)_2C_6H_3)_4$], **45**

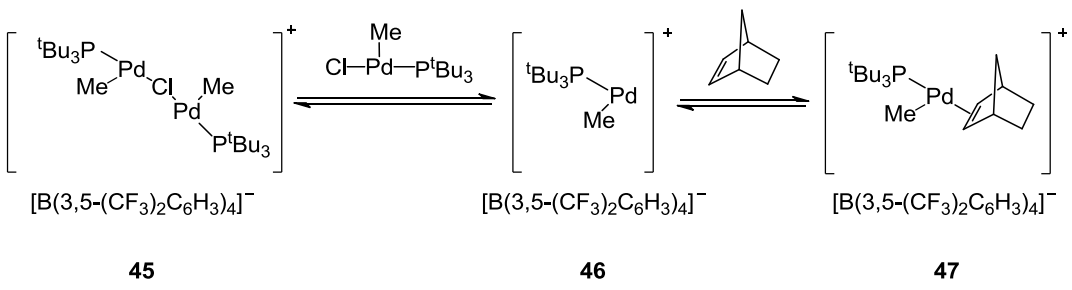

Scheme 1.12 Equilibrium between the coordinatively unsaturated cationic palladium species **46**, and corresponding palladium complex with bound norbornene monomer **47**.

Over the past decade, a wide range of both neutral and cationic nickel and palladium complexes (including chiral palladium complexes, which allow the possibility for stereo control within the backbone chain) have been investigated as initiators for the vinyl polymerisations of norbornene derivatives.[51-52,56-57,95-108] However, high activities usually require the use of co-initiators such as MAO, which make them less attractive in comparison with the cationic palladium complexes discussed above. A notable exception to this rule is the complex [(η^6-toluene)Ni(C_6F_5)$_2$], which is extremely active in the polymerisation of functionalised norbornene derivatives, without the need for a co-catalyst.[110]

1.5 Mechanistic insights in to the polymerisation of norbornene using late-transition metal initiators

The polymerisation of olefins such as norbornene, initiated using the cationic palladium(II) complex, [Pd(CH_3CN)$_4$][BF_4]$_2$ (**1**) was initially though to proceed by a cationic mechanism, as described by Sen in 1981.[64] However, further studies by Risse showed that the polymerisation was uninhibited in the presence of water which is a known trap for free carbocations.[111] This observation hence suggested that a cationic polymerisation mechanism was unlikely.

As an alternative, Risse proposed a mechanism based upon insertion of norbornene into a palladium carbon bond, which more recent studies have since confirmed to be correct. The polymerisation of norbornene and a substituted derivative, 2-acetoxymethyl-5-norbornene ($NBCH_2OAc$) using complex **1** was reported to be living (*i.e.* the absence of chain transfer or termination), and the authors suggest that "the Pd-C bond of the polymer end group remained intact after all of the monomer had been consumed", an observation which supports a living polymerisation mechanism.[25,111] A living mechanism is understandable as insertion of norbornene into a palladium carbon bond generates a structure, which does not contain hydrogen atoms that are suitably positioned for β-hydrogen elimination to occur (Figure 1.2).

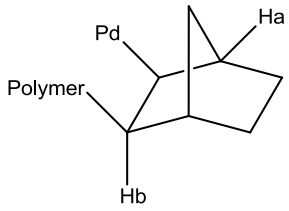

Figure 1.2 β-hydrogen atoms of a generic inserted-palladium norbornene species

An interesting rearrangement of an inserted palladium-norbornene complex in the polymerisation of *endo*-/*exo*-2-acetoxymethyl-5-norbornene using **1** is reported by Rhodes and co-workers.[112] The authors report the formation of a low molecular weight (~1000 Daltons) polymer with an unusual, saturated end group, *via* β, γ-carbon-carbon bond cleavage and subsequent rearrangement of the norbornene end group moiety (Scheme 1.13).

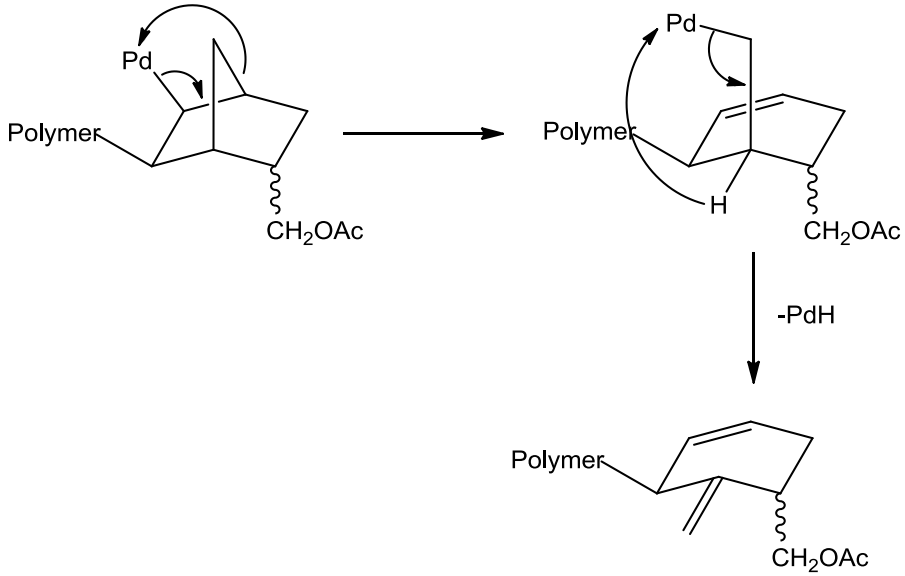

Scheme 1.13 Formation of poly(*endo*-/*exo*-NBCH$_2$OAc) with unsaturated end groups *via* β, γ-carbon-carbon bond cleavage

Brookhart and co-workers have undertaken detailed studies into the first insertion products of the polymerisation of norbornene using allyl-nickel and palladium initiators.[113-114] They report formation of an interesting palladium norbornene complex in which the norbornene moiety acts as a bidentate ligand, binding to the palladium centre *via* the π system of the olefin and a γ-agostic interaction of the *syn* hydrogen of C7 (Figure 1.3).[113] The nature of the agostic intermediate was confirmed using NMR spectroscopy and X-ray molecular structure determination. NMR spectroscopic studies suggest that the rate limiting step in the polymerisation of norbornene is insertion of monomer into the agostic intermediate and opening of the chelate, with subsequent insertions shown to be extremely fast.

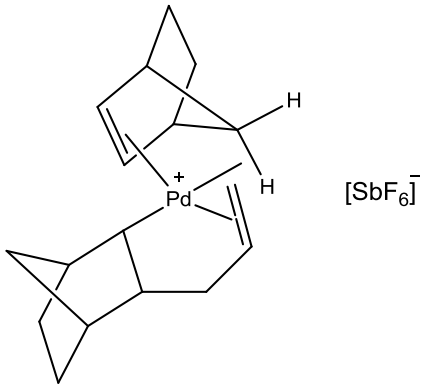

Figure 1.3 Bidentate bind of norbornene to a cationic palladium centre *via* the olefin and a γ-agostic interaction of the *syn* hydrogen of C7

1.6 The effect of *endo*-/*exo*- substituents in the polymerisation of functionalised-norbornene monomers

It is well documented that *endo*-functionalised norbornenes are polymerised more slowly than their *exo* counterparts, however despite extensive experimental[20,23-29,31-36,115] and theoretical[116-118] investigations, the precise origins of this effect remain unclear. A detailed understanding of this phenomenon requires consideration of a number of factors, all of which may contribute to the overall observed polymerisation rate. A simple series of functionalised norbornenes that can be used to study the effect of substituents in the *endo*- and *exo*-positions are norbornenes bearing alkyl groups (*endo*-/*exo*-NB$(CH_2)_nCH_3$). Sen and co-workers examined the polymerisation of a series of these *endo*- and *exo*-alkyl-functionalised norbornenes with varying alkyl chain length, (n = 3-9).[29] Polymerisations were carried out in TCE and initiated using [Pd(Cl)(Me)(COD)] in combination with one equivalent of PCy_3. Analysis of total monomer consumption was monitored as a function of time by GC. The resulting data were fitted to *pseudo*-first order kinetics and demonstrated a decrease in overall polymerisation rate in the order butyl-NB > hexyl-NB > decyl-NB. The decrease in polymerisation rate with increasing chain length can be rationalised in terms of the steric demands of the functional group. In order for polymerisation to take place, the norbornene monomer unit must insert into a metal-alkyl or metal-hydride bond, a process that requires re-hybridisation of carbon centres of the norbornene moiety from sp^2 to sp^3 hybrids (Scheme 1.14) together with an associated change in geometry.[29] Sen suggests that the larger the steric bulk of a group in the *endo* position, the greater the interaction will be between the hydrogen of the double bond and the functionality,

during the rehybridisation process. The more unfavourable the re-hybridisation process, the slower the observed polymerisation rate.

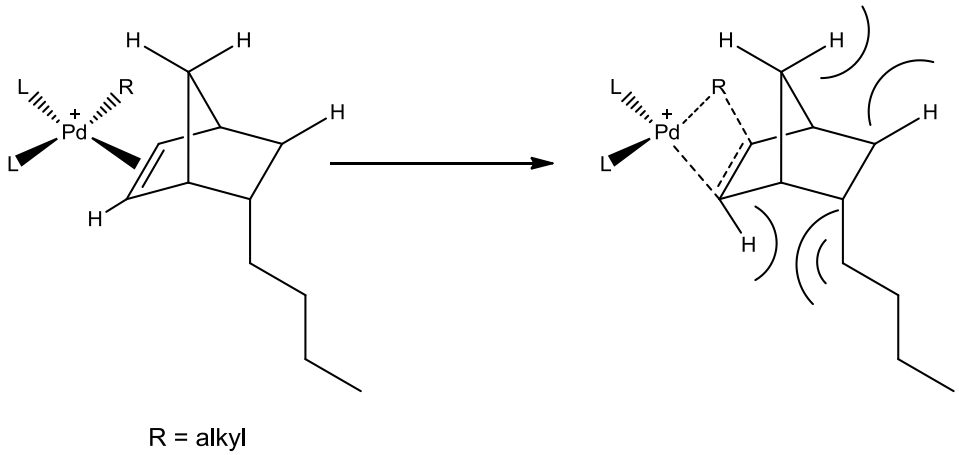

Scheme 1.14 Steric interactions in the insertion of *endo* alkyl functionalised norbornenes into a palladium alkyl-bond.[29]

Further studies on the polymerisation of alkyl-functionalised norbornenes explored the use of ^{1}H NMR spectroscopy to examine the rates of polymerisation of *endo* and *exo* isomers independently within a mixture.[20] Polymerisation reactions were initiated using **Pd1388** and the resulting data fitted to *pseudo*-first order kinetics. The polymerisation of *exo*-functionalised alkyl norbornenes within a mixture showed similar rates, irrespective of chain length. However, in the presence of an alkyl substituent the rate of polymerisation was lower than that for the parent, un-substituted norbornene. For *endo* alkyl functionalised norbornenes, a decrease in polymerisation rate was observed as chain length was increased, confirming the sterics argument proposed by Sen.[29]

1.6.1 The effect of polar, coordinating substituents on polymerisation rate

The polymerisation of norbornenes bearing polar substituents such as oxygen- or nitrogen-containing functionalities adds an extra layer of complexity to understanding the difference in polymerisation rate between *endo* and *exo* isomers. Functionalities such as esters and carboxylic acids present the possibility of coordination to the metal centre *via* the carbonyl moiety in preference to, or in combination with, the olefin moiety. Coordination of functionalised norbornenes to a metal centre is possible in a number of orientations. These include coordination of the olefin to the metal centre as desired (**a**), coordination of the functional group to the metal (**b**) or coordination of both olefin and functional group as part of a chelate (**c**) (Figure 1.4).[28-29]

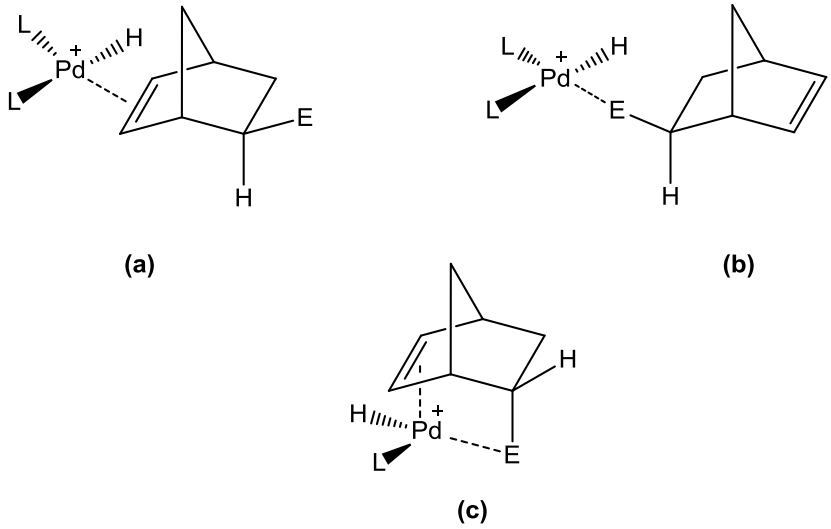

Figure 1.4 Possible coordination modes of functionalised norbornenes to a generic, cationic palladium centre (counter anion not shown). **a**) Coordination of the norbornene double bond, **b**) coordination of the functional group E, which is a potential Lewis base and **c**) formation of a chelate *via* coordination of both the olefin and E to the metal centre.[28-29]

Coordination of a polar group to the metal centre will attenuate polymerisation rate, regardless of whether the coordinating functionality is part of the monomer structure or not. The effect of coordination is highlighted by reduced polymerisation rates for norbornenes when polymerisation reactions are carried out in coordinating solvents such as acetonitrile or ethyl acetate.[28-29] Coordinating solvents compete with monomer units for binding to the metal centre, reducing the likelihood of coordination of the olefin and subsequent insertion of monomer units into the growing polymer chain.

1.6.1.1 The effect of polar substituents in the *exo* position

In the case of pure *exo*-substituted norbornenes, formation of a chelate involving coordination of both the double bond and the functionality, E, to a metal centre is unfavourable. The lack of chelate formation for pure *exo*-isomers makes them ideal candidates to study the effect of systematic changes to their substituents on observed polymerisation rate. Liu and co-workers examined the palladium-catalysed polymerisation behaviour of *exo*-functionalised norbornenes bearing dimethyl carboxylate (**a**) and dialkyl ester groups (**b**) (Figure 1.5).[119] By systematically varying the length of the alkyl chain, R, the contribution of the substituent to the observed rate of polymerisation could be determined.

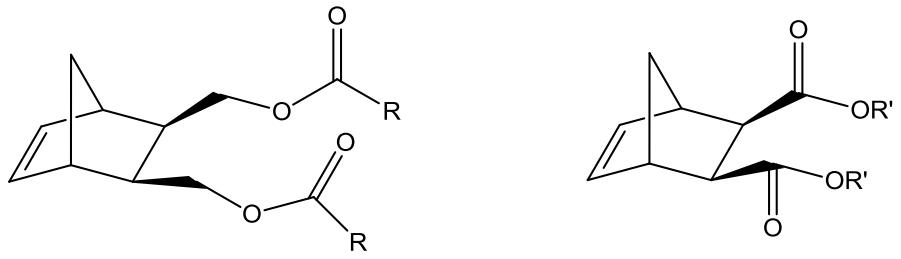

Figure 1.5 a) Dimethyl carboxylate-functionalised norbornenes and **b**) dialkyl ester-functionalised norbornenes.[119]

For the series of dimethyl carboxylate-functionalised norbornenes (**a**), the polymerisation rate was shown to decrease in the order R = acetate > propionate > butyrate. Analysis of the carbonyl stretching frequencies of these monomers by IR spectroscopy indicates similar basicity and hence coordinating ability in all cases, suggesting that the effects in polymerisation behaviour observed are related primarily to steric rather than electronic interactions.

A similar decrease in polymerisation rate with increasing chain length of the substituent (R'), is observed for the series of dialkyl ester-functionalised norbornenes (Figure 1.5, **b**). Comparison between monomer types (**a**) and (**b**) containing the same number of carbon atoms in the alkyl chain R and R', indicates increased polymerisation activity for the dimethyl carboxylate analogue. The reduced reactivity of type (**b**) monomers may be attributed to the closer proximity of the functional group to the norbornene skeleton and hence increased contribution to steric interactions between the functionality and the metal centre.

1.6.1.2 The effect of polar substituents in the *endo* position – formation of metal norbornene-containing chelates

The formation of a chelate involving coordination of both E and the norbornene double bond has two detrimental effects on polymerisation rate. Firstly, chelation strengthens the metal olefin interaction which raises the energy barrier for any migratory insertion step. Secondly, chelation requires coordination of the olefin and hence any subsequent insertion to occur through the *endo* face of the norbornene (Figure 1.6, **a**).[28-29] Insertion

through the *endo* face goes against the known preference for norbornenes to undergo insertion into a metal-carbon bond through the less hindered *exo* face (Figure 1.6 **b**).[31-36, 120-121] The propensity of *endo*-norbornenes bearing ester functionalities to form chelates was confirmed by Sen and co-workers *via* isolation of a discrete platinum norbornene chelate complex following insertion of the alkenyl moiety of the norbornene into the platinum hydride bond (Figure 1.7).[28]

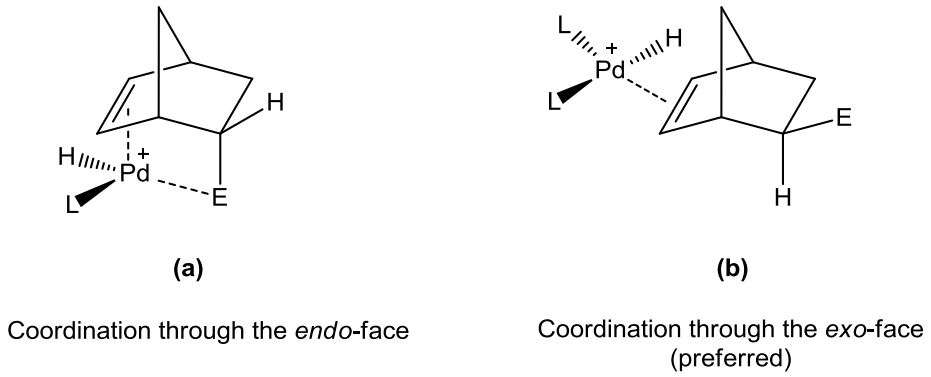

Figure 1.6 Coordination of the norbornene double bond to a generic palladium centre through the *endo* (**a**) and *exo* (**b**) face (counter anions not shown).[28-29]

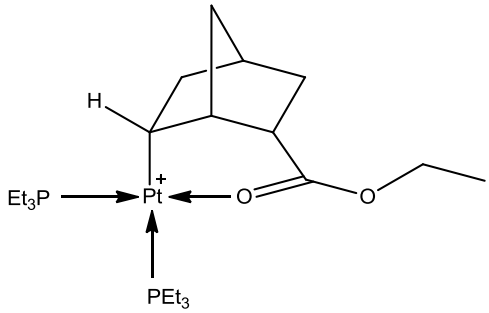

Figure 1.7 Structure of the platinum-norbornene chelate formed upon insertion of *endo*-norbornene ethyl ester into a platinum hydride bond (counter anion not shown).[28]

In order to determine the relative importance of coordination versus chelate formation, Sen and co-workers examined the relative abilities of *endo*-norbornene ethyl ester (Figure 1.8, **a**) and its corresponding saturated norbornane analogue (Figure 1.8, **b**) to reduce the rate of palladium-catalysed polymerisation of n-butyl norbornene.[29] The formation of a stable chelate (**a**) increases the energy barrier to insertion of monomer, whilst coordination of the ester functionality without chelation (**b**), simply blocks one of

the coordination sites on the palladium centre. The unsaturated norbornene ester (**a**) was significantly more effective in reducing polymerisation rate, confirming that for this system, chelate formation, rather than coordination is the dominant factor in attenuating the rate of polymerisation.

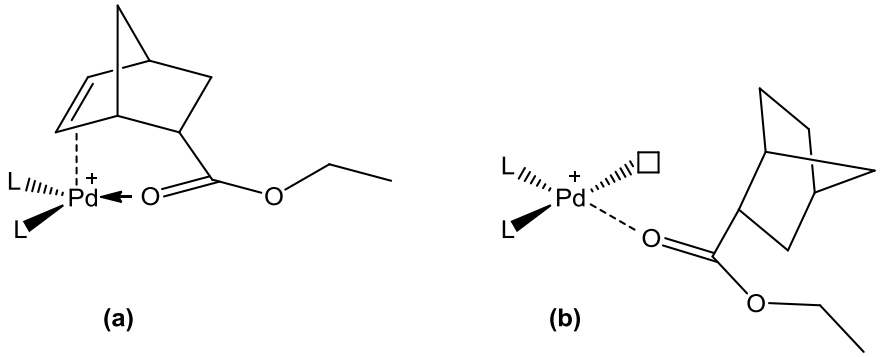

Figure 1.8 Coordination of **a**) *endo*-norbornene ethyl ester and **b**) *endo*-norbornane ethyl ester to a generic palladium centre (counter anions not shown). Formation of a chelate is only possible for the unsaturated analogue (**a**).[29]

1.6.1.3 Disrupting chelate formation *via* the introduction of spacer groups

One possible method to reduce the likelihood of chelate formation is to space the functionality away from the norbornene skeleton by means of an alkyl or ether chain (homologation). The introduction of a spacer group reduces the proximity of any functionality on the monomer to the metal centre, making coordination less likely to occur. In addition, if sufficient methylene spacers are used, chelate formation would require the generation of a medium (> 6-membered) ring that is unfavourable due to both ring strain and transannular interactions. The effect of chelate ring size on polymerisation rate is illustrated in an example by Sen and co-workers who demonstrate that *endo*-norbornene ethyl ester (Figure 1.9, **a**) is significantly more effective at attenuating the uptake of n-butyl norbornene than methyl acetate norbornene (Figure 1.9, **b**).[29] The effectiveness of the ester in preference to the acetate can be explained by the reduced stability of the 8-membered chelate likely to be formed if chelation were to occur in the latter example (Figure 1.9).

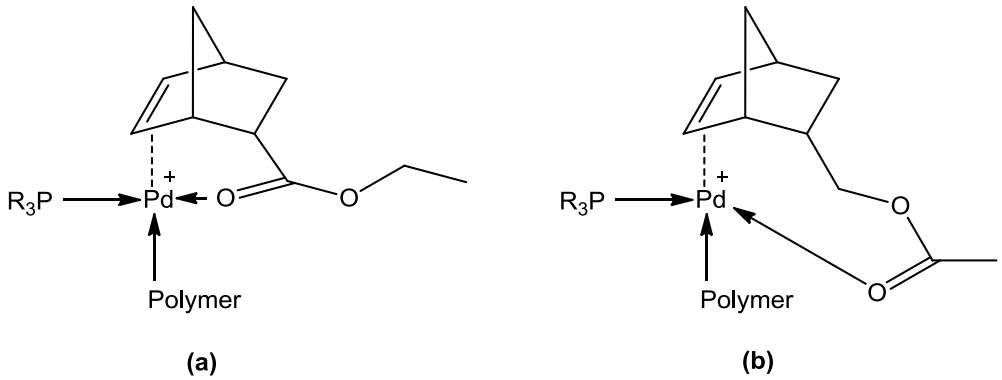

Figure 1.9 Possible chelate structures formed *via* coordination of **a**) *endo*-norbornene ethyl ester and **b**) *endo*-norbornene methyl acetate to a palladium centre (counter anions not shown).[29]

The effect of spacer group on polymerisation rate was examined in preliminary studies within our group, for the polymerisation of a number of different functionalised norbornene monomers using **Pd1388** (Figure 1.10).[20] In general, an increase in the number of methylene units, n, between a given oxygen- or nitrogen-containing functionality (E) and the norbornene skeleton results in a corresponding increase in polymerisation rate, for both the *exo* and *endo* isomers (Figure 1.10, **a**). In sharp contrast, the opposite effect is observed for alkyl norbornenes (Figure 1.10, **b**), where increased chain length for *endo*-alkyl-functionalised monomers results in a decrease in polymerisation rate. The effect of introducing increasing numbers of methylene spacer groups between the norbornene skeleton and a particular functionality results in a delicate balance between steric and electronic effects.

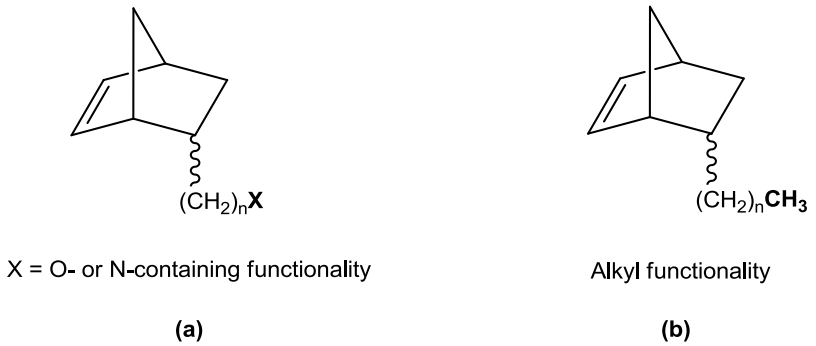

Figure 1.10 Functionalised norbornene monomers containing various numbers (n) of methylene spacer units. **a**), oxygen- and nitrogen-containing functionalities, **b**) alkyl functionalities

The introduction of methylene spacer groups between a given functionality and the norbornene skeleton has also been shown to have an effect on the properties of poly(norbornenes). Müller and co-workers have recently examined the homo- and co-polymers of hexyl norbornene (*endo*-/*exo*-$NB(CH_2)_5CH_3$) and $NB(CH_2)_8CO_2C_2H_5$ (Figure 1.11, **a**).[122] The study demonstrates the facile palladium-catalysed polymerisation of *endo*-/*exo*-$NB(CH_2)_8CO_2C_2H_5$ to high conversion (88%) after 20 minutes at ambient temperature. Polymerisation of *endo*-/*exo*-$NBCO_2C_2H_5$ is considerably more difficult due to formation of a chelate (Figure 1.11, **b**). However, despite the rapid polymerisation of *endo*-/*exo*-$NB(CH_2)_8CO_2C_2H_5$, the solubility of the resulting polymer is poor. Copolymerisation of $NB(CH_2)_8CO_2C_2H_5$ with *endo*-/*exo*-$NB(CH_2)_5CH_3$ allows the solubility, T_g and mechanical properties of the resulting copolymers to be tailored by varying the feed ratio of the two monomers. Spacing of oxygen- and nitrogen-containing functional groups hence allows easy incorporation of polar monomers into copolymers, without the inherent problems of chelate formation and subsequent attenuation of polymerisation rate.

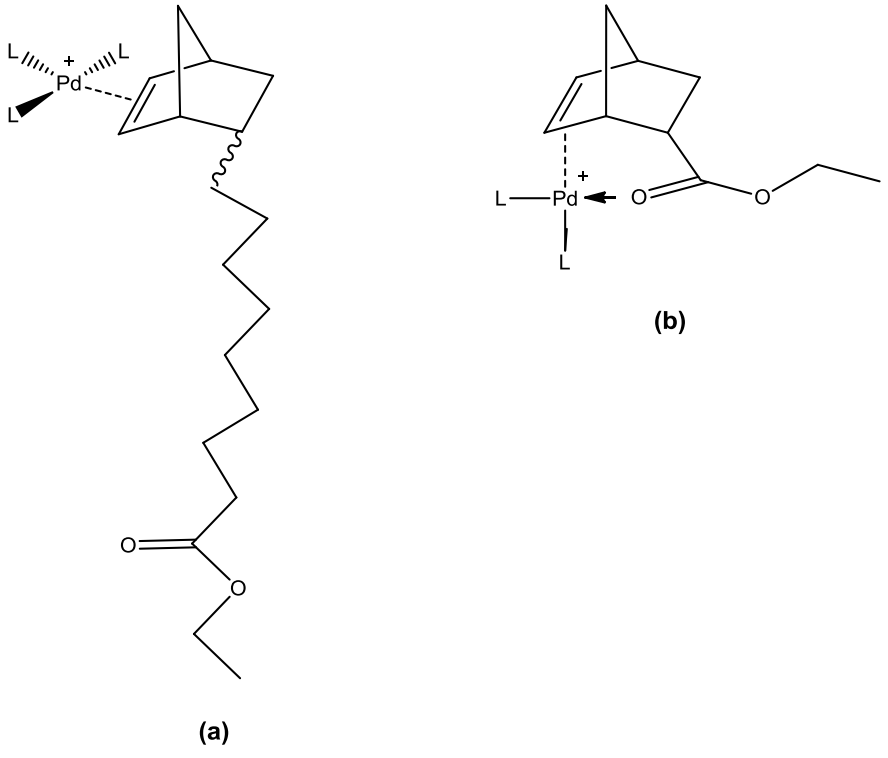

Figure 1.11 The effect of alkyl spacing upon the coordination of ester-functionalised norbornenes to a generic cationic palladium centre (counter anions not shown).[122]

Sections 1.1-1.6 have outlined the key palladium initiators and mechanistic processes involved in the polymerisation of generic norbornene derivatives. In this work, the norbornene monomers studied are very specific and are of commercial interest to Promerus LLC within the area of photolithography. An introduction to the subject of photolithography and the key monomers of interest in this thesis will be described in the following sections.

1.7 Introduction to hexafluoropropanol-functionalised norbornene monomers

Polynorbornenes with pendant functionalities find use in a wide range of commercial applications as their properties are easily tailored to meet a given specification.[20] Of significant interest to Promerus LLC are monomers bearing the hexafluoropropanol functionality, which are key components of polymeric binders in photoresist formulations for 157 nm photolithography, due to their transparency in the deep UV region.[10-16] A key monomer employed in this process is α,α-*bis*(trifluoromethyl)bicyclo[2.2.1]hept-5-ene-2-ethanol ($NBCH_2C(CF_3)_2OH$, also known as HFA norbornene and by the code **SXN4** within this thesis), the structure of which is shown in Figure 1.11.[10-16,123-131]

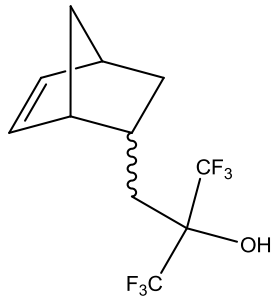

Figure 1.11 Structure of *endo*/*exo* HFA norbornene (**SXN4**)

1.8 Introduction to Photolithography

Photolithography is a technique used in the semiconductor industry to transfer circuitry information inscribed on photo masks onto the surface of silicon substrates.[9,132] This task is accomplished in a number of steps, which are illustrated in Figure 1.12. A liquid photosensitive formulation (or photoresist) is spin coated from an organic solvent on to the surface of a silicon wafer and dried to form a thin photosensitive film. The film is then covered with a mask bearing the desired pattern and exposed to UV light. Exposed areas of the film undergo a photoinduced chemical reaction which changes the solubility of the resist material. There are two types of photoresist: positive and negative, of which positive are now predominantly used and will form the focus of this review. Irradiation of a positive resist increases the solubility of the exposed film. The photo mask used is an exact copy of the pattern to be transferred to the surface and the resist is exposed wherever the underlying material is to be removed. The exposed resist is then simply washed away using developer solution (typically aqueous base), leaving a three-dimensional relief image of the mask in the photo resist film. Negative resists behave in the opposite manner. Exposure to UV light causes a polymerisation reaction to occur, rendering the resist insoluble in the developer solution. The negative resist remains on the silicon surface wherever it is exposed, with the developer removing all unexposed portions. Masks used for negative photo resists therefore contain the inverse (or photographic negative) of the pattern to be transferred. In both cases, the image is transferred to the underlying silicon surface *via* plasma etching, a process to which the remaining photoresist film is resistant.

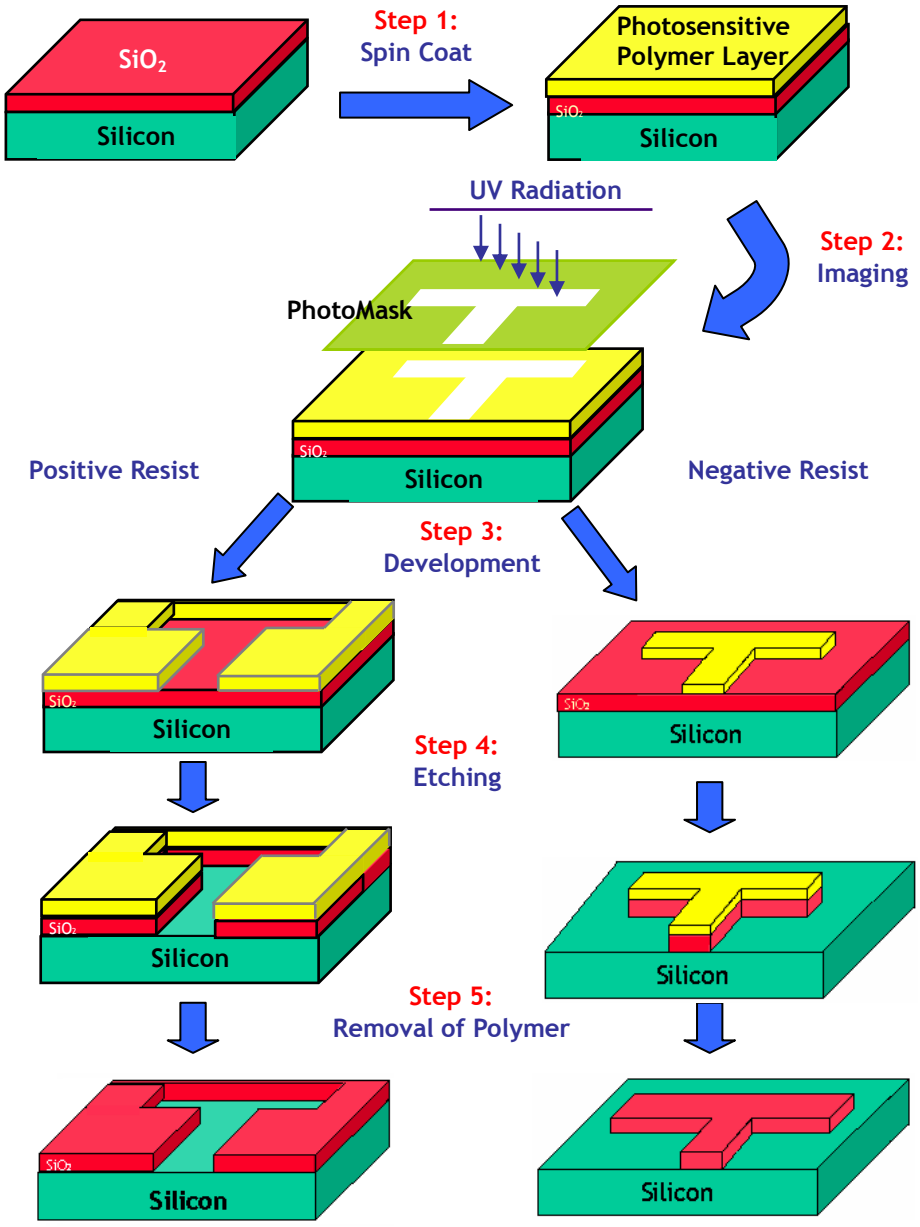

Figure 1.12 Schematic representation of the photolithographic process for positive and negative resists (adapted from an unpublished presentation, Promerus LLC)

1.9 Photolithographic Imaging

The minimum achievable feature size on a silicon chip is directly proportional to the imaging wavelength used, with modern optics allowing generation of feature sizes approximately one half the size of the imaging wavelength. Advances in photoresist materials have enabled a transition from imaging using ≥ 365 nm (i-line and g-line radiation) through 248 nm (KrF laser) and 193 nm (ArF laser) to the current state of the art of 157 nm (F_2 laser) light (Figure 1.13).[9,13-16] The key to these advances is the design of materials that are sufficiently transparent at the desired imaging wavelength, as without sufficient transparency, light cannot penetrate to the bottom of the resist film, resulting in poorly defined features.

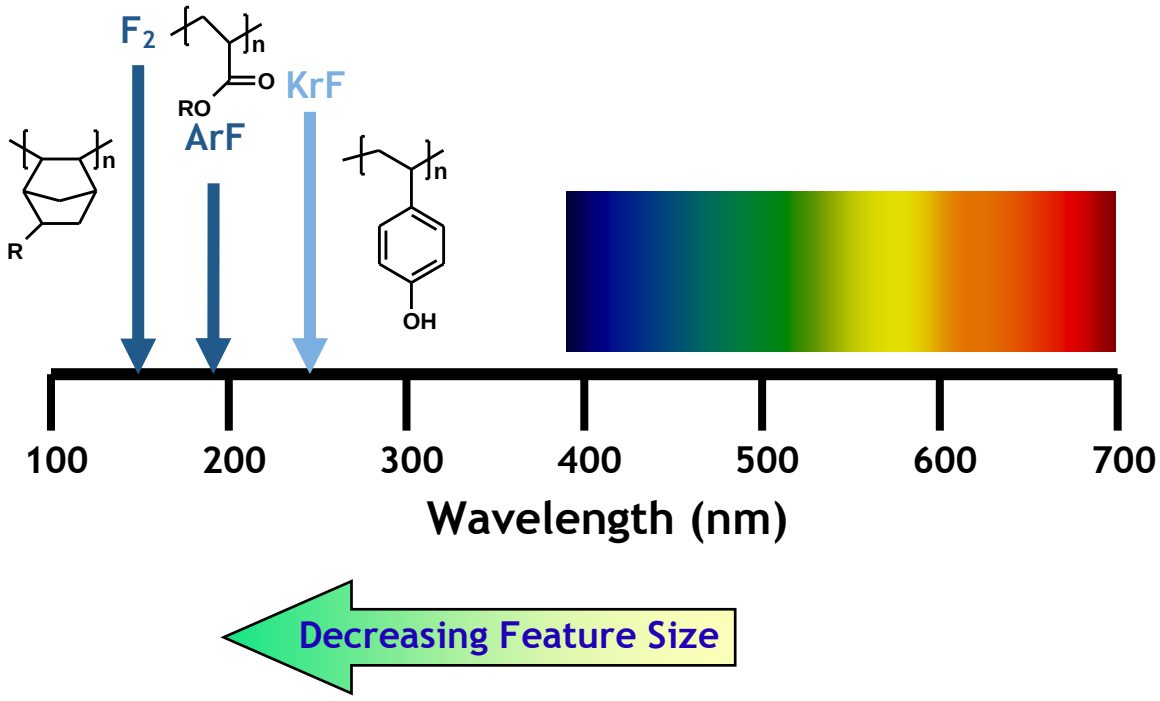

Figure 1.13 Key polymeric materials of used in photolithography, carried out at a variety of imaging wavelengths. (Figure taken from an unpublished presentation, Promerus LLC).

In addition to sufficient transparency, a photoresist formulation must also display a number of other crucial properties, and these are usually tailored through judicious choice of a polymeric binder.[133] The binder must demonstrate excellent etch resistance, solubility in selected organic solvents to allow spin coating, adhesion to the

silicon surface, tuneable functionality and molecular weight to permit dissolution whilst maintaining acceptable mechanical properties, be of extremely high purity (parts per billion levels) and finally be manufacturable on an appropriate scale at an acceptable cost.

1.9.1 Polymeric materials for photolithographic imaging at 248 nm

Lithography at 248 nm makes use of poly(*para*-hydroxy styrene) as a binder resin in which a proportion of the hydroxyl groups are protected as acid-labile *tert*-butyl carbonates.[134] The formulation also contains a photoacid generator (PAG) such as a triarylsulfonium perfluoroalkylsulfonate, which decomposes upon irradiation to generate a strong acid. The protected polymer is insoluble in aqueous base but acid-catalysed deprotection in the irradiated areas renders the exposed polymer soluble allowing effective removal. The presence of benzene rings within the polymer is advantageous, giving superior etch resistance. Carbon-rich organics have been shown to have superior etch resistance to those containing higher amounts of hydrogen or oxygen.[135] Unfortunately, polymers containing benzene rings are unsuitable for use below 248 nm due to their high absorbencies in this region.

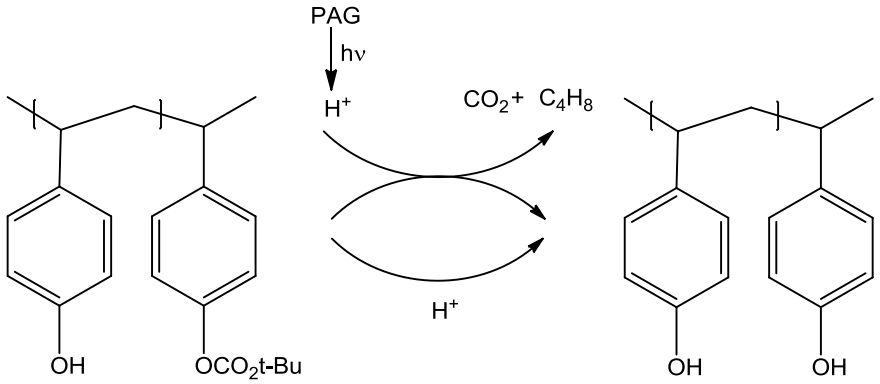

Scheme 1.15 Deprotection of ester-functionalised poly(*para*-hydroxy styrene) in the presence of a photoacid generator.[14]

1.9.2 Polymeric materials for photolithographic imaging at 193 nm

A number of polymeric materials fulfil the requirements for 193 nm photoresists. These include norbornene/maleic anhydride copolymers, norbornene/maleic anhydride/acrylate terpolymers, vinyl addition norbornene polymers and poly methacrylates containing polycyclic (*e.g.* adamantly) groups in their side chains (Figure

1.14).[16,136-141] The key to all of the above are polycylic groups which are sufficiently transparent at 193 nm and provide adequate etch resistance.

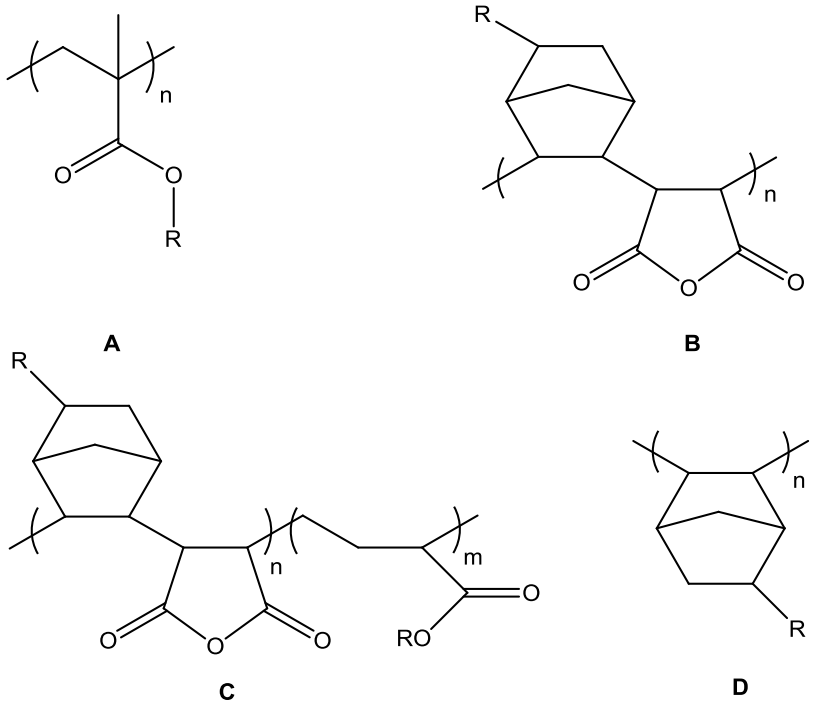

Figure 1.14 Polymeric materials which are transparent at 193 nm: methacrylates (**A**), norbornene/maleic anhydride copolymers (**B**), norbornene/maleic anhydride/acrylate polymers, (**C**) and vinyl addition norbornene polymers (**D**).[16]

1.9.3 Requirements for imaging at 157 nm and suitable polymeric materials

The move to 157 nm imaging presents a particular challenge in materials design, as water, oxygen gas and even simple hydrocarbons such as polyethylene absorb strongly in this spectral region. Hence, there is a need for a polymer that not only demonstrates sufficient transparency at this wavelength, but also is acidic enough to provide solubility in base developers and has sufficient rigidity to provide the necessary etch resistance.

It has been demonstrated that the use of fluorinated polymers, in particular the incorporation of the hexafluoropropanol ($C(CF_3)_2OH$) fragment into the polymer chain can overcome these difficulties.[10-16, 123-132] ($C(CF_3)_2OH$) shows similar acidity to phenol which has been used successfully in lithographic imaging at longer wavelengths and if rigid structure is incorporated into the polymeric backbone (as for 193 nm resists) then a suitable polymer can be obtained.

Incorporation of the $C(CF_3)_2OH$ group into organic molecules is possible *via* a number of routes. These include reactions of hexafluoroacetone with organic substrates, reaction of the synthetic equivalents of the trifluoromethyl anion, especially CF_3SiMe_3 with carbonyl compounds and more recently, ring opening of the fluorinated epoxide 2,2-*bis*(trifluoromethyl) oxirane (HFIBO).[142] The following sections will concentrate on the synthesis of norbornenes bearing the hexafluoropropanol group.

1.10 Hexafluoropropanol-functionalised norbornenes for use in 157 nm photolithography

The first synthesis of a hexafluoropropanol-functionalised norbornene derivative was described in a 2002 patent by Ito and co-workers.[143] The resulting monomer, *endo*-/*exo*-$NBCH_2C(CF_3)_2OH$, commonly referred to as HFANB was isolated in 31% yield as a mixture of *endo* and *exo* isomers in the ratio 80:20, *via* reaction of cyclopentadiene with 1,1,1-trifluoro-2-trifluoromethyl-4-penten-2-ol (Scheme 1.16).

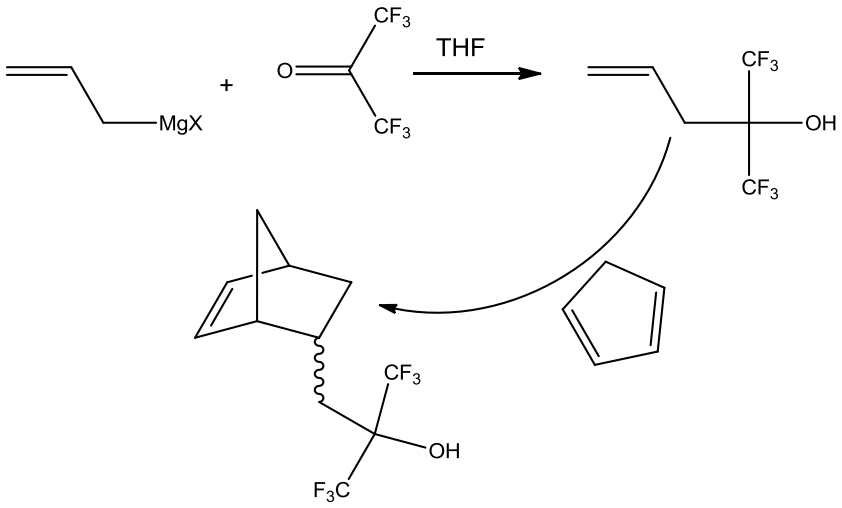

Scheme 1.16 Synthesis of HFANB

The synthesis of the pure *exo* isomer of HFANB (**SX2**) is disclosed in a 2005 patent by Fiering and co-workers.[11] Isolation of the pure isomer requires a multistep synthesis starting from an *endo*/*exo* mixture of 5-norbornene-2-chloride (Scheme 1.17). A second route to HFANB, which contains a predominantly the *exo* isomer, is also disclosed (Scheme 1.18). The product is obtained in high yield (91%) with a ratio of *exo:endo* isomers of >97:3.

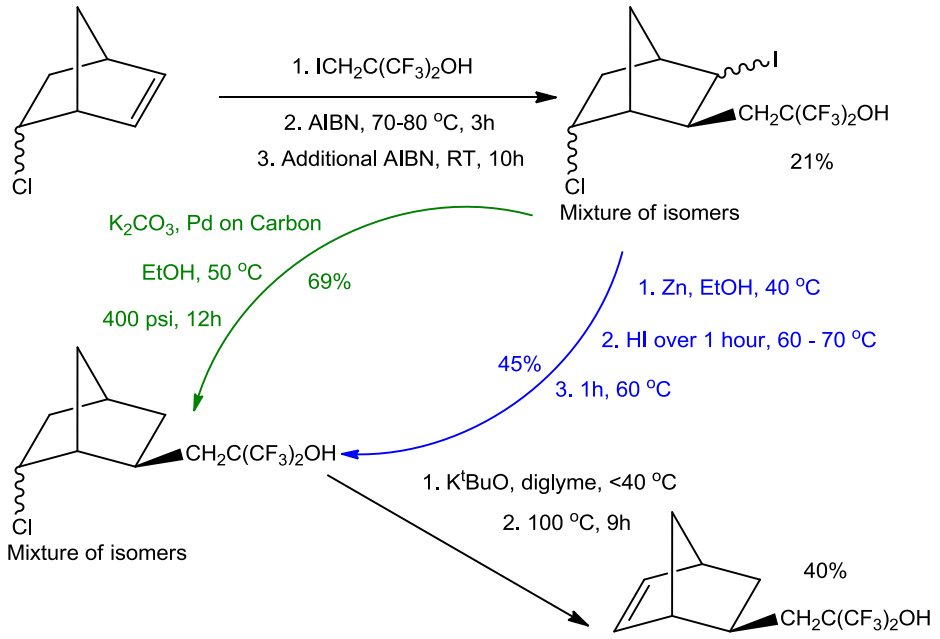

Scheme 1.17 Synthesis of *exo*-HFANB

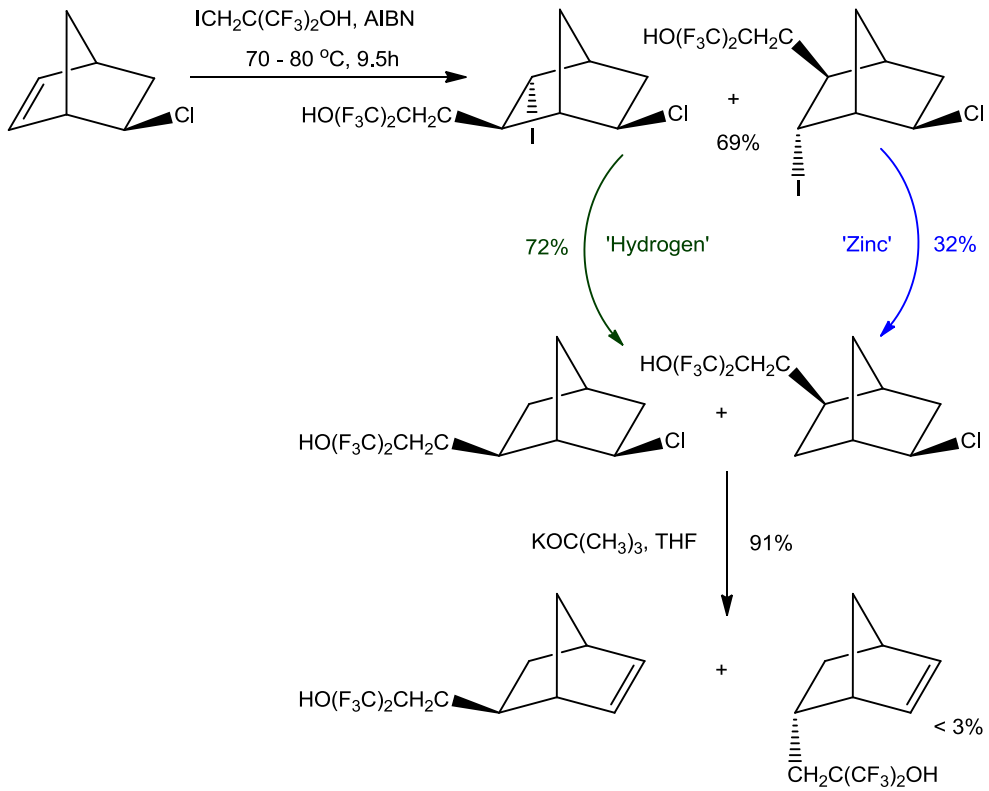

Scheme 1.18 Synthesis of an *endo*/*exo* mixture of HFANB, with *exo*:*endo* ratio of 97:3

The synthesis of similar monomers to HFANB, such as (5-norbornen-2-yl)-1,1,1,3,3,3-hexafluoro-2-propanol, which differs from HFANB only in the number of methylene units between the HFP-functionality and the norbornene skeleton was reported in a 2007 patent by Araki and co-workers.[144] The synthesis of $NBC(CF_3)_2OH$ is shown in Scheme 1.19, with the product obtained in reasonable yield as a mixture of *endo*/*exo* isomers.

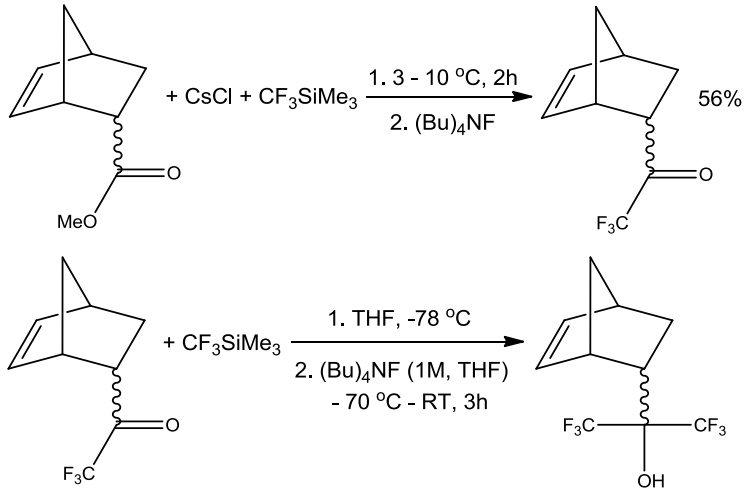

Scheme 1.19 Synthesis of *endo*-/*exo*-(5-norbornen-2-yl)-1,1,1,3,3,3-hexafluoro-2-propanol

HFANB and similar HFP-functionalised analogues were quickly recognised to be ideal candidates for use in polymeric binders for both 193 and 157 nm photolithography due to their transparency in the deep UV region and rigidity resulting from the bicyclic ring structure. Addition copolymers of HFANB and other norbornenes bearing a protected acidic group (such as ^{t}butyl esters) as a solubility switch were investigated by Grubbs and co-workers.[13] The synthesis of three examples of these copolymers which demonstrated promising lithographic performance are summarised in Scheme 1.20.

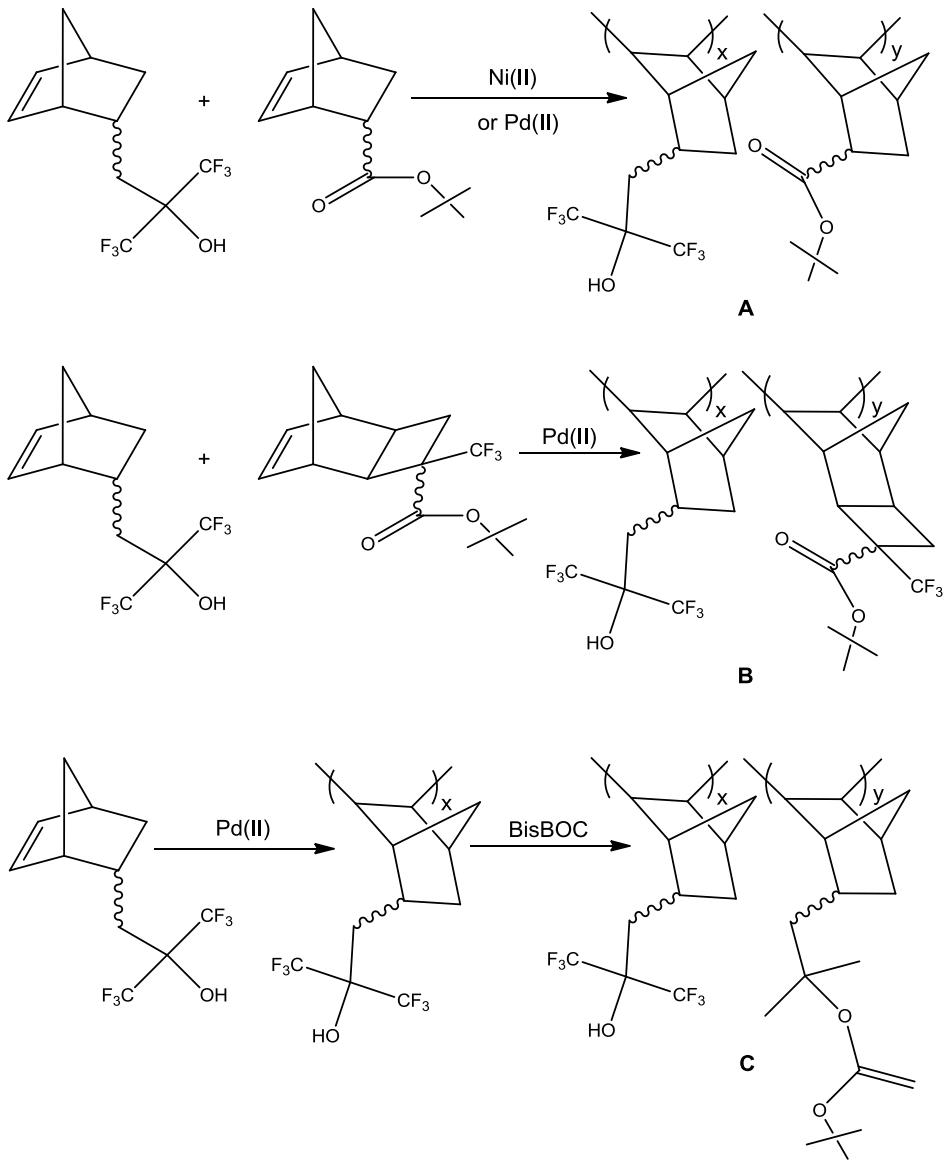

Scheme 1.20 Synthesis of HFANB-containing copolymers for use in 157 nm lithographic imaging.[13]

5.10.1 Synthesis of functionalised norbornenes using 2,2-bis(trifluoromethyl)oxirane (HFIBO)

Despite being first investigated in the 1960s and 70s, the reactivity of HFIBO had until recently, remained poorly studied.[145] A simple and practical synthesis developed by DuPont allowed production on a multigram scale, triggering a thorough investigation of reactivity.[146]

The reaction between HFIBO and alcohols provides a convenient route to the introduction of the HFP functionality, with the use of HFIBO in the synthesis of HFP functionalised norbornenes being first documented in 2003.[14] A DMF solution of *exo*-5-

norbornene-2-ol treated sequentially with excess sodium hydride and HFIBO (Scheme 1.21). Quenching with methanol, solvent removal and subsequent work up with acetic acid yields the crude product which is purified *via* Kügelrohr distillation. A 90% yield is reported.

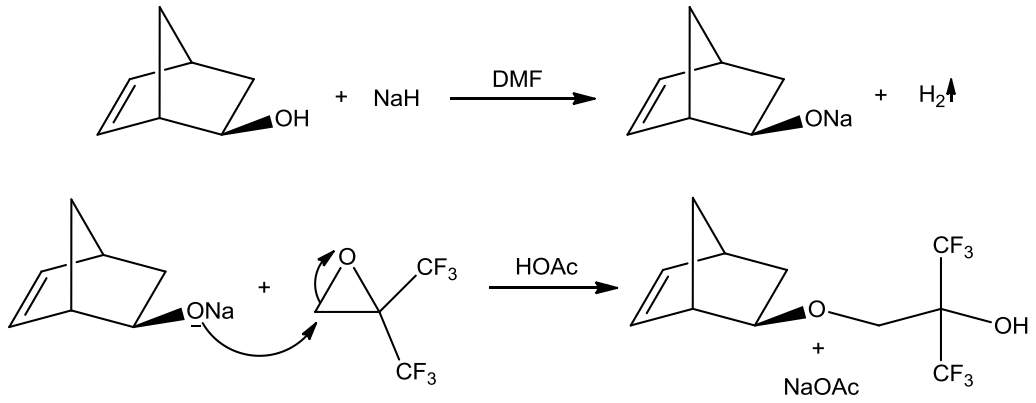

Scheme 1.21 Synthesis of *exo*-NBOCH$_2$C(CF$_3$)$_2$OH

The ease of synthesis of NBOCH$_2$C(CF$_3$)$_2$OH highlights this synthetic method as an ideal route to a spectrum of HFP-functionalised monomers using simple alcohol-functionalised norbornenes as starting materials. The resulting products are structurally very similar to HFANB and related analogues, differing only in an ether linkage in the alkyl chain connecting the HFP functionality to the norbornene skeleton (Figure 1.15). The number of methylene units, n, can be systematically varied by reaction of HFIBO with an appropriate alcohol-functionalised norbornene.

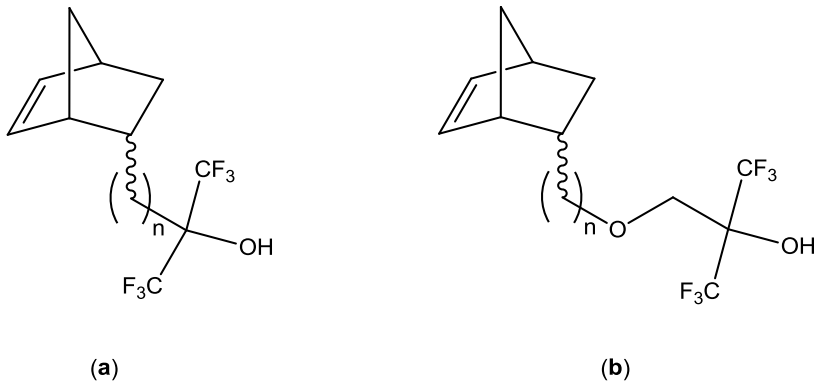

Figure 1.15 Structures of HFP-functionalised norbornenes. (**a**) HFA – type norbornenes NB(CH$_2$)$_n$C(CF$_3$)$_2$OH) and (**b**) norbornenes prepared *via* reaction of NB(CH$_2$)$_n$OH with HFIBO

1.11 The effect of *endo*/*exo* isomer content within a HFP-functionalised polynorbornene on photolithographic imaging

Ito and co-workers examined the effect of the properties of polyHFANB on photolithographic imaging.[15] The polymer demonstrated approximately linear dissolution kinetics in 0.26 M tetramethylammonium hydroxide (TMAH) developer, however complex multistage swelling and dissolution is observed in weaker developer solutions. Dissolution rate in 0.26 M developer solution was found to be independent of molecular weight,[146-147] however a complex relationship was reported in 0.19 M TMAH developer.[148]

As discussed in previous sections, the rates of incorporation of *endo* and *exo* isomers during polymerisation of a mixture have been shown to differ, resulting in a heterogeneous distribution of isomers within the polymer structure. Ito and co-workers have demonstrated that the *endo*:*exo* ratio within a polymer will influence the dissolution rate as well as the extent of hydrogen bonding between chains and interactions with a photoacid generator. [15] Polymers containing higher concentrations of the *exo* isomer exhibit less hydrogen bonding, and interact more strongly with a photoacid generator, resulting in slower dissolution kinetics. Subsequently, the *endo*:*exo* ratio has also been shown to have an effect on imaging performance with polymers with higher *exo* content producing considerably better feature definition. For this reason, control over the incorporation of *endo*:*exo* isomers is extremely important, and hence a detailed understanding of polymerisation kinetics is vital.

1.12 Introduction to the work reported in this thesis

As discussed in sections 1.7-1.11 hexafluoropropanol functionalised norbornenes are of key importance in binder resins for deep UV photolithography. The quality of the photolithographic image obtained is strongly influenced by polymer structure (due to factors such as dissolution rate and hydrogen bonding), with the ratio of *endo*/*exo* isomers within the polymer making a major contribution to imaging performance. It has been well documented that the rates of polymerisation and hence incorporation into the final polymer of *endo* and *exo* isomers differ significantly, with preferential uptake of the *exo* isomer. This difference in rate leads to a heterogeneous distribution of isomers within the polymer chain which may subsequently have a negative impact upon lithographic performance.

The rate of polymerisation of functionalised norbornenes is strongly influenced by the nature of the substituent. For alkyl-functionalised norbornenes, polymerisation rate has also been shown to be a function of alkyl chain length with a decrease in polymerisation rate observed upon increasing chain length. The polymerisation behaviour of hexafluoropropanol-functionalised norbornenes is considerably more complicated than simple alkyl systems due to the presence of heteroatoms such as oxygen and fluorine within the monomer structure. Previous studies have demonstrated that norbornenes functionalised with polar groups behave somewhat differently to simple alkyl systems, hence it is crucial to understand in detail the polymerisation behaviour specific to HFP-functionalised systems used commercially.

In this work, a series of HFP-functionalised norbornenes were prepared (Chapter II) that differ in the number of methylene groups n, separating the HFP-functional groups from the norbornene skeleton (Figure 5.10), in order to study the impact of n on polymerisation rate and the properties of the final polymers obtained. Commercially (Promerus LLC), HFP-functionalised norbornenes are polymerised using the palladium-hydride complex $[Pd(H)(MeCN)(PCy_3)_2][B(C_6F_5)_4]$, however the counter anion is extremely expensive. With a view to determination of the effects of the anion on the polymerisation process, a series of palladium hydride complexes of the type $[Pd(H)(MeCN)(PCy_3)_2][X]$ (where X is a weakly coordinating anion) were prepared.

In the study of the polymerisation behaviour of HFP-functionalised monomers, it is crucial to replicate the conditions used commercially. An in-depth study of the polymerisation process and behaviour of the initiator under commercially relevant conditions is described for a model system in Chapter III. Once the key details of the polymerisation process had been established, the behaviour of other HFP-functionalised monomers prepared in Chapter II was studied. A series of pure *endo* and *exo* isomers, differing in the number of methylene units (n), were examined (Chapter IV) in order to determine the effect of methylene spacing upon the polymerisation process. The study was further extended to mixtures of *endo*/*exo* isomers in Chapter V. Finally, the effect of the weakly coordinating anion, X, on polymerisation rate was examined with a view to developing a cheaper alternative to **Pd1388**.

1.13 References

1. C. Janiak and P.G. Lassahn, *J. Mol. Catal. A: Chem*., 2001, **166**, 193-209
2. R.R. Schrock, *Pure and Appl. Chem.,* 1994, **66**, 1447-1454
3. S.T. Nguyen, L.K. Johnson and R.H Grubbs, *J. Am. Chem. Soc.,* 1992, **114**, 3974-3975
4. C. Pariya, K.N. Jayaprakash and A. Sarkar, *Coordination Chemistry Reviews.,* 1998, **168**, 1-48
5. N.G. Gaylord, B.M. Mandal and M. Martan, *J. Polym. Sci. Polym. Lett.,* 1976, **14**, 555-559
6. N.G. Gaylord, A.B. Deshpande, B.M. Mandal and M.Martan, *J. Macromol. Sci. Chem.,* 1977, **11**, 1053-1070
7. N.G. Gaylord and A.B. Deshpande, *J. Polym. Sci. Polym. Lett.,* 1976, **14**, 613-617
8. J.P. Kennedy and H.S. Makowski, *J. Macromol. Sci. Chem.,* 1967, **1**, 345-370
9. E. Reichmanis, O. Nalamasu and F.M. Houlihan, Acc. Chem Res. 1999, **32**, 659-667
10. A.E. Feiring, V.A. Petrov and F.L. Schadt III, US 2005/00588932 A1, 2005
11. A.E. Feiring, V.A. Petrov and F.L. Schadt III, US 2005/6875555 B1, 2005
12. A.E. Feiring, J. Feldman, F.L. Schadt III, G. Newton Taylor, US 2005/6884564 B2, 2005
13. H.V. Tran, R.J. Hung, T. Chiba, S. Yamada, T. Mrozec, T-Y. Hsieh, C.R. Chambers, B.P. Osborn, B.C. Trinque, J.P. Matthew, S.A. MacDonald, C.G. Willson, D.P Sanders, E.F. Connor, R.H. Grubbs and W. Conley *Macromolecules,* 2002, **35**, 6539-6549
14. A.E. Feiring, M.K. Crawford, W.B. Farnham, J. Feldman, R.H. French, K.W. Leffew, V.A. Petrov, F.L. Schadt III, R.C. Wheland and F.C. Zumsteg, *J. Fluorine Chem.*, 2003, **122**, 11-16
15. H. Ito, H.D. Truong, L.F. Rhodes, C. Chang, L.J. Langdorf, H.A. Sidaway, K. Maeda and S. Sumida, *Journal of Photopolymer Science and Technology,* 2004, **17**, 609-620
16. C. Chang, J. Lipian, D.A. Barnes, L. Seger, C. Burns, B. Bennett, L. Bonney, L.F. Rhodes, G. M. Benedikt, R. Lattimer, S.S. Huang and V.W. Day, *Macromol. Chem. Phys.*, 2005, **206**, 1988-2000
17. F. Blank and C. Janiak, *Coord. Chem. Rev.*, 2009, **253**, 827-861

18. R. Ma, Y. Hou, J. Gao and F. Bao, *J. Macromol. Sci., C: Polym. Rev.* 2009, **49**, 249-287

19. J. Clayden, N. Greeves, S. Warren and P. Wothers, *Organic Chemistry*, Oxford University Press, Oxford, 2001, p. 912

20. A.T. Cooper, Ph.D Thesis, Durham University, 2008

21. A. Bell, B. Knapp, D. Jablonski, D. Fabricius, and P.W. Newsome, US2010/7662996, 2010

22. S.J. Cristol, T.C. Morrill and R.A. Sanchez, *J. Org. Chem*, 1966, **31**, 2719-2725

23. J. Melia, E. Connor, S. Rush, S. Breunig, C. Mehler and W. Risse, *Makromol. Chem. Macrol. Symp.* 1995, **89**, 433-442

24. S. Breunig and W. Risse, *Makromol. Chem.*, 1992, **193**, 2915-2927

25. B.S. Heinz, F.P. Alt and W. Heitz, *Macromol. Rapid Commun.*, 1998, **19**, 251-256

26. A. Reinmuth, J.P. Mathew, J. Melina and W. Risse, *Macromol. Rapid. Commun.*, 1996, **17**, 173-180

27. J.P. Mathew, A. Reinmuth, W. Risse, W. Melia and N. Swords, *Macromolecules*, 1996, **29**, 2755-2763

28. A.D. Hennis, J.D. Polley, G.S. Long, A. Sen, D. Yandulov, J. Lipian, G.M. Benedikt, L.F. Rhodes and J. Huffman, *Organometallics*, 2001, **20**, 2802-2812

29. J.K. Funk, C.E. Andes and A. Sen, *Organometallics*, 2004, **23**, 1680-1683

30. M. Kang and A. Sen, *Organometallics*, 2004, **23**, 5396-5398

31. A. Sen, *Acc. Chem. Res.* 1993, **26**, 303-310

32. B.A. Markies, D. Kruis, M.H.P. Rietveld, K.A.N. Verkerk, J. Boersma, H. Kooijman, T.M. Lakin, A.L. Spek and G. van Koten, *J. Am. Chem. Soc.* 1995, **117**, 5263-5274

33. R. van Asselt, E.E.C.G. Gielens, R.E. Rülke, K. Vrieze and C.J. Elsevier, *J. Am. Chem. Soc.* 1994, **116**, 977-985

34. M. Zocchi and G. Tieghi, *J. Chem. Soc., Dalton Trans.*, 1979, 944-947

35. N. Carr, D.J. Dunne, A.G. Orpen and J.L. Spencer, *J. Chem. Soc., Chem. Commun.*, 1988, 926-928

36. J.G.P. Delis, P.B. Aubel, D. Vrieze, P.W.N.M. van Leeuwen, N. Veldman and A.L. Spek, *Organometallics*, 1997, **16**, 4150-4160

37. G. Sartori, F.C. Ciampelli and N. Cameli, *Chim. Ind. (Milan)*, 1963, **45**, 1478-1482

38. T. Tsujino, T. Saegusa and J. Furukawa, *Makromol. Chem.*, 1965, **85**, 71-79

39. N. Seehof, C. Mehler, S.Breunig and W Risse, *J. Mol. Catal*., 1992, 76, 219-228
40. B.L. Goodall, L.H. McIntosh III and L.F. Rhodes, *Macromol. Chem. Macromol. Symp.*, 1995, **89**, 421-432
41. T. Saegusa, T. Tsujino and J. Furukawa, *Makromol. Chem.*, 1964, **78**, 231-133
42. W. Kaminsky, A Bark and M. Arndt, *Makromol. Chem. Macromol. Symp.*,1991, **47**, 83-93
43. W. Kaminsky and A. Noll, *Polym. Bull.*, 1993, **31**, 175-182
44. H. Herfert, P. Montag and G Fink, *Makromol. Chem.*, 1993, **194**, 3167-3182
45. H.G. Alt and A. Köppl, *Chem. Rev.*, 2000, **100**, 1205-1221
46. L. Resconi, L. Cavallo, A. Fait and F. Piemontesi, *Chem. Rev.*, 2000, **100**, 1253-1345
47. M. Bochmann, *J. Organomet. Chem*., **2004**, ***689***, 3982-3998
48. C. Janiak, K.C.H. Lage, U Versteeg, D. Lentz and P.H.M. Budzelaar, *Chem Ber.*, 1996, **129**, 1517-1529
49. R.J. Minchak and J.T. Ware, Patent EP0291970, 1988, B.F. Goodrich Co. (US)
50. U. Peuckert and W. Heitz, *Macromol. Chem. Phys.*, 1998, **199**, 1951-1956
51. F.P. Alt and W. Heitz, *Acta Polym.*, 1998, **49**, 477-481
52. F.P. Alt and W. Heitz, *Macromol. Chem. Phys.*, 1998, **199**, 1951-1956
53. F. Peruch, H. Cramail and A. Deffieux, *Macromol. Chem. Phys.*, 1998, **199**, 2221-2227
54. M. Arndt and M. Grosmann, *Polym. Bull.*, 1998, **41**, 433-440
55. F. Pelascini, F. Peruch, P.J. Lutz, M. Wesolek and J. Kress, *Macromol. Rapid. Commun*,. 2003, **24**, 768-771
56. Y. Sato, Y. Nakayama and H. Yasuda, *J. Organometal. Chem.*, 2004, **689**, 744-750
57. J. Chen, Y. Huang, Z. Lei, Z. Zhang, C. Wei, T. Lan and W. Zhang, *J. Mol. Catal. A: Chem.*, 2006, **259**, 133-141
58. Y.X. Chen and T.J. Marks, *Chem. Rev.*, 2000, **100**, 1391-1434
59. N. Thirupathi, D. Amoroso, A. Bell and J.D. Protasiewicz, *J. Polym. Sci. A: Polym. Chem.* 2009, **47**, 103-110
60. A. Bell, D. Amoroso, J.D. Protasiewicz and N. Thirupathi, US 2005/0187398, 2005
61. R.G. Schultz, *Polym. Lett.*, 1966, **4**, 541-546
62. J.E. Mckeon and P.S. Starcher; Patent US 3330815, 1967 Union Carbide Corp.

63. C. Taniélian, A Kiennemann and T. Osparpucu, *Can. J. Chem.*, 1979, **57**, 2022-2027

64. A Sen and T.W. Lai, *J. Am. Chem. Soc*., 1981, **103**, 4627-4629

65. A Sen and T.W. Lai, *Organometallics*, 1982, **1**, 415-417

66. A Sen, T.W. Lai and R.R. Thomas, *J. Organomet. Chem.*, 1988, **358**, 567-588

67. Y. Yano, M.T. Fairhurst and T.W. Swaddle, *Inorg. Chem.*, 1980, **19**, 3267-3270

68. F.K. Mayer, K.E. Newman and A.E. Merbach, *Inorg. Chem.*, 1979, **18**, 2142-2148

69. K.E. Newman, F.K. Mayer and A.E. Merbach, *J. Am. Chem. Soc.*, 1979, **101**, 1470-1476

70. C. Mehler and W. Risse, *Makromol. Chem., Rapid Commun.*, 1991, **12**, 255-259

71. C. Mehler and W. Risse, *Makromol. Chem., Rapid Commun,*. 1992, **13**, 455-459

72. P.W. Atkins, C.H. Langford, and D.F. Shriver, *Inorganic Chemistry*, 2nd edtn., Oxford University Press, Oxford, 1993, p. 213

73. T.F.A. Haselwander, W. Heitz, S.A. Krügel and J.H. Wendorff, *Macromol. Chem. Phys.*, 1996, **197**, 3435-3453

74. T.F.A. Haselwander, W. Heitz and M. Maskos, *Macromol. Rapid. Commun,*. 1997, **118**, 689-697

75. A. L. Safir and B.M. Novak, *Macromolecules*, 1995, **28**, 5396-5398

76. B.M. Novak and A. L. Safir, *Polym. Prepr*., 1996, **37**, 335-336

77. A. L. Safir and B.M. Novak, *Polymer Prepr. (Am. Chem. Soc., Div. Polym. Chem.)*, 1995, **36**, 227-228

78. F. Hojabri, M.M. Mohaddes and A. Talab, *Polymer*, 1976, **17**, 710-712

79. B.L. Goodall, G.M. Benedikt, L.H. McIntosh III and D.A. Barnes U.S.A. 5,468,819, 1995, B.F. Goodrich

80. S. Heinz, W. Heitz, S.A. Krügel, F. Raubacher and J.H. Wendorff, *Acta Polym.*, 1997, **48**, 385-391

81. M.R. Colsman, T.D. Newbound, L.J. Marshall, M.D. Noirot, M.M. Miller, G.P. Wulfsberg, J.S. Frye, O.P. Anderson and S.H. Strauss, *J. Am. Chem. Soc.*, 1990, **112**, 2349-2362

82. G.M. DiRenzo, P.S. White and M. Brookhart, *J. Am. Chem. Soc.*, 1996, **118**, 6225-623

83. Y. Tatsuno and T. Yoshida, *Inorganic Synthesis*, D.F. Shriver (Ed.), John Wiley and Sons, New York, 1979, p 220

84. J. Powell and B.L Shaw, *Inorg. Phys. Theor*, 1967, 1839

85. J. Lipian, R.A. Mimna, J.C. Fondran, D. Yandulov, R.A. Shick, B.L. Goodall and L.F. Rhodes, *Organometallics*, 2002, **35**, 8969-8977

86. R.H. Crabtree '*The Organometallic Chemistry of the Transition Metals*' Wiley-Interscience, New York, 1988, p 71

87. C.A. Tolman, *Chem Rev.*, 1977, **3**, 313-347

88. N. Thirupathi, D. Amoroso, A. Bell and J.D. Protasiewicz, *Organometallics*, 2005, **24**, 4099-4102

89. V.S. Tkach, D.S. Suslov, G. Myagmarsuren, G.V. Ratovskii, A.V. Rohin, T. Felix and F.K. Shmidt, *J. Organometal. Chem.*, 2008, **693**, 2069-2073

90. M. Sommovigo, M. Pasquali, P. Leoni, P. Sabatio and D. Braga, *J. Organometal. Chem.*, 1991, **418**, 119-126

91. P. Leoni, M. Sommovigo, M. Pasquali, S. Midollini and D. Braga; P. Sabatio, *Organometallics*, 1991, **10**, 1038-1044

92. A.B. Goel and S.A. Goel, *Inorganica Chimica Acta*, 1980, **45**, L85-L86

93. D. Nguyen, G. Laurenczy, M. Urrutigoïty and P. Kalck, *Eur. J. Inorg. Chem.*, 2005, 4215-4225

94. M. Yamashita, I. Takamiya, K. Jin and K. Nozaki, *Organometallics*, 2006, **25**, 4588-4595

95. S.R. Foley, H. Shen, U.A. Qadeer and R.F. Jordan, *Organometallics*, 2004, **23**, 600-609

96. T.J. Deming and B.M. Novak, *Macromolecules*, 1993, **26**, 7089-7091

97. W. Massa, N. Faza, H.-C. Cang, C. Focke and W. Heitz, *Acta. Polym.*, 1997, **48**, 385-391

98. C. Mast, M. Krieger, K. Dehnicke and A. Greiner, *Macromol. Rapid. Commun.*, 1999, **20**, 232-235

99. S. Borkar and P.K. Saxena, *Polym. Bull.*, 2000, **44**, 167-172

100. T.R. Younkin, E.F. Connor, J.I. Henderson, S.K. Friedrich, R.H. Grubbs and D.A. Bansleben, *Science*, 2000, **287**, 460-462

101. G.M. Benedikt, E. Elce, B.L. Goodall, H.A. Kalamarides, L.H. McIntosh III, L.F. Rhodes, K.T. Selvy, C.E. Andes, K. Oyler and A. Sen, *Macromolecues*, 2002, **35**, 8978-8988

102. C. Shikada, S. Kaita, Y. Maruyama, M. Takei and Y. Wakatsuki, *Macromol. Rapid, Commun.*, 2008, **29**, 219-223

103. F. He, Y. Chen, X. He, M. Chen, W. Zhou and Q. Wu, *J. Polym. Sci A: Polym. Chem.*, 2009, **47**, 3990-4000

[104] J. Berding, M. Lutz, A.L. Spek and E. Bouwman, *Appl. Organometal. Chem.*, 2011, **25**, 76-81

[105] P.G. Lassahn, V. Lozan, B. Wu, A.S. Weller and C. Janiak, *Dalton. Trans.*, 2003, 4437-4450

[106] T. Hu, Y.G. Li, Y.S. Li and N.H. Hu, *J. Mol. Catal. A: Chem.*, 2006, **253**, 155-164

[107] A. S. Abu-Surrah, U. Thewalt and B. Rieger, *J. Organometal. Chem.*, 1999, **587**, 58-66

[108] G. Siedle, P.G. Lassahn, V. Lozan, C. Janiak and B. Kersting, *Dalton Trans.*, 2007, 52-61

[109] H. Morishita, A. Sudo and T. Endo, *J. Polym. Sci A: Polym. Chem.*, 2009, **47**, 3982-3989

[110] D.A. Barnes, G.M. Benedikt, B.L. Goodall, S.H. Huang, H.A. Kalamarides, S. Lenhard, L.H. McIntosh III, K.T. Selvy, R.A. Shick and L.F. Rhodes, *Macromolecules*, 2003, **36**, 2623-2632

[111] C. Mehler and W. Risse, *Macromolecules*, 1992, **25**, 4226-4228

[112] J. McDermott, C. Chang, L.F. Martin, L.F. Rhodes, G.M Benedikt and R.P. Lattimer, *Macromolecules*, 2008, **41**, 2984-2986

[113] M.D. Walter, R.A. Moorhouse, S.A. Urbin, P.S. White and M. Brookhart, *J. Am. Chem. Soc.*, 2009, **131**, 9055-9069

[114] M.D. Walter, R.A. Moorhouse, P.S. White and M. Brookhart, *J. Polym. Sci. A: Polym. Chem.*, **47**, 2009, 2560-2573

[115] I. Takamiya, M. Yamashita and K. Nozaki, *Organometallics*, 2008, **27**, 5347-5352

[116] N. Koga, T. Ozawa and K. Morokuma, *J. Phys. Org. Chem.*, 1990, **3**, 519-533

[117] K.H. Kim, Y.K. Han, S. U. Lee, S.H. Chun and J. H. Ok, *J. Mol. Model.*, 2003, **9**, 304-307

[118] K. Damodaran, N.R. Dhumal and R.T. Mathers, *J. Mol. Struct:Theorochem*, 2008, **867**, 5-9

[119] B. Liu, Y. Li, B.G. Shin, D. Yeung Yoon, I. Kim, L. Zhang, W. Yan . *J. Polym. Sci. A: Polym. Chem.* 2007, 3391-3399

[120] C.S. Li, D.C. Jou and C.H. Cheng, *Organometallics*, 1993, **12**, 3945-3954

[121] R.P Hughes and J. Powell, *J. Organomet. Chem.* 1973, **60**, 427-441

[122] K. Müller, Y. Jung, D.Y. Yoon, S. Agarwal and A. Greiner, *Macromol. Chem Phys.* 2010, **221**, 1595-1601

123. H. Ito, N. Seehof, R. Sato, T. Nakayama and M. Ueda, *ACS Symp. Ser.,* 1998, **706**, 208-223

124. H. Ito, G. Wallraff, N. Fender, P.J. Brock, C.E. Larson, H.D. Truong, G. Breyta, D. C. Miller, M.H. Sherwood and R.D. Allen, *J. Photopolym. Sci. Technol.,* 2001, **14**, 583-593

125. M. Padmanaban, E. Almey, J.B.Bae, W.K. Kim, T. Kudo, S. Masuda, D. Rahman, R. Sakamuri, R. Dammel, J.C. Jung, S.K. Lee and K.S. Shin, *J. Photopolym. Sci. Technol*, 2001, **14**, 631-642

126. H. Ito, H.D. Truong, M. Okazaki, D. C. Miller, N. Fender, P.J. Brock, G.M. Wallraff, C.E. Lawson and R.D. Allen, *J. Photopolym. Sci. Technol*, 2002, **15**, 591-602

127. M. Toriumi, T. Ishikawa, T. Kodani, M. Koh, T. Moriya, T.. Araki, H. Aoyame, T. Yamashita, T. Yamazaki, T. Furukawa and T. Itani, *J. Photopolym. Sci. Technol*, 2003, **16**, 607-613

128. T. Chiba, R.J. Hung, S. Yamada, B. Trinque, M. Yamachika, C. Brodsky, K. Patterson, A. Van der Heyden, A. Jamison, S.H. Lin, M. Somervell, J. Bayers, W. Canley and C.G. Willson, *J. Photopolym. Sci. Technol*, 2000, **13**, 657-664

129. R.R. Dammel, R. Sakamuri, T. Kudo, A. Romano, L. Rhodes, R. Vicari, C. Hawker, W. Conley and D. Miller, *J. Photopolym. Sci. Technol*, 2001, **14**, 603-611

130. H.V. Tran, R.J. Hung, T. Chiba, S. Yamada, T. Mrozec, T-Y. Hsieh, C.R. Chambers, B.P. Osborn, B.C. Trinque, M.J. Pinnow, D.P. Sanders, E.F. Connor, R.H. Grubbs, W. Conley S.A. MacDonald and C.G. Willson, *J. Photopolym. Sci. Technol*, 2001, **14**, 669-674

131. F. Houliham, A. Romano, D. Rentkiewicz, R. Sakamuri, R. R. Dammel, W. Conley, G. Rich, D. Miller, L. Rhodes, J. McDaniel and C. Chang, *J. Photopolym. Sci. Technol*, 2003, **16**, 581-590

132. L.F. Thompson, C.G. Willson and M.J. Bowden, *Introduction to Microlithography*, 2nd Edition, American Chemical Society, Washington, D.C., 1994, p212

133. H. Ito, C.G Willson and J.M.J. Frechet, US 1985/4,491628, 1985

134. H. Gokan, S. Esho and Y. Ohnishi, *J. Electrochem. Soc*., 1983, **130**, 143-146

135. B.L. Goodall, S. Jayaraman, R.A. Shick and L.F. Rhodes, US2000/6136499, 2000

136. U. Okoroanyanwu, T. Shimokawa, J. Byres and C.G. Willson, *Chem. Mater.*, 1998, **10**, 3319-3327

137. U. Okoroanyanwu, T. Shimokawa, J. Byres and C.G. Willson, *J. Mol. Catal. A: Chem*, 1998, **133**, 93-114

138. T. Wallow, P. Brock, R. DiPietro, R. Allen, J. Opitz, R. Sooriyakamaran, D. Hofer, J. Byres, G. Rich, M. McCallum, S. Schuetze, S. Jayaraman, K. Hullihen, R. Vicari, L.F. Rhodes, B.L. Goodall and R.A. Shick, Proc. *SPIE-Int. Soc. Opt. Eng.*, 1998, **3333**, 92-101

139. P.R. Varanasi, J. Maniscalo, A.M. Mewherter, M.C. Lawson, G. Jordhamo, R.D. Allen, J. Opitz, H. Ito, T.I. Wallow, D. Hofer, L. Langsdorf, S. Jayaraman and R. Vicari, *SPIE-Int. Soc. Opt. Eng.*, 1999, **3678**, 51-63

140. P.R. Varanasi, A.M. Mewherter, M. C. Lawson, G. Jordhamo, R.D. Allen, J. Opitz, H. Ito, T.I. Wallow and D. Hofer, *J. Photopolym. Sci. Technol.*, 1999, **12**, 493-500

141. V.A. Petrov, *Synthesis*, 2002, **15**, 2225-2231

142. H. Ito, P.J. Brock and G. M. Wallraff, 2002/01024901/A1, 2002

143. T. Akari, T. Ishikawa, T. Kume and A. Yamamoto, 2007/71867731/B2, 2007

144. T. Katagiri and K. Uneyama, *J. Fluorine Chem.*, 2000, 105, 285-293

145. V.A. Petrov, A.E. Feiring and J. Feldmann, WO00/66575, PCT/US/00/11746, 2000

146. H. Ito, W.D. Hinsberg, L.F. Rhodes and C. Chang, *Proc. SPIE*, 2003, **5039**, 70-79

147. H. Ito, H.D. Truong, M. Okazaki and R.A. DiPietro, *J. Photopolym. Sci. Technol.*, 2003, **16**, 523-536

148. T. Hoskins, W.J. Chung, P.J. Ludovice, C.L. Henderson, L.D. Seger, L.F. Rhodes and R.A. Shick, *Proc. SPIE*, 2003, **5039**, 600-611

Chapter II

Preparation of hexafluoropropanol-functionalised norbornene monomers and palladium hydride initiators

Chapter II

Preparation of hexafluoropropanol-functionalised norbornene monomers and palladium hydride initiators

2.1. Introduction

Polynorbornenes bearing the hexafluoropropanol (HFP) functionality provide a key component in binder resin formulations for use in deep UV photolithography, making them of significant commercial interest.[1-3] The majority of research to date has focused on the vinyl polymerisation of three specific HFP-functionalised norbornene (NB) monomers, $NBCH_2C(CF_3)_2OH$ (HFANB) and $NB(CH_2)_nOCH_2C(CF_3)_2OH$ (where n = 0-1).[1-7] The polymerisation of such monomers has been shown to be initiated using a multitude of group X transition metal-based complexes. However, this thesis will focus on polymerisations using the cationic palladium hydride complex $[Pd(H)(MeCN)(PCy_3)_2][B(C_6F_5)_4]$ (**Pd1388**) developed by Promerus.[8-9]

In this chapter, the synthesis of a series of HFP-monomers of the type $NB(CH_2)_nC(CF_3)_2OH$ (Figure 2.1, **a**) and $NB(CH_2)_nOCH_2C(CF_3)_2OH$ (Figure 2.1, **b**) will be described with a view to sequentially conducting detailed studies on their polymerisation behaviour using **Pd1388**. In addition to the synthesis of HFP-functionalised monomers, the synthesis of palladium hydride pro-initiators will also be discussed.

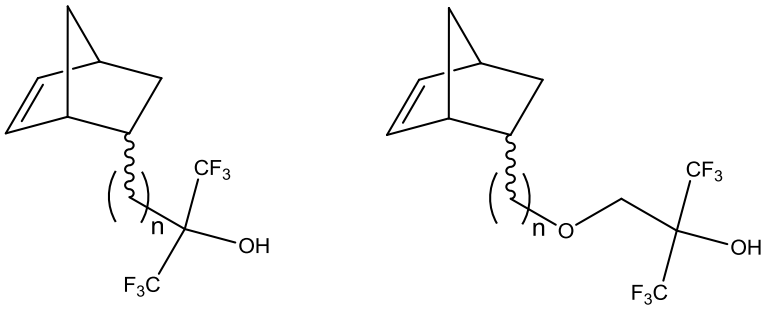

Figure 2.1 Generic structures of hexafluoropropanol-functionalised norbornene monomers. $NB(CH_2)_nC(CF_3)_2OH$ (**a**) and $NB(CH_2)_nOCH_2C(CF_3)_2OH$ (**b**)

2.2 Results and Discussion

2.2.1 Synthesis of $NBOCH_2C(CF_3)_2OH$ monomers (n = 0)

The synthesis of $NBOCH_2C(CF_3)_2OH$ monomers relies on the preparation of the alcohol starting material, 5-norbornene-2-ol (NBOH) and subsequent reaction with 2,2-bis(trifluoromethyl)oxirane (HFIBO).[10] NBOH may be purchased commercially from Sigma Aldrich as a mixture of *endo*/*exo* isomers (ratio 74:26 by ^1H NMR spectroscopy) or synthesised as pure isomeric materials according to literature procedures.[11-13]

2.2.1.1 Synthesis of *endo-/exo*-$NBOCH_2C(CF_3)_2OH$ (ZXN2)

The synthesis of *endo/exo*-$NBOCH_2C(CF_3)_2OH$ (**ZXN2**) was carried out using a modified version of the method reported in the literature.[1-3] A THF solution of *endo/exo*-NBOH (**ZXN1**) was treated sequentially with NaH and HFIBO (Scheme 2.1). Following work-up and distillation, **ZXN2** was isolated in 51% yield along with **ZXN1** starting material (20%). The two compounds were separated chromatographically to yield **ZXN2** (10% overall yield) as a colourless oil (70:30 *endo*:*exo*).

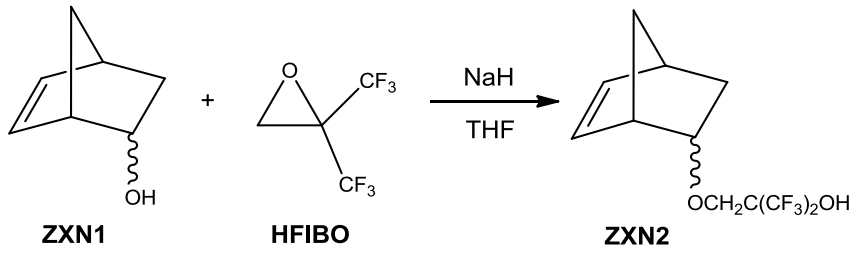

Scheme 2.1 Synthesis of *endo-/exo*-$NBOCH_2C(CF_3)_2OH$ (**ZXN2**)

2.2.1.2 Synthesis of *exo*-$NBOCH_2C(CF_3)_2OH$ (ZX3)

The synthesis of **ZX3** first requires isolation of the alcohol starting material *exo*-NBOH **(ZX2).** Several synthetic routes to *exo*-NBOH (**ZX2**) have been documented in the literature dating back to the 1960s. These include chromatographic separation of a mixture of *endo/exo* NBOH isomers, hydroboration of norbornadiene with sodium borohydride, oxymercuration of norbornadiene and reaction of norbornadiene with acetic acid to form the norbornene acetate (NBOAc, **ZX1**) followed by saponification.[11, 12] This latter approach is unusual in that formation of NBOAc occurs with *exo*:*endo* selectivity of 98:2 in the absence of a catalyst.[12] Saponification of **ZX1** was selected as the method of choice for this study due to the ready availability of the **ZX1** starting

material (Promerus). Reaction of **ZX1** with aqueous sodium hydroxide followed by subsequent work-up and recrystallisation yields **ZX2** as a white solid (85%), which was obtained with retention of *exo*:*endo* ratio (98:2) (Scheme 2.2).

Sequential treatment of a THF solution of **ZX2** with NaH and HFIBO followed by distillation yields a crude mixture of **ZX3** (51%) and residual **ZX2** starting material (20%) as a yellow oil. Separation of the two compounds is achieved using column chromatography giving **ZX3** (*exo*:*endo* ratio 98:2) as a colourless oil, however the isolated yield of the pure product was extremely low (3%). The majority of the **ZX3** product proved to be inseparable from **ZX2** starting material using either distillation or column chromatography.

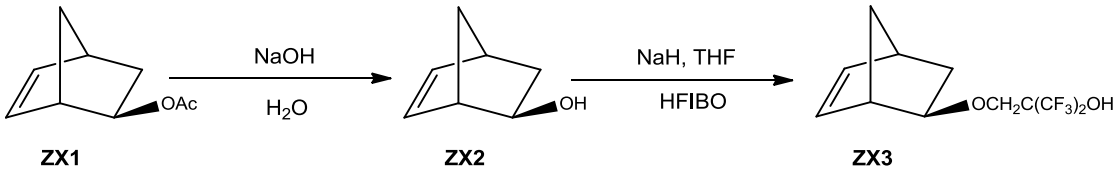

Scheme 2.2 Synthesis of *exo*-NBOCH$_2$C(CF$_3$)$_2$OH (**ZX3**)

2.2.1.3 Attempted synthesis of *endo*-NBOCH$_2$C(CF$_3$)$_2$OH (ZN2)

The synthesis of **ZN2** first requires isolation of the starting alcohol *endo*-NBOH **(ZN1)** (Scheme 2.3). Synthetic routes for the synthesis of **ZN2** that have been documented in the literature include chromatographic separation of an isomeric mixture of NBOH, (**ZXN1**) and reduction of 5-norbornene-2-one (**ZNO**) using sodium borohydride.[13] The latter approach was selected as the method of choice for this study as it is more suitable for preparation of **ZN1** on a multigram scale.

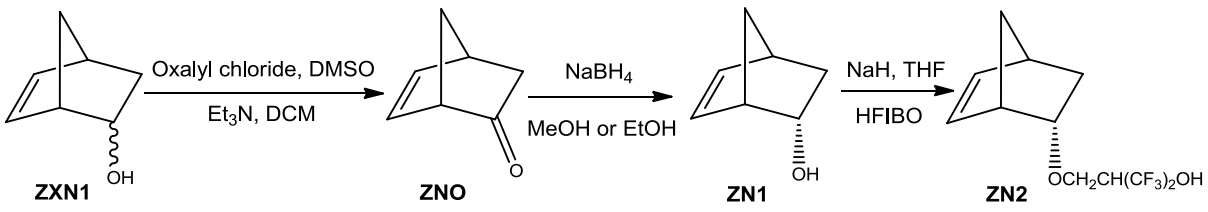

Scheme 2.3 Synthetic route to *endo*-NBOCH$_2$C(CF$_3$)$_2$OH (**ZN2**)

2.2.1.4 Synthesis of 5-norbornene-2-one (ZNO)

Several routes are documented in the literature for the synthesis of 5-norbornene-2-one (**ZNO**). These include Diels-Alder reaction between 2-chloroacrylonitrile and cyclopentadiene to form 2-chloro-2-cycanonorbornene followed by treatment with DMSO and potassium hydroxide, oxidation of *exo*-NBOH (**ZX1**) using CrO_3 and Swerne oxidation of *endo/exo*-NBOH (**ZXN1**).[11,14,15] In this current work Swerne oxidation was selected as the method of choice since this latter approach avoids the use of toxic metals such as chromium(VI) and can be performed under mild conditions. However, a drawback is formation of the malodorous side product dimethyl sulphide (DMS).

A proposed mechanism for the formation of **ZNO** from Swerne oxidation of **ZXN1** is given in Scheme 2.4.[16] The oxidation proceeds *via* reaction of DMSO with oxalyl chloride to generate the dimethylchlorosulphonium salt *in situ.* Subsequent reaction with the alcohol **ZXN1** at -78 ºC leads to an alkoxysulphonium salt. Deprotonation of this intermediate gives a sulphur ylide, which undergoes intramolecular deprotonation *via* a five-membered ring transition state and fragmentation to yield the ketone product and DMS. Low temperatures are required to prevent the possible formation of thioacetals (Scheme 2.5)

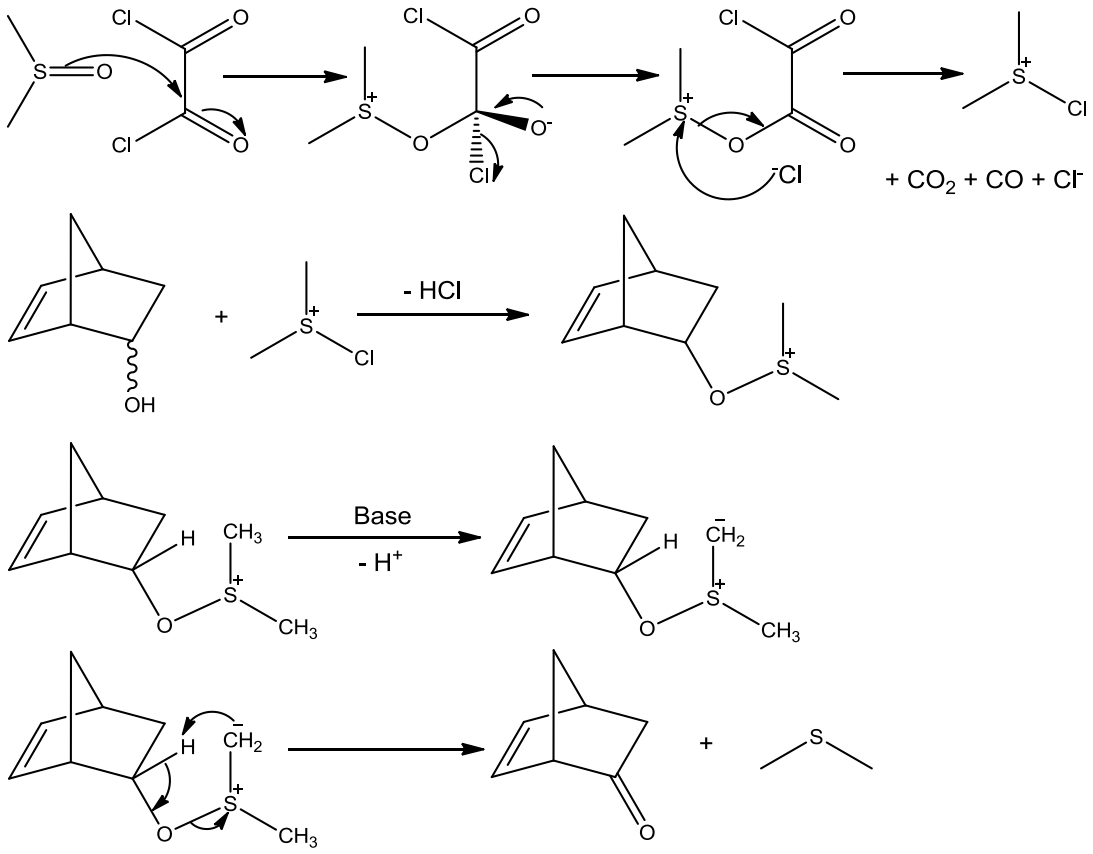

Scheme 2.4 Mechanism for the Swerne oxidation of *endo/exo*-NBOH (**ZXN1**) to 5-norbornene-2-one (**ZNO**)

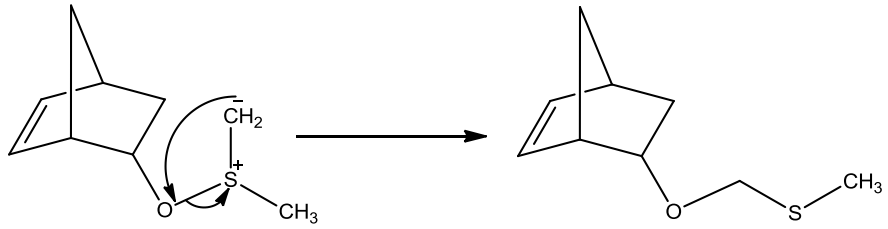

Scheme 2.5 Rearrangement of the dimethylchlorosulphonium salt to yield a thioacetal at temperatures above -78 °C

A solution of **ZXN1** in DCM was treated with oxalyl chloride and dimethylsulphoxide, followed by triethylamine. Subsequent work-up and distillation yields a mixture of **ZNO** (88%) and residual DMSO (7%), which are extremely difficult to separate. Vigorous drying of all starting materials prior to use was essential as the yield drops to 39% in the absence of the drying process. Separation of **ZNO** and DMSO is possible chromatographically, however it proves to be extremely time consuming and the purification process results in a substantial loss of material.

2.2.1.5 Reduction of 5-norbornene-2-one (ZNO)

Previous reports suggest that reduction of **ZNO** using sodium borohydride in methanol generates *endo*-NBOH in good yield (61%) with *endo:exo* selectivity of 99:1.[14,17] This process was attempted with both pure **ZNO** and samples containing residual DMSO. However, in both cases it was found to be difficult to drive the reaction to completion and subsequently isolate the **ZN1** product from the methanol solvent, giving rise to an extremely low yield (3%). To counter this, the reaction solvent was changed to ethanol which gave marginally improved results in terms of conversion, however the isolated yields were still found to be extremely low (4%). The main problem in each case was removal of the alcohol solvent as the majority of the product was found to co-distil during both solvent evaporation on a rotary evaporator or during fractional distillation at ambient pressure using a Vigreux column. Small amounts of **ZN1** were eventually obtained and purified using sublimation, however the majority of the material was not easily purified in this manner. The ratio of *endo*:*exo* isomers in the sublimed material was >99:1.

2.2.1.6 Attempted synthesis of *endo*-NBOCH$_2$C(CF$_3$)$_2$OH (ZN2)

The synthesis of *endo*-NBOCH$_2$C(CF$_3$)$_2$OH (**ZN3**) was attempted on a small scale (0.8 g of **ZN2** starting material). A THF solution of **ZN2** was treated sequentially with NaH and HFIBO followed by work up and distillation. Multinuclear NMR spectroscopic analysis confirmed the presence of the desired **ZN3** product, however the pure product could not be obtained, despite attempts to isolate pure **ZN3** chromatographically.

2.2.2 Synthesis of NB(CH$_2$)$_2$OCH$_2$C(CF$_3$)$_2$OH monomers (n=2)

Diels-Alder reaction between cyclopentadiene and a dienophile results in a mixture of *endo* and *exo* norbornene isomers, with the *endo:exo* ratio being dependent upon variables such as the nature of the dienophile and reaction temperature. A problematic side reaction in the Diels-Alder synthesis of norbornenes is the formation of cyclopentadiene trimer (CP trimer), generated *via* reaction of cyclopentadiene (CP) with dicyclopentadiene (DCPD) (Scheme 2.6). This poses a significant problem in the synthesis of functionalised norbornenes as the trimer has a boiling point that is often very similar to that of the desired product, making the two very difficult to separate. This issue can be avoided, however, by carrying out the Diels-Alder synthesis in the presence of a large excess of the dienophile.

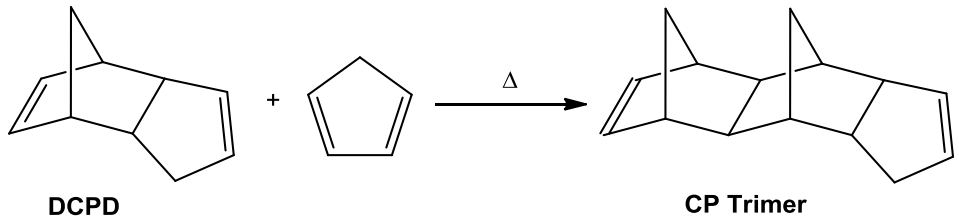

Scheme 2.6 Reaction between cyclopentadiene and dicyclopentadiene to form CP trimer

Diels-Alder reaction between cyclopentadiene and 3-butenol was used to prepare *endo/exo*-NB$(CH_2)_2$OH (**DXN1**) (Scheme 2.7). The synthesis of **DXN1** was first attempted on a small scale in a sealed Carius tube. An eight times molar excess of 3-butenol was reacted with high purity dicyclopentadiene (>99%) at 220 ºC for 6 hours. Subsequently **DXN1** was isolated *via* distillation as a colourless oil (72%). Scale up of the reaction was achieved using a 0.5 L stainless steel autoclave, fitted with a rocking mechanism. **DXN1** was isolated in reasonable yield (62%) with the ratio of *endo*:*exo* isomers determined to be 79:21 by ^{1}H NMR spectroscopic and GCMS analyses. The reaction was scaled further using a 2 L stainless steel autoclave. **DXN1** was isolated as a 70:30 mixture of *endo*:*exo* isomers (^{1}H NMR spectroscopic and GCMS analyses), however the yield on this scale was lower (36%).

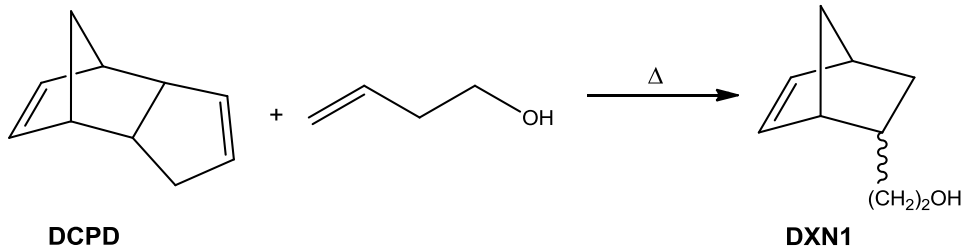

Scheme 2.7 Diels-Alder synthesis of *endo-/exo* –NB$(CH_2)_2$OH (**DXN1**)

2.2.2.1 Synthesis of *endo-/exo*-NB$(CH_2)_2OCH_2C(CF_3)_2$OH (DXN2)

A THF solution of **DXN1** was treated sequentially with NaH and HFIBO (Scheme 2.8). Following work-up and distillation, a colourless oil was obtained in moderate yield (38%), which was found to be a crude solution containing **DXN2**. Treatment of the oil with sodium hydroxide, subsequent recrystallisation of the solid obtained from heptane, acidic work-up and distillation gave pure **DXN2** as a colourless oil, however the yield of the pure product was very low (3%). The ratio of *endo*:*exo* isomers was determined

to be 68:32 by ^{1}H NMR spectroscopic and GCMS analyses. Attempts were made to isolate further material from the heptane recrystallisation liquor, however these proved to be of lower purity than the original batch and so were discarded.

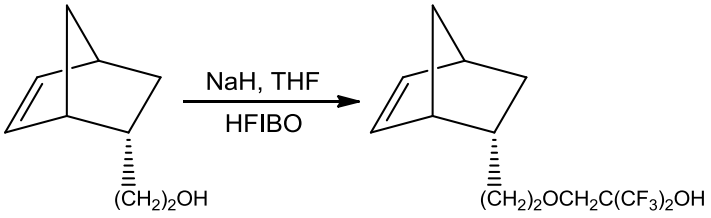

DXN1 **DXN2**

Scheme 2.8 Synthesis of *endo-/exo*-NB$(CH_2)_2OCH_2C(CF_3)_2OH$ (**DXN2**)

2.2.2.2 Iodolactonisation as a technique to separate *endo*- and *exo*-functionalised norbornene monomers

The synthesis of lactones, iodolactones and iodoethers from norbornene carboxylic acids and alcohols dates back to the 1950s and has been studied in detail. Of these reactions, a technique that has found widespread use as a means to separate *endo*- and *exo*-functionalised norbornene monomers is iodolactonisation.[18-22] Treatment of a mixture of *endo* and *exo* isomers of a norbornene carboxylic acid with iodine and potassium iodide yields an iodolactone species *via* reaction with the *endo* isomer; the *exo* isomer is unreactive and remains in solution allowing the two to be separated (Scheme 2.9). In the majority of cases, the *exo* isomer has been the desired product (due to its higher reactivity in polymerisation reactions) and the *endo* isomer simply disregarded. However, for the purpose of this study, iodolactonisation provides a convenient route to pure *endo* norbornenes.

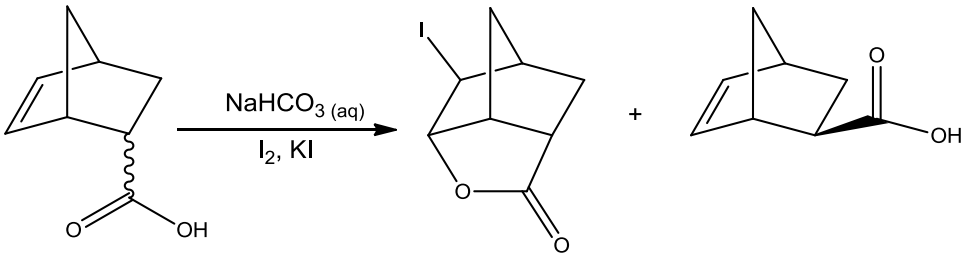

Scheme 2.9 Iodolactonisation of *endo-/exo*-NBCO_2H

2.2.2.3 Synthesis of 6-*endo*-hydroxy-5-*exo*-iodonorbornan-2-*endo*-2ylacetic acid δ-lactone (I1), a precursor to *endo*-NB$(CH_2)_2OCH_2C(CF_3)_2OH$ (DN1)

endo-/exo-$NBCH_2CO_2H$ (**SXN2**) was obtained *via* the deprotection of *endo-/exo*-$NBCH_2CO_2TMS$ (**SXN1**) (kindly supplied by Promerus) in acidic solution. The desired carboxylic acid **SXN2** was isolated as a pale yellow oil in quantitative yield with the ratio of *endo:exo* isomers determined to be 84:16 by ^1H NMR spectroscopic analysis.

Crude 6-*endo*-hydroxy-5-*exo*-iodonorbornan-2-*endo*-2ylacetic acid δ-lactone (**I1**) was prepared *via* treatment of an aqueous solution of **SXN2** with sodium hydrogen carbonate, iodine and potassium iodide (Scheme 2.10).[19] Pure **I1** was isolated as colourless needles (85%) upon recrystallisation from chloroform.

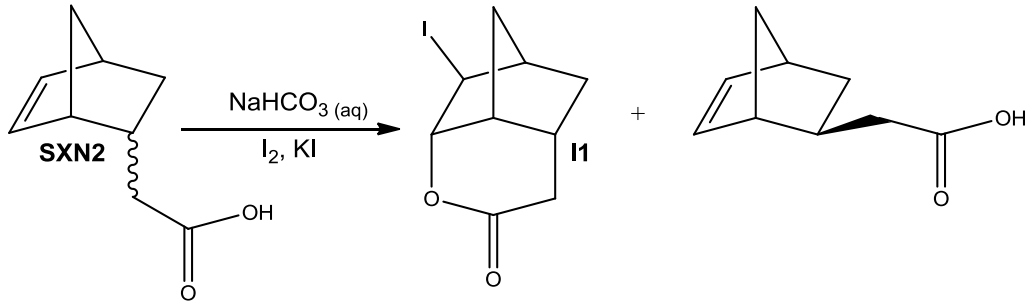

Scheme 2.10 Synthesis of 6-*endo*-hydroxy-5-*exo*-iodonorbornan-2-*endo*-2ylacetic acid δ-lactone (**I1**)

Single crystals of the iodolactone **I1** were grown by slow evaporation from a saturated chloroform solution at ambient temperature and isolated as colourless prisms. Subsequently, the molecular structure was determined by X-ray diffraction analysis (Dr Andrei Batsanov, Durham University), which revealed the expected atom connectivity (Figure 2.2). The structure of the bicyclic norbornene fragment was unremarkable, although the presence of the fused lactone ring causes a small expansion of the C6-C1-C2 bond angle (107.41(17)°), compared to that for the related unsubstituted C5-C4-C3 (105.92(17)°) moiety. Comparison of the C6-C1-C2 bond angle of **I1** (107.41(17)°), with the corresponding angle in a previously characterised carboxylic acid-functionalised norbornene, *endo*-$NBCO_2H$, (103.05(10)°) (Figure 2.3, **a**) shows an expansion of the C6-C1-C2 moiety in the iodolactone-functionalised norbornene, **I1**.[17] The six-membered lactone ring is again unexceptional, with the metric parameters describing the ester functionality being comparable to those for a related structure 1,5-dimethyl-2,6-dioxapentacyclo[6.5.O.$O^{4,12}$.$O^{5,10}$.$O^{9,13}$] tridecane-3,7-dione (Figure 2.3, **b**) previously structurally characterised.[23]

C5-I	2.173(2)	C6-C1-C2	107.41(17)
C1-C2	1.533(3)	C5-C4-C3	105.92(17)
C2-C3	1.552(3)	C6-O1-C9	122.48(16)
C3-C4	1.536(3)	O1-C9-C8	119.30(18)
C4-C5	1.538(3)	C6-C5-C4	103.11(16)
C5-C6	1.551(3)	C4-C5-I	111.06(14)
C1-C6	1.537(3)	C2-C3-C4	104.08(17)
O1-C6	1.457(2)		
O1-C9	1.351(3)		
O2-C9	1.209(3)		

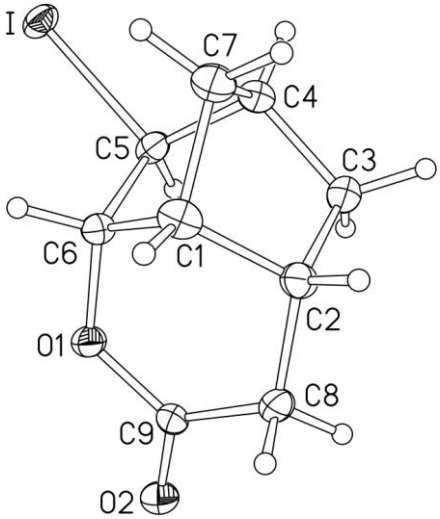

Figure 2.2 Molecular structure and selected bond distances (Å) and bond angles (°) of iodolactone **I1**; ORTEPS set at the 50% probability level.

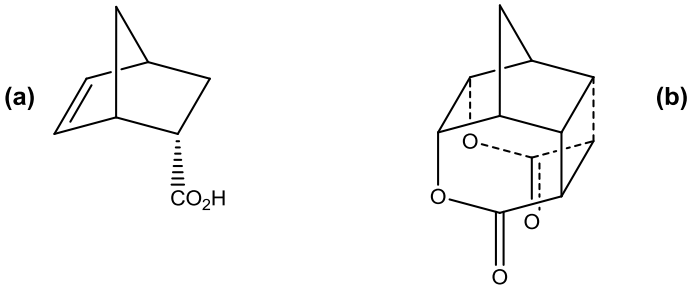

Figure 2.3 Structures of **a**) *endo*-$NBCO_2H$[17] and **b**) 1,5-dimethyl-2,6-dioxapentacyclo[6.5.O.$O^{4,12}$.$O^{5,10}$.$O^{9,13}$] tridecane-3,7-dione[23]

2.2.2.4 Synthesis of *endo*-$NBCH_2CO_2H$ (SN1)

Iodolactone **I1** was treated with zinc powder and copper(I) bromide in methanol followed by filtration through Celite and work-up to give an off white powder.[24] Subsequent dissolution of the powder in acidic solution followed by work-up yields crude $NBCH_2CO_2H$ (**SN1**) as purely the *endo* isomer, *via* opening of the lactone ring to regenerate the norbornene carboxylic acid moiety. The *exo* isomer was not detected by either ^1H NMR spectroscopic or GCMS analysis. Attempted purification of crude **SN1** *via* distillation was unsuccessful, hence the carboxylic acid was used in the next step of the synthesis without further purification.

2.2.2.5 Synthesis of *endo*-NB(CH$_2$)$_2$OH (DN1)

endo-NB(CH$_2$)$_2$OH (**DN1**) was prepared from e*ndo*-NBCH$_2$CO$_2$H (**SN1**) *via* reduction using lithium aluminium hydride in diethyl ether and subsequent work-up. **DN1** was isolated as a colourless oil in reasonable yield (45%). The presence of the alcohol functionality was confirmed by means of IR and ^{1}H NMR (D$_2$O shake) spectroscopies and the molecular ion was confirmed by mass spectrometry (accurate mass). Coupled GC mass spectrometry showed the presence of a single species possessing a molecular ion corresponding to that of the desired product.

2.2.2.6 Attempted synthesis of *endo*-NB(CH$_2$)$_2$OCH$_2$C(CF$_3$)$_2$OH (DN2)

A THF solution of *endo*-NB(CH$_2$)$_2$OH (**DN1**) was treated sequentially with NaH and HFIBO. However, despite numerous attempts, the reaction was shown by GC to only proceed with low conversion (<30%), generating a mixture containing ~40% unreacted alcohol as well as numerous other species. Increasing the reaction time (up to one month) and/or heating (40 ºC) were found to make little difference to the extent of conversion. Treatment of the reaction mixture with an excess of HFIBO led to the generation of a complex mixture of products, which proved impossible to separate. In basic solution the hexafluoropropanol-moiety is believed to be deprotonated and react with further equivalents of HFIBO to form a 'double HFIBO adduct' (Scheme 2.11). Functionalised norbornenes of this type may account for one or more of the species observed in the mixture observed in the reaction of **DN1** with HFIBO.

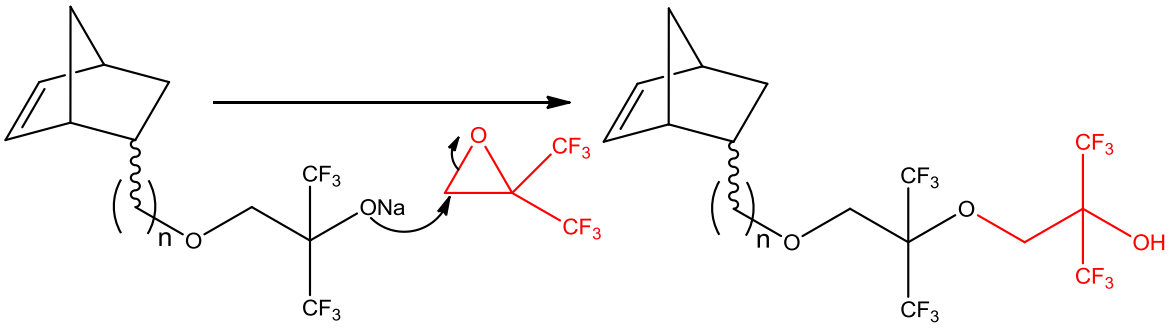

Scheme 2.11 Possible side reaction between NB(CH$_2$)$_n$OCH$_2$C(CF$_3$)$_2$ONa and HFIBO

2.2.2.7 Synthesis of *endo*-NB(CH$_2$)$_2$OMs (DN3)

The low reactivity of **DN1** with HFIBO, discussed in section 2.3.6, was unexpected as HFIBO was found to react readily with all of the other norborneneol monomers studied, including the mixture of isomers *endo-/exo*-NB(CH$_2$)$_2$OH (**DXN1**). In order to examine whether the low reactivity of **DN1** was specific to reaction with HFIBO or more

generic, a reaction was carried out between **DN1** and methanesulfonoyl chloride. A cooled DCM solution of **DN1** was treated with methanesulfonyl chloride followed by triethylamine (scheme 2.11). Subsequent work-up afforded the mesylate product, **DN3**, as a yellow oil in good yield (84%). The ease of formation of **DN3** seems to rule out low reactivity the alcohol functionality of **DN1** and at the present time a satisfactory explanation for the low reactivity with HFIBO has not been established.

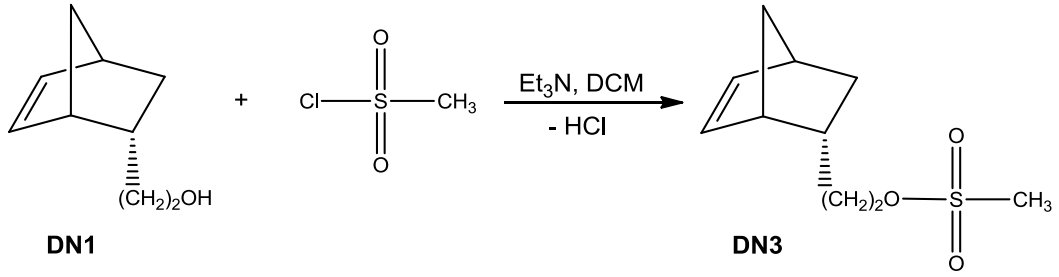

DN1 **DN3**

Scheme 2.12 Synthesis of *endo*-NB$(CH_2)_2$OMs (**DN3**)

2.2.3 Synthesis of NB$(CH_2)_3OCH_2C(CF_3)_2$OH monomers (n=3)

2.2.3.1 Attempted synthesis of *endo-/exo*-NB$(CH_2)_2$OH (TXN1)

The synthesis of *endo-/exo*-NB$(CH_2)_3$OH (**TXN1**) by Diels-Alder was first attempted on a small scale *via* reaction of cyclopentadiene with 4-pentenol in a sealed Carius tube, using a route analogous to that discussed in section 2.3.2. However, a mixture of **TXN1**, cyclopentadiene trimer and residual 4-pentenol was obtained from which the pure **TXN1** product could not be isolated. The reaction was repeated on a larger scale using a 0.5 L stainless steel autoclave fitted with a rocking mechanism. Purification of **TXN1** was attempted using a variety of distillation techniques and conditions however a mixture of **TXN1** and residual 4-pentenol (~7%) was obtained in all cases. Separation of **TXN1** and 4-pentenol using column chromatography was also unsuccessful due to the similarity of the Rf values of both compounds.

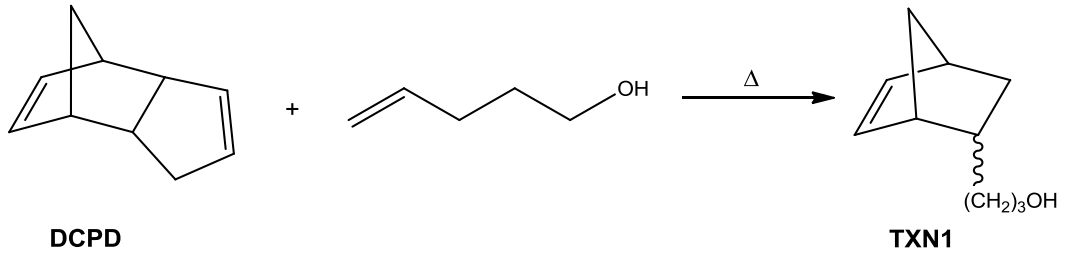

Scheme 2.12 Synthesis of *endo-/exo*-NB$(CH_2)_3$OH (**TXN1**) *via* Diels-Alder reaction

2.2.3.2 Attempted synthesis of *endo-/exo*-NB$(CH_2)_3$OAc (TXN2)

In an attempt to aid separation of the mixture of **TXN1** and 4-pentenol described in section 2.4.1, the corresponding acetates were prepared. A cooled diethyl ether solution of **TXN1** was treated with triethylamine and acetyl chloride (scheme 2.13). Following work-up and distillation a colourless oil was obtained which was shown by ^{1}H NMR and GCMS to be a mixture of **TXN2** and $H_2CCH(CH_2)_3OAc$. As with the parent alcohols, the two compounds proved to be inseparable by distillation or column chromatography.

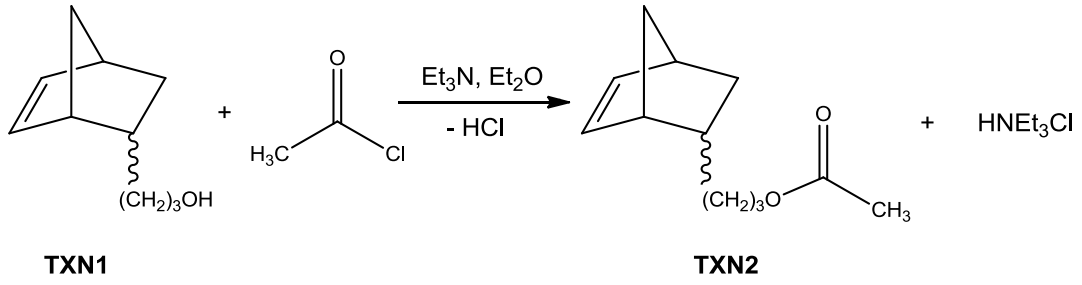

Scheme 2.13 Synthesis of *endo-/exo*-NB$(CH_2)_3$OAc (**TXN2**)

2.2.3.3 Synthesis of *endo-/exo*-NB$(CH_2)_3$OH (TXN1) and *exo*-NB$(CH_2)_3$OH (TX1)

Due to the difficulties experienced in the isolation of **TXN1** from the Diels-Alder reaction of cyclopentadiene with 4-pentenol alternative routes to **TXN1** were sought. The synthesis of *endo-/exo*-NB$(CH_2)_2$COOH **DXN4** *via* treatment of dicyclopentadiene with pentenoic acid at high temperature and pressure is reported in the literature and provides a possible route to **TXN1** *via* reduction to the corresponding alcohol.[19] An alternative is the chain extension of shorter alcohols (such as NB$(CH_2)_2$OH) *via* preparation of the corresponding mesylate or tosylate and subsequent reaction with sodium cyanide.[21] However whilst effective, this process requires several steps and was

rejected in favour of carboxylic acid reduction. Due to the fewer synthetic steps required, reduction of carboxylic acids and esters to alcohols was selected as the method of choice in this work.

Treatment of *endo-/exo*-NB$(CH_2)_2CO_2Et$ (**DXN3**, supplied by Promerus) with lithium aluminium hydride in diethyl ether followed by subsequent work up gave the **TXN1** product in good yield (76%) with an *endo:exo* ratio of 80:20. Treatment of *exo*-NB$(CH_2)_2CO_2H$ (**DX1**, supplied by Promerus) in an analogous reaction gave *exo*-NB$(CH_2)_3OH$ (**TX1**) in reasonable yield (41%). The *endo* isomer was not detected by ^1H NMR spectroscopic or GCMS analyses.

2.2.3.4 Synthesis of *endo-/exo*-NB$(CH_2)_3OCH_2C(CF_3)_2OH$ (TXN3) and *exo*-NB$(CH_2)_3OCH_2C(CF_3)_2OH$ (TX2)

A THF solution of **TXN1** was treated sequentially with NaH and HFIBO. Following work-up, distillation and column chromatography **TXN3** was obtained as a colourless oil, however the isolated yield was low (9%).

Reaction of **TX1** in an identical manner to that described for **TXN3** generates **TX2** again in low yield (3%), as a colourless oil. The low yields of these reactions can be attributed to the small scale at which they were carried out and subsequent loss of material during purification.

2.2.3.5 Iodolactonisation of *endo-/exo*-NB$(CH_2)_2CO_2H$ (DXN4) - synthesis of 3-(2-*endo*-hydroxy-7-anti-iodonorbornan-2-*exo*-yl)propionic acid γ-lactone (I2)

endo-/exo-NB$(CH_2)_2CO_2H$ (**DXN4**) was obtained as a colourless oil in good yield (73%) *via* de-esterification of *endo-/exo*-NB$(CH_2)_2CO_2Et$ (**DXN3**) under alkaline conditions. Crude iodolactone (**I2**) was prepared *via* treatment of an aqueous solution of **DXN4** with sodium hydrogen carbonate, iodine and potassium iodide and isolated as a yellow oil (8% crude yield).[19] Purification was achieved using column chromatography and recrystallisation from diethyl ether to yield **I2** as colourless needles, however the isolated yield is extremely low (5%).

Unlike the iodolactonisation reaction of *endo-/exo*-$NBCH_2CO_2H$ (**SXN2**) to form **I1**, the product obtained from the iodolactonisation reaction of *endo-/exo*-$NB(CH_2)_2CO_2H$ (**DXN4**) is the γ-lactone, 3-(2-*endo*-hydroxy-7-anti-iodonorbornan-2-*exo*-yl) propionic acid, **I2**, rather than the seven-membered lactone which would result from attack of the norbornene double bond (scheme 2.14). Given the unfavourable nature of medium-sized (>6-membered) rings (attributed to ring strain and transannular interactions) the preference for generation of the 5-memeberd γ-lactone is expected.[25]

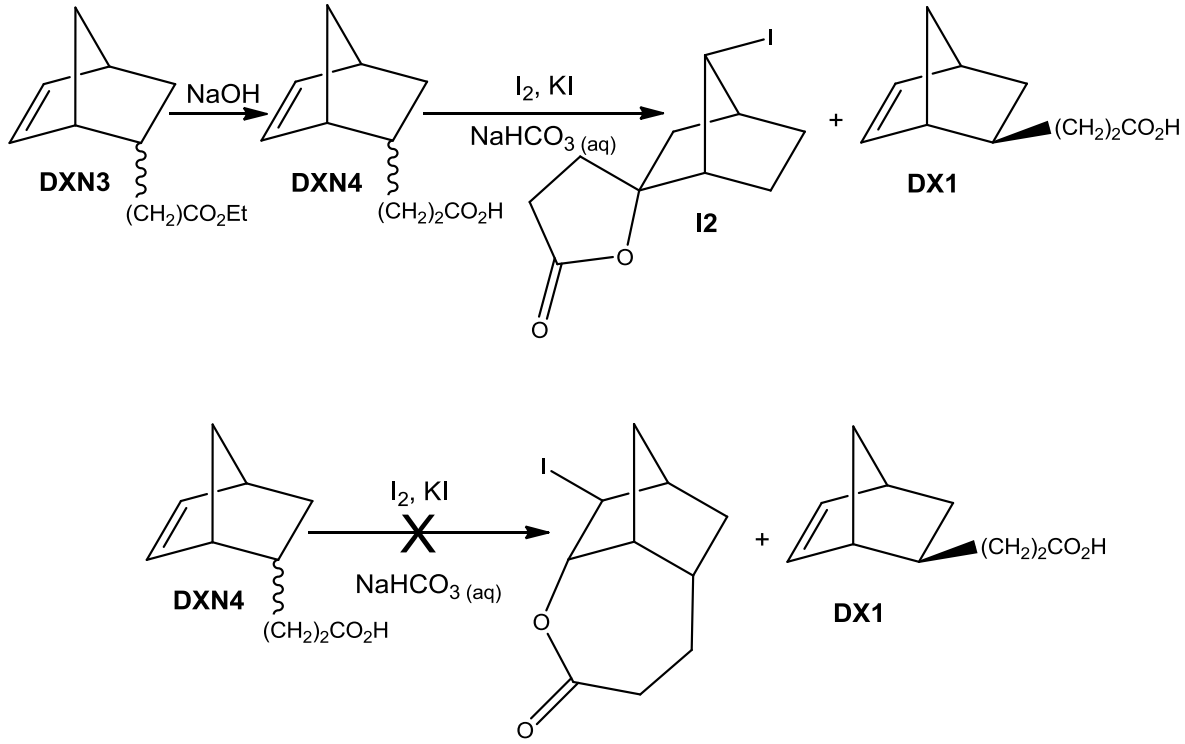

Scheme 2.14 Synthesis of 3-(2-*endo*-hydroxy-7-anti-iodonorbornan-2-*exo*-yl) propionic acid γ-lactone (**I2**)

Single crystals of the iodolactone **I2** were grown by slow evaporation from a saturated diethyl ether solution at ambient temperature and isolated as colourless prisms. Subsequently, the molecular structure was determined by X-ray diffraction analysis (Dr Andrei Batsanov, Durham University), which revealed the expected atom connectivity (Figure 2.4). The structure of the bicyclic norbornene fragment was unremarkable, with the presence of the γ-lactone ring substituent having little effect on the C6-C1-C2 bond angle (109.27(13)°), compared to that for the related unsubstituted C5-C4-C3 (108.41(13)°) moiety. However, comparison of **I2** with *endo*-$NBCO_2H$ (Figure 2.5, **a**) shows a large expansion of the C6-C1-C2 (103.05(10)º) moiety; C5-C4-

C3 (107.56(12)º) is similar in both the lactone and carboxylic acid structures.[17] The five-membered lactone ring is again unexceptional, with the metric parameters of the ester functionality being comparable to that for a related structure, *trans* 8-tert-butyl-1-oxaspiro[4.5]decan-2-one (Figure 2.6, **b**) previously structurally characterised.[26]

C1-C2	1.550(2)	C6-C1-C2	109.27(13)
C2-C3	1.545(3)	C6-C5-C4	103.22(13)
C3-C4	1.541(2)	C5-C4-C3	108.41(13)
C4-C5	1.542(2)	C3-C2-C1	103.37(13)
C5-C6	1.556(2)	C2-O1-C8	110.73(12)
C1-C6	1.539(2)	O1-C2-C3	110.41(12)
C1-C7	1.534(2)	O1-C2-C10	103.76(12)
O1-C2	1.459(3)	C1-C7-I	114.69(10)
O1-C8	1.355(2)		
O2-C8	1.207(2)		
C7-I	2.163(1)		

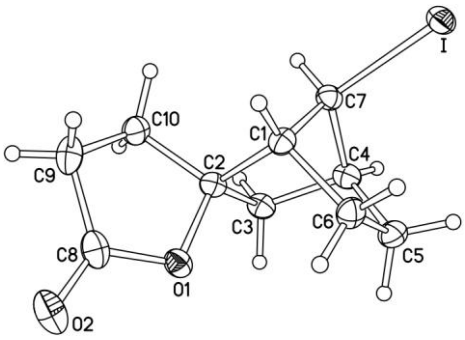

Figure 2.4 Molecular structure and selected bond distances (Å) and bond angles (°) of iodolactone (**I2**); ORTEPS set at the 50% probability level.

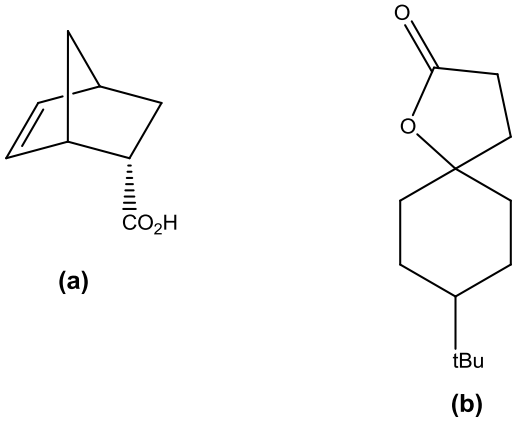

Figure 2.5 Structures of (**a**) *endo*-$NBCO_2H$[17] and (**b**) *trans* 8-tert-butyl-1-oxaspiro[4.5]decan-2-one[26]

2.2.4 Isolation of *endo*-NBCH$_2$C(CF$_3$)$_2$OH (SN3)

An alternative method to the iodolactonisation process for the isolation of *endo*-functionalised monomers involves polymerisation of an *endo*/*exo* mixture of isomers and subsequent separation of residual *endo* monomer. Such a separation is possible due to the difference in polymerisation rates between *endo* and *exo* isomers; uptake of the *exo* isomer is preferred, leaving residual *endo* isomer in solution.[27-29] A drawback of this route is the need for sufficient quantities of the *endo*/*exo* starting material (several grams) and the poor yield of the isolated *endo* isomer, which results from the need ensure that all of the (unwanted) *exo* isomer has been consumed.

Residual *endo*-NBCH$_2$C(CF$_3$)$_2$OH (**SN3**) was isolated from the reaction mixture following the polymerisation of *endo*-/*exo*-NBCH$_2$C(CF$_3$)$_2$OH (**SXN4**) using **Pd1388** (Scheme 2.15). The isolated yield of **SN3** was very low (3%), however the monomer obtained is exclusively the desired *endo*-isomer, confirmed by ^{1}H NMR spectroscopic and GCMS analyses.

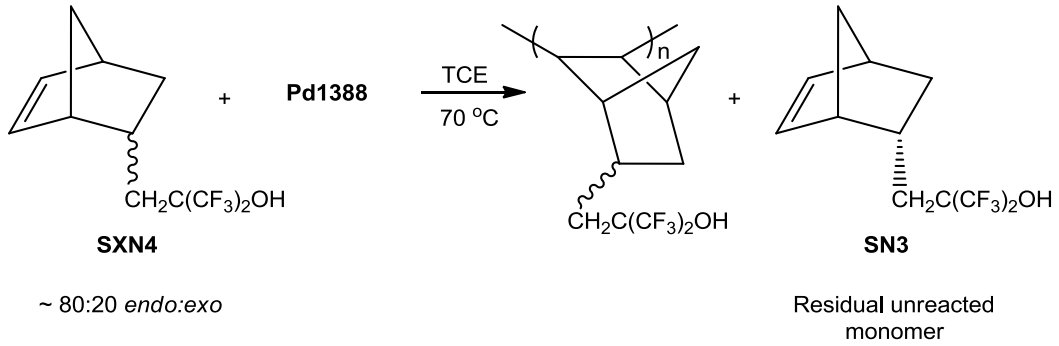

Scheme 2.15 Polymerisation of **SXN4** to recover residual **SN3**

2.2.5 Synthesis of palladium hydride pro-initiators for the polymerisation of HFP-functionalised norbornenes

The polymerisation of HFP-functionalised norbornenes is possible using a number of late transition metal based initiators, including palladium hydrides.[8-9] [Pd(H)(MeCN)(PCy$_3$)$_2$][B(C$_6$F$_5$)$_4$] (**Pd1388**) is used commercially in the polymerisation of HFP-functionalised monomers and was selected to initiate the polymerisations conducted in this thesis. However, a drawback to the use of **Pd1388** commercially is that the [B(C$_6$F$_5$)$_4$] counter anion is extremely expensive. In this section, the synthesis of the series of palladium hydride complexes, [Pd(H)(MeCN)(PCy$_3$)$_2$][X] will be discussed with a view to later examination of their potential as alternative initiators to **Pd1388**. It is hoped that a systematic study of the effect of the weakly coordinating

anion (WCA) X will highlight if the nature of the anion impacts on polymerisation and hence potentially allow a cheaper initiator package to be developed that exhibits comparable reactivity to **Pd1388**.

2.2.5.1 Synthesis and characterisation of [Pd(H)(MeCN)(PCy_3)$_2$][X] complexes

Complexes of the type [Pd(H)(MeCN)(PCy_3)$_2$][X] are readily prepared *via* oxidative addition to Pd(PCy_3)$_2$. A number of syntheses of Pd(PCy_3)$_2$ have been reported in the literature.[30-33] The synthetic method of choice for this study is a modification of that reported by Osakada.[33] Initially, $PdMe_2$(TMEDA) was synthesised according to the literature method and subsequently reacted with two equivalents of PCy_3 which upon appropriate work-up yields Pd(PCy_3)$_2$ as a white powder in good yield (85%) following evolution of ethane.[34-35]

Oxidative addition to Pd(PCy_3)$_2$ to generate palladium hydride complexes may be achieved using two synthetic routes: addition of an anilinium salt of a weakly coordinating anion (such as [$HNMe_2Ph$][$B(C_6F_5)_4$]) to the palladium(0) *bis*-phosphine (Scheme 2.16) or addition of an acid of a weakly coordinating anion (such as HCl or HBF_4) (Scheme 2.17).[8, 36-38] These two synthetic strategies will be discussed in turn.

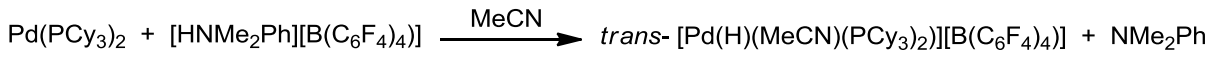

Scheme 2.16 Oxidative addition of [$HNMe_2Ph$][$B(C_6F_5)_4$] to Pd(PCy_3)$_2$ - synthesis of [Pd(H)(MeCN)(PCy_3)$_2$][$B(C_6F_5)_4$] **(Pd1388)**

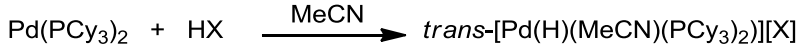

Scheme 2.17 Oxidative addition of HX to Pd(PCy_3)$_2$ - synthesis of [Pd(H)(MeCN)(PCy_3)$_2$][X]

2.2.5.2 Oxidative addition of an anilinium salt to $Pd(PCy_3)_2$ - synthesis of $[Pd(H)(MeCN)(PCy_3)_2][B(C_6F_5)_4]$ (Pd1388)

$[Pd(H)(MeCN)(PCy_3)_2][B(C_6F_5)_4]$ was prepared *via* addition of an acetonitrile solution of $[HNMe_2Ph][B(C_6F_5)_4]$ to a suspension of $Pd(PCy_3)_2$ in toluene (scheme 2.16).[8] Following work-up and purification, **Pd1388** is isolated as an off-white powder in high yield (95%). Both ^1H and ^{31}P NMR spectroscopic analysis confirm a *trans* arrangement of phosphines, as evidenced by triplet splitting of the characteristic palladium hydride proton resonance at δ -15.4 ppm ($^2J_{P-H}$ = 8.0 Hz).

2.2.5.3 Oxidative addition of HX to $Pd(PCy_3)_2$

Addition of aqueous tetrafluoroboric acid to a suspension of $Pd(PCy_3)_2$ in acetonitrile affords the desired product $[Pd(H)(MeCN)(PCy_3)_2][BF_4]$ (**Pd796**) as a yellow-brown powder in good yield (69%).[37] Analysis by ^1H NMR spectroscopy shows a triplet at δ -15.5 ppm (Pd-H, $^2J_{P-H}$ = 6.8 Hz) confirming a *trans* arrangement of phosphines. Addition of aqueous hexafluorophosphoric acid to a suspension of $Pd(PCy_3)_2$ in acetonitrile affords the desired product *trans*-$[Pd(H)(MeCN)(PCy_3)_2][PF_6]$ (**Pd854**) as a pale orange-brown solid in reasonable yield (54%). Treatment of a solution of $Pd(PCy_3)_2$ in toluene with a solution of HCl in diethyl ether gives the desired palladium hydride complex, *trans*-$[Pd(Cl)(H)(PCy_3)_2]$ (**Pd704**), as a sand coloured powder in high yield (83%).[38]

2.2.5.4 Reaction of $[Pd(Cl)(H)(PCy_3)_2]$ with MX

Reaction of **Pd704** with sodium hexafluoroantimonate in the presence of acetonitrile yields *trans*-$[Pd(H)(MeCN)(PCy_3)_2][SbF_6]$ (**Pd945**), as a pinky-brown powder in reasonable yield (68%). Analogous reaction of **Pd704** with silver triflate yields a yellow solid, **Pd817**, (55%). Analysis of **Pd817** by ^1H NMR spectroscopy shows a Pd-H resonance at δ -19.6 ppm however the splitting is unresolved hence it is not possible to confirm if the phosphine arrangement is *cis* or *trans*. The palladium hydride resonance appears further upfield than that of the other palladium hydride complexes studied (such as **Pd1388**), by 4.2 ppm, suggesting that the structure of **Pd817** is the expected $[Pd(H)(OTf)(PCy_3)_2]$ in which triflate is bound directly to the palladium centre, rather than one in which the triflate acts as a weakly coordinating anion. A similar complex in which triflate is bound to a palladium centre is the palladium methyl complex $[Pd(Me)(OTf)(P^tBu_3)]$ (**43**), which is discussed in Chapter I.[39]

2.2.5.5 Reaction of [Pd(Cl)(H)(MeCN)(PCy_3)$_2$] with $^tBu_4NI$

Reaction of [Pd(Cl)(H)(PCy_3)$_2$] with stoichiometric amounts of tetrabutylammonium iodide and acetonitrile on an NMR scale (10 mg of [Pd(Cl)(H)(PCy_3)$_2$]) led to the formation of a mixture of two palladium hydride-containing products, characterised by resonances at δ -12.2 and δ -15.4 ppm in approximately a 1:1 ratio by ^{1}H NMR spectroscopic analysis (Figure 2.7). Overlapping multiplets in the region δ + 0.5 - 2 ppm were also observed corresponding to tricyclohexyl and acetonitrile protons. The resonance at δ -15.4 ppm is a triplet ($^2J_{P-H}$ = 4.4 Hz) and was attributed to the complex *trans*-[Pd(H)(MeCN)(PCy_3)$_2$][I] (**Pd836**) in which the iodide acts as a weakly coordinating counter ion, and the remaining coordination site is occupied by acetonitrile. The position of the hydride resonance is in agreement with that of that of the analogous complex [Pd(H)(MeCN)(PCy_3)$_2$][B(C_6F_5)$_4$] in which the hydride also appears at δ -15.4 ppm.

The resonance at δ -12.2 ppm also appears as a triplet ($^2J_{P-H}$ = 8.4 Hz) and is assigned to the complex *trans*-[Pd(H)(I)(PCy_3)$_2$] (**Pd795**) in which the iodide is bound to the palladium centre. The ratio between **Pd836** and **Pd795** is influenced by addition of tetrabutylammonium iodide (0.5 equivalents) or MeCN (1 equivalent), both of which surprisingly cause an increase in the proportion of **Pd795** within the mixture (30:70 and 35:65 **Pd836:Pd795**, respectively). The ^{31}P{^{1}H} NMR spectrum of the **Pd836**/**Pd795** mixture shows two singlets at δ + 41.6 and δ + 42.2 ppm, which were assigned to **Pd836** and **Pd795**, respectively.

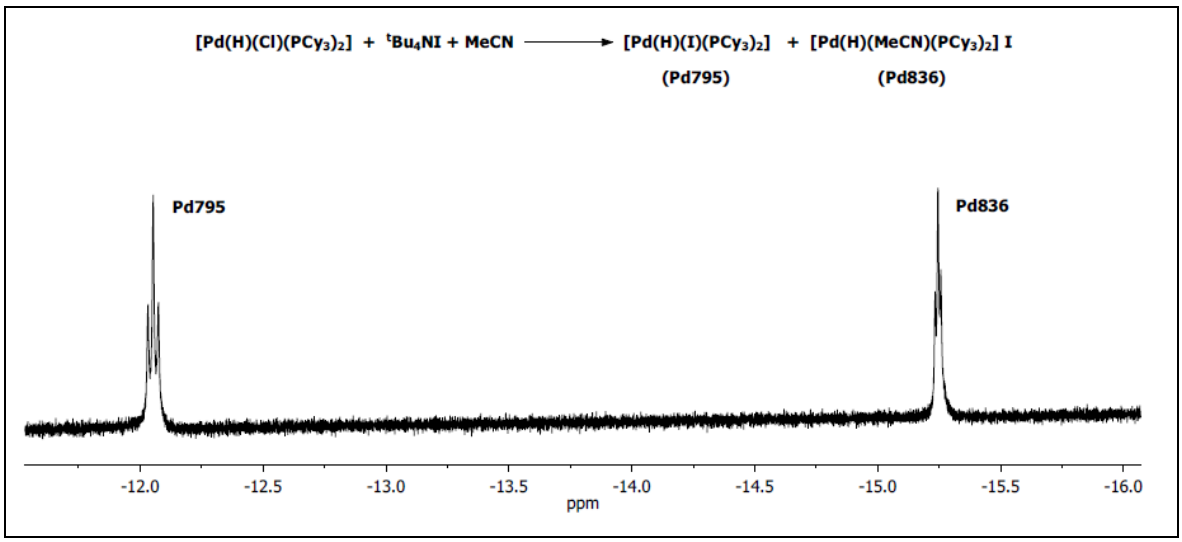

Figure 2.7 ^{1}H NMR spectra of a mixture of *trans*-[Pd(H)(MeCN)(PCy_3)$_2$]I (**Pd836**) and *trans*-[Pd(H)(I)(PCy_3)$_2$] (**Pd795**) showing the palladium hydride resonances

2.3 Summary

A series of HFP-functionalised norbornene monomers of the type $NB(CH_2)_nC(CF_3)_2OH$ (n = 1) and $NB(CH_2)_nOCH_2C(CF_3)_2OH$ (n = 0-3) have been prepared along with the series of palladium hydride initiators, [Pd(H)(MeCN)(PCy_3)$_2$][X]. The polymerisation kinetics of the HFP-functionalised monomers prepared will be discussed in subsequent chapters. The effect of the weakly coordinating anion of the initiator upon polymerisation rate will be explored in Chapter V.

2.4 References

1. A.E. Feiring, V.A. Petrov and F.L. Schadt III, US 2005/00588932 A1, 2005
2. A.E. Feiring, V.A. Petrov and F.L. Schadt III, US 2005/6875555 B1, 2005
3. A.E. Feiring, J. Feldman, F.L. Schadt III, G. Newton Taylor, US 2005/6884564 B2, 2005
4. H.V. Tran, R.J. Hung, T. Chiba, S. Yamada, T. Mrozec, T-Y. Hsieh, C.R. Chambers, B.P. Osborn, B.C. Trinque, J.P. Matthew, S.A. MacDonald and C.G. Wilson, *Macromolecules,* 2002, **35**, 6539-6549
5. A.E. Feiring, M.K. Crawford, W.B. Farnham, J. Feldman, R.H. French, K.W. Leffew, V.A. Petrov, F.L. Schadt III, R.C. Wheland and F.C. Zumsteg, *J. Fluorine Chem.*, 2003, **122**, 11-16

6. H. Ito, H.D. Truong, L.F. Rhodes, C. Chang, L.J. Langdorf, H.A. Sidaway, K. Maeda and S. Sumida, *Journal of Photopolymer Science and Technology*, 2004, **17**, 609-620
7. C. Chang, J. Lipian, D.A. Barnes, L. Seger, C. Burns, B. Bennett, L. Bonney, L.F. Rhodes, G. M. Benedikt, R. Lattimer, S.S. Huang and V.W. Day, *Macromol. Chem. Phys.*, 2005, **206**, 1988-2000
8. N. Thirupathi, D. Amoroso, A. Bell and J.D. Protasiewicz, *J. Polym. Sci. A: Polym. Chem.* 2009, **47**, 103-110
9. A. Bell, D. Amoroso, J.D. Protasiewicz and N. Thirupathi, US 2005/0187398, 2005
10. V.A. Petrov, *Synthesis*, 2002, **15**, 2225-2231
11. P. Mayo, G. Orlova, J.D. Goddard and W. Tam, *J. Org. Chem.*, 2001, **66**, 5182-5191
12. S.J. Cristol, T.C. Morrill and R.A. Sanchez, *J. Org. Chem*. 1966, **31**, 2719-2725
13. W. Oppolzer, C. Chapuis, D. Dupuis and M. Guo, *Helvetica Chimica Acta*, 1985, **68**, 2100-1114
14. C. Le Drian and A.E. Greene, *J. Am. Chem. Soc.* 1982, **104**, 5473-5483; H. Kreiger, *Suom. Kemistil. B.* 1963, **36**, 68; P.K. Freeman, D.M. Balls and D.J. Brown, *J. Org. Chem.* 1968, **33**, 2211-2214
15. G.T. Wang, S. Wang, Y. Chen, R. Gentles and T. Sowin, *J. Org. Chem.*, 2001, **66**, 2052-2056
16. J. Clayden, N. Greeves, S. Warren and P. Wothers, *Organic Chemistry*, Oxford University Press, Oxford, 2001, p. 1271-1272
17. A.T. Cooper, Ph.D Thesis, Durham University, 2008
18. C.D. Ver Nooy and C.S. Rondestvert, Jr, 1955, *J. Am. Chem. Soc*, 1955, **77**, 3583-3586
19. D.I. Davies and M.D. Dowle, J. *Chem. Soc. Perkin Trans. 1*, 1976, 2267-2270
20. D.I. Davies and M.D. Dowle, J. *Chem. Soc. Perkin Trans. 1*, 1978, 227-231
21. A. bin Sadikun and D.I. Davies, J. *Chem. Soc. Perkin Trans. 1*, 1982, 2461-2465
22. Y. Inoue, *Bull. Chem. Soc. Jpn.*, 1987, **60**, 1954-1956
23. A. P. Marchand and W. H. Watson, Private communication to CSD, CCDC 623402.
24. Y. Kawanami, T. Katsuki and M. Yamaguchi, *Bull. Chem. Soc. Jpn.*, 1987, **60**, 4190-4192

25. M. Grossel, *Alicyclic Chemistry*, Oxford University Press, Oxford, 1997, p13, 20, 81-83
26. B. Busetta, G. Precigoux and Y. Barrans, *Crystal Structure Communications*, 1975, **4**, 597
27. Promerus, Unpublished Work
28. A.D. Hennis, J.D. Polley, G.S. Long, A. Sen, D. Yandulov, J. Lipian, G.M. Benedikt and L.F. Rhodes, *Organometallics*, 2001, **20**, 2802-2812
29. J.K. Funk, C. Andes and A. Sen, *Organometallics*, 2004, **23**, 1680-1683
30. W. Kuran and A. Musco, *Inorg. Chim. Acta*., 1975, **12**, 187-193
31. S. Otsuka, T. Yoshida, M. Matsumoto and K. Nakatsu, *J. Am. Chem. Soc.* 1976, **98**, 5850-5858
32. V.V. Grushin, C. Bensimon and H. Alper, *Inorg. Chem*., 1994, **33**, 4804-4806
33. M. Tanabe, N. Ishikawa and K. Osakada, *Organometallics*, 2006, **25**, 796-798
34. J. Boersma; W. de Graff, D. Grove, G. van Koten andA.L. Spek, *Rec. Trav. Chim*., 1988, **107**, 299-301
35. J. Boersma, W. de Graff, G. van Koten, J.J. Smeets and A.L. Spek, *Organometallics*, 1989, **8**, 2907-2917
36. M. Sommovigo, M. Pasquali, P. Leoni, P. Sabatio and D. Braga, *J. Organometal. Chem.* 1991 **418** 119-126
37. P. Leoni, M. Sommovigo, M. Pasquali, S. Midollini, D. Braga and P. Sabatio, *Organometallics*, 1991, **10**, 1038-1044
38. D. Nguyen, G. Laurenczy, M. Urrutigoïty and P. Kalck, *Eur. J. Inorg. Chem.* 2005, 4215-4225
39. M. Yamashita, I. Takamiya, K. Jin and K. Nozaki, *Organometallics*, 2006, **25**, 4588-4595

Chapter III

Stability and reactivity of Pd1388 with hexafluoropropanol-functionalised norbornene monomers

Chapter III

Stability and reactivity of Pd1388 with hexafluoropropanol-functionalised norbornene monomers

3.1 Introduction

The vinyl polymerisation of functionalised-norbornene (NB) monomers is initiated by a wide variety of transition metal-based complexes, in particular, those based on the group X metals palladium and nickel.[1-2] Cationic palladium(II) complexes bearing allyl, alkyl or hydride ligands have demonstrated high tolerance to and activity for the polymerisation of functionalised-norbornenes bearing oxygen-containing functionalities (such as carboxylic acids, ethers and esters), which traditionally has proven difficult to achieve. An excellent example of such an initiator is the palladium hydride complex $[Pd(H)(MeCN)(PCy_3)_2][B(C_6F_5)_4]$ (**Pd1388**), developed by Promerus, which is employed commercially in the vinyl polymerisation of hexafluoropropanol-functionalised norbornenes for use in binder resins for deep UV photolithography.[3-4] Polymerisation of these alcohol-functionalised monomers is traditionally carried out in halogenated polar solvents such as chlorobenzene or 1,1,2,2-tetrachloroethane (TCE), which serve to solubilise the palladium initiator as well as allowing the reaction to be carried out at elevated temperatures (~50-70 °C).[5-6] Although the desired polymeric materials are obtained using this methodology, the stability of **Pd1388** under these conditions of sustained heating is unknown, which poses the question as to the nature of the actual active species involved the polymerisation reaction. Is a palladium hydride solely responsible? Does **Pd1388** decompose into other complexes that are involved in the reaction or does the polymerisation in fact, rely on a mixture of the two?

From an industrial perspective, it is vital to have a detailed understanding of the polymerisation process in order to predict and ultimately control the properties of the polymers obtained. In general, a rapid, but controlled polymerisation reaction is desired in order to produce well-defined materials in high yield and on a short time scale. Therefore, it is necessary to develop a detailed understanding of the kinetics of the polymerisation process for these types of industrially relevant system.

3.2 Polymerisation kinetics

The kinetics of a wide variety of polymerisation reactions have been studied extensively. Examples include living radical polymerisations (*e.g.* ATRP and RAFT), the polymerisation of olefins using metallocene catalysts and the ring opening metathesis polymerisation of norbornenes.[7-10] In contrast, the vinyl (addition) polymerisation of norbornenes has received considerably less attention.[11-14] Studies to date concerning the metal-catalysed polymerisation of functionalised norbornenes have been described using *pseudo*-first order kinetics (equation 3.1), in which k is a rate constant (typically that of propagation), [C] represents the number of active centres and $\alpha = 1$. The overall polymerisation rate is assumed to be independent of monomer conversion. Whilst the vast majority of polymerisation reactions can be described as being first-order in monomer, in some instances, a non-integer dependence on [M] has been observed with values of α ranging between 0 and 2. Values of α greater than unity suggest the involvement of a second monomer unit in the transition state.[15-19] The mechanistic complexity of vinyl norbornene polymerisations initiated using **Pd1388** presents the possibility that a *pseudo*-first order kinetic treatment may not be sufficient.

$$\frac{d[M]}{dt} = -k[C][M]^{\alpha} \quad \text{Equation 3.1}$$

3.2.1 Preliminary studies on the vinyl polymerisation kinetics of *exo*-$NBCH_2OCH_2C(CF_3)_2OH$ (SX1)

Preliminary studies were carried out in which the vinyl polymerisation of *exo*-$NBCH_2OCH_2C(CF_3)_2OH$ using **Pd1388** was examined using ^1H NMR spectroscopy. The polymerisation reaction was carried out in two different solvents for comparison. Data corresponding to monomer concentration as a function of time were analysed using *pseudo*-first order kinetics. The resulting logarithmic plots of $\ln([M]/[M]_0)$ (where $[M]_0$ is initial monomer concentration at time = 0) did not produce a linear relationship (Figure 3.1) suggesting that a more rigorous model for treatment of these data is required. In order to develop such a model, it is necessary to consider the mechanism of polymerisation in detail.

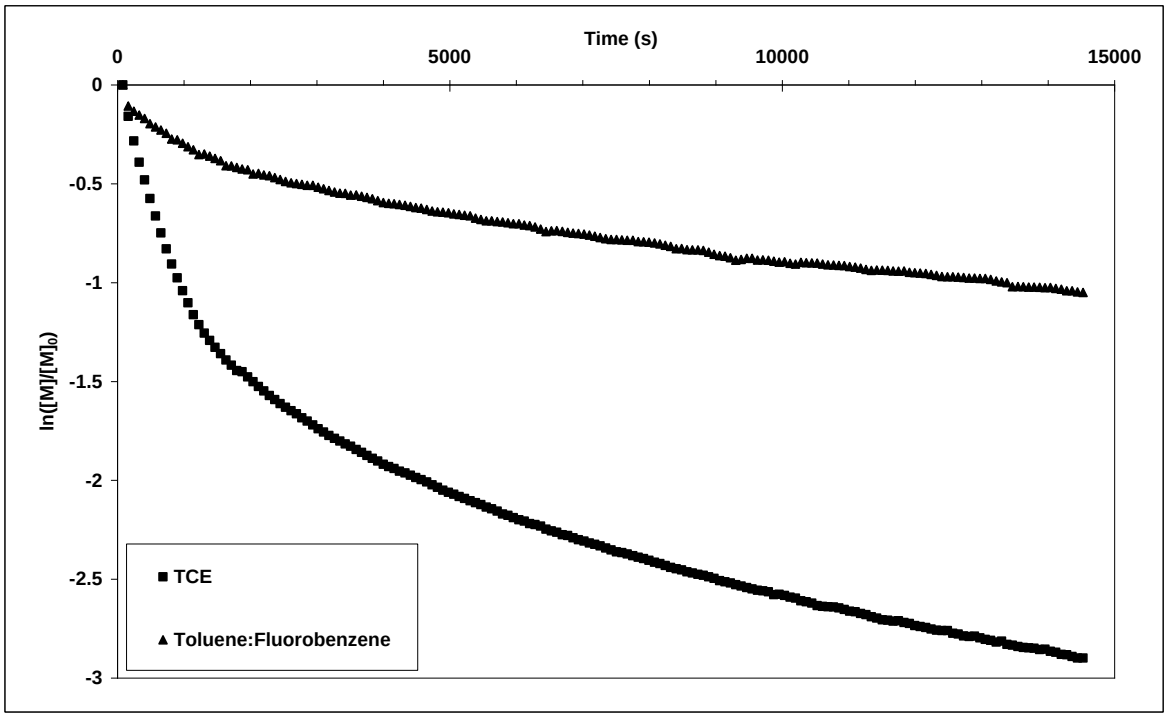

Figure 3.1 Plot of ln([M]/[M_0]) versus time for the vinyl polymerisation of *exo*-$NBCH_2OCH_2C(CF_3)_2OH$ using **Pd1388** at 70 °C in TCE and a 5:1 (v/v) mixture of toluene:fluorobenzene.

3.3 Proposed mechanism for the polymerisation of norbornene monomers using Pd1388

Although the hydride complex $[Pd(H)(MeCN)(PCy_3)_2][B(C_6F_5)_4]$ (**Pd1388**) has been used to initiate the polymerisation of norbornene, its mode of action has not been established experimentally. Due to its d^8, 16-electron, four-coordinate disposition, **Pd1388** should be regarded as a polymerisation pro-initiator since a vacant coordination site must be generated in order to bind the norbornene substrate prior to the onset of the polymerisation process. This may be achieved with dissociation of PCy_3 and/or loss of acetonitrile, a process/processes that must be followed by *cis*/*trans* isomerism in order to locate the alkene *cis* to the hydride moiety in order to allow the necessary migratory insertion prior to subsequent polymerisation (Scheme 3.1). *cis*/*trans* isomerism and phosphine dissociation were not explored experimentally in this system due to the high temperature (70 °C) used in commercial polymerisation reactions.

The acetonitrile ligand of **Pd1388** is likely to be extremely labile, especially given that it is situated *trans* to a hydride moiety. The soft tricyclohexyl phosphine donors on the other hand would be expected to be bound more strongly to the soft

palladium centre.[20] Although high solvent polarity may weaken the palladium phosphine interaction, it is most likely that loss of acetonitrile will provide the first step in the polymerisation process.

As shown in Scheme 3.1, the initiation process involves a complex series of equilibria, hence it is not possible to attribute loss of palladium hydride (measured experimentally) directly to rate of initiation. Experimental determination of monomer concentration as a function of time is somewhat more useful and can be used as a basis to calculate the rate of propagation in a polymerisation reaction.

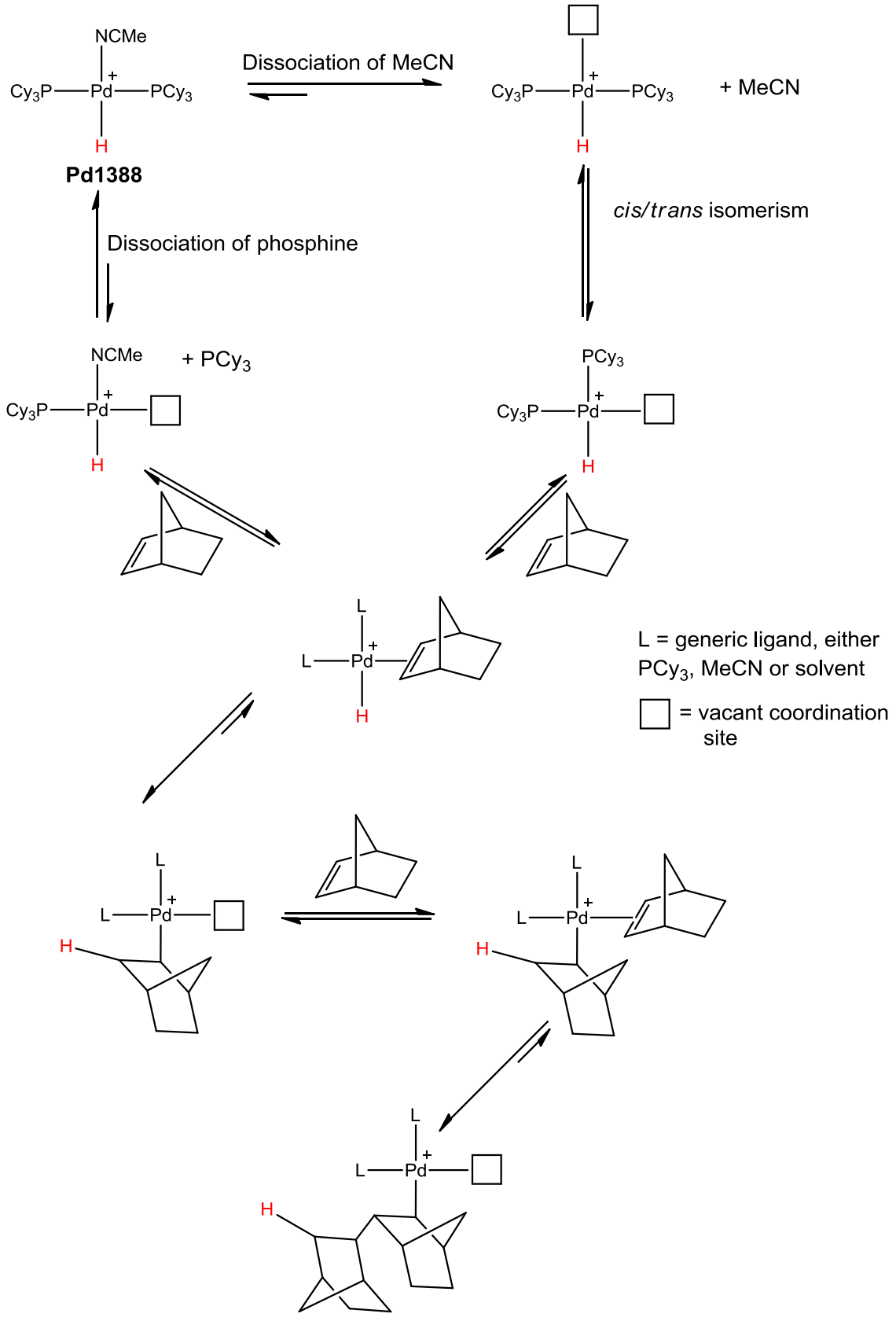

Scheme 3.1 Proposed mechanism for the polymerisation of norbornene monomers using **Pd1388**. In all steps, the counter ion is $[B(C_6F_5)_4]^-$. In the absence of experimental evidence it is not possible to determine the nature of the ligands during each stage of the polymerisation process, hence they are denoted as generic ligands, L.

3.4 Towards a kinetic model to describe the polymerisation of norbornenes using Pd1388

As described in Scheme 3.1, the first step in the polymerisation of norbornene (NB) will involve insertion of a monomer unit into a palladium hydride bond. It is therefore reasonable to assume that such an insertion will demonstrate a first order dependence upon both initiator and monomer concentration. However, subsequent insertion steps will involve insertion of monomer into a palladium alkyl (palladium norbornene) bond and the nature of this bond will change throughout the course of the reaction (Pd-NB dimer, Pd-NB trimer, *etc*.). Consequently, the kinetics of the propagation process could be considered to be time dependent, with a different value of *k* for each insertion step. It is also possible that additional monomer units are involved in the transition state, and that polymerisation rate is influenced by the changing viscosity of the system as the reaction progresses, resulting in kinetic behaviour which is considerably more complex than that expected for a *pseudo*-first order system. It is not practical (or even necessarily possible) to measure the rate of each insertion step independently; instead it is more useful to have a model that accurately describes the monomer consumption data obtained as a function of time, which gives an approximation of the polymerisation rate over the course of the reaction.

In order to determine an overall rate constant of polymerisation, it is necessary to consider the amount of monomer consumed, as well as the concentration of monomer remaining in solution at any given time. The concentration of free monomer as a function of time, [M], is readily determined experimentally, whilst the concentration of monomer at the start of the reaction is also a known value, $[M]_0$. The amount of monomer consumed is given by ($[M]_0 - [M]$), which can be linked to conversion {($[M]_0 - [M]$)/$[M]_0$)}. It is now possible to define a second rate constant, k_2, which considers both ($[M]_0 - [M]$) and free monomer concentration [M].

As discussed previously, the initiation process relies upon a complex series of equilibria which make it extremely difficult to study experimentally under conditions of commercial relevance. In addition, initiation is likely to be a function of catalyst concentration, which necessitates additional parameters within any model used to study the process, such as those described elsewhere by Bochmann and co-workers.[8-9] In order to simplify the requirements of a kinetic model used to approximate the overall rate of polymerisation, only data corresponding to the propagation process (*i.e.* insertion of monomer into palladium-norbornene bonds) will be considered. For this reason all rate constants subsequently described are *pseudo*-rate constants in which the concentration

of active centres is considered within the value of *k*. The concentration of **Pd1388** remained constant for all of the polymerisation reactions carried out within this thesis.

3.4.1 A note on nomenclature - $[M]_0$, $[M]_0'$ and conversion

The concentration of monomer at the start of the polymerisation reaction, $[M]_0$, is a known value (typically 0.3 M). However, the proposed kinetic model (section 3.4.2) does not take into account the initiation step of the process. This means that in order to calculate k_2 correctly, it is necessary to determine the monomer concentration at the start of the propagation process, denoted $[M]_0'$ to avoid any confusion. It would also be feasible to consider the extent of conversion at the start of the propagation process, however for the model discussed in this work, monomer concentrations were chosen instead. It is not possible to measure $[M]_0'$ experimentally as during the initial stages of the polymerisation, initiation and propagation processes will be in competition. However, it is possible to extrapolate monomer concentration data for the propagation process alone (*i.e.* when the palladium hydride is no longer present) to time = zero, which should provide a good approximation for $[M]_0'$ within the kinetic model proposed in section 3.4.2.

3.4.2 Proposed kinetic model for the polymerisation of functionalised-norbornene monomers using Pd1388

Combining the process described by k_1 and k_2, it is possible to suggest a kinetic model for the polymerisation of norbornene monomers *via* a step-wise addition mechanism, which will provide an appropriate means of fitting monomer concentration data as a function of time and an indication of overall polymerisation rate. The model that will subsequently be used to analyse polymerisation kinetic data in this thesis is given by equation 3.2. The integrated form of equation 3.2 was solved using Mathematica software (equation 3.3). As will be demonstrated later in this chapter, although not perfect, this model does give a more accurate view of the **Pd1388**-initiated functionalised norbornene polymerisation process than simple treatment of the data using first order kinetics. It also provides an excellent fit to experimental data.

$$\frac{d[M]}{dt} = -((k_1 - k_2([M]_0^{'} - [M]))[M] \qquad \text{Equation 3.2}$$

$$[M] = \frac{[M]_0^{'}(k_1 - [M]_0^{'}k_2)e^{-(k_1 - [M]_0^{'}k_2)t}}{k_1 - [M]_0^{'}k_2 e^{-(k_1 - [M]_0^{'}k_2)t}} \qquad \text{Equation 3.3}$$

3.4.3 Experimental techniques to study the vinyl polymerisation of functionalised norbornenes

A number of analytical techniques have been used successfully to study the kinetics of polymerisation reactions and these include ^{1}H NMR spectroscopy, gas chromatography, IR spectroscopy and UV-Vis spectroscopy. UV-Vis spectroscopy relies upon the presence of a chromophore within the monomer, whilst IR spectroscopy requires the presence of a strong band within the spectrum (such as a carbonyl) that changes sufficiently during polymerisation, something that makes both techniques unsuitable for the study of the vinyl polymerisation of hexafluoropropanol-functionalised norbornenes of interest here.

^{1}H NMR spectroscopy was selected in preference to GC as the former technique permits the study of both the characteristic palladium-hydride resonance of the pro-initiator at δ -15.5 ppm and the *endo* (~ δ + 6.2, + 5.9 ppm) and *exo* (~ δ + 6.1 – 6.0 ppm) resonances of vinyl monomers independently as a function of time. Although it is possible to separate the *endo* and *exo* signals using GC techniques, very careful choice of both column type and method are required to ensure that the retention times of the two isomers do not overlap.

3.5 Exploring the stability and reactivity of Pd1388

The generic mechanism for polymerisation of norbornene monomers using **Pd1388** was explored in section 3.3, and a model proposed to describe the kinetics of polymerisation in such systems (sections 3.4.1-3.4.3). However, in systems of industrial relevance, such as the polymerisation of hexafluoropropanol (HFP)-functionalised norbornenes using **Pd1388**, a further complication arises. Such polymerisations are carried out in chlorinated solvents such as TCE or chlorobenzene and at elevated temperatures (~50-70 ^{o}C) to ensure solubility of the pro-initiator and a high degree of monomer conversion on a short time scale.[6] However, the stability of **Pd1388** under such forcing conditions is unknown. In the following sections, a detailed study of both the stability, and reactivity

of **Pd1388** under the standard conditions used commercially for polymerisation of hexafluoropropanol-functionalised monomers will be described.

3.5.1 Stability of Pd1388 under standard commercial polymerisation conditions

For stability studies concerning **Pd1388**, a temperature of 70 ^{o}C was selected to ensure that testing was carried out under conditions comparable to those used commercially. TCE was selected as the polymerisation solvent due to its higher polarity compared with chlorobenzene, high temperature stability and ease of availability of the deuterated analogue. TCE is an excellent solvent in which to perform polymerisations, however is far from ideal from an industrial perspective due to its high level of toxicity.

3.5.2 Stability of Pd1388 in chlorinated solvents at 70 °C

Variable temperature ^{31}P NMR spectroscopy was used to examine the stability of **Pd1388** in d_2-TCE as a function of time. Initially (<5 minutes at 70 ^{o}C) only a single resonance is observed in the ^{31}P NMR spectrum, corresponding to the *trans* cyclohexyl phosphines of $[Pd(H)(MeCN)(PCy_3)_2][B(C_6F_5)_4]$ (δ + 44.6 ppm). However, on continued heating, **Pd1388** undergoes decomposition and/or reaction with the TCE solvent as indicated by the formation of three new phosphorus-containing species, characterised by ^{31}P resonances of δ + 26.8 (**a**), + 34.9 (**b**) and + 35.7 (**c**) ppm (Figure 3.2). The phosphorus-containing decomposition products **a**, **b** and **c** were also analysed using ^{1}H NMR spectroscopy. The starting complex $[Pd(H)(MeCN)(PCy_3)_2][B(C_6F_5)_4]$ (**Pd1388**) gives rise to a characteristic triplet resonance at δ –15.5 ppm for the hydride moiety, as well as broad multiplets in the region δ + 0.5 - 2 ppm corresponding to tricyclohexyl phosphine and acetonitrile protons. In contrast, the ^{1}H NMR spectrum of a mixture of the **Pd1388** decomposition products **a**, **b** and **c** showed only broad multiplets in the region δ + 0.5 - 2 ppm, and no evidence for any hydride species was observed.

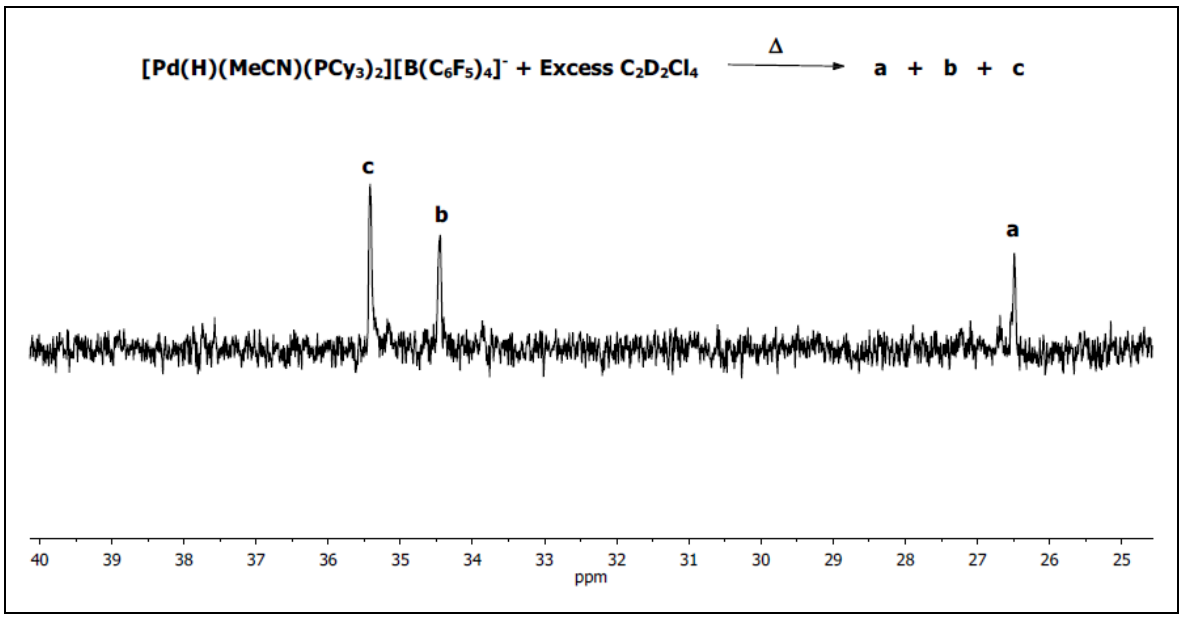

Figure 3.2 Scheme illustrating reaction between **Pd1388** and TCE at 70 ºC to form decomposition products **a**, **b** and **c** and $^{31}P\{^{1}H\}$ NMR spectrum illustrating decomposition products **a**, **b** and **c**

The decomposition of **Pd1388** as a function of time as monitored by ^{31}P NMR spectroscopy is given in Figure 3.3. The integral of each resonance within the ^{31}P NMR spectrum was determined relative to an internal standard contained within an external lock tube ($O=PH(OH)_2$ in d_6-benzene, δ + 7.8 ppm). The decay curve corresponding to the disappearance of the hydride initiator (δ + 44.6 ppm, solid black line) was analysed, with the decomposition of **Pd1388** demonstrating a reasonable fit to *pseudo*-first order kinetics ($R^2 = 0.966$). The half-life ($t_{½}$) for the decomposition process at 70 °C is around 35 minutes with a rate constant, k_d, of the order 10^{-4} s^{-1} (Figure 3.4). Typically polymerisations carried out commercially are run over a period of hours hence the rate of decomposition observed for **Pd1388** in the absence of monomer could be significant.

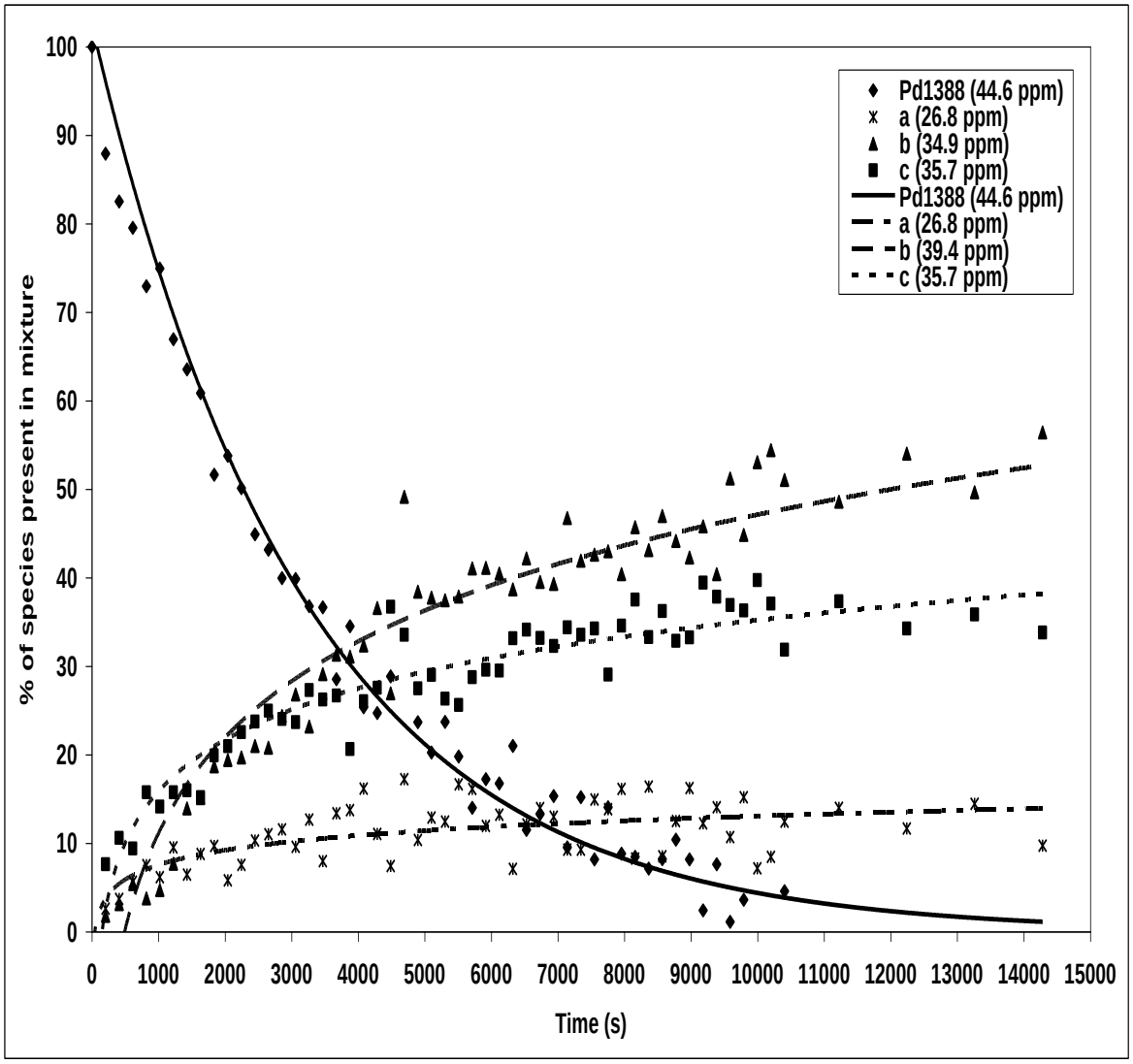

Figure 3.3 Decomposition as a function of time for a solution of **Pd1388** in TCE at 70 °C monitored by ^{31}P NMR spectroscopy.

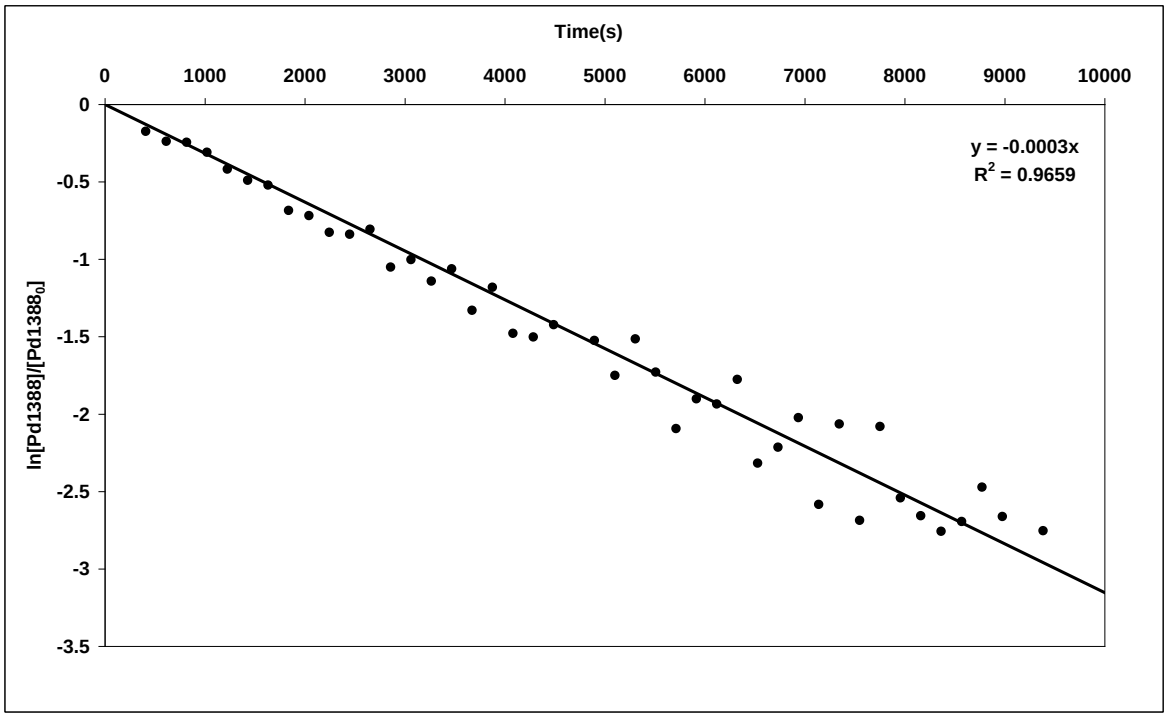

Figure 3.4 Plot of ln([Pd1388]/[Pd1388]$_0$) versus time illustrating the *pseudo*-first order kinetics for the decomposition of **Pd1388** in TCE at 70 °C.

The stability of **Pd1388** was also considered in chlorobenzene in order to determine if the decomposition observed was related to specific reaction of **Pd1388** with TCE, rather than generic reaction with chlorinated solvents. The decomposition process appears to be identical (*i.e.* same three phosphorus-containing products **a-c** obtained in comparable ratio) irrespective of the chlorinated solvent used.

3.5.3 Stability of Pd1388 in non-chlorinated solvents at 70 °C

To determine whether the decomposition of **Pd1388** observed in TCE is a consequence solely of temperature or a combination of temperature and solvent effects, the stability of the **Pd1388** was also tested in a non-chlorinated/non-reactive solvent mix. A 5:1 (v/v) mixture of toluene:fluorobenzene (C_6H_5F) was selected for its combination of solubility and non-reactivity (**Pd1388** is not soluble in neat toluene at ambient temperature). No change was observed in the ^{31}P NMR spectrum of the **Pd1388** dissolved in this solvent mix, even after prolonged heating (21 hours at 70 °C), confirming that the instability of **Pd1388** observed in TCE is related to the solvent and is not purely a thermal decomposition process (Figure 3.5).

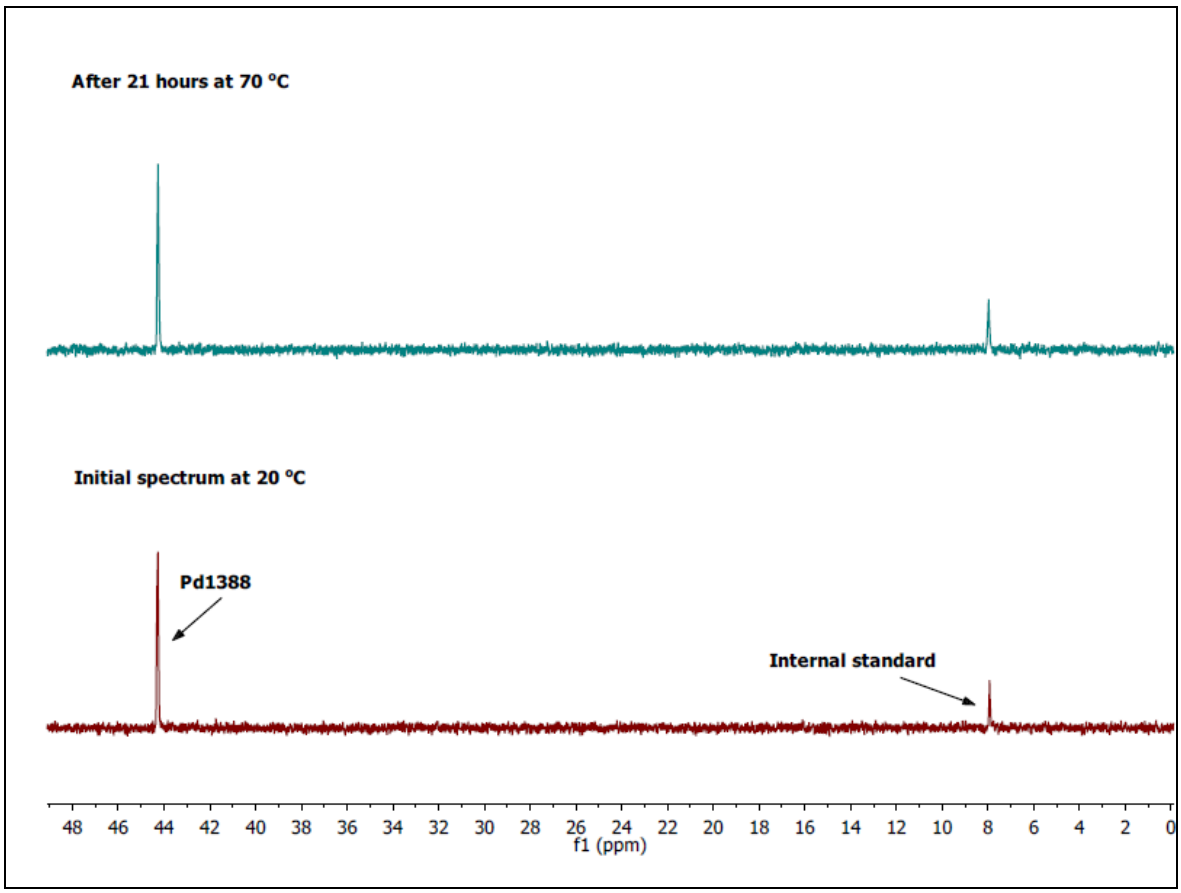

Figure 3.5 $^{31}P\{^{1}H\}$ NMR spectra of **Pd1388** in a 5:1 mixture of toluene:fluorobenzene at ambient temperature and after 21 hours at 70 °C

3.5.4 Reactivity of Pd1388 with TCE

As discussed in the preceding section, the decomposition of **Pd1388** observed in TCE is not purely a thermal process, indicating that **Pd1388** reacts directly with these types of chlorinated solvent. To further examine the possibility of this reactivity, **Pd1388** was treated with one molar equivalent of TCE in a 5:1 (v/v) mixture of toluene:fluorobenzene, a solvent combination found not to react with **Pd1388** (*vide supra*). Formation of decomposition products **a**, **b** and **c** was again observed after heating for 1 hour at 70 °C, however the process proceeds much more slowly than in neat TCE with ~ 90% of the initiator remaining after 1 hour (*c.f.* 30% in TCE) and ~80% remaining after 4 hours at 70 °C (Figure 3.6). Addition of excess TCE (5 equivalents) leads to further decomposition, with ~45% of the initiator remaining after heating for 1 hour at 70 °C, the remainder of the solution being composed of decomposition products **a**, **b** and **c** in the approximate ratio 5:1:4, respectively.

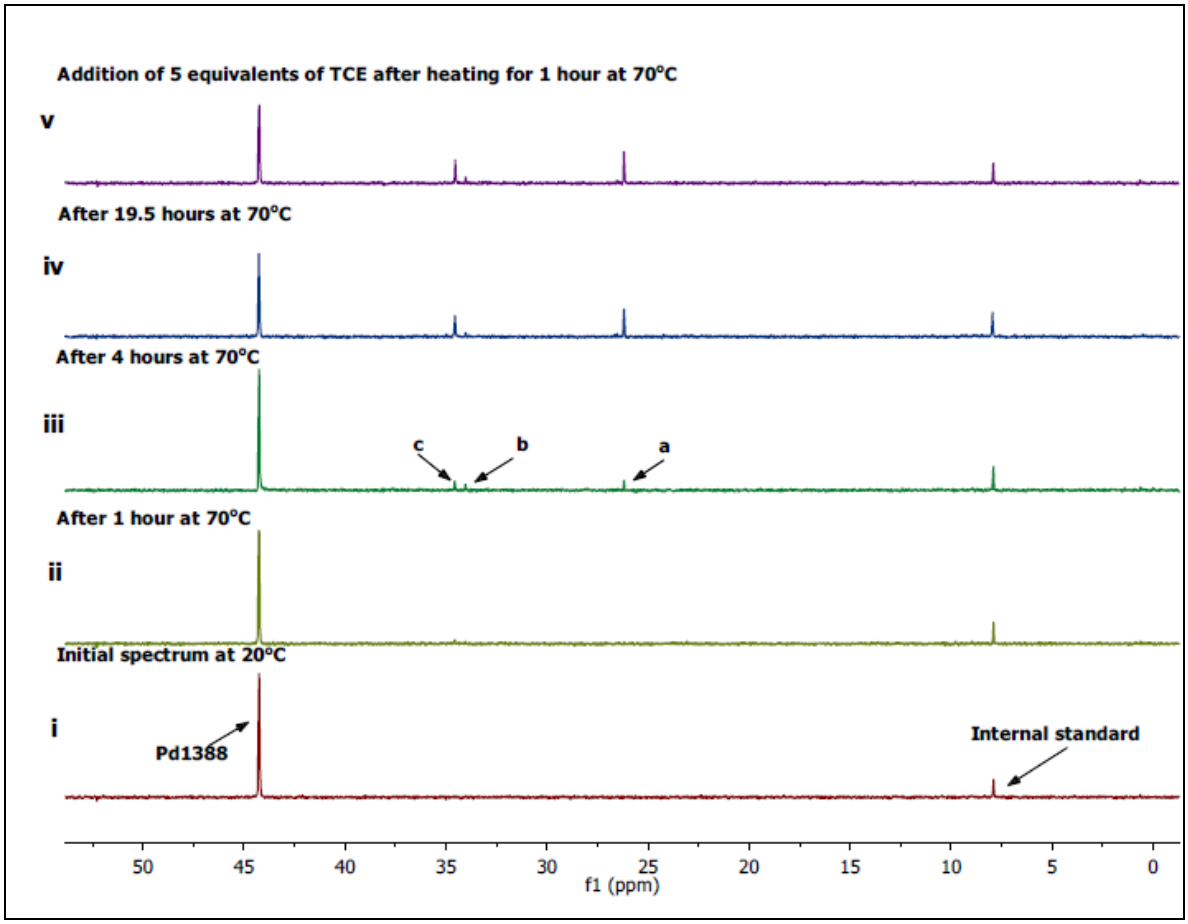

Figure 3.6 (**i-iv**) $^{31}P\{^{1}H\}$ NMR spectra of **Pd1388** treated with one molar equivalent of TCE in a 5:1 (v/v) mixture of toluene:fluorobenzene as a function of time; (**v**) $^{31}P\{^{1}H\}$ NMR spectra of **Pd1388** in a 5:1 mixture (v/v) of toluene:fluorobenzene, heated for 19.5 hours at 70 °C with one molar equivalent of TCE followed by treatment with excess TCE (5 equivalents) at ambient temperature and (**vi**) after heating for an additional 1 hour at 70 °C.

The decomposition observed in the chlorinated solvents examined here could possibly be attributed to the presence of HCl as an impurity in the tetrachloroethane solvent used. To eliminate this possibility a sample of protic TCE was dried over calcium hydride (as an alternative to P_2O_5 used in previous experiments) to remove any residual traces of acid and the decomposition of **Pd1388** re-examined. The same decomposition peaks are observed irrespective of the solvent drying agent used.

One possible cause of decomposition and/or reactivity of **Pd1388** in chlorinated solvents could be related to the lability of the phosphine ligands in solution (rapid

association/dissociation) and loss of PCy_3 by reaction of free phosphine. Such processes are often cited as a common catalyst degradation pathway in homogeneous catalysis involving metal phosphine complexes. In order to probe the theory that **Pd1388** decomposes as a consequence of dissociation of PCy_3, with the then unbound phosphine reacting with TCE, the ^{31}P NMR spectra of tricyclohexyl phosphine were studied at 70 °C under identical conditions to those discussed for **Pd1388** in sections 3.6.1-3.6.3

3.5.5 Stability and reactivity of tricyclohexyl phosphine (PCy_3) at 70 °C

The stability and reactivity of tricyclohexyl phosphine in a selection of solvents was examined using ^{31}P NMR spectroscopy. Solutions of PCy_3 were prepared in either d_2-TCE or d_8-toluene, whilst a third was prepared in toluene and subsequently treated with one molar equivalent of TCE (relative to PCy_3). The solutions were heated to 70 °C and ^{31}P resonance integrals monitored as a function of time relative to an internal standard contained within a lock tube ($O=PH(OH)_2$ in d_6-benzene).

A solution of PCy_3 in toluene shows a single ^{31}P resonance at δ + 10.9 ppm and no change is observed, even after prolonged heating at 70 °C (27 hours). Following treatment of a toluene solution of PCy_3 with one molar equivalent of TCE accompanied by heating to 70 °C, the phosphine undergoes reaction to form a new species, **d**, characterised by a singlet resonance in its $^{31}P\{^1H\}$ NMR spectrum at δ + 48.3 ppm. Conversion of PCy_3 to **d** is ~30% after 24 hours at 70 °C (Figure 3.7, **ii**). Addition of excess TCE (5 equivalents) to the PCy_3 solution previously heated for 24 hours, (Figure 3.7, spectrum **ii**) followed by prolonged heating (16 h at 70 °C) leads to further reaction of PCy_3 (60% conversion) to generate **d** and a second species **e**, characterised by a singlet resonance at δ + 106.5 ppm in approximately a 2:3 ratio respectively (Figure 3.7, **iii**). When TCE is used as the solvent, complete conversion of PCy_3 to **e** is observed after 90 minutes at 70 °C.

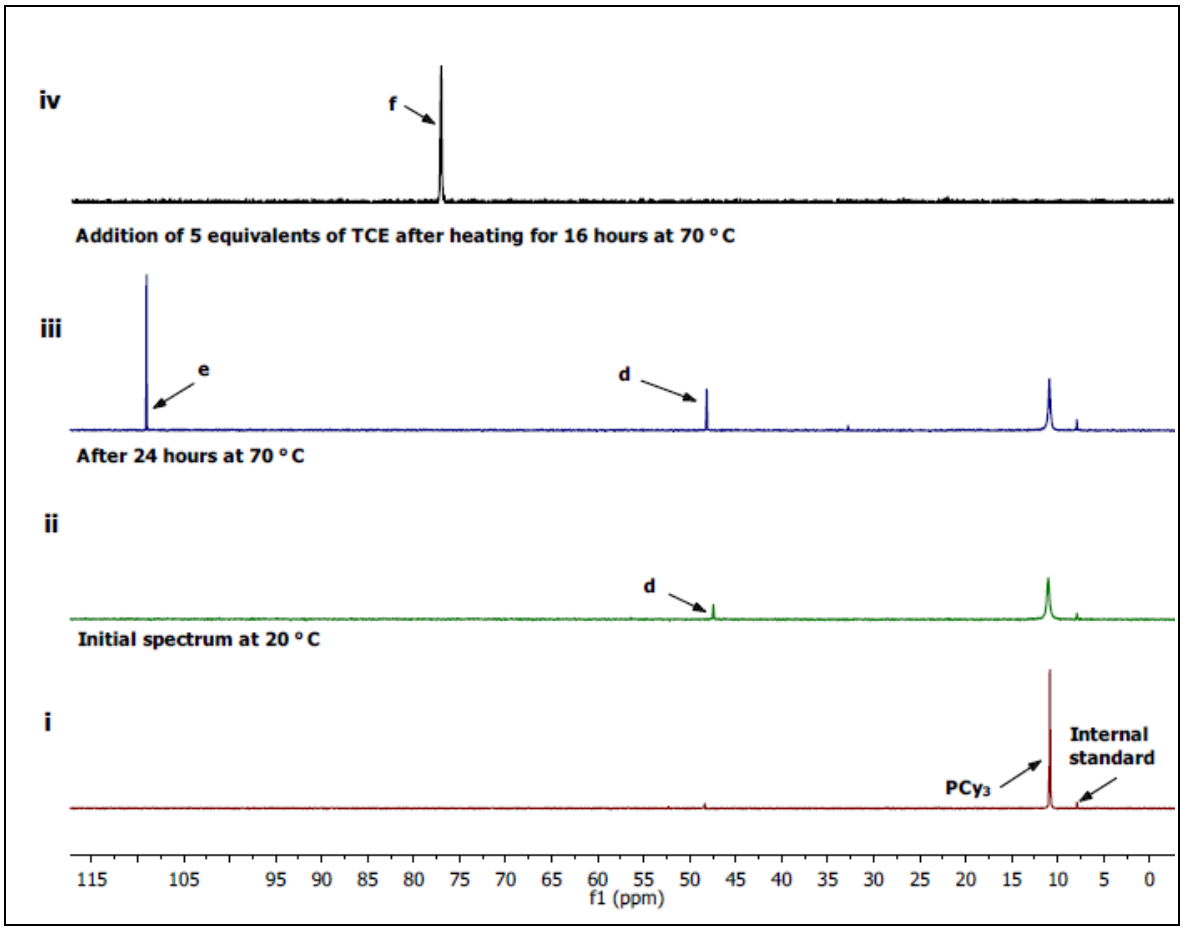

Figure 3.7 (**i-ii**) $^{31}P\{^{1}H\}$ NMR spectra of PCy_3 treated with one molar equivalent of TCE in a 5:1 mixture of toluene:fluorobenzene as a function of time; (**iii**) $^{31}P\{^{1}H\}$ NMR spectra of PCy_3 in a 5:1 mixture (v/v) of toluene:fluorobenzene, heated for 24 hours at 70 °C with one molar equivalent of TCE followed by treatment with excess TCE (5 equivalents) and heating for an additional 16 hours at 70 °C; (**iv**) $^{31}P\{^{1}H\}$ of species **f** (PCy_3Cl_2)

3.5.5.1 Synthesis of tricyclohexyl phosphine oxide

Several possibilities have been considered to explain the nature of products **d** and **e**, resulting from reaction of PCy_3 with TCE. A simple explanation could be formation of the oxide, $O{=}PCy_3$. This was tested *via* direct reaction of PCy_3 with an excess of H_2O_2 in TCE, which led to the formation of a single product displaying a singlet resonance in the $^{31}P\{^{1}H\}$ NMR spectrum at δ + 56.4 ppm; GCMS analysis confirmed the product to be the expected product, $O{=}PCy_3$. The chemical shift of tricyclohexyl phosphine oxide is not consistent with the ^{31}P NMR resonances observed in the reaction of PCy_3 with TCE, hence $O{=}PCy_3$ can be discounted.

3.5.5.2 Reaction of PCy_3 with hydrochloric acid in TCE

An alternative explanation for the presence of **d** and **e** could be the formation of the phosphonium salt $[HPCy_3]Cl$ as a result of reaction of PCy_3 with any residual hydrochloric acid within the TCE solvent. This possibility was examined *via* direct reaction of PCy_3 with excess hydrochloric acid in d_2-TCE. The phosphonium salt is characterised by a singlet resonance at δ + 25.4 ppm by $^{31}P\{^1H\}$ NMR spectroscopy and a doublet resonance (J_{P-H} = 487 Hz) by $^{31}P[^1H]$ NMR spectroscopy. Reaction of PCy_3 with excess HCl in TCE at ambient temperature also results in the generation of **e** and an additional species **f** characterised by a singlet resonances at δ + 76.8 ppm in both the $^{31}P\{^1H\}$ and $^{31}P[^1H]$ NMR spectra (Figure 3.7, **iv**). Species **f** has been assigned as PCy_3Cl_2, which has a reported ^{31}P NMR chemical shift of δ + 76.6 ppm ($CDCl_3$).[21] Hexachloroethane is known to be a chlorinating agent for tricyclohexyl phosphine, generating PCy_3Cl_2 and tetrachloroethene.[22] It is therefore reasonable to assume that a similar reaction can occur with tetrachloroethane, to generate PCy_3Cl_2 and dichloroethene, the presence of which is confirmed by ^1H and ^{13}C NMR spectroscopy of the reaction mixture. PCy_3Cl_2 is formed during reaction of PCy_3 with HCl using TCE as a solvent. However, in the direct reaction of PCy_3 with neat tetrachloroethane in the absence of HCl the formation of PCy_3Cl_2 is not observed with species **e** being the only reaction product.

An alternative explanation of the origins of species **e** could be formation a chlorophosphine such as PCy_2Cl or $PCyCl_2$ *via* halogen exchange of tricyclohexyl phosphine with the chlorinated solvent (Scheme 3.2, **a**). However, the ^{31}P chemical shifts of the aforementioned chlorophosphines (δ + 128.9 and + 204.0 ppm, respectively, $CDCl_3$) are not consistent with that observed for **e** (δ + 106.5 ppm, $C_2D_2Cl_4$; δ + 107.7 ppm, $CDCl_3$) hence they have also been ruled out.[23] One final possibility to explain the presence of species **e** is generation of a phosphonium salt of the type $[RPCy_3]Cl$ *via* direct reaction of PCy_3 with tetrachloroethane (R = $C_2D_2Cl_3$) (Scheme 3.2, **b**).

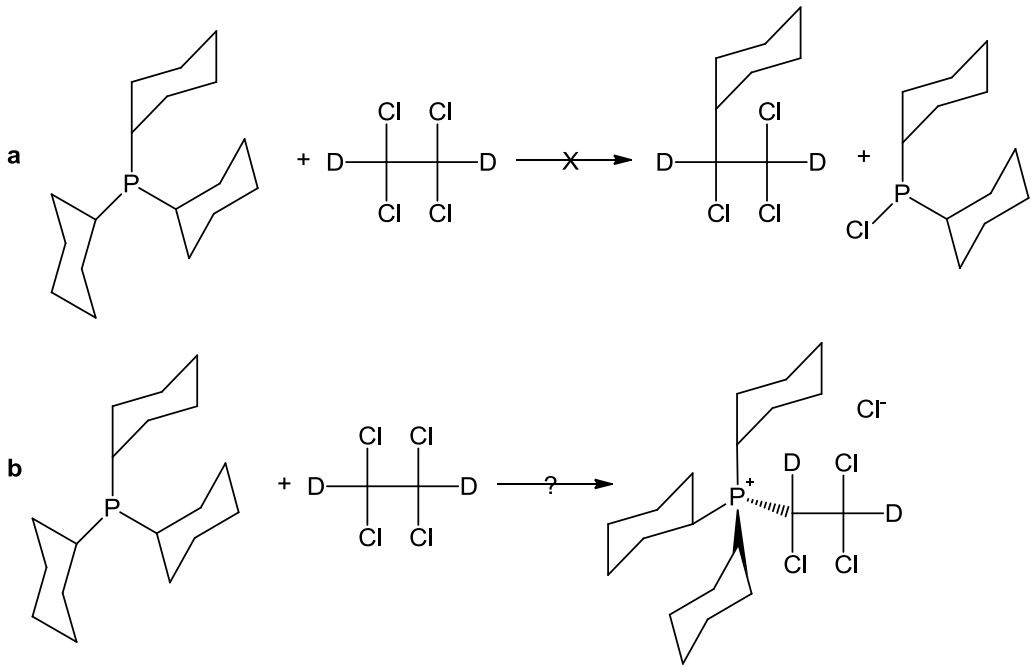

Scheme 3.2 Possible reactions between PCy_3 and TCE. a) ligand exchange to generate chlorophosphines; b) formation of a phosphonium salt

3.5.5.3 Attempted characterisation of the reaction product, e

Analysis of a solution of **e** in TCE *via* mass spectrometry was attempted, however only the presence of tricyclohexyl phosphine oxide ($O=PCy_3$) was detected irrespective of the MS experiment used. ^{1}H and ^{13}C NMR spectroscopy were also inconclusive, showing only resonances assigned as tricylohexyl groups. Attempts to isolate a pure solid sample of **e** *via* removal of TCE *in vacuo* resulted in the formation of a sticky white solid after *ca.* 12 h at ambient temperature. The solid was assigned as PCy_3Cl_2 based upon ^{31}P NMR chemical shifts upon re-dissolution in either TCE or $CDCl_3$, confirming that **e** is unstable under prolonged periods *in vacuo*. The conversion of **e** to PCy_3Cl_2 is not reversible.

3.5.5.4 Exploring the ability of product e to act as a ligand

To obtain further information regarding the nature of **e**, its ability to act as a ligand was examined. A pure solution of **e** in TCE was treated with a source of palladium(II) containing labile ligands, $[PdCl_2(MeCN)_2]$, which can readily undergo substitution by phosphines. Analysis of the reaction solution containing $[PdCl_2(MeCN)_2]$ and **e** by ^{31}P NMR spectroscopy shows only one resonance corresponding to the 'free' species **e** at δ

+ 106.5 ppm. No change was observed in the ^{31}P NMR spectrum after 3 hours at ambient temperature suggesting that no ligand substitution at palladium had taken place.

3.5.6 Analysis of the decomposition products of Pd1388 in TCE

The experiments detailed in section 3.5.5 indicate that neither free PCy_3 nor any of the products formed during reaction of PCy_3 with TCE account for the ^{31}P NMR spectroscopic resonances observed following the decomposition of **Pd1388** in TCE. Consequently, it is tentatively suggested that these species are indeed likely to be palladium-phosphine complexes. One possibility is formation of $PdCl_2(PCy_3)_2$ *via* reaction of either **Pd1388** itself, or an unstable decomposition product, with the chlorinated solvent. A genuine solution of *trans*-$PdCl_2(PCy_3)_2$ in TCE was prepared *via* reaction of $PdCl_2(MeCN)_2$ with 2 equivalents of PCy_3. The resulting $PdCl_2(PCy_3)_2$ product showed a singlet resonance in the $^{31}P\{^1H\}$ NMR spectrum at δ + 26.2 ppm (literature δ + 25.4 ppm ($CDCl_3$))[24] confirming that one of the decomposition products of **Pd1388**, **a**, in TCE is indeed $PdCl_2(PCy_3)_2$. Unfortunately, it has not been possible to assign decomposition products **b** and **c** corresponding to the resonances at δ + 34.9 and + 35.7 ppm, respectively.

3.6 Pd1388 as a polymerisation initiator – vinyl polymerisation of *exo*-$NBCH_2OCH_2C(CF_3)_2OH$ (SX1)

The decomposition of **Pd1388** in the absence of monomer has been discussed in detail in section 3.5 however the behaviour of **Pd1388** in the presence of monomer is expected to be somewhat different. In the following sections, the use of **Pd1388** as a vinyl polymerisation initiator will be explored in detail in a selection of solvents. Previous kinetic studies of vinyl norbornene polymerisation reactions using ^1H NMR spectroscopy have demonstrated that a monomer:initiator ratio of 50:1 is optimal in this type of study as both the palladium hydride and vinylic resonances are clearly visible.[6] The monomer selected for preliminary polymerisation studies was $NBCH_2OCH_2C(CF_3)_2OH$ as it is easily accessible in suitable quantities as the pure *exo* isomer. Pure isomers were deemed necessary at this early stage to avoid the inherent complication of *endo*/*exo* effects upon rates of polymerisation; the study of mixtures of isomers will be considered in Chapter V. Prior to beginning polymerisation studies, a blank run was carried out in which a solution of *exo*-$NBCH_2OCH_2C(CF_3)_2OH$ (**SX1**) monomer in TCE was heated to 70 ºC for 4 hours to rule out any contamination of the monomer or solvent; no polymerisation was observed.

3.6.1 Polymerisation of SX1 in d_2-TCE

Variable temperature ^{1}H NMR spectroscopy was used to monitor the reaction of **Pd1388** with 50 equivalents of **SX1** at 70 °C in d_2-TCE as a function of time. Using a wide spectral window (δ -15 to + 12 ppm), it was possible to measure the concentration of both the palladium hydride pro-initiator and free monomer over the course of the reaction. As discussed in section 3.3 (Scheme 3.1) the initiation process for the vinyl polymerisation of norbornenes relies upon a complex series of equilibria. For this reason, although the rate of hydride consumption, k_H, is related to the rate of initiation, the two rate constants are not necessarily equivalent. However, values of k_H do provide an interesting comparison between different solvents, and in later chapters, different monomers. In addition, comparison between k_H and the rate of decomposition of **Pd1388** gives an indication to the relative importance of hydride consumption *via* initiation and decomposition pathways during a polymerisation reaction.

For the polymerisation of **SX1** using **Pd1388** at 70 °C in d_2-TCE, loss of palladium hydride is rapid (complete within 300 seconds) and demonstrates an excellent fit to *pseudo*-first order kinetics. A first order rate constant (k_H) of 7.36 ± 0.2 x 10^{-3} s^{-1} is obtained with a corresponding R^2 value of 0.998. k_H is an order of magnitude faster than the rate of decomposition of **Pd1388** in the absence of monomer, k_d, for which a value of is 3.15 ± 0.08 x 10^{-4} s^{-1} is obtained (R^2 = 0.966) (Figure 3.8). The difference in rates suggests that for polymerisations carried out in TCE, consumption of **Pd1388** *via* monomer insertion is likely to be of greater significance than corresponding loss of **Pd1388** *via* a competing decomposition pathway which is 23 times slower.

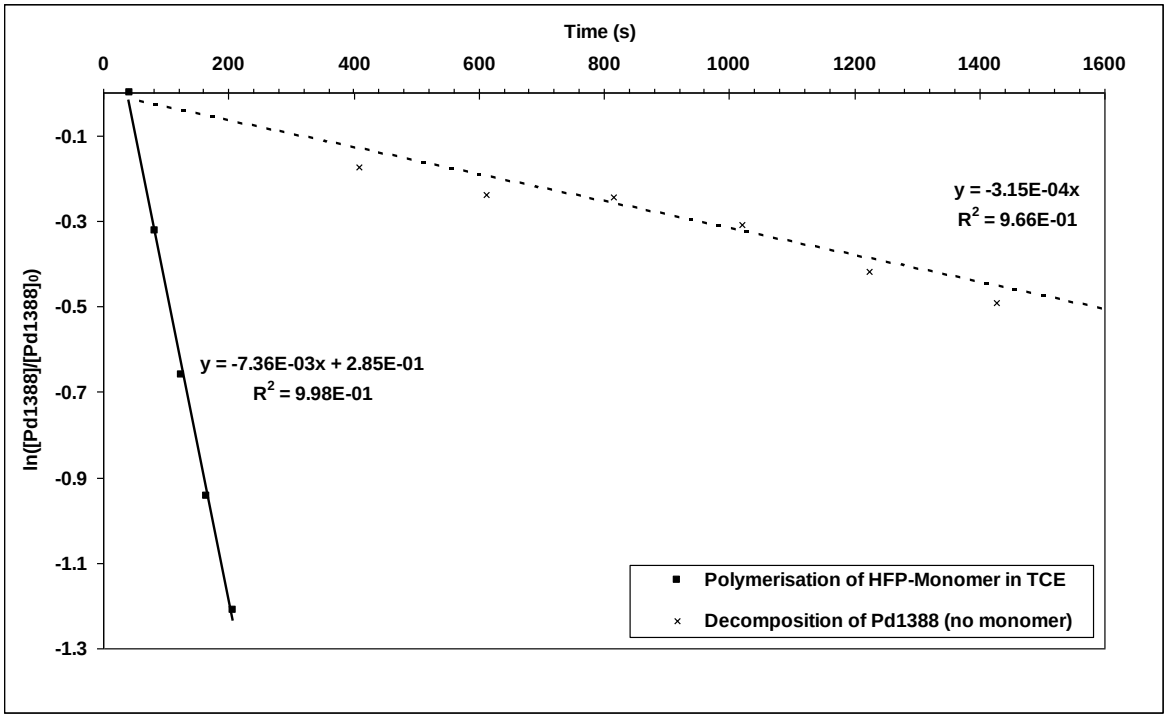

Figure 3.8 Plot of ln([Pd1388]/[Pd1388]$_0$) versus time illustrating the *pseudo* first order kinetics for loss of hydride in the polymerisation of **SX1** using **Pd1388** and for decomposition of **Pd1388** in the absence of monomer at 70 °C in TCE.

The propagation process for the polymerisation of **SX1** using **Pd1388** was studied using the kinetic model described in section 3.4.2. Origin 8.1 software was used to perform non-linear curve fitting analysis of the monomer consumption data (NMR integral areas) obtained for the polymerisation of **SX1** in TCE to equation 3.3 (Figure 3.9). An excellent fit (R^2 = 0.995) was obtained with the model accurately describing the polymerisation kinetics to 94% conversion. If the data is analysed up to ~70% conversion, a fit of R^2 = 0.999 is obtained. The improvement in fit at lower conversions is proposed to possibly be attributable to changes in the viscosity of the polymerisation solution as the reaction nears completion.

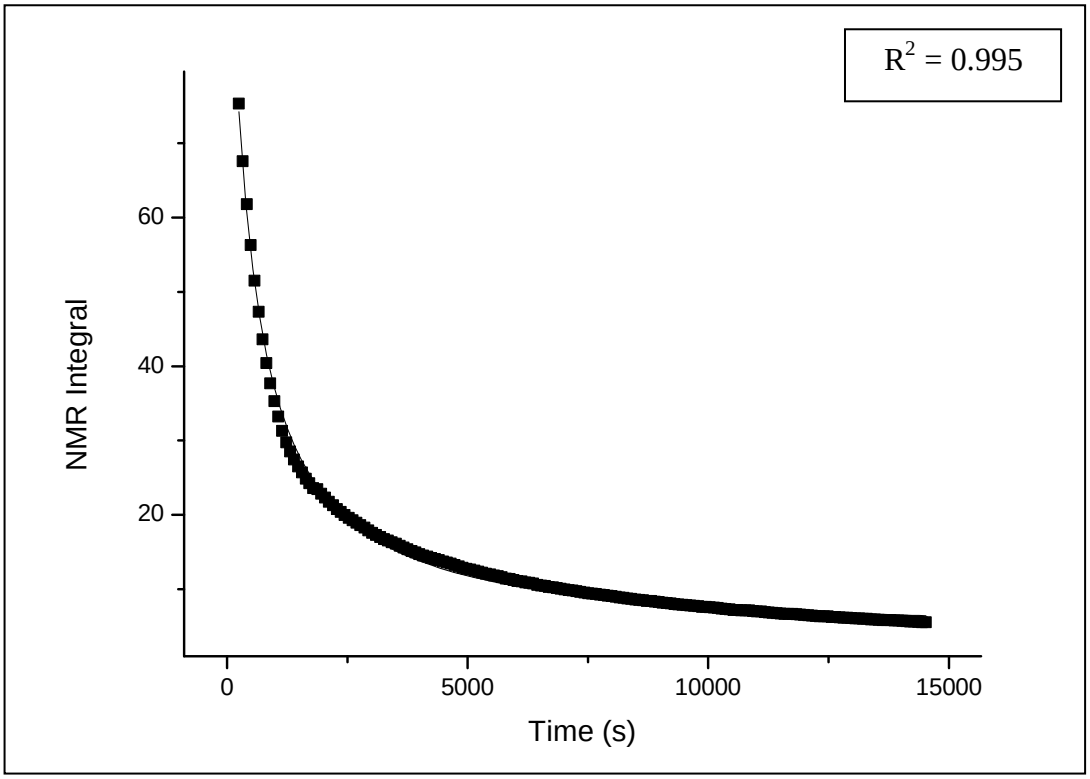

Figure 3.9 Plot of NMR integral intensity as a function of time for the vinyl resonances of **SX1**, polymerised using **Pd1388** in TCE at 70 ºC. The data has been fitted to equation 3.3 using non-linear curve fitting in Origin 8.1.

Non-linear curve fitting of monomer consumption data (NMR integral areas) obtained in the polymerisation of **SX1** to equation 3.3 results in the generation of three values, corresponding to the three parameters within the kinetic model: $[M]_0^{'}$, k_1 and k_2 (as discussed in section 3.4.2). Each parameter is obtained with an associated error in the fit which is discussed in Appendix 3.

$[M]_0^{'}$ is the concentration of monomer at the start of the propagation process and is obtained *via* extrapolation of the experimental data to t = 0. This is necessary since the value of $[M]_0^{'}$ is needed in order to obtain values of k_2 in meaningful units. The process of converting k_2 values into units of $mol^{-1}dm^3s^{-1}$ will be discussed in section 3.7.1.1. Unlike values of k_2, k_1 values can be determined directly from fitting of raw experimental NMR integral data (the total area vinylic resonance) to the kinetic model. In the case of polymerisation of **SX1** using **Pd1388** at 70 ºC in TCE, a k_1 value of 2.22 ± 0.5 x 10^{-3} s^{-1} is obtained. In polar solvents such as TCE, loss of hydride is approximately 3 times faster than propagation, hence insertion of monomer units into palladium-norbornene bonds is rate limiting.

3.6.1.1 Generic calculation of k_2 values from curve fitting of experimental data for monomer consumption to equation 3.3

The rate constant k_2 is a function of both [M] and ($[M]_0^{'}$ – [M]), making it a second order rate constant. Second order rate constants are concentration dependent and in order for the final values to have the desired units of $mol^{-1}dm^3s^{-1}$, the conversion of NMR integral areas into explicit concentrations is required. The concentration of monomer at the start of the polymerisation reaction, $[M]_0$, is a known value of 0.3 M. The concentration of **Pd1388** pro-initiator is also known (6 mM), *i.e.* monomer:Pd ratio of 50:1. Hence, if it is assumed that during the initiation process, one monomer unit is inserted into each palladium hydride bond, then at the start of the propagation reaction the ratio of free monomer:inserted norbornene-palladium complex will be 49:1. This will leave a concentration of free monomer in solution, $[M]_0^{'}$, of 0.294 M. However, data for monomer concentration measured experimentally is given in dimensionless units of NMR integral areas rather than mol dm^{-3}. Hence, it is necessary to first determine a value of $[M]_0^{'}$ in terms of NMR integral area in order for experimental data to be converted into explicit concentrations.

As discussed in section 3.4.1, the ^{1}H NMR integral area at the start of the propagation process can be approximated *via* extrapolation of experimental data for monomer consumption to time = 0. If the value for $[M]_0^{'}$ in units of ^{1}H NMR integral area is now set equal to 0.294 M and all other ^{1}H NMR integrals obtained experimentally normalised relative to this value, then a set of explicit monomer concentrations throughout the reaction are obtained. If the concentration of monomer at time = t, [M], in units of mol dm^{-3} is now plotted as a function of time, and the data refitted to equation 3.3, then a value of k_2 is obtained in the desired units of $mol^{-1}dm^3s^{-1}$.

It is worthwhile highlighting at this point that values of k_2 are only an approximation, as their calculation relies upon the extrapolation of experimental data. However, the purpose of the studies within this thesis is to explore relative rates of polymerisation in systems of industrial relevance in terms of solvent, monomer type *etc*. and for this reason, the calculation of absolute values of rate constants is not required. Values of k_2, whilst only approximations, do provide an interesting insight into the effect of polymer chain length on polymerisation rate and hence provide a useful, relative comparison between systems.

3.6.1.2 The k_2 value for polymerisation of SX1 using Pd1388

For the polymerisation of **SX1** using **Pd1388** at 70 ºC in TCE, a k_2 value of 7.91 ± 0.09 x 10^{-3} $mol^{-1}dm^3s^{-1}$ is obtained. For this system, k_2 is ~3.5 times faster than the corresponding value of k_1, suggesting that under the conditions studied, increasing polymer chain length makes a substantial contribution to retardation of polymerisation rate.

3.6.2 Polymerisation of SX1 in toluene:fluorobenzene

Polymerisation of **SX1** was carried out in a 5:1 (v/v) mixture of toluene:fluorobenzene in a manner analogous to that discussed in section 3.7.1. For reactions carried out in this solvent combination, **Pd1388** pro-initiator remained present throughout the entire course of the reaction, with consumption of ~20% of the palladium hydride after 30 minutes and ~30% after 4 hours. The presence of the pro-initiator throughout the polymerisation of **SX1**, which proceeds to 65% conversion over a period of 4 hours suggests that in this solvent combination, insertion of monomer into a palladium norbornene is favoured over insertion into palladium hydride *i.e.* the initiation process is the rate limiting step.

As the palladium–hydride pro-initiator remains present during the propagation process, fitting of monomer consumption data to equation 3.3 will result in rate constants which account for loss of monomer *via* palladium-hydride insertion as well as propagation. However, as the majority of the monomer is consumed *via* propagation, then the contribution to the overall observed rate from palladium hydride insertions is expected to be limited. For this reason, approximate values of k_1 and k_2 may be obtained as a means to compare overall polymerisation rate in TCE with that in a toluene:fluorobenzene mixture.

Fitting of monomer consumption data for the polymerisation of **SX1** in toluene:fluorobenzene using **Pd1388** to equation 3.3 generates values of k_1 = 1.76 ± 0.04 x 10^{-4} s^{-1} and k_2 = 0.91 ± 0.02 x 10^{-3} $mol^{-1}dm^3s^{-1}$ with an R^2 value of 0.993 (Figure 3.10). The excellent fit of experimental data to the kinetic model described by equation 3.3 suggests that this model does provide a good approximation of the overall rate of polymerisation in this system.

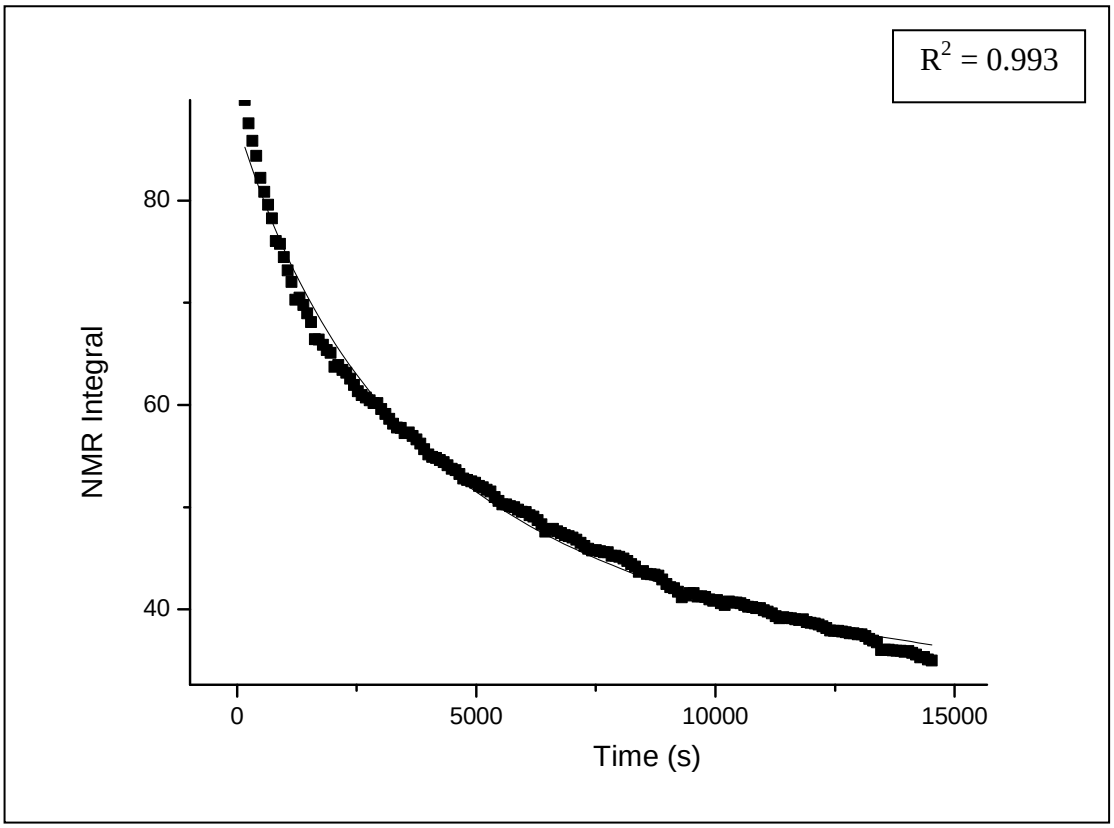

Figure 3.10 Plot of NMR integral intensity as a function of time for the vinyl resonances of **SX1**, polymerised using **Pd1388** in a 5:1(v/v) mixture of toluene:fluorobenzene at 70 ºC. The data has been fitted to equation 3.3 using non-linear curve fitting in Origin 8.1.

3.6.3 Polymerisation of SX1 using decomposed Pd1388 in TCE

Pd1388 has been shown to undergo decomposition in TCE at 70 ºC in the absence of monomer (section 3.6). However, the ability of decomposition products $PdCl_2(PCy_3)_2$ (**a**), and also **b** and **c** to act as polymerisation initiators remains unknown. Consequently, a sample of 'decomposed **Pd1388**' was prepared by heating a solution of **Pd1388** to 70 °C overnight in d_2-TCE. The solution was then subsequently treated with 50 equivalents of monomer and monitored as a function of time at 70 °C using ^{1}H NMR spectroscopy. It is important to note that polymerisation of **SX1** still occurs, even when the original palladium hydride initiator has been 'destroyed' as a result of decomposition.

At the present time, it has not been possible to conclude the nature of the active initiator species in the 'decomposed' system. A study by ^{1}H NMR spectroscopy as a function of time for the polymerisation of **SX1** using decomposed **Pd1388** shows only resonances corresponding to tricyclohexyl phosphine groups and the vinyl signals of the norbornene monomer. The polymerisation reaction using decomposed **Pd1388** was also

monitored using ^{31}P NMR spectroscopy and the areas of the three **Pd1388** decomposition products ($PdCl_2(PCy_3)_2$) (**a**), and also **b** and **c** carefully integrated against an internal standard ($O=PH(OH)_2$ in d_6-benzene), however no change in any of the resonances was detected within the error limits of the experiment, nor were any new resonances observed. It may be possible that one or more of the decomposition products is an active initiator. However, only a tiny amount of the species may be necessary for the polymerisation reaction to proceed, hence no change in the intensities would be visible within the error limit of the experiment. It is equally likely that the active initiator does not contain phosphine groups (such as colloidal palladium), hence would be invisible in the ^{31}P NMR spectrum.

An estimation for the overall rate of polymerisation of **SX1** using decomposed **Pd1388** was obtained via fitting of monomer consumption data to equation 3.3 (Figure 3.11). Values of $k_1 = 1.07 \pm 0.01 \times 10^{-4}$ s^{-1} and $k_2 = 0.86 \pm 0.008 \times 10^{-3}$ $mol^{-1}dm^3s^{-1}$ were obtained with a corresponding R^2 value of 0.997. The fit of the experimental data to equation 3.3 is excellent, suggesting that the kinetic model described in section 3.4.2 is suitable to provide an approximation of the overall rate of polymerisation of **SX1** using decomposed **Pd1388**.

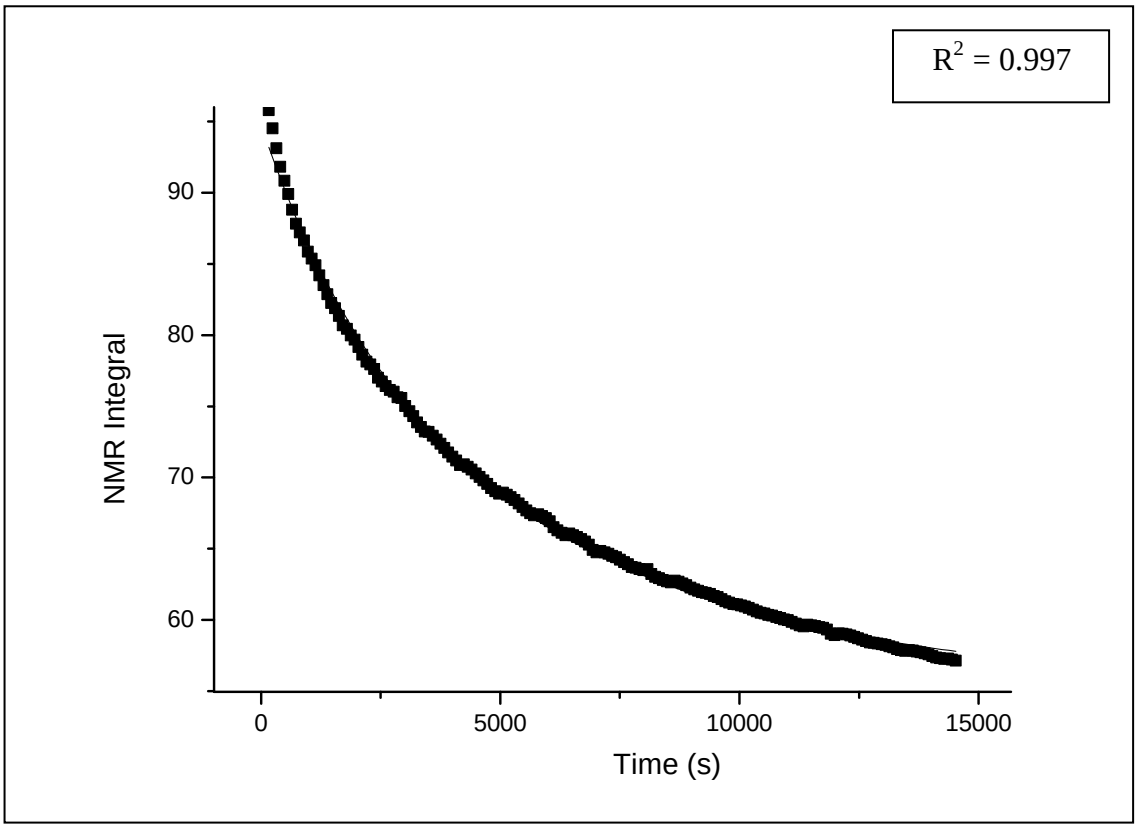

Figure 3.11 Plot of NMR integral intensity as a function of time for the vinyl resonances of *exo*-$NBCH_2OCH_2C(CF_3)_2OH$, polymerised using 'decomposed **Pd1388'** in TCE at 70 ºC. The data has been fitted to equation 3.3 using non-linear curve fitting in Origin 8.1.

3.6.4. Comparison of kinetics data for the polymerisation of SX1

The kinetics data obtained in sections 3.6.1-3.6.3 are summarised in Table 3.1. The conversion of monomer to polymer as a function of time for each of the systems studied is given in Figure 3.12. The highest degree of conversion of the three systems studied is observed using **Pd1388** in TCE (94%) compared with 65% in a 5:1 mixture of toluene:fluorobenzene. In TCE, conversion using decomposed **Pd1388** is approximately half that achieved when **Pd1388** is used as a pro-initiator.

The use of TCE as a reaction solvent for the polymerisation of **SX1** results in values of both k_1 and k_2 that are an order of magnitude (~12 times) faster than in a 5:1 toluene:fluorobenzene mixture (v/v). For reactions carried out in TCE, the use of decomposed **Pd1388** as the initiator system results in rate constants which are an order of magnitude lower than those obtained using the **Pd1388** pro-initiator.

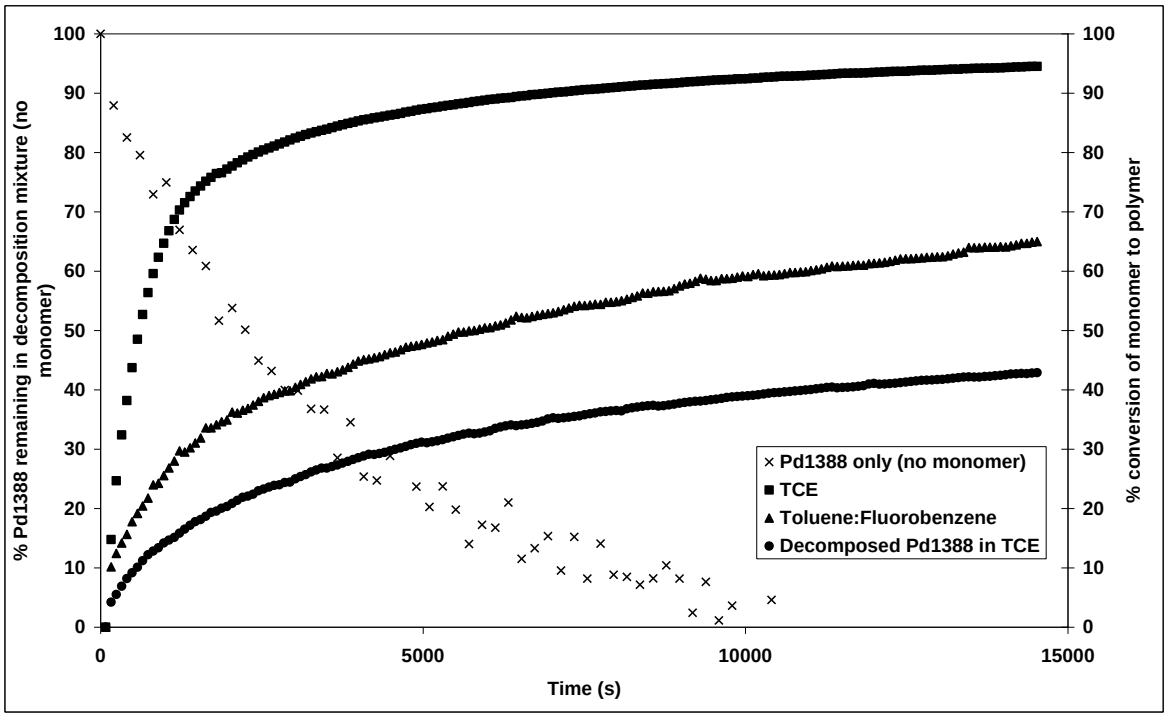

Figure 3.12 Percentage conversion of monomer to polymer for the polymerisation of *exo*-$NBCH_2OCH_2C(CF_3)_2OH$ at 70 °C using **Pd1388**, monitored by ^1H NMR spectroscopy. The percentage decomposition of **Pd1388** as a function of time in the absence of monomer under identical conditions (monitored separately by ^{31}P NMR spectroscopy) is also superimposed.

Table 3.1 Summary of conversion of monomer to polymer after 4 hours and rate constants for polymerisation of *exo*-$NBCH_2OCH_2C(CF_3)_2OH$ at 70 ºC

Solvent	**Conversion (%)**	k_1 **(10^{-4} s^{-1})**	k_2 **(10^{-3} Mol^{-1} dm^3s^{-1})**	R^2
TCE	94	22.2 ± 0.5	7.91 ± 0.09	0.995
Toluene:Fbenzene	65	1.76 ± 0.04	0.91 ± 0.02	0.993
TCE (Dec. Pd1388)	43	1.07 ± 0.01	0.86 ± 0.008	0.997

Previous studies relating to the vinyl polymerisation of a mixture of *endo* and *exo* decyl norbornene, also initiated using **Pd1388**, have demonstrated that solvent polarity can have a significant impact upon the rate of polymerisation, with polymerisation reactions proceeding more quickly as solvent polarity is increased.[6] This

effect is presumed to result from the fact that the initiator complex **Pd1388**, consists of a cationic palladium component $[Pd(H)(MeCN)(PCy_3)_2]^+$, (or more relevantly its active form $[Pd(H)L_2]^+$ in which one of the ligands has dissociated), stabilised by a weakly coordinating anion, $[B(C_6F_5)_4]$. Greater solvent polarity decreases the extent of cation-anion interaction resulting in an increase in polymerisation rate. The solvent effects observed may be attributed to the higher polarity of TCE, which has a dielectric constant of 8.4 (20 ºC) compared with those of either toluene or fluorobenzene, 2.4 (25 ºC) and 5.4 (24 ºC), respectively.[25]

3.7 Polymers of *exo*-$NBCH_2OCH_2C(CF_3)_2OH$ (SX1) prepared using Pd1388

The kinetics of a particular polymerisation reaction give an interesting insight into the polymerisation process, however they do not provide information about the structure and properties of the final polymers obtained. Detailed information relating to the molecular weight and polydispersity index (PDI) of polymeric materials is readily obtained using GPC.

3.7.1 A note on the use of GPC techniques in the analysis of HFP-functionalised polynorbornenes

Analysis of the polymers obtained in section 3.7.2 was attempted using GPC with a triple detector system (refractive index, viscometry and light scattering) in order to determine molecular weights and PDI. However, the polymers prepared are of relatively low molecular weight (due to the high initiator loading of 50:1) and are also highly fluorinated, resulting in poor light scattering behaviour.[26] The d_n/d_c ratio value calculated for poly(*exo*-$NBCH_2OCH_2C(CF_3)_2OH$) in THF was found to be extremely low, 0.0348, (*c.f.* 0.185 for polystyrene). The d_n/d_c was also calculated for poly (decyl norbornene) as a comparison and found to be 0.0924. The combination of low d_n/d_c and low molecular weight of HFP-functionalised norbornenes made analysis by light scattering difficult. Therefore, all molecular weight values quoted are relative to polystyrene standards and hence are not absolute values, as the hydrodynamic volumes of polystyrene and polynorbornene are somewhat different.[27] Absolute molecular weights could be calculated by preparing polynorbornenes with a range of molecular weights to generate a calibration curve and hence provide a 'correction factor', relative to polystyrene. However, for the majority of the polymers prepared in this work, insufficient monomer was available to make such experiments possible. Despite the non-absolute values, molecular weights relative to polystyrene and PDI provide a useful

means of comparison between polynorbornenes of similar structure, such as those prepared using a variety of solvent systems.

3.7.2 GPC analysis of poly(SX1) prepared using Pd1388

The polymers obtained upon completion of each of the reactions studied in sections 3.6.1-3.6.4 were isolated and analysed by GPC using THF as eluent. Molecular weight and polydispersity data are given in Table 3.2.

Table 3.2 Molecular weight, polydispersity and conversion data for the polymerisation of *exo*-$NBCH_2OCH_2C(CF_3)_2OH$ after 4 hours at 70 ºC using **Pd1388** in various solvent systems.

	Solvent	Conversion (%)	M_n (Daltons)	M_w (Daltons)	PDI
1	TCE	94	15900	22900	1.4
2	Toluene:Fbenzene	65	4300	7300	1.4
3	TCE (Dec. Pd1388)	43	7200	16500	2.2

The polymer obtained from **Pd1388** in neat TCE (1) shows the highest number average molecular weight of the three systems studied along with the corresponding highest degree of conversion. The PDI is also reasonably low for the polymers obtained from HFP-functionalised monomers polymerised using palladium – based initiators, suggesting a fairly well controlled polymerisation reaction. As a comparison, Feiring and co workers reported a PDI of 1.9 for the polymerisation of 100 equivalents of an *endo*/*exo* mixture of $NBCH_2OCH_2C(CF_3)_2OH$ initiated using the allyl palladium complex [η^3-allyl$PdCl_2$] and silver hexafluoroantimonate in chlorobenzene at ambient temperature.[5]

In a mixture of toluene:fluorobenzene (2), the molecular weight of the polymer obtained is somewhat lower than that observed in TCE. However, the PDI of the polymer is similar to that obtained using TCE, also suggesting a well controlled polymerisation despite the lower degree of conversion.

When decomposed **Pd1388** is used as the initiator system (3), the molecular weight of the polymer is lower than that achieved using **Pd1388** in TCE (1), which is not entirely unexpected considering a lower degree of conversion. However, the PDI is

somewhat broader than that of the polymer in system 1, which may be attributable to the presence of chain transfer and chain termination processes.

Comparison of the three systems studied highlights that **Pd1388** in TCE allows the generation of well defined polymers of reasonably narrow polydispersity with a high degree of conversion in a reasonable timescale. For this reason, it was decided to conduct all subsequent polymerisation studies in TCE, despite the now established decomposition of **Pd1388** in this solvent medium.

3.8 Conclusions

The discrete complex $[Pd(H)(MeCN)(PCy_3)_2][B(C_6F_5)_4]$ (**Pd1388**) is unstable in TCE at a temperature of 70 °C and decomposes to form $PdCl_2(PCy_3)_2$ and two further species, **b** and **c**, which could not be identified. In TCE both **Pd1388** itself and **Pd1388** in its decomposed form (*i.e.* a mixture of $PdCl_2(PCy_3)_2$, **b** and **c**) are able to act as pro-initiator systems in the polymerisation of *exo*-$NBCH_2OCH_2C(CF_3)_2OH$ (**SX1**).

The kinetics of polymerisation of **SX1** can be approximated using a kinetic model denoted by equation 3.3. The model contains two rate constants, k_1 and k_2, which together provide an excellent approximation of the overall observed rate of polymerisation. k_1 is a function of monomer concentration, [M], at a given time and describes the rate of polymerisation in terms of *pseudo*-first order kinetics. k_2 considers both free monomer concentration, [M], and the amount of monomer consumed ($[M]_0$-[M]). For this model we assume that any monomer consumed has been incorporated into a polymer chain.

Values of k_1, k_2 and $[M]_0$' are obtained *via* non-linear curve fitting of experimentally-determined monomer consumption data to equation 3.3 using Origin 8.1. The model was shown to provide an excellent fit to the data for polymerisation of **SX1** using **Pd1388** and its decomposed form in both TCE and a 5:1 (v/v) mixture of toluene:fluorobenzene with R^2 values of 0.993 or greater. For polymerisation of **SX1**, both k_1 and k_2 are highest using **Pd1388** in polar solvents such as TCE and these rapid polymerisation kinetics correlate well with the high degree of conversion (94%) observed. The polymerisation reaction proceeds more slowly using decomposed **Pd1388** and conversion is approximately half that achieved using **Pd1388** itself in the same time frame, resulting in a HFP-functionalised poly(norbornene) of lower molecular weight and higher polydispersity. **Pd1388** will also act as a pro-initiator in a 5:1 (v/v) mixture of toluene:fluorobenzene, however conversion and polymerisation rate are significantly lower than in the more polar solvent TCE, resulting in a HFP-

functionalised poly(norbornene) of lower molecular weight. High conversion is of vital importance industrially to generate the maximum yield of polymer in the shortest possible time frame.

Although not perfect, the kinetic model proposed goes some way to describing the rate of polymerisation of **SX1** over the course of the reaction, required by industry in order to compare different solvent system and ultimately different monomers, and provides an excellent fit to experimental data for monomer consumption as a function of time. In the following chapters, the kinetic model will be applied more generally to the polymerisation of a series of HFP-functionalised norbornenes of commercial importance.

3.9 References

1. C. Janiak and P.G. Lassahn, *J. Mol. Catal. A: Chem*. 2001, **166**, 193-209
2. F. Blank and C. Janiak, *Coord. Chem. Rev.* 2009, **253**, 827-861
3. N. Thirupathi, D. Amoroso, A. Bell and J.D. Protasiewicz, *J. Polym. Sci. A: Polym. Chem.* 2009, 47, 103-110
4. A. Bell, D. Amoroso, J.D. Protasiewicz and N. Thirupathi, US 2005/0187398, 2005
5. A.E. Feiring, J. Feldman, F.L. Schadt, III, G. Newton Taylor, US 2005/6884564 B2
6. A.T. Cooper, PhD Thesis, Durham University, 2008
7. A. Goto and T. Fukuda, *Prog. Polym. Sci.* 2004, 29, 329-385
8. F. Song, R.D. Cannon and M. Bochmann, *J. Am. Chem. Soc.*, 2003, **125**, 7641-7653
9. M. Bochmann, *J. Organometal. Chem.* 2004, **689**, 3982-3998
10. A. Duda and A. Kowalski, *Handbook of Ring Opening Polymerisation* (P. Dubois, O. Coulembier and J.M. Raquez (eds), Wiley-VCH, Weinheim, 2009, p. 1-51
11. C. Andes, L. Fischetti, A. Hennis and A. Sen, *Polym. Prepr.* 2002, **43**, 963-964
12. J.K. Funk, C. Andes and A. Sen, *Polym. Prepr.* 2003, **44**, 681-682
13. J.K. Funk, C. Andes and A. Sen, *Organometallics*, 2004, **23**, 1680-1683
14. M. Kang and A. Sen, *Organometallics*, 2004, **23**, 5396-5398
15. N. Nerfert and G. Fink, *Makromol. Chem., Macromol. Sym.*, 1993, **66**, 157-170
16. S. Jüngling, R. Mülhaupt, U. Stehling, H.H. Brintzinger, D. Fischer and F. Langhauser, *Makromol. Chem., Macromol. Sym.*, 1995, **97**, 205-216
17. M. Ystenes, *J. Catal*., 1991, **129**, 383-401
18. K. Thorshaug, J. Støvneng, E. Rytter and M. Ystenes, *Macromolecules*, 1998, **31**, 7149-7165

19. R.J. Muñoz-Escalona, V. Cruz and J. Martinez-Salazar, *J. Polym. Sci, A: Polym. Chem.*, 2000, **38**, 571-582

20. P.W. Atkins, C.H. Langford, and D.F. Shriver, *Inorganic Chemistry*, 2nd edtn., Oxford University Press, Oxford, 1993, p. 213

21. S.M. Godfrey, C.A. McAuliffe, R.G. Pritchard, J.M. Sheffield and G.M. Thompson, *J. Chem. Soc., Dalton Trans.* 1997, **24**, 4823-4827

22. R. Appel and H. Schöler, 1977, *Chem. Ber*. **110**, 2382

23. P.K. Monks, Ph.D Thesis, Durham University, 2007

24. V.V. Grushin, C. Bensimon and H. Alper, *Inorg. Chem.* 1994, **33**, 4804-4806

25. R.C. Weast, *Handbook of Chemistry and Physics,* 63rd edtn, CRC Press, Florida, 1982, E53

26. M. Haney, P. Clarke, B. Postama, and Viscotrek: *New Technologies in GPC and Viscosities, GPC Masterclass: An Advanced GPC/SEC Training School* September/October 1997, Course Material

27. Y. Li and S. Bo, *Chromatographia*, 2004, **59**, 299-303

Chapter IV

Polymerisation of *endo*- and *exo*-hexafluoropropanol functionalised norbornene monomers

Chapter IV

Polymerisation of *endo*- and *exo*-hexafluoropropanol-functionalised norbornene monomers

4.1 Introduction

The polymerisation of hexafluoropropanol-functionalised (HFP) norbornenes is of key industrial importance and forms the basis of this thesis. Previous chapters have described the synthesis of a series of such monomers and a preliminary study of the polymerisation behaviour for a model monomer system, *exo*-$NBCH_2OCH_2C(CF_3)_2OH$ (**SX1**), under conditions of industrial relevance. This chapter will build on this work and extend the ideas and kinetic model discussed to the polymerisation behaviour of a series of pure *endo*- and pure *exo*-HFP-functionalised norbornene monomers.

4.2 Results and Discussion

4.2.1 Kinetics of the vinyl polymerisation of hexafluoropropanol-functionalised norbornene monomers using Pd1388

In Chapter III a kinetic model, given by equation 3.2 and its integrated form, equation 3.3, was proposed in order to accurately describe the polymerisation kinetics of a model system, *exo*-$NBCH_2OCH_2C(CF_3)_2OH$ (**SX1**) initiated using **Pd1388**. The model contains two rate constants, k_1 and k_2, which together provide an excellent approximation of the overall observed rate of polymerisation. k_1 is a function of monomer concentration, [M], at a given time and describes the rate of polymerisation in terms of *pseudo*-first order kinetics. k_2 considers both free monomer concentration, [M], and the amount of monomer consumed ($[M]_0$-[M]). For this model we assume that any monomer consumed has been incorporated into a polymer chain.

$$\frac{d[M]}{dt} = -((k_1 - k_2([M]_0^{'} - [M]))[M] \qquad \text{Equation 3.2}$$

$$[M] = \frac{[M]_0^{'}(k_1 - [M]_0^{'}k_2)e^{-(k_1 - [M]_0^{'}k_2)t}}{k_1 - [M]_0^{'}k_2 e^{-(k_1 - [M]_0^{'}k_2)t}} \qquad \text{Equation 3.3}$$

In order to test the wider suitability of the kinetic model to the study of other HFP-functionalised monomers, the polymerisation behaviour of the series of monomers of the type $NB(CH_2)_nOCH_2C(CF_3)_2OH$ (n = 0-3) and $NB(CH_2)_nC(CF_3)_2OH$ (n = 1) was examined in detail. The study was also used to examine the effect of various numbers of methylene spacer groups, (n), separating the HFP-functionality from the norbornene skeleton, on polymerisation rate. Work in this chapter describes the polymerisation of pure *endo*- and pure-*exo* isomers; mixtures of isomers will be considered in chapter V.

Polymerisation reactions were carried out for a series of pure *exo* and pure *endo* HFP-functionalised norbornenes and was initiated using **Pd1388** (50:1 monomer:initiator) in d_2-TCE at 70 ºC, conditions optimised in Chapter III. Reactions were monitored using ^{1}H NMR spectroscopy and the resulting monomer consumption data fitted to equation 3.3 using non-linear curve fitting in Origin 8.1. Where possible, the rate of hydride loss was also measured and analysed according to *pseudo*-first order kinetics. In each case, polymerisation reactions were repeated at least three times under identical conditions unless otherwise stated. Rate constants are quoted as mean values with their associated standard deviation. Full details of the kinetic analysis, including the errors in each of the rate constants, determined from the fitting of experimental data to equation 3.3 and corresponding R^2 values are given in Appendix 3.

4.2.1.1 Rates of hydride consumption, k_H, in the polymerisation of HFP-functionalised norbornenes

As discussed in section 3.3 (Scheme 3.1), the initiation process for the vinyl polymerisation of norbornenes using palladium-hydride initiators relies upon a complex series of equilibria. For this reason, although the rate of hydride consumption (k_H), measured experimentally contributes to the rate of initiation, the two rate constants are not necessarily equivalent. Rates of hydride (**Pd1388**) consumption (k_H) were obtained by analysis of hydride consumption data (measured experimentally) using *pseudo* first-order kinetics, as discussed in section 3.6.1, and are summarised in Table 4.1.

Table 4.1 Rates of hydride consumption, k_H, and rate constants of propagation (k_1 and k_2) for the polymerisation of a series of hexafluoropropanol-functionalised norbornene monomers polymerised using **Pd1388** at 70 ºC in d_2-TCE

Monomer	Code	n	k_H (10^{-3} s^{-1})	k_1 (10^{-4} s^{-1})	k_2 (10^{-3} $Mol^{-1}dm^3s^{-1}$)
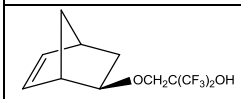	**ZX3**	0[§]	3.00 ± 0.02	1.15 ± 0.05	3.51 ± 0.2
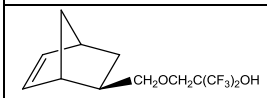	**SX1**	1	7.36 ± 1	22.4 ± 0.2	7.21 ± 0.6
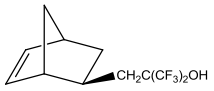	**SX2**	1	13.3 ± 2	30.0 ± 9	8.88 ± 1
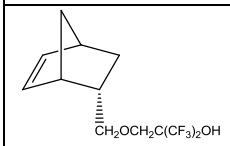	**SN2**	1	2.64 ± 0.1	0.40 ± 0.005	0.63 ± 0.007
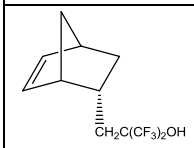	**SN3**	1	2.93 ± 0.4	0.75 ± 0.01	0.165 ± 0.03
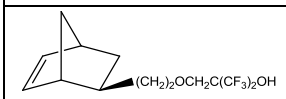	**DX2**	2	-*	120 ± 0.5	29.9 ± 2
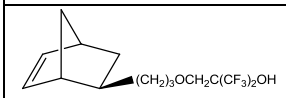	**TX2**	3	-*	269 ± 15	50.3 ± 9

[§] Monomer contains 2% of the *endo* isomer, see section 2.2.2

* Reaction was too rapid for k_H to be determined under conditions used

Comparison between the rate of hydride loss observed during polymerisation of **SX1** (*exo*-$NBCH_2OCH_2C(CF_3)_2OH$) with that observed for **SX2** (*exo*-$NBCH_2C(CF_3)_2OH$), for both of which n = 1, indicates more rapid consumption of the hydride in the latter case. Possible explanations for the difference in the rate between **SX1** and **SX2** could relate to the presence of an ether oxygen in the spacer group

separating the $C(CF_3)_2OH$ from the norbornene skeleton (CH_2OCH_2 for **SX1** versus CH_2 for **SX2**) or may simply be a result of the spacer chain length.

Interestingly, the rates of hydride loss observed for polymerisation of pure *endo*-monomers **SN2** and **SN3** are identical within the error limits of the experiment. This is in contrast to the difference observed between their *exo* counterparts, **SX1** and **SX2**, respectively. For both types of monomer, $NBCH_2OCH_2C(CF_3)_2OH$ (**SX1** and **SN2**) and $NBCH_2C(CF_3)_2OH$ (**SX2** and **SN3**), the rate of hydride loss is considerably (>3 times) greater for the *exo* isomer (**SX1** and **SX2**) than its *endo* counterpart (**SN2** and **SN3**, respectively).

The rate of hydride consumption was also measured for the monomer **ZX3** for which n = 0. However, **ZX3** contains 2% of the *endo* isomer (see section 2.2.2). As the contribution of the *endo* isomer within a mixture to the rate of hydride loss is at the present time unknown, direct comparison of the values of k_H observed for **ZX3** with rates observed for pure *exo* isomers is not possible.

For the polymerisation of **DX2** and **TX2** (n = 2 and 3 respectively), the rate of hydride consumption was extremely rapid, with complete disappearance of the hydride resonance within the time taken to acquire 2-3 ^{1}H NMR spectra (<2 minutes), hence insufficient data points were available from which to calculate k_H. However, a qualitative assessment of spectra indicates that the rate of hydride consumption is faster during the polymerisation of **TX2** (n = 3) than for **DX2** (n = 2) suggesting that in general, an increase in chain length results in a corresponding increase in the rate of hydride loss observed.

4.2.2.2 First- and second-order rate constants of propagation (k_1 and k_2) for the polymerisation of HFP-functionalised norbornenes

Monomer consumption data for the series of monomers $NB(CH_2)_nOCH_2C(CF_3)_2OH$ and $NB(CH_2)_nC(CF_3)_2OH$ was fitted to equation 3.3, as described in chapter III. The rate constants of propagation (k_1 and k_2) obtained from the fit of the experimental data to the model described by equation 3.3 are summarised in Table 4.1 and Figures 4.1 and 4.2.

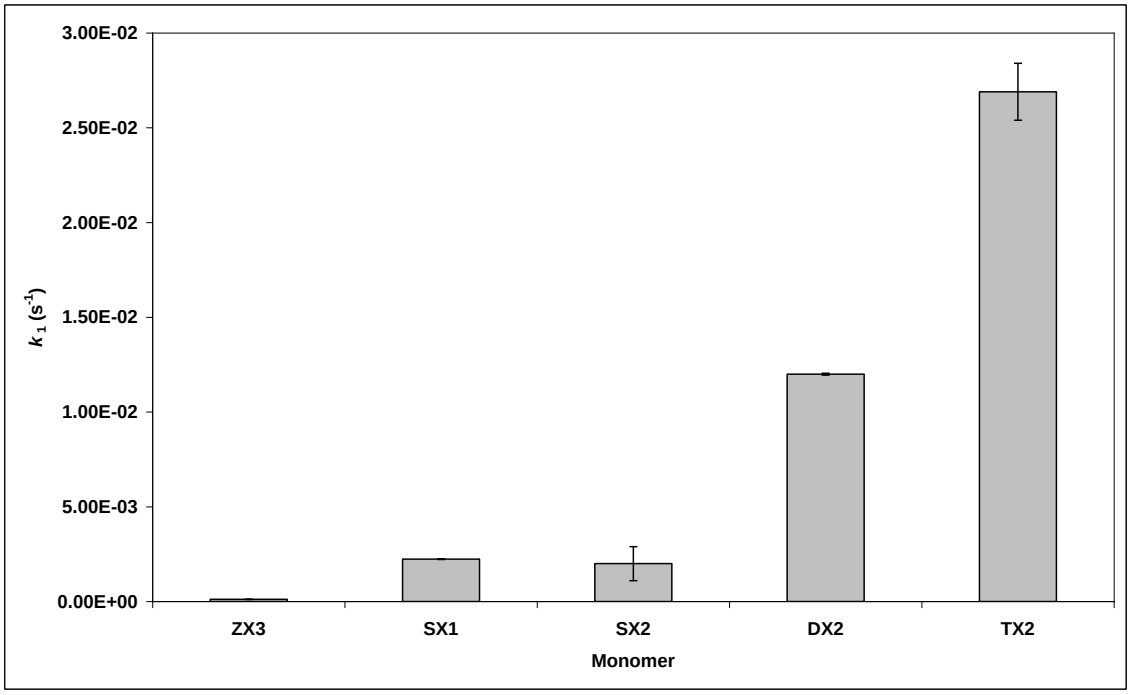

Figure 4.1 Comparison of first-order rate constants (with errors) of propagation for a series of *exo* hexafluoropropanol-functionalised norbornene monomers polymerised using **Pd1388** at 70 ºC in d_2-TCE

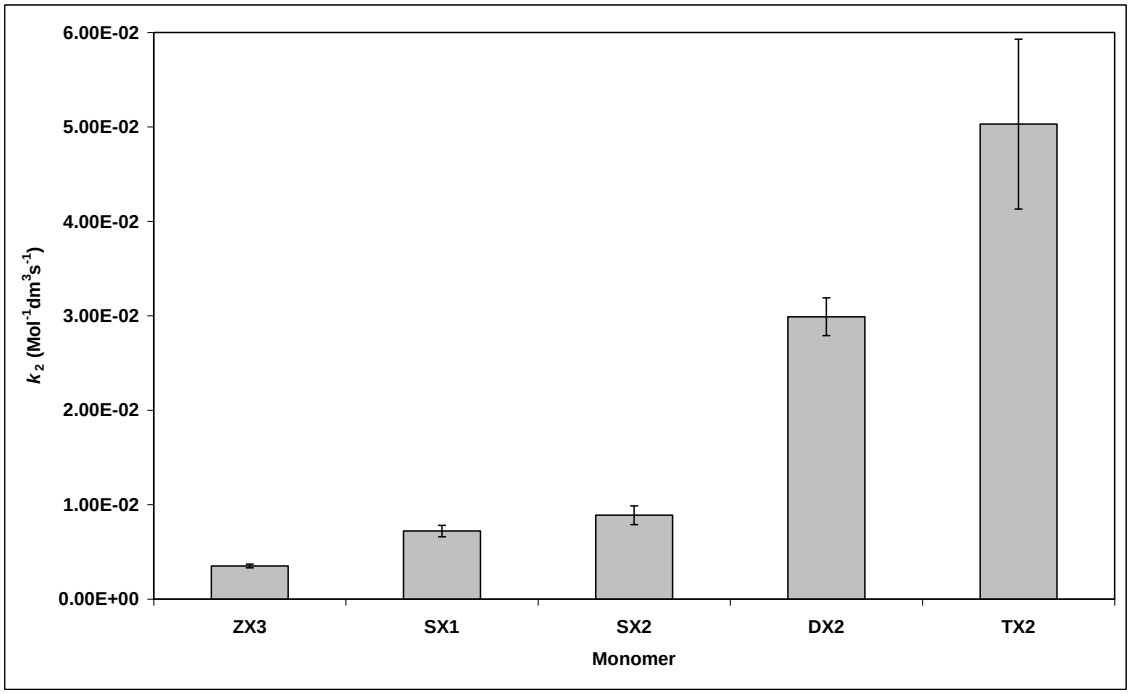

Figure 4.2 Comparison of second-order rate constants (with errors) of propagation for a series of *exo* hexafluoropropanol-functionalised norbornene monomers polymerised using **Pd1388** at 70 ºC in d_2-TCE

For each of the monomers studied, equation 3.3 provides an excellent fit to experimental data with R^2 values of 0.993 or greater for each of the individual polymerisation reactions carried out. For the series of *exo*-functionalised norbornene monomers, $NB(CH_2)_nOCH_2C(CF_3)_2OH$, an increase in the value of n from 0 to 3 leads to an increase in k_1 by two orders of magnitude. A corresponding increase is also observed in k_2, however the magnitude of this increase is much smaller than for k_1. As discussed in section 4.4.1, the n = 0 **ZX3** system contains 2% of the *endo* isomer, hence comparison with pure *exo* systems is purely qualitative. However, the observed increase in polymerisation rates between n = 1 (**ZX1**) and n = 3 (**TX2**) confirms that spacing the HFP functionality further away from the norbornene skeleton leads to an increase in overall polymerisation rate. The rates observed for **ZX3** (n = 0) correlate well with the expected trend. The increase in k_1 observed following the addition of each subsequent CH_2 unit becomes less apparent as n is increased. Moving from n = 1 (**SX1**) to n = 2 (**DX2**) leads to a 5 times increase in rate, however on moving from n = 2 (**DX2**) to n = 3 (**TX3**) a doubling of polymerisation rate is observed.

In the case of the pure *endo* analogues of **SX1** and **SX2** namely **SN2** and **SN3**, respectively, comparable rates are not observed. In the polymerisation of **SN3**, k_1 is approximately double that of **SN2**. However, for the rate constant k_2, the trend is reversed with the k_2 value for polymerisation of **SN2** being significantly higher. For both types of monomer, $NBCH_2OCH_2C(CF_3)_2OH$ (**SX1** and **SN2**) and $NBCH_2C(CF_3)_2OH$ (**SX2** and **SN3**), both k_1 and k_2 are considerably higher for the *exo*-isomer (**SX1** and **SX2**) than its *endo* counterpart (**SN2** and **SN3**, respectively). The difference in k_1 between *endo* and *exo* isomers is monomer dependant (56 and 40 times greater for *exo*-$NBCH_2OCH_2C(CF_3)_2OH$ and *exo*-$NBCH_2C(CF_3)_2OH$ versus the corresponding *endo*-isomer, respectively.) For each of the monomers studied, k_2 is significantly larger than k_1, however the magnitude of the difference between the two rate constants is monomer-dependent.

4.2.2 Polymerisation of hexafluoropropanol-functionalised norbornenes - the effect of the number of methylene spacer groups (n) on polymer molecular weight and PDI

Polymerisation reactions were carried out in Young's tap NMR tubes, and percentage conversion determined using ^1H NMR spectroscopic analysis with mesitylene as an internal standard. Polymers were isolated *via* precipitation into hexane and analysed using GPC (THF). A summary of molecular weight, polydispersity and conversion data

is given in Table 4.2. All values of molecular weight are quoted relative to polystyrene standards due to the poor light scattering of the polymers (see section 3.7.1) and are hence not absolute.

For the series of pure *exo* hexafluoropropanol-functionalised monomers, $NB(CH_2)_nOCH_2C(CF_3)_2OH$ an increase in the value of n from 1 to 3 (is accompanied by an increase in conversion as well as a corresponding increase in both number and weight average molecular weights of the polymers obtained. The polymers display monomodal GPC traces with values of PDI that are fairly consistent, irrespective of the value of n, ranging between 1.2 and 1.4 for each of the pure *exo* polymers studied.

In the case of the pure *endo* monomers **SN2** and **SN3**, conversions are relatively low (20 and 27%, respectively). Polymerisation of **SN2** results in a polymer of low molecular weight with moderate polydispersity (1.7). However, polymerisation of **SN3** generates a polymer with a bimodal character, consisting of species with M_P = 34,000 and 9000 Daltons, respectively, a result which was completely reproducible. The *endo*-/*exo*- mixture of $NBCH_2C(CF_3)_2OH$ (**SXN4**) also shows a bimodal distribution, as discussed in Chapter V. However whilst consistent, a satisfactory explanation for the bimodal distribution observed for this particular monomer has not been established.

Table 4.2 Experimentally-determined molecular weight, polydispersity and conversion data for a series of hexafluoropropanol-functionalised norbornene monomers polymerised using **Pd1388**, after 3 hours at 70 °C in d_2-TCE

Monomer	Code	M_n (Daltons) *	M_w (Daltons) *	M_p (Daltons) *	PDI	Conversion (%)[§]
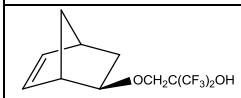	**ZX3**	4500	6500	8200	1.4	**17**
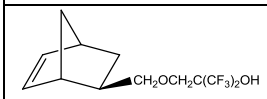	**SX1**	5900	6800	7300	1.2	**94**
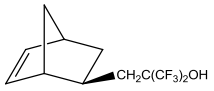	**SX2**	8500	11100	12500	1.3	**99**
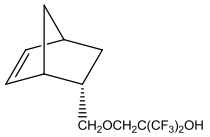	**SN2**	4500	7900	8200	1.7	**20**
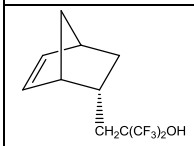	**SN3**	27100 4900	33300 5700	34400 9400	-[‡]	**27**
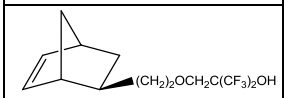	**DX2**	8600	11100	13500	1.3	**100**
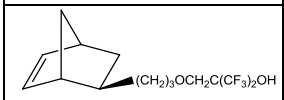	**TX2**	11300	15600	19600	1.4	**100**

* All molecular weights are relative to polystyrene standards

[§] Percentage conversion determined using ^{1}H NMR spectroscopy

[‡] The GPC trace shows a bimodal distribution hence it is not possible to determine a meaningful value of PDI.

4.2.3 Exploring the polymerisation behaviour of hexafluoropropanol-functionalised norbornenes as a function of time - GPC studies

The kinetics of polymerisation of a series of pure *exo* and pure *endo* hexafluoropropanol (HFP)-functionalised norbornenes has been discussed in detail in section 4.3 along with analysis of the resultant polymers in section 4.4. However, whilst analysis of polymerisation kinetics data gives an insight into polymerisation rate, it provides no information relating to the properties of the polymer (such as molecular weight and polydispersity) as the reaction progresses. To address this issue, studies were conducted in which the molecular weight, PDI and conversion were monitored at various time intervals throughout the course of a series of polymerisation reactions.

Polymerisations were conducted under similar conditions to those used in order to determine the polymerisation kinetics. A 50:1 ratio of monomer:initiator (**Pd1388**) was maintained along with a reaction temperature of 70 ºC. Reactions were conducted in either TCE or a mixture of toluene and fluorobenzene, containing nonane as an internal standard. Reactions were carried out on a scale between 1-5 g to allow numerous samples to be extracted from the reaction vessel over a period of time. The polymerisation reactions were heated by means of an oil bath and stirred vigorously using a magnetic stirrer bar. Samples were extracted at various intervals between 1 minute and 3 hours using a pre-heated glass syringe fitted with a wide bore needle. Warming of the syringe setup was necessary as polymer started to precipitate from the reaction solution upon cooling. Samples were immediately quenched in methanol to prevent further reaction and an aliquot of the methanol/TCE reaction mixture removed for analysis by GC. The methanol/TCE solution was reduced to dryness and redissolved in the minimum of THF. The THF solution was then filtered through Celite to remove colloidal palladium and the polymers isolated *via* precipitation into hexane and dried overnight at 40 °C *in vacuo*. After a 3 hour reaction time at 70 °C, the reaction vessel was treated with methanol to quench the polymerisation and the final polymer isolated.

4.2.3.1 Polymerisation of *exo*-$NBCH_2OCH_2C(CF_3)_2OH$ (SX1)

The polymerisation of **SX1** using **Pd1388** highlights a number of interesting features. Firstly, high molecular weight polymer is formed within one minute of starting the reaction, at a corresponding degree of conversion of 35%. Secondly, the polymer obtained after 1 minute reaction time consists of three distinct species, each with different molecular weights (M_p = 4000, 21,000 and 70,000 Daltons, respectively, Table 4.3), characterised by the trimodal GPC trace illustrated in Figure 4.3 (red line).

Thirdly, and perhaps most interestingly, the molecular weight of the polymer obtained changes as a function of time, with loss of both high and low molecular weight species to yield a final polymer with peak average molecular weight of 22,000 Daltons and moderately low polydispersity of 1.4 (Figure 4.3, black line). The low molecular weight species was attributed to oligomers of around ten monomer units and its disappearance as a function of time is expected with contained growth of the polymer chain. Loss of the high molecular weight species, which is complete within 25 minutes, is extremely unusual, and consequently much more difficult to explain. The molecular weight and conversion data for a selection of the polymer samples obtained are summarised in Table 4.6. It is worthwhile to note that differences in conversion observed at 11 and 18 minutes (82 and 76 %, respectively) suggest the possibility of a 'depolymerisation' reaction. However, the difference is only marginally beyond the error limit of the experiment, hence it is not possible to draw any firm conclusions. The error limits of the GPC analysis are considered in this instance, to be a maximum of ± 2000 Daltons, with all values quoted relative to polystyrene standards.

The polymerisation of **SX1** by **Pd1388** was followed by ^{1}H NMR spectroscopy at 70 °C as a function of time. This study of **Pd1388** showed the steady disappearance of both the palladium hydride resonance of initiator (δ -15.5 ppm) and the vinyl resonances of the monomer (δ + 6 ppm). The kinetics of these processes are discussed in sections 4.2.1.1 and 4.2.1.2, respectively.

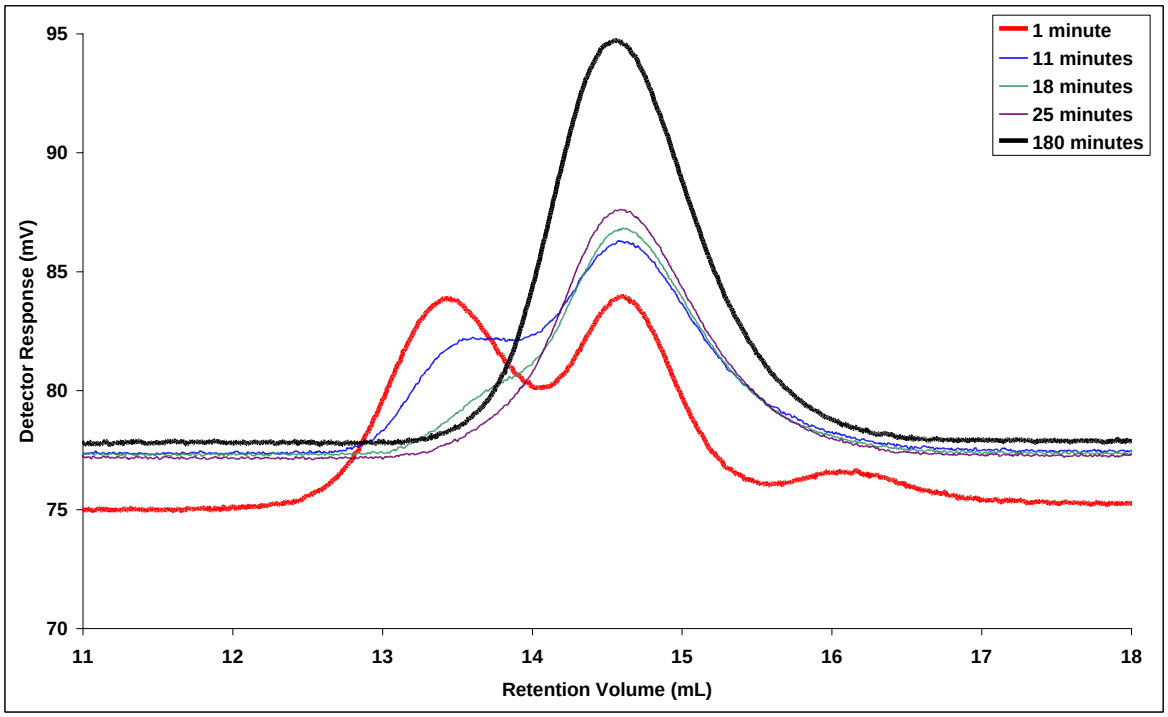

Figure 4.3 GPC traces as a function of time for the polymerisation of *exo*-$NBCH_2OCH_2C(CF_3)_2OH$ (**SX1**) in TCE at 70 ºC using **Pd1388**

Table 4.3 Molecular weight, polydispersity and conversion data as a function of time for the polymerisation of *exo*-$NBCH_2OCH_2C(CF_3)_2OH$ (**SX1**) in TCE at 70 ºC using **Pd1388**

Time (mins)	M_n (Daltons)*	M_w (Daltons)*	M_p (Daltons)*	PDI	Conversion (%)
1	65400 18400 3600	77100 20700 4400	69600 20900 4300	-	35
11	51900 16900	59600 18077	64200 11600	-	82
18	59300 14600	61800 20100	46800 20700	-	76
25	15300	21600	20900	1.4	83
180	16000	22000	21900	1.4	96

* All molecular weights are quoted relative to polystyrene standards

‡ Determined using GC analysis, relative to an internal standard (nonane), error = ± 2%

In order to rule out solvent effects as an explanation for the loss of high molecular weight polymer observed during the polymerisation of **SX1**, the same polymerisation reaction was repeated in a mixture of toluene and fluorobenzene (17:1, v/v). The fluorobenzene was required in order to solubilise the **Pd1388** pro-initiator. Similar effects are observed in toluene:fluorobenzene to those seen in TCE, with an overall change from a trimodal to monomodal system, as illustrated in Figure 4.4. The polymer obtained after 1 minute is characterised by a trimodal trace with species of M_p = 27,000 and 62,000 Daltons, as well as low molecular weight oligomers. On heating the reaction for 180 minutes and subsequent isolation the resulting material exhibits monomodal character with M_p = 15,000 Daltons and PDI = 2.5. The differences in peak molecular weights of the materials obtained in TCE and toluene:fluorobenzene are believed to be related to the different rates of polymerisation, as discussed previously in Chapter III.

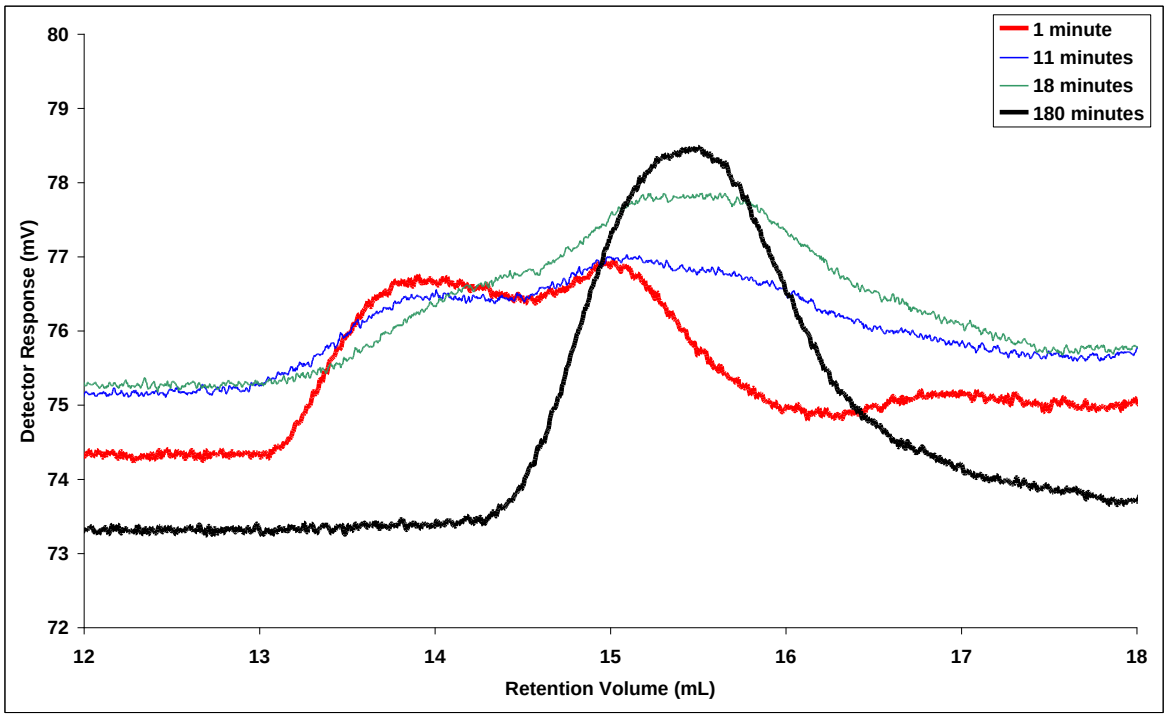

Figure 4.4 GPC traces as a function of time for the polymerisation of *exo*-$NBCH_2OCH_2C(CF_3)_2OH$ (**SX1**) in a 17:1 mixture of toluene:fluorobenzene at 70 ºC using **Pd1388**

4.2.3.2 Polymerisation of *endo*-$NBCH_2OCH_2C(CF_3)_2OH$ (SN2)

The polymerisation of **SN2** was carried out in a manner analogous to that used for polymerisation of the corresponding *exo* isomer, **SX1**, in TCE. The molecular weights of the polymer obtained throughout the reaction range between M_p = 2000 and 7000 Daltons, as illustrated in Figure 4.5 and Table 4.4, with the final polymer obtained after 3 hours characterised by M_p = 3000 Daltons and PDI = 1.4. Overall conversion is 37%, which can be rationalised in terms of the slow polymerisation kinetics observed in section 4.2.1.2.

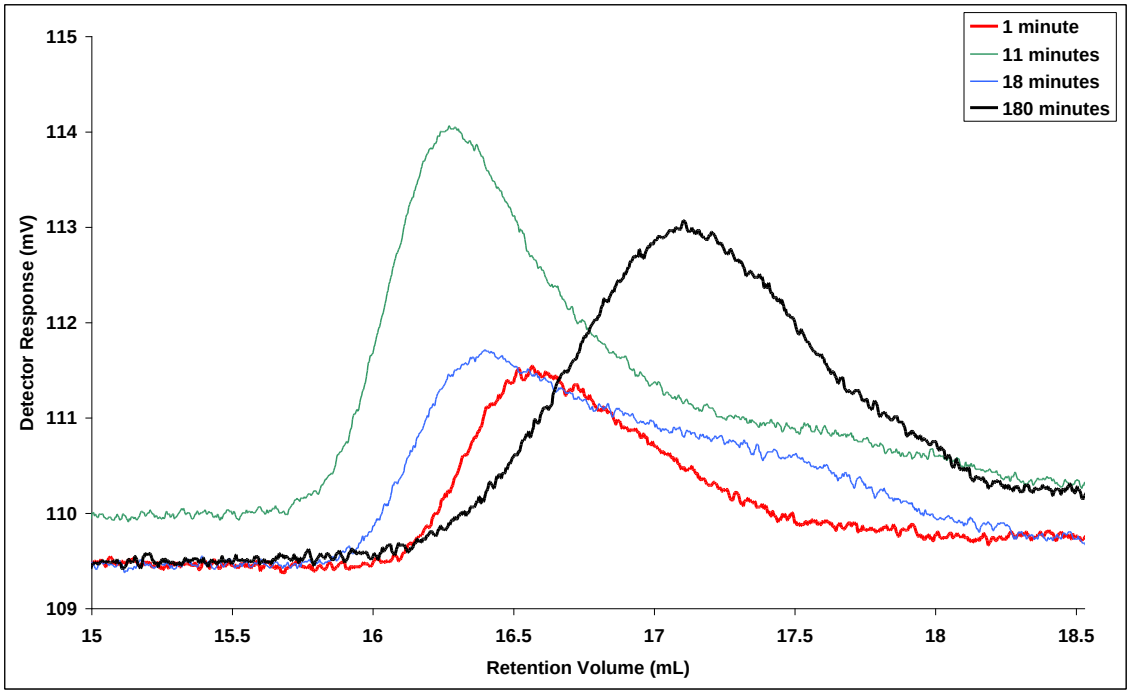

Figure 4.5 GPC traces as a function of time for the polymerisation of *endo*-$NBCH_2OCH_2C(CF_3)_2OH$ (**SN2**) in TCE at 70 ºC using **Pd1388**

Table 4.4 Molecular weight, polydispersity and conversion data as a function of time for the polymerisation of *endo*-$NBCH_2OCH_2C(CF_3)_2OH$ (**SN2**) in TCE at 70 ºC using **Pd1388**

Time (mins)	M_n (Daltons)*	M_w (Daltons)*	M_p (Daltons)*	PDI	Conversion (%)‡
1	3000	4100	5200	1.3	17
11	5500 1200	6300 1500	7300 2400	-	22
18	5300 1600	5800 1900	6300 3000	-	24
180	2000	2900	2900	1.4	37

* All molecular weights are quoted relative to polystyrene standards

‡ Determined using GC analysis, relative to an internal standard (nonane)

4.2.3.3 Polymerisation of *exo*-$NBCH_2C(CF_3)_2OH$ (SX2)

The polymerisation of **SX2** was carried out in a manner analogous to that used for polymerisation of **SX1** in TCE, to confirm if the loss of high molecular weight species observed as a function of time was specific to monomers of the type $NB(CH_2)_nOCH_2C(CF_3)_2OH$ or also occurred in the polymerisation of similar monomers such as $NBCH_2C(CF_3)_2OH$. As illustrated in Figure 4.6, and Table 4.5, a reduction in peak average molecular weight of approximately 15,000 Daltons is observed over the course of the reaction, however all of the polymers obtained show monomodal traces with polydispersities of 1.3 or less. The consistent monomodal character as a function of time is in contrast to the polymerisation of **SX2** which shows a change from trimodal to monomodal character as the reaction progresses. However in both cases, the loss of high molecular weight species is observed as a function of time to yield a polymer with relatively narrow PDI.

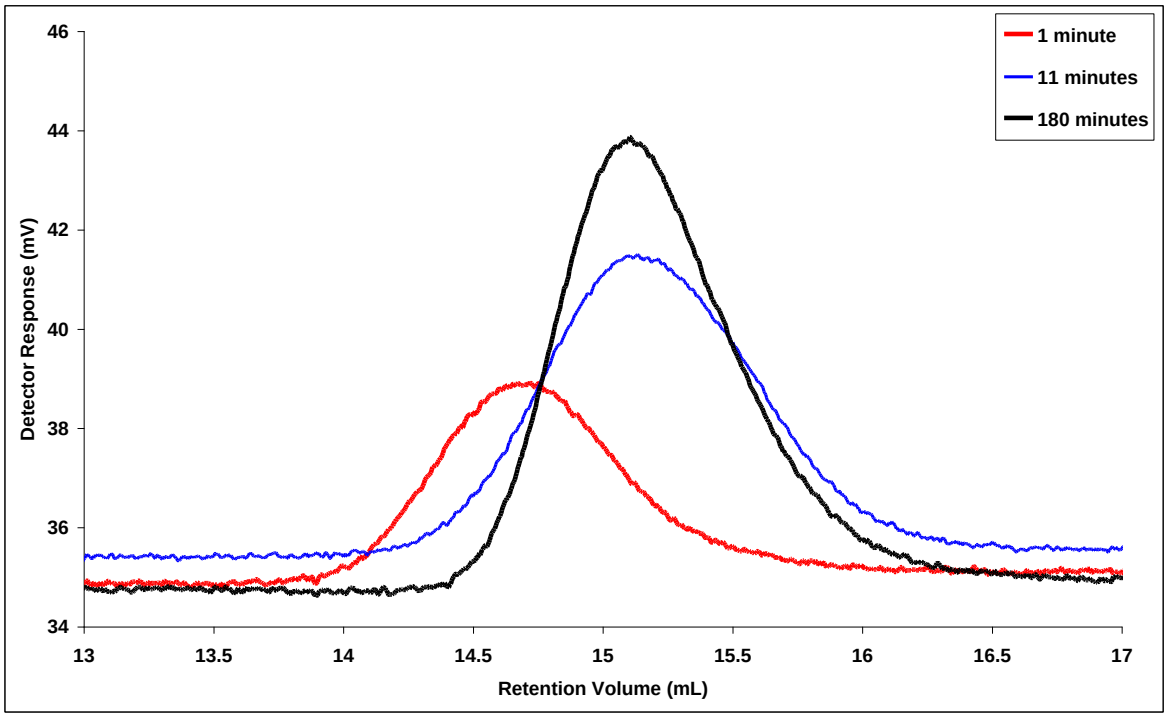

Figure 4.6 GPC traces as a function of time for the polymerisation of *exo*-$NBCH_2C(CF_3)_2OH$ (**SX2**) in TCE at 70 ºC using **Pd1388**

Table 4.5 Molecular weight, polydispersity and conversion data as a function of time for the polymerisation of *exo*-$NBCH_2C(CF_3)_2OH$ (**SX2**) in TCE at 70 ºC using **Pd1388**

Time (mins)	**M_n (Daltons)***	**M_w (Daltons)***	**M_p (Daltons)***	**PDI**	**Conversion (%)‡**
1	27600	36500	38,000	1.3	50
11	18000	23000	22,800	1.3	63
180	17200	21700	23,500	1.3	94

* All molecular weights are quoted relative to polystyrene standards

‡ Determined using GC analysis, relative to an internal standard (nonane)

4.2.3.4 Exploring the reaction of poly(*exo*-$NBCH_2OCH_2C(CF_3)_2OH$) with Pd1388

The observed reduction in molecular weight during the polymerisation of HFP-functionalised norbornenes is extremely unusual. In order to further probe the changes in molecular weight, the reactivity of a sample of isolated poly(*exo*-$NBCH_2OCH_2C(CF_3)_2OH$) with **Pd1388** was explored. A sample of poly(*exo*-$NBCH_2OCH_2C(CF_3)_2OH$), prepared in TCE and of known molecular weight (trimodal, M_p = 69,600, 20,900 and 4300 Daltons, Scheme 4.1, **1**) was treated with a solution of

Pd1388 in TCE and heated for 30 minutes at 70 °C. Polymer (**1**) was insoluble in the reaction solvent, however did swell appreciably. After 30 minutes at 70 °C the resulting polymer (Scheme 4.1, **2**) was isolated *via* work-up and precipitation into hexane, as described previously in section 4.6.1, and analysed using GPC (THF). The molecular weight data obtained for polymers **1** and **2** are given in Table 4.6.

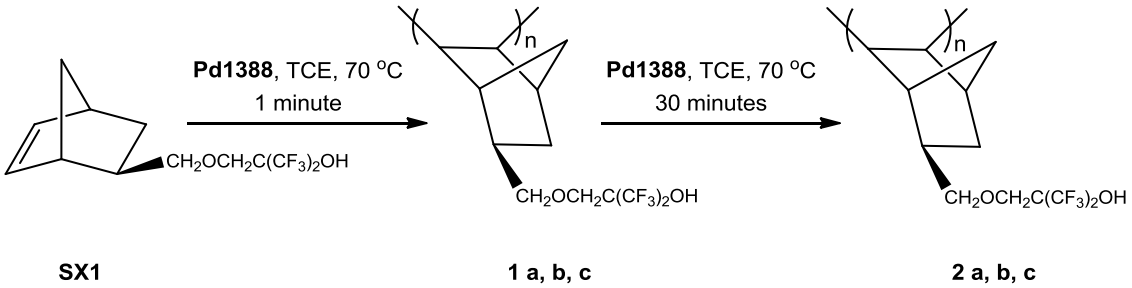

Scheme 4.1 Preparation of poly(*exo*-$NBCH_2OCH_2C(CF_3)_2OH$) and subsequent reaction with **Pd1388** in TCE at 70 °C

Table 4.6 Molecular weight data for poly(*exo*-$NBCH_2OCH_2C(CF_3)_2OH$), before (**1**) and after (**2**) reaction with **Pd1388** at 70 °C.

Polymer	M_n (Daltons)*	M_w (Daltons)*	M_p (Daltons)*
(1)	**65400 (a)**	**77100(a)**	**69600 (a)**
	18400 (**b**)	20700 (**b**)	20900 (**b**)
	3600 (**c**)	4400 (**c**)	4300 (**c**)
(2)	**59100**	**65200**	**60300**
	18200	20400	20900
	4400	4800	7700

* All molecular weights are quoted relative to polystyrene standards

Treatment of poly(*exo*-$NBCH_2OCH_2C(CF_3)_2OH$) (**1**) with **Pd1388** at 70 °C in TCE results in a substantial reduction in the molecular weight of the high molecular weight species of the polymer, (Table 4.6, **a**). The change in Mp is ~ 9000 which is above the error limit of the experiment. The molecular weights of the moderate and low molecular weight species, (**b**) and (**c**), respectively, remain essentially unchanged, within the error limits of the experiment which is assumed be approximately ± 2000 Daltons.

4.2.3.5 Thermal stability of poly(*exo*-$NBCH_2OCH_2C(CF_3)_2OH$) in TCE

In order to explore the stability of poly(*exo*-$NBCH_2OCH_2C(CF_3)_2OH$) in TCE in the absence of **Pd1388**, a sample of poly(*exo*-$NBCH_2OCH_2C(CF_3)_2OH$) of known molecular weight (**3**) (see footnote)[‡] was treated with TCE and heated to 70 °C. After heating overnight, the polymer (**4**) was isolated as discussed previously (Scheme 4.2). The molecular weight data obtained for polymers (**3**) and (**4**) are given in Table 4.7.

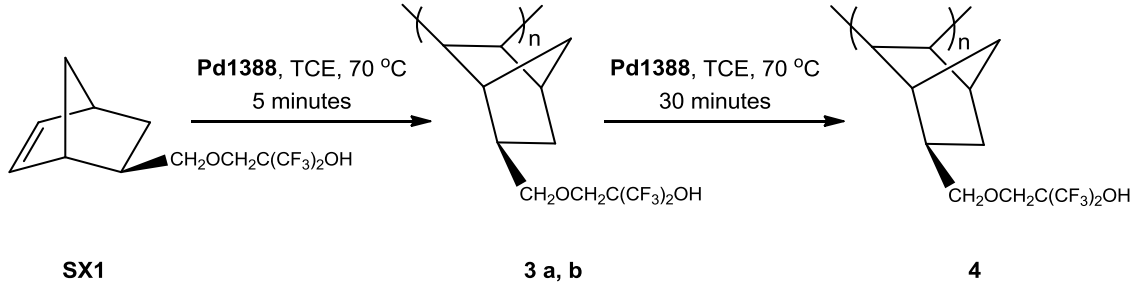

Scheme 4.2 Preparation of poly(*exo*-$NBCH_2OCH_2C(CF_3)_2OH$), (**3**) and (**4**)

Table 4.7 Molecular weight data for poly(*exo*-$NBCH_2OCH_2C(CF_3)_2OH$), before (**3**) and after (**4**) heating to 70 °C overnight.

Polymer	M_n (Daltons)*	M_w (Daltons)*	M_p (Daltons)*
(3)	69100	85100	79600
	10800	14600	12700
(4)	29200	54100	64300

* All molecular weights are quoted relative to polystyrene standards

Heating of poly(*exo*-$NBCH_2OCH_2C(CF_3)_2OH$) (**3**) in TCE leads to a reduction in the molecular weight of the of polymer, to form a new material **4**. Unlike polymer **3** which shows a bimodal GPC trace, the trace for material **4** is monomodal with a polydispersity value of 1.9. The origins of these observations are presently unknown.

[‡]Sufficient quantities of polymer (**1**) were not available for both reactions, hence a similar polymer, (**3**) was used. Polymer (**3**) was isolated from the same reaction vessel as polymer (**1**), the only difference being the time at which the polymer samples were taken (1 and 5 minutes for polymers (**1**) and (**3**) respectively.)

4.2.3.6 'Depolymerisation' behaviour of HFP-functionalised norbornenes – ceiling temperature, T_c

The observed 'depolymerisation' of HFP-functionalised norbornenes is somewhat unusual as in general, any thermal or metal mediated process that could impact upon polymer molecular weight would be expected to be random in nature, and hence result in a broadening of the molecular weight distribution. However, one possible explanation for the depolymerisation behaviour observed could stem from the thermodynamics of the polymerisation reaction, in particular, the phenomena of ceiling temperature, T_c.[1] The Gibbs free energy of a reaction is given by equation 4.1 and is function of the enthalpy and entropy of the reaction as well as reaction temperature.

$$\Delta G_P = \Delta H_P - T\Delta S_P \qquad \text{Equation 4.1}$$

ΔH_P for the polymerisation of an alkene is a negative value, since the formation of a σ-bond from a π-bond is an exothermic process. The process is especially favourable for the vinyl polymerisation of norbornenes due to the strained nature of the norbornene skeleton. However, the change in entropy upon polymerisation is unfavourable (ΔS_P is positive) due to the increased order of covalently bonded polymeric chains in comparison with free monomer. Typical values of ΔS_P range between 100-130 J K^{-1} mol^{-1} whilst values of ΔH_P are of the order 30 to 150 kJ mol^{-1}, resulting in a negative Gibbs free energy and a polymerisation reaction that is thermodynamically feasible.[1]

As the reaction temperature is increased, the polymerisation becomes more unfavourable (i.e. ΔG_p becomes 'less negative') resulting in shorter polymer chain lengths and at sufficiently high temperature, the depolymerisation reaction also becomes an important factor. Eventually a temperature is reached at which the rate of polymerisation (k_p) and depolymerisation (k_{dp}) reactions equal one another giving a value of $\Delta G_p = 0$. This temperature is referred to as the ceiling temperature, T_c. Ceiling temperature is also a function of free monomer concentration, as an equilibrium is established between free monomer and polymer chains, hence there will be a specific ceiling temperature for any given equilibrium monomer concentration, $[M_e]$.

Detailed investigation into the thermodynamics of norbornene polymerisation has, to date, received little attention, however one example of such a study has been reported by Lebedev.[2] Thermodynamic parameters are reported for the bulk polymerisation of norbornene at temperatures up to 330 K (~57 °C) for which values of

ΔH_p = 65 kJ mol^{-1}, ΔS_p = 58 J K^{-1} mol^{-1} and ΔG_p = 45 kJ mol^{-1} are quoted. Similar values are obtained under standard conditions (289 K, 1 atm), giving an equilibrium monomer concentration, $[M_e]$, of 1.7 x 10^{-9} mol dm^{-3}, which is comparable to that of vinyl acetate.[1-2] The reaction equilibrium almost exclusively favours polymer formation and estimation of a theoretical ceiling temperature gives T_c ~1000 K which is considerably higher than the thermal decomposition temperature of the polymer.

The vinyl polymerisation of HFP-functionalised monomers will be somewhat different to that for bulk polymerisation of norbornene, hence currently no benchmark exists which could aid in the estimation of the ceiling temperatures for the monomers studied in this work. However, if T_c proved to be close to the reaction temperature of 70 °C used in the polymerisation reactions then a thermodynamics-based argument could provide a plausible explanation for the depolymerisation behaviour observed.

4.3 Conclusions

The kinetics of polymerisation have been determined for the series of HFP-functionalised norbornenes of the type $NB(CH_2)_nOCH_2C(CF_3)_2OH$ and $NB(CH_2)_nC(CF_3)_2OH$. For pure *exo* HFP-functionalised norbornenes, an increase in the number of methylene groups, n, spacing the HFP functionality away from the norbornene skeleton leads to an enhancement in polymerisation rate and overall conversion. For the two cases studied, pure *exo*-functionalised norbornenes polymerise much more quickly than their *endo* counterparts (**SX1** and **SN2**) and (**SX2** and **SN3**), respectively. An increase in the number of methylene spacer groups also leads to a corresponding increase in the molecular weight of the polymers obtained, which may be rationalised in terms of faster polymerisation kinetics. The polymers obtained after 3 hours are of fairly low polydispersity, with values ranging between 1.2 and 1.4 irrespective of the value of n.

The polymerisations of a selection of HFP-functionalised norbornenes (**SX1**, **SX2** and **SN2**) using **Pd1388** were also studied using GPC to monitor the molecular weight of the polymers as a function of time. A number of interesting effects were observed, including the formation of high molecular weight material at relatively low monomer conversion (<35%). In addition, during the early stages of the polymerisation reaction (<30 minutes) a reduction in the molecular weight of the polymer is observed as a function of time. For the polymerisation of **SX1** in TCE, a polymer of trimodal character (M_p = 4000, 21000 and 70,000 Daltons, respectively) was obtained after 1 minute at 70 °C, however over the course of the reaction, loss of both the high and low

molecular weight species is observed to yield a final polymer (3 hours at 70 °C) of M_p = 22,000 Daltons and moderately low polydispersity of 1.4. An identical effect is observed during the polymerisation of **SX1** in a 17:1 (v/v) mixture of toluene:fluorobenzene. The low molecular weight species was attributed to oligomers of around ten monomer units and its' disappearance as a function of time is expected with continued growth of the polymer chain. Loss of the high molecular weight species, which is complete within 25 minutes, is more unusual and consequently more difficult to explain.

The polymerisation of **SX2** using **Pd1388** in TCE shows similar behaviour to that observed for **SX1**, with a reduction in peak average molecular weight of approximately 15,000 Daltons over the course of the 3 hour reaction, however all of the polymers obtained show monomodal character with polydispersities of 1.3 or less. Loss or molecular weight reduction of high molecular weight species, with retention of low PDI is extremely difficult to rationalise in terms of either thermal or metal-mediated processes, both of which would be expected to be random in nature hence resulting in a broadening of the molecular weight distribution. However, one explanation could relate to the ceiling temperature of the polymerisation reaction and its possible proximity to the reaction temperature of 70 °C, however further work is needed to confirm whether this is indeed the case.

4.4 References

1. J.M. Cowie, *Polymers: Physics and Chemistry of Modern Materials*, 2nd Edition, Blackie Academic and Professional, London, 1993, p74-77
2. B. Lebedev, N. Smirnova, Y. Kiparisova and K. Makovetsky, *Makromol. Chem.*, 1992, **193**, 1399-1411

Chapter V

Polymerisation of mixtures of *endo*- and *exo*- hexafluoropropanol-functionalised norbornenes

Chapter V

Polymerisation of mixtures of *endo*- and *exo*- hexafluoropropanol-functionalised norbornenes

5.1 Introduction

In Chapter IV the polymerisation behaviour of pure *endo*- and pure *exo*-hexafluoropropanol-functionalised norbornenes was discussed in detail. The use of single isomers simplifies the analysis of polymerisation kinetics, however, their synthesis is often non-trivial, requiring multi-step processes.[1-8] In contrast, the preparation of mixtures of *endo*-/*exo*-isomers of functionalised norbornenes *via* Diels-Alder syntheses is considerably more straightforward.[9-11] In this chapter the polymerisation of *endo*-/*exo*- mixtures of hexafluoropropanol-functionalised norbornenes of the type $NB(CH_2)_nOCH_2C(CF_3)_2OH$ (Figure 5.1, **a**) and $NB(CH_2)_nC(CF_3)_2OH$ (Figure 5.1, **b**) will be discussed. The polymerisation kinetics will be determined in order to examine the effect of the methylene spacer group, n, separating the HFP-functionality from the norbornene skeleton, on polymerisation rate. Subsequently, the polymerisation of *endo*-/*exo*-$NBCH_2C(CF_3)_2OH$ (**SXN4**), which has found widespread use in photolithography,[5-9, 12-13] will be examined using a selection of palladium hydride-based initiators of the type $[Pd(H)(MeCN)(PCy_3)_2][X]$ (where X is a weakly coordinating anion) in order to determine the effect of the anion on polymerisation rate.

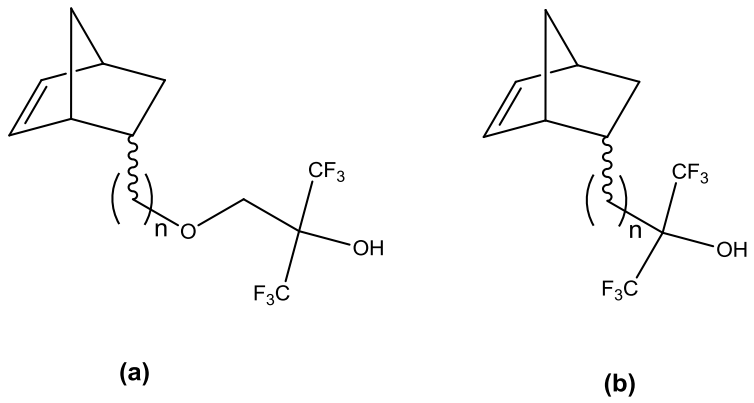

Figure 5.1 Generic structure of hexafluoropropanol-functionalised norbornene monomers

5.2 Results and discussion

5.2.1 The polymerisation of mixtures of *endo*- and *exo*- isomers – *pseudo*-copolymerisation reactions

Polymerisations of a mixture of *endo* and *exo* isomers of a substituted norbornene would ordinarily be considered as homopolymerisation reactions, as the two differ only in the orientation of the substituent. However, the reactivities of the two isomers have been shown to differ widely, with preferential uptake of the *exo* isomer into the polymer chain.[4, 14-19] This preference essentially leads to a *pseudo*-copolymerisation reaction, hence the polymerisation kinetics of such reactions must be treated accordingly.

The kinetics of copolymerisation of a wide variety of monomers using radical polymerisation techniques such as ATRP and RAFT have been studied in detail.[20] In comparison, the vinyl and ROMP copolymerisation of functionalised-norbornene monomers have received considerably less attention.[21-23] The copolymerisation kinetics of two monomer, M_1 and M_2 are usually discussed in terms of the monomer reactivity ratios, r_1 and r_2, which describe the relative rates of self versus cross propagation reactions. Reactivity ratios are extremely useful as they give an insight into the structure of the copolymer, for example if it is random, alternating etc.

Reactivity ratios have been determined for a multitude of copolymerisation reactions including the copolymerisation of norbornene with styrene and ethylene, using a variety of catalysts.[41, 43-46] The nature of the insertion of each monomer has also been confirmed *via* detailed analysis of triad and tetrad structures by high resolution ^{13}C NMR spectroscopy.[41] By comparison, only two reports detailing the reactivity ratios of copolymerisations concerning functionalised-norbornene derivatives are found in the literature.[21-22] To the best of our knowledge, the concept of reactivity ratios has not been applied to the study of the copolymerisation of *endo*-/*exo*-isomers.

5.2.1.1 Experimental determination of monomer reactivity ratios

Experimentally, reactivity ratios can be determined using a number of methods, however the simplest of these was described by Finemann and Ross in which the composition of a copolymer formed from various ratios of monomer feed is considered.[20, 24] The polymerisation is analysed at low conversion (5-10%) to minimise the effects of composition drift. The mole fractions are calculated in the monomer feed (f) and in the resulting copolymer (F) and fitted to equation 5.1. A linear plot of f(1-f)/F versus f^2/F yields values of r_1 and r_2 from the slope and intercept, respectively.

$$\frac{f(1-F)}{F} = r_2 - \frac{f^2}{F} r_1 \qquad \text{Equation 5.1}$$

The Finemann Ross method has a number of drawbacks. Firstly, the calculation of copolymer composition at low conversion has a very large associated error. In addition, the Finemann Ross method assumes that the reaction behaves according to the terminal model of copolymerisation, which was first proposed by Dostal in 1936,[25] and subsequently extended by input from many other groups.[26-28] The terminal model is based on the assumption that the reactivity of a propagating polymer chain is independent of the size or composition of the chain and is influenced only by the active end group.[29] Whilst these assumptions are not always completely accurate, the terminal model does provide a relatively straightforward method to evaluate the copolymerisation behaviour of various monomer pairs.

Due to its simplicity, analysis of the reactivity ratios for the polymerisation of a selection of HFP-functionalised norbornenes was attempted using the Finemann Ross method, as illustrated in Figures 5.2 – 5.4. However, the huge errors associated in the determination of f and F suggest that the values of r_{endo} and r_{exo} obtained are not particularly reliable, hence an alternative description of copolymerisation kinetics was sought.

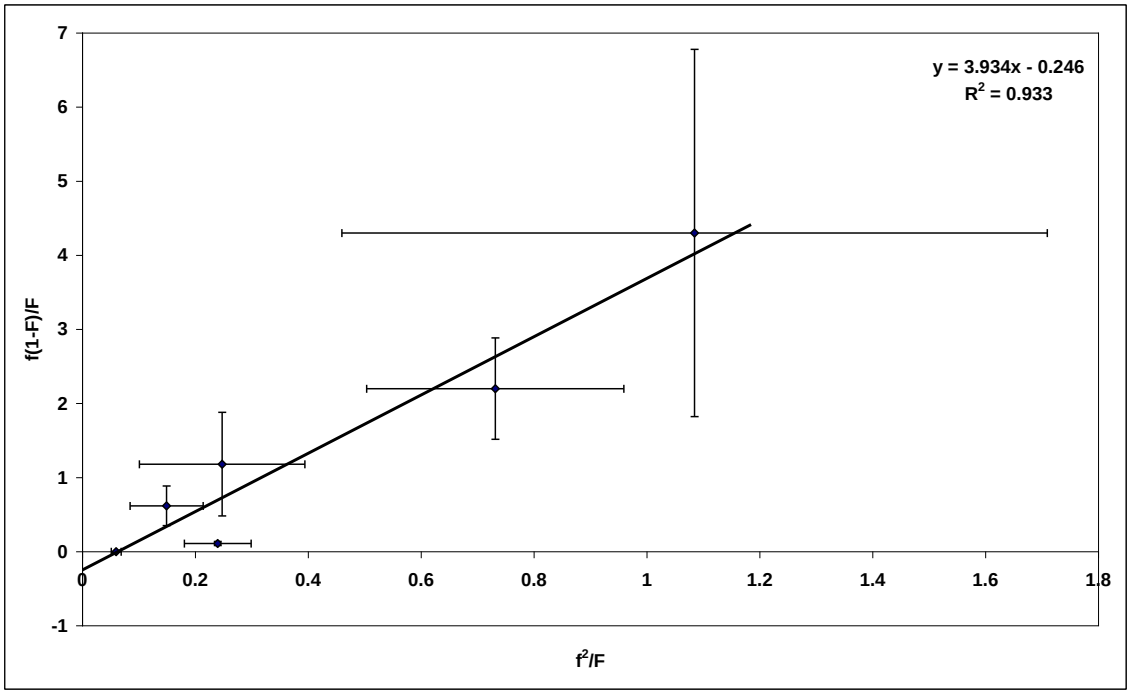

Figure 5.2 Plot of f(1-f)/F versus f^2/F to determine the reactivity ratios r_{endo} and r_{exo} for the polymerisation of mixtures of *endo*- and *exo*-$NBCH_2OCH_2C(CF_3)_2OH$ (**SN2** and **SX1**) using **Pd1388** in TCE at 70 °C.

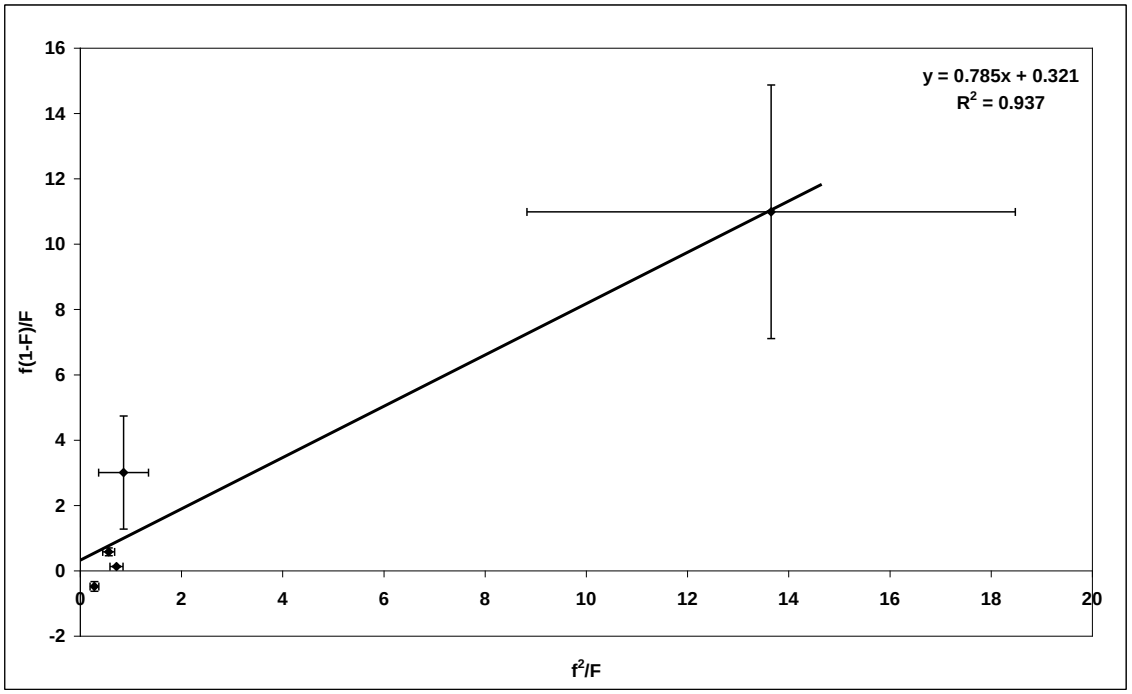

Figure 5.3 Plot of f(1-f)/F versus f^2/F to determine the reactivity ratios r_{endo} and r_{exo} for the polymerisation of mixtures of *endo*- and *exo*-$NBCH_2C(CF_3)_2OH$ (**SN3** and **SX2**) using **Pd1388** in TCE at 70 °C.

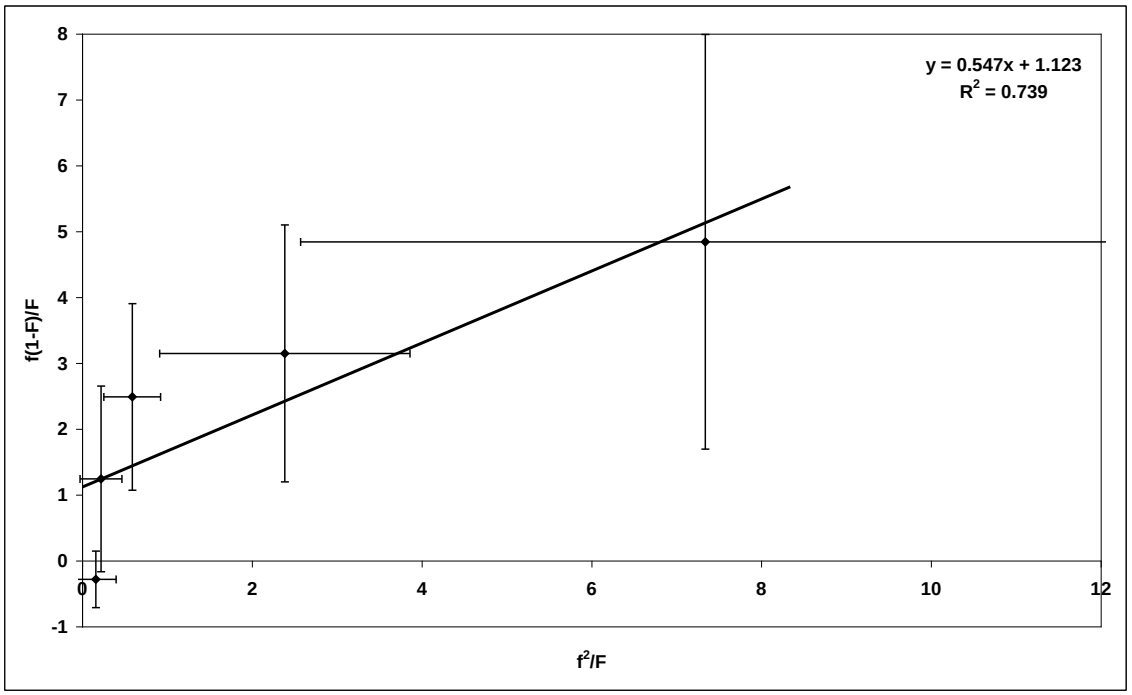

Figure 5.4 Plot of f(1-f)/F versus f^2/F to determine the reactivity ratios r_{endo} and r_{exo} for the polymerisation of mixtures of *endo*- and *exo*-$NB(CH_2)_2OCH_2C(CF_3)_2OH$ (**DXN2** and **DX2**) using **Pd1388** in TCE at 70 °C.

An alternative to the terminal model is the penultimate model, in which the copolymerisation reaction is significantly influenced by the penultimate monomer unit, in an effect known as the penultimate group effect.[30-34] The effect of the penultimate unit on the kinetics of copolymerisation was first reported by Merz and co-workers[35] and later by Barb[36] and Ham.[37] A number of copolymerisation reactions have been studied in which the experimental data showed better agreement with a penultimate model than with the terminal model. A selection of the comonomers which have been studied using the penultimate model include vinyl chloride,[38] butadiene,[39] maleic anhydride,[40] methyl methacrylate[41] acrylonitrile,[34] and styrene,[41] as well as the copolymerisation of ethylene with norbornene.[42] However, a drawback is that application of the penultimate model is significantly more complicated and time consuming than the terminal model and for this reason, analysis using the terminal model is preferred, where possible.

Determination of reactivity ratios in which the penultimate model is assumed is carried out using a non-linear least squares approach. [21-22, 41-42, 44-45, 47-49] This method takes into account conversion data over the course of the entire reaction using a variety

of monomer feeds and provides a much more accurate indication of r_1 and r_2. The possibility of calculating reactivity ratios r_{exo} and r_{endo} for HFP-functionalised norbornenes using a non-linear least squares approach was considered, however it was decided that a better description of the polymerisation kinetics of the *endo*-/*exo*-mixtures of isomers of interest in this work, could be provided using the kinetic model discussed in Chapter III. In addition, a non-linear least squares approach would require large amounts of NMR spectrometer time at elevated temperature to allow for sufficient repeats of results.

5.2.2 Introduction to the polymerisation kinetics of *endo*/*exo* mixtures of hexafluoropropanol-functionalised norbornenes

In Chapters III and IV, a kinetic model was introduced that was shown to accurately describe the polymerisation behaviour of pure isomers of HFP-functionalised norbornene monomers. This kinetic model is readily extended to encompass the polymerisation of *endo*/*exo* mixtures of monomers, although a number of additional factors need to be taken into consideration. Firstly, the polymerisation of mixtures of isomers can be considered in terms of three monomer concentrations, $[M]_{total}$, which covers the total monomer concentration, and $[M]_{endo}$ and $[M]_{exo}$ that separately consider the *endo* and *exo* components within a mixture. The determination of overall polymerisation rate from total monomer concentrations is straightforward and the rate constants k_1 and k_2 (first- and second-order rate constants of propagation, respectively) can be calculated in an analogous fashion to that used for pure isomers.

5.2.2.1 Calculation of second-order rate constants, k_2, for individual *endo*- and *exo*-components within mixtures of isomers

The calculation of the second-order rate constants, k_2, becomes more complicated when the rates of polymerisation of the individual *endo* and *exo* components are calculated independently. Fitting of monomer consumption data for each isomer within the mixture to the kinetic model described by equation 3.3 generates values of k_1, however in order to obtain values of k_2, the NMR integral areas obtained must be converted into absolute monomer concentrations. The conversion process relies upon extrapolation of experimental data for monomer consumption to determine the concentration of monomer at the start of the propagation process, $[M]_0$' (*i.e* data obtained when all of the palladium hydride initiator has been consumed) and normalisation of all NMR integrals relative to this value, as discussed in section 3.4. The model assumes that upon

completion of the initiation process, one monomer unit has inserted into each palladium hydride bond, leaving a concentration of free monomer in solution of 0.294 M. For mixtures of *endo* and *exo* isomers, the relative rates of insertion of each isomer into the palladium hydride bond are unknown, although they are likely to depend upon the ratio of each isomer in a particular reaction mixture as well as the nature of the particular monomers being used.

5.2.2.2 Calculation of second-order rate constants, k_2, based upon *endo*-/*exo*-monomer feed ratios

One possible way in which to calculate k_2 values is to assume that the rates of insertion of *endo*- and *exo*-monomers are the same and that the values of $[M]_0$' obtained *via* extrapolation are simply a function of the initial ratio of monomers within the mixture. For example, using a 70:30 mixture of *endo*:*exo* isomers, $[M]_0'_{endo}$ = 0.7 x 0.294 M, whilst $[M]_0'_{exo}$ = 0.3 x 0.294 M. This is an extremely crude approximation for a number of reasons. Firstly, a number of studies have highlighted the preference for uptake of the *exo* isomer within a mixture hence the rates of insertion are expected to be different.[4, 14-19] Also, the ratio of *endo*:*exo* isomers in solution will be time-dependent, changing as insertion into each palladium hydride bond occurs. For this reason, the values of k_2 obtained from fitting of individual *endo*- and *exo*-monomer concentration data within a mixture to equation 3.3 are by no means absolute and are included for illustrative purposes only. Values of k_1 however, provide an excellent means of comparison between monomer systems. Despite the non-absolute values of k_2 for individual components, fitting of data to equation 3.3 provides a much better approximation for the overall rate of polymerisation than simple treatment of the data using *pseudo*-first order kinetics, which has been used in previous studies relating to vinyl norbornene kinetics.[4,19]

5.2.3 Experimental determination of polymerisation kinetics of *endo*-/*exo*-mixtures of hexafluoropropanol-functionalised norbornenes

In this work, the polymerisation kinetics of a series of monomers of the type *endo*-/*exo*-$NB(CH_2)_nOCH_2C(CF_3)_2OH$ (n = 0-4, 6) and *endo*-/*exo*-$NB(CH_2)_nC(CF_3)_2OH$ (n = 1, 2), prepared *via* Diels-Alder synthesis, have been studied in detail. The compositions of the mixtures prepared ranged between ~70-80% of the *endo* isomer and are summarised in Table 5.1.

Table 5.1 Composition of *endo*-/*exo*-mixtures and rates of hydride consumption, k_H, for the polymerisation of hexafluoropropanol-functionalised norbornenes initiated using **Pd1388** at 70 °C in d_2-TCE

Monomer	Code	n	% *endo* isomer in mixture[§]	k_H (10^{-3} s^{-1})
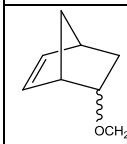	**ZXN3**	0	70	2.82 ± 0.03
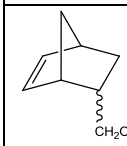	**SXN3**	1	80	5.21 ± 0.2
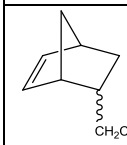	**SXN4**	1	76	4.78 ± 0.5
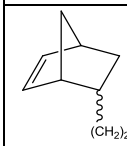	**DXN2**	2	68	-*
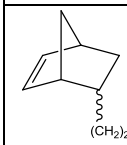	**DXN5**	2	79	-*
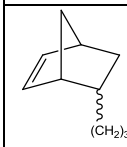	**TXN3**	3	81	-*
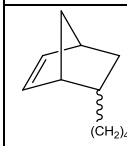	**QXN1**	4	77	-*
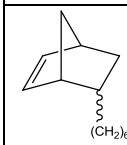	**HXN1**	6	80	-*

[§]The ratio of *endo*:*exo* isomers was determined using ^{1}H NMR spectroscopic analysis

* Reaction was too rapid for k_H to be determined under conditions used

5.2.3.1 Rates of hydride consumption, k_H, in the polymerisation of HFP-functionalised norbornenes

As discussed in section 3.3 (Scheme 3.1), the initiation process for the vinyl polymerisation of norbornenes using palladium-hydride initiators relies upon a complex series of equilibria. For this reason, although the rate of hydride consumption (k_H) measured experimentally contributes to the rate of initiation, the two rate constants are not necessarily equivalent. Rates of hydride consumption were measured, where possible, and are summarised in Table 5.1.

For the majority of the polymerisation reactions studied, the rate of hydride consumption was extremely rapid, with complete disappearance of the hydride resonance within the time taken to acquire 2-3 ^{1}H NMR spectra (< 2 minutes), hence insufficient data points were available from which to calculate k_H. The rates of hydride loss were determined for monomers in which n = 0, 1, with an approximate doubling of k_H upon moving from zero (**ZXN2**) to one (**SXN3**) methylene spacer units being observed. The rates of hydride loss for monomers **SXN3** and **SXN4**, (for both of which n = 1) are identical within the error limits of the experiment.

5.2.3.2 First-order rate constants of propagation, k_1, for the polymerisation of *endo*-/*exo*- HFP-functionalised norbornenes

First-order rate constants, k_1, are given for overall polymerisation rate (total isomers) and independently for the *endo* and *exo* components within a given mixture and are summarised in Table 5.2 and Figure 5.5. As discussed in Chapter III, the rate constant k_1 describes the rate of polymerisation in terms of *pseudo* first-order kinetics. Quantitative comparison between the rate constants, k_1, obtained for each *endo*-/*exo*- monomer system studied is not possible, due to the slightly different *endo*:*exo* ratio of each particular monomer within a mixture. However, a qualitative assessment indicates a number of interesting results. In general, an increase in the number of methylene spacer units separating the HFP-functionality from the NB skeleton leads to a corresponding increase in the first-order rate constant of propagation, k_1. The increase in rate is observed whether data for total isomer content (k_{1total}) or individual *endo* (k_{1endo}) and *exo* (k_{1exo}) components are considered. However, despite an increase in overall rate, no difference is observed in k_{1exo}, upon moving from four (**QXN1**) to six (**HXN1**) methylene spacer units. The increase in the overall polymerisation rate observed for **HXN1** is thought to derive purely from the increased rate of polymerisation of the *endo* component of the mixture, with increasing values of n. Clearly for the *exo* component, a

limit is reached in the value of n above which incorporation of additional methylene units do not lead to an enhancement in rate.

Table 5.2 First-order rate constants of propagation, k_1, for the polymerisation of a series of hexafluoropropanol-functionalised norbornene monomers polymerised using **Pd1388** at 70 ºC in d_2-TCE

Monomer	Code	n	k_{1total} (10^{-4} s^{-1})	k_{1endo} (10^{-4} s^{-1})	k_{1exo} (10^{-4} s^{-1})
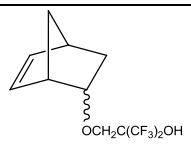	**ZXN2**	0	1.11 ± 0.6	1.33 ± 0.2	*
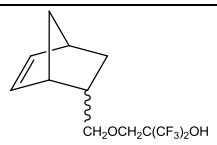	**SXN3**	1	2.68 ± 0.4	1.79 ± 0.3	7.90 ± 0.3
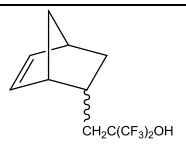	**SXN4**	1	6.58 ± 0.8	2.35 ± 0.4	17.0 ± 2
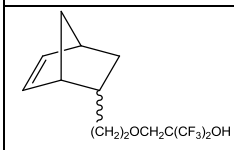	**DXN2**	2	20.9 ± 0.6	12.5 ± 0.5	52.4 ± 0.8
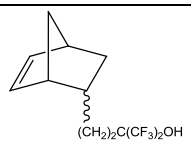	**DXN5**	2	17.4 ± 2	13.7 ± 1	36.7 ± 3
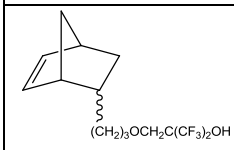	**TXN3**	3	49.5 ± 2	38.0 ± 1	117 ± 20
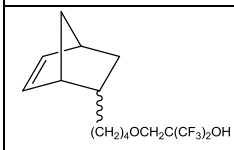	**QXN1**	4	58.2 ± 9	45.6 ± 2	177 ± 10
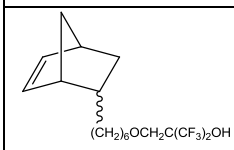	**HXN1**	6	75.9 ± 2	67.0 ± 2	173 ± 30

* Rate constant too slow to measure but not zero

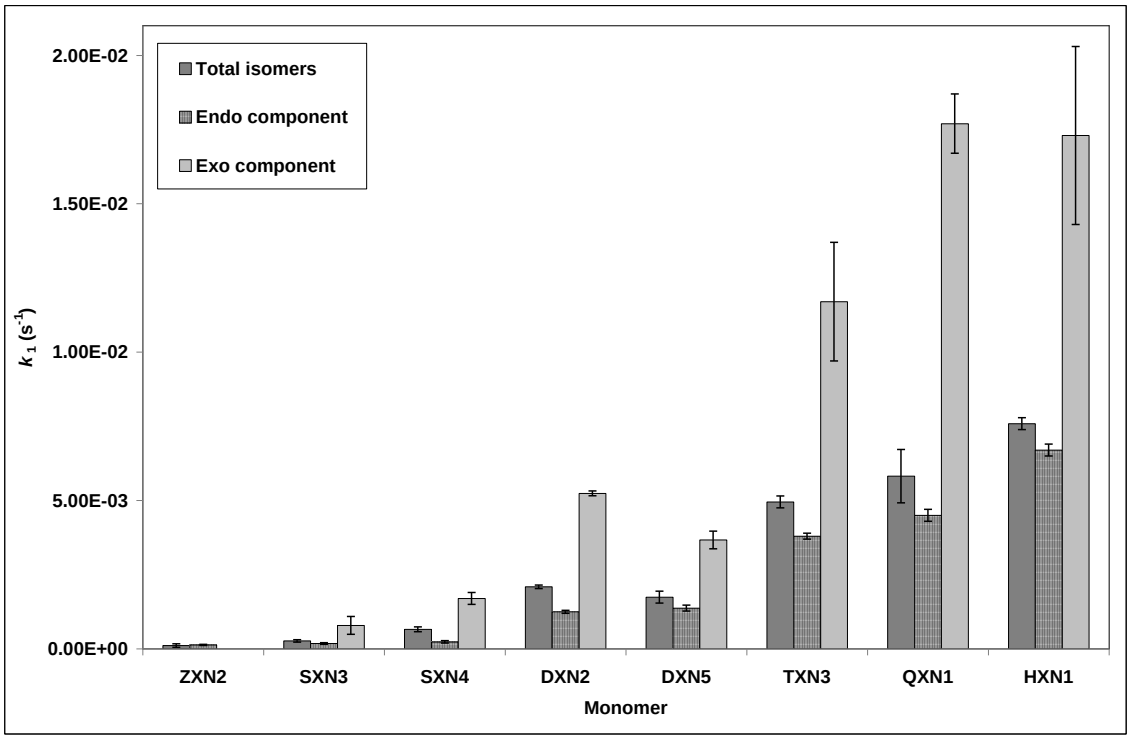

Figure 5.5 Comparison (with errors) of first-order rate constants of propagation, k_1, for a series of *endo*-/*exo*- hexafluoropropanol-functionalised norbornene monomers polymerised using **Pd1388** at 70 ºC in d_2-TCE. 'Total isomers' refers to analysis of the total monomer concentration (*endo* + *exo* isomers within the mixture).

A second interesting effect is that an increase in the value of n leads to a corresponding increase in polymerisation rate for the *endo* component within a mixture. Such an increase is in contrast to the effects observed by Sen for the polymerisation of *endo*-/*exo*-alkyl-functionalised norbornenes in which increasing chain length resulted in a reduction in polymerisation rate.[19] The effects observed by Sen were attributed to the increased steric bulk of the substituent, which hinders the insertion of monomer units into the polymer chain, as discussed in section 4.2.

In the case of the HFP-functionalised norbornenes studied in this work, the electronic effects of spacing the functionality further from the norbornene skeleton appear to outweigh the increase in the steric demands of the functional group. Such an increase in rate is possibly linked to the proximity to, and subsequent interaction of, the HFP-functional group with the metal centre. Theoretical studies have found no evidence to suggest that increasing the number separation (i.e. the number of methylene units in this instance) of a functional group from the norbornene skeleton contributes to changes

in the structure of the norbornene skeleton itself or more importantly, the properties of the double bond.[4]

For the majority of the monomers studied in this work, the rate of polymerisation of the *exo* component within the mixture is considerably faster than for the corresponding *endo* component. The magnitude of k_{1exo}/k_{1endo} is monomer-dependent, ranging between 2.6 to 7.2, however no trend as a function of n is observed, within the error limits of the experiment. Such values for the difference in the polymerisation rate are within the range of those reported previously for *endo*-/*exo*-mixtures of functionalised norbornenes.[4]

A final point to note is that for **ZXN2**, for which n = 0, the rate of polymerisation of the *exo* component was too slow for its associated rate constant to be obtained with any degree of accuracy. The change in the raw NMR integral area over the time frame of the reaction studied was ~1 'unit', hence the error associated with each data point is considerable. However, the *endo* component of the mixture readily undergoes polymerisation. Interestingly, the monomer **ZX3** (discussed in chapter IV), which has an *exo*:*endo* ratio of 98:2 does undergo polymerisation with a value of k_1 ($1.15 \pm 0.05 \times 10^{-4}$ s^{-1}) comparable to that for **ZXN2** ($k_{1total} = 1.11 \pm 0.6 \times 10^{-4}$ s^{-1}). The extremely low reactivity of the *exo*-component within the **ZXN2** mixture is in sharp contrast to the effects observed with every other *endo*-/*exo*-HFP-functionalised monomer system studied in this work, and also for the polymerisation of other norbornene monomers using cationic palladium initiators, for which k_{1exo} is several times faster than k_{1endo}.[4, 18-19]

There are reports for which uptake of the *endo* isomer is comparable to that of the *exo* isomer, however such instances occur when the polymerisation is carried out using neutral, late-transition metal-based initiators.[50-52] Theoretical calculations by Ziegler demonstrate that interaction of an oxygen-containing functional group with a metal centre is weaker for neutral versus cationic systems, however the vinyl bond is not significantly affected.[53] The weaker interaction between a metal centre and a functionality in the *endo*-position, for neutral versus cationic initiator complexes may provide an explanation for the similar rates of polymerisation of *endo* and *exo* isomers observed using neutral initiators. However, a satisfactory explanation for the low *exo* reactivity observed for polymerisation of **ZXN2** using **Pd1888** in this work has not, to date, been established.

5.2.3.3 Second-order rate constants of propagation, k_2, for the polymerisation of *endo*-/*exo*- HFP-functionalised norbornenes

As discussed in Chapter III, the second order rate constant, k_2, considers both the free monomer concentration at a given time ([M]) and the amount of monomer consumed ($[M]_0$-[M]). The calculation of second-order rate constants for mixtures of *endo*/*exo* isomers was discussed in section 5.3.1.1. In general, only the value of k_2 relating to total isomer consumption (k_{2total}) is of importance, with k_{2endo} and k_{2exo} being included purely for illustrative purposes. Second-order rate constants, k_2, are summarised in Tables 5.3 and Figure 5.6.

The observed changes in k_{2total} with increasing chain length are interesting in the fact that an increase is observed up to a value of n = 3, however for systems with n>3, the value of k_{2total} begins to decrease. The differences in $k_{2\text{total}}$ suggest that the number of methylene units dictates the relative contribution of the polymer chain bound to the metal centre, to the overall rate of polymerisation observed.

In the case where $k_{2total} = 0$, only a first-order rate constant of polymerisation, k_1, can be determined, hence the polymerisation reaction is described by *pseudo*-first order kinetics. A situation in which $k_{2total} = 0$ arises when the rate of insertion of monomers is so rapid that the polymer bound to the metal centre has no effect on the overall polymerisation rate observed.

Table 5.3 Second-order rate constants of propagation, k_2, for the polymerisation of a series of hexafluoropropanol-functionalised norbornene monomers polymerised using **Pd1388** at 70 ºC in d_2-TCE.

Monomer	Code	n	k_{2total} (10^{-3} Mol^{-1}dm^{3}s^{-1})	k_{2endo} (10^{-3} Mol^{-1}dm^{3}s^{-1})	k_{2exo} (10^{-2} Mol^{-1}dm^{3}s^{-1})
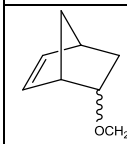	**ZXN2**	0	0	2.48 ± 0.6	0
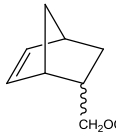	**SXN3**	1	4.09 ± 0.4	5.13 ± 0.9	1.79 ± 0.2
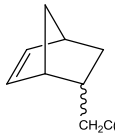	**SXN4**	1	4.77 ± 0.5	3.09 ± 0.7	2.60 ± 0.3
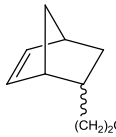	**DXN2**	2	9.52 ± 0.3	8.93 ± 0.3	3.46 ± 0.5
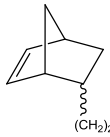	**DXN5**	2	8.62 ± 1	9.30 ± 1	5.30 ± 0.5
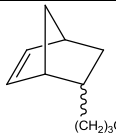	**TXN3**	3	24.4 ± 1	25.3 ± 1	13.8 ± 5
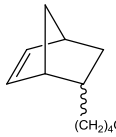	**QXN1**	4	18.4 ± 3	17.8 ± 0.9	12.1 ± 0.2
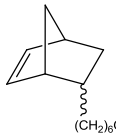	**HXN1**	6	10.9 ± 1	9.18 ± 1	0

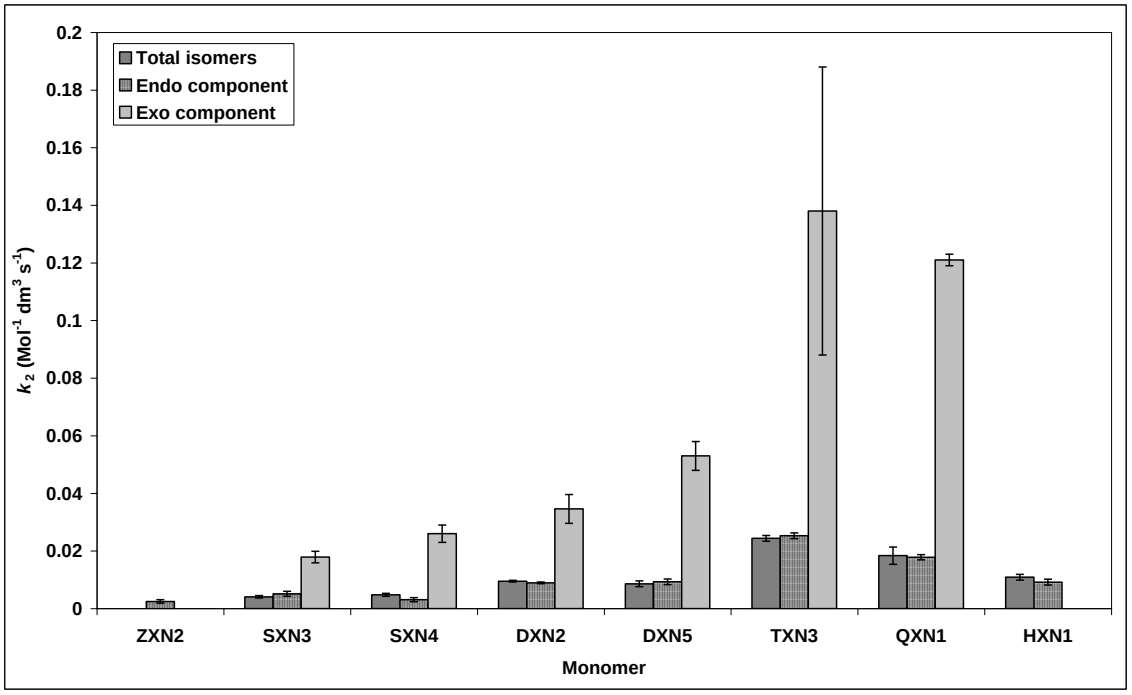

Figure 5.6 Comparison (with errors) of second-order rate constants of propagation, k_2, for a series of *endo*-/*exo*- hexafluoropropanol-functionalised norbornene monomers polymerised using **Pd1388** at 70 ºC in d_2-TCE. 'Total isomers' refers to analysis of the total monomer concentration (*endo* + *exo* isomers within the mixture).

5.2.4 The effect of methylene spacer groups on the molecular weight and PDI of *endo*-/*exo*- hexafluoropropanol-functionalised poly(norbornenes)

Polymerisation reactions for a series of HFP-functionalised monomers were carried out in Young's tap NMR tubes. Monomer feeds were determined using ^{1}H NMR spectroscopic analysis. Copolymer composition was calculated by comparing monomer feeds with residual norbornene monomers present in solution upon completion of the polymerisation reaction and assuming that any monomer consumed is incorporated into a polymer chain. All integral values were measure relative to an internal standard (mesitylene). Percentage conversion were also determined using ^{1}H NMR spectroscopic analysis with percentage conversion of the *endo*- and *exo*-components within the mixture determined by comparing the integrals of each isomer independently within the monomer feed and at the end of the reaction. After 3 hours at 70 °C the resulting polymers were isolated *via* precipitation into hexane and analysed using GPC (THF). A summary of monomer feed composition, conversion, copolymer composition, molecular weight and PDI data are given in Table 5.4. All values of molecular weight are quoted relative to polystyrene standards. Conversion data is also summarised in Figure 5.7

Table 5.4 Monomer feed, copolymer composition, conversion, molecular weight and PDI data for a series of *endo*-/*exo*-hexafluoropropanol-functionalised norbornene monomers, polymerised using **Pd1388**, after 3 hours at 70 °C in d_2-TCE. 'Total isomers' refers to combined analysis of both isomers (*i.e.* the *endo* + *exo* components within the mixture).

	Monomer feed (%)		**Copolymer composition (%)**		**Conversion (%)**			**M_n**	**M_w**	**M_p**	**PDI**
Monomer	***endo***	***exo***	***endo***	***exo***	***endo* isomer**	***exo* isomer**	**Total isomers**	**(Daltons) ***	**(Daltons) ***	**(Daltons) ***	
ZXN2	70	30	84	16	35	15	**29**	10500	16800	19500	1.6
SXN3	80	20	50	50	22	84	**34**	7100	12200	16000	1.7
SXN4	76	24	55	45	35	92	**49**	10500 30300	12600 32200	16500 29700	-
DXN2	68	32	63	37	80	100	**86**	5000	10300	8300	2.0
DXN5	79	21	72	28	69	97	**75**	11800	16700	16700	1.4
TXN3	81	19	78	22	82	100	**86**	11900	16300	19200	1.4
QXN1	77	23	75	25	93	100	**95**	12900	16900	19900	1.3
HXN1	80	20	80	20	99	100	**99**	17600	22400	21000	1.3

* All molecular weights are quoted relative to polystyrene standards

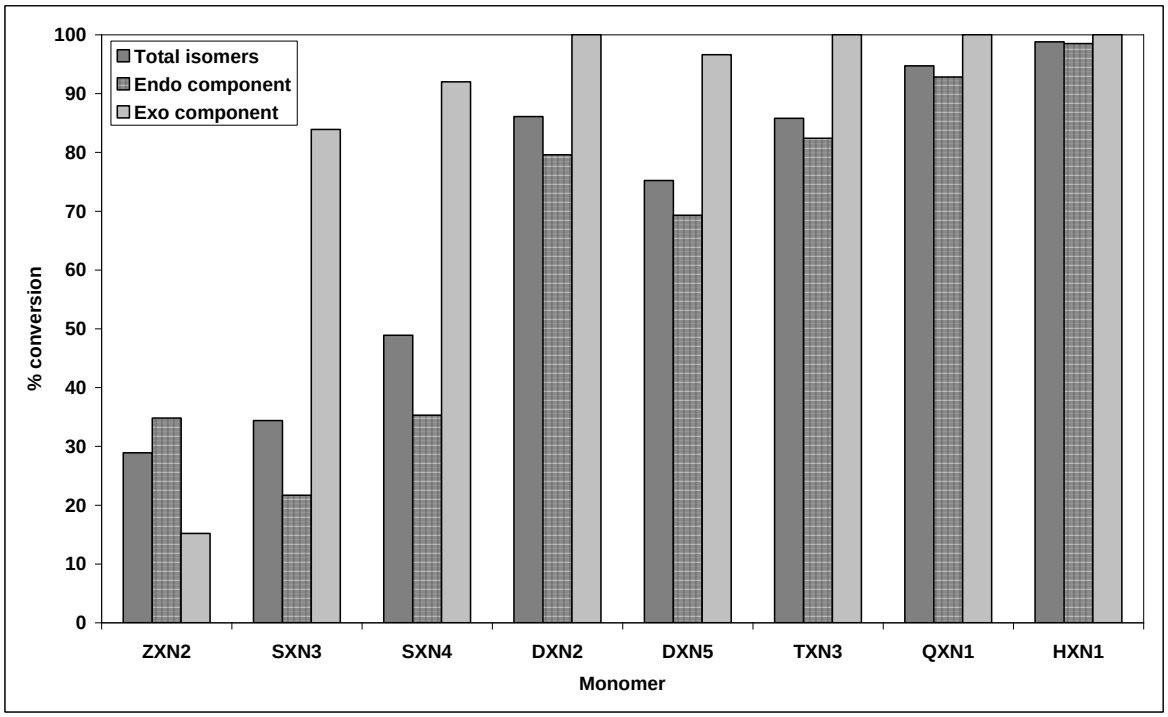

Figure 5.7 Comparison of conversion data for a series of *endo*-/*exo*-hexafluoropropanol-functionalised norbornene monomers, polymerised using **Pd1388**, after 3 hours at 70 °C in d_2-TCE. 'Total isomers' refers to combined analysis of both isomers (i.e. the *endo* + *exo* components within the mixture.)

In general, an increase in the number of methylene spacer groups, n, separating the HFP-functionality from the norbornene skeleton leads to a corresponding increase in overall conversion. The exception to the trend is for the polymerisation **ZXN2**, in which n = 0. In this instance, incorporation of the *endo* isomer into the polymer is preferred over its *exo* counterpart, resulting in a polymer with an *endo*:*exo* ratio of 84:16 (monomer feed = 70:30 *endo*:*exo*). The preferential uptake of the *endo* isomer was discussed quantitatively in section 5.3.2.2, in terms of rate constants of propagation. At the present time, no satisfactory explanation for the differing behaviour of **ZXN2** compared with other HFP-functionalised monomers has been established.

As discussed in Chapter III, the molecular weights of the polymers were analysed relative to polystyrene standard due to their poor light scattering behaviour. For this reason, the values of molecular weight quoted are not accurate due to the differences in hydrodynamic volume between polystyrene and poly(HFP-functionalised norbornenes).

No particular trend is observed in polymer molecular weight as a function of n, with the peak molecular weights of the polymers obtained ranging between 8000 (**DXN2**) and 21000 Daltons (**HXN1**). The PDIs of the polymers obtained vary between 1.3 and 2 and, in general, are narrower for polymers with n≥3 methylene units. When compared with polymers obtained from pure *exo*-isomers, studied in section 4.4, the polydispersity of the materials obtained from *endo*/*exo* mixtures is slightly broader. For example, the PDI of the pure *exo* isomer, **SX1**, is 1.2, whereas for the *endo*/*exo* mixture, **SXN3**, the PDI of the polymer is 1.7. The polymer obtained from **SXN4** (*endo*-/*exo*-$NBCH_2C(CF_3)_2OH$) is bimodal, showing peak molecular weights of 10500 and 30000. Similar bimodal character is observed for the polymer obtained from the pure *endo* analogue of this monomer, **SN3**, discussed in Chapter IV. It is unclear why the polymers obtained for **SXN4** and **SN3** differ from the monomodal character observed for the other HFP-functionalised systems studied in this work.

5.2.5 The effect of the *endo*:*exo* ratio within *endo*/*exo* mixtures of HFP-functionalised norbornenes on conversion, polymer molecular weight and PDI

The effect of the *endo*:*exo* ratio of monomers in a mixture was studied for a selection of HFP-functionalised norbornenes. The monomers selected were *endo*-/*exo*-$NB(CH_2)_nOCH_2C(CF_3)_2OH$ (n = 0-2) and *endo*-/*exo*-$NBCH_2C(CF_3)_2OH$, as sufficient quantities were available of both an *endo*/*exo* mixture (*via* Diels-Alder synthesis) and of the pure *exo* isomers. In each case, a range of monomer feeds were prepared and subsequently polymerised. The extent of conversion was determined using ^1H NMR spectroscopic analysis and where possible, the resulting polymers isolated as described previously in section 5.3. The resulting conversion, copolymer composition, molecular weight and PDI data are given in Tables 5.7–5.13. Figure 5.8 highlights the effect of increasing the percentage of *endo*-isomer within a mixture on overall conversion.

Table 5.5 Monomer feed, copolymer composition and conversion data for *endo*-/*exo*-$NBOCH_2C(CF_3)_2OH$, polymerised using **Pd1388**, after 3 hours at 70 °C in d_2-TCE

Monomer feed (%)		**Copolymer composition (%)**		**Conversion (%)**		
endo	***exo***	***endo***	***exo***	***endo* isomer**	***exo* isomer**	**Total isomers**
70	30	84	16	35	15	29
47	53	56	44	35	25	29
37	63	51	49	36	20	25
24	76	39	61	34	17	21
2	98	34	97	21	17	17

Table 5.6 Monomer feed, copolymer composition, conversion, molecular weight and PDI data for *endo*-/*exo*-$NBCH_2OCH_2C(CF_3)_2OH$, polymerised using **Pd1388**, after 3 hours at 70 °C in d_2-TCE

Monomer feed (%)		**Copolymer composition (%)**		**Conversion (%)**			**M_n (Daltons) ***	**M_w (Daltons) ***	**M_p (Daltons) ***	**PDI**
endo	***exo***	***endo***	***exo***	***endo* isomer**	***exo* isomer**	**Total isomers**				
100	0	100	0	20	0	20	4500	7900	8200	1.7
80	20	50	50	22	84	34	5300	8100	8800	1.5
57	43	27	73	23	85	50	82300 7200	85600 9900	89500 11200	-
42	58	17	83	23	83	58	7300	10800	12000	1.5
25	75	9	91	25	88	72	6500	8800	9900	1.4
0	100	0	100	0	94	94	5900	6800	7300	1.2

* All molecular weights are quoted relative to polystyrene standards

Table 5.7 Monomer feed, copolymer composition, conversion, molecular weight and PDI data for *endo*-/*exo*-$NBCH_2C(CF_3)_2OH$, polymerised using **Pd1388**, after 3 hours at 70 °C in d_2-TCE

Monomer feed (%)		**Copolymer composition (%)**		**Conversion (%)**			**M_n**	**M_w**	**M_p**	**PDI**
endo	***exo***	***endo***	***exo***	***endo* isomer**	***exo* isomer**	**Total isomers**	**(Daltons) ***	**(Daltons) ***	**(Daltons) ***	
100	0	100	0	27	0	27	27100 4900	33300 5700	34400 9400	-
76	24	55	45	35	92	49	30300 10500	32200 12600	29700 16500	-
56	44	27	73	25	87	52	10700	13600	14000	1.3
43	57	18	82	24	85	59	9600	13900	14200	1.4
26	74	8	92	23	91	73	7900	10600	11500	1.3
0	100	0	100	0	99	99	8500	11100	12500	1.3

* All molecular weights are quoted relative to polystyrene standards

Table 5.8 Monomer feed, copolymer composition, conversion, molecular weight and PDI data for *endo*-/*exo*-$NB(CH_2)_2OCH_2C(CF_3)_2OH$, polymerised using **Pd1388**, after 3 hours at 70 °C in d_2-TCE

Monomer feed (%)		**Copolymer composition (%)**		**Conversion (%)**			**M_n**	**M_w**	**M_p**	**PDI**
endo	***exo***	***endo***	***exo***	***endo* isomer**	***exo* isomer**	**Total isomers**	**(Daltons) ***	**(Daltons) ***	**(Daltons) ***	
68	32	63	37	80	100	86	5000	10300	8300	2.0
58	42	47	53	64	100	79	7000	8500	9700	1.2
46	54	39	62	74	100	88	6500	8300	9600	1.3
28	72	25	75	87	100	96	6700	7800	8800	1.2
0	100	0	100	0	100	100	8600	11100	13500	1.3

* All molecular weights are quoted relative to polystyrene standards

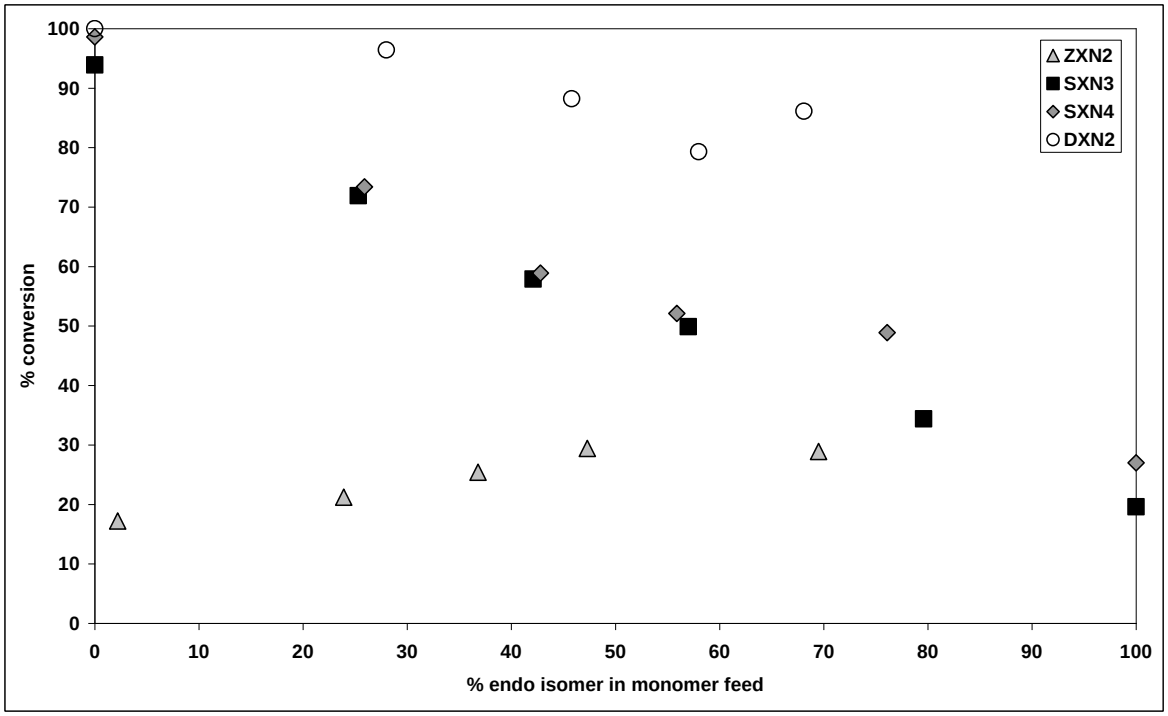

Figure 5.8 The effect of increasing the percentage of *endo*-isomer within a mixture on overall conversion for a series of HFP-functionalised norbornenes polymerised using **Pd1388**, after 3 hours at 70 °C in d_2-TCE.

For the majority of the monomers studied, a preference is observed for uptake of the *exo*-component within a mixture, as discussed previously. The exception is for the polymerisation of *endo*-/*exo*-$NBOCH_2C(CF_3)_2OH$, where uptake of the *endo* isomer is preferred, which again, was discussed in sections 5.3 and 5.4. In general, increasing the *endo* component within a mixture, leads to reduction in overall conversion (Figure 5.8). Again, the exception is *endo*-/*exo*-$NBOCH_2C(CF_3)_2OH$ (**ZXN2**) for which conversion ranges between 20 and 30%, irrespective of the *endo*:*exo* ratio in the monomer feed.

The molecular weight of the polymers obtained from **ZXN2**, **SXN3**, **SXN4** and **DXN2** show no apparent trend with variations in the *endo*:*exo* ratio, irrespective of the monomer used. Values of PDI are fairly narrow (< 1.5), however a few of the polymers obtained do show broader polydispersities or bimodal character (**SXN4** and **SN3**). It is unclear why certain reactions behave differently to the majority studied. In the case of *endo*-/*exo*-$NBOCH_2C(CF_3)_2OH$, insufficient material was isolated from the polymerisations reactions for analysis to be carried out.

5.2.6 Polymerisation of HFP-functionalised norbornene using palladium-hydride initiators – anion effects

The majority of the work in this thesis has focused on the vinyl polymerisation of functionalised norbornenes using $[Pd(H)(MeCN)(PCy_3)_2][B(C_6F_5)_4]$ (**Pd1388**), which has been shown to be an effective pro-initiator. However, as discussed previously, the $[B(C_6F_5)_4]$ counter anion is extremely expensive. In Chapter II, the synthesis of a selection of alternative palladium hydride initiators bearing different weakly coordinating anions was described. In the following sections, the ability of these pro-initiators to polymerise an *endo*/*exo* mixture of a HFP-functionalised norbornene derivative of commercial relevance (**SXN4**) will be described.

5.2.6.1 Small-scale test polymerisations of SXN4 using palladium-hydride initiators

Each of the initiators prepared in section 2.6 (with the exception of **Pd1388**) were tested for activity in the vinyl polymerisation of **SXN4**. The complex *trans*-$[Pd(H)(MeCN)(PCy_3)_2][PF_3(C_2F_5)_3]$ (**Pd1154**), supplied by Promerus was also examined. Polymerisation reactions were carried out in Young's tap NMR tubes under identical conditions to those used for polymerisations initiated using **Pd1388** (70 °C, d_2-TCE, 50:1 monomer: initiator). Of the initiators studied, only the complexes **Pd1154**, **Pd945** and **Pd854** (counter anions *mer*-$[PF_3(C_2F_5)_3]$, $[SbF_6]$ and $[BF_4]$ respectively) were found to be active pro-initiators for the polymerisation of **SXN4**. The other palladium-hydride complexes studied ($[Pd(H)(MeCN)(PCy_3)_2][PF_6]$, $[Pd(Cl)(H)(PCy_3)_2]$, $[Pd(H)(OTf)(PCy_3)_2]$ and the mixture $[Pd(H)(MeCN)(PCy_3)_2][I]$/$[Pd((H)(I)(PCy_3)_2]$, were either found to be completely inactive or the reaction did not proceed beyond the first insertion product.

5.2.6.2 Kinetics of polymerisation of SXN4 using palladium-hydride pro-initiators in TCE

The kinetics of polymerisation of **SXN4** using **Pd1154**, **Pd945** and **Pd854** were analysed as discussed previously for the analogous polymerisation reaction using **Pd1388**. Values of k_H and k_1 were obtained and are summarised in Table 5.9 and Figure 5.9. Values of k_2 are summarised in Table 5.10.

Table 5.9 Rates of hydride consumption, k_H, and first-order constants of propagation, k_1, for the polymerisation of **SXN4** initiated using a selection of palladium-hydride pro-initiators of the type $[Pd(H)(MeCN)(PCy_3)_2][X]$ at 70 ºC in d_2-TCE

Anion, X	Initiator	k_H (10^{-3} s^{-1})	k_{1total} (10^{-4} s^{-1})	k_{1endo} (10^{-4} s^{-1})	k_{1exo} (10^{-3} s^{-1})
$[BF_4]$	**Pd796**	5.69 ± 0.5*	3.13 ± 0.6	1.21 ± 0.3	0.76 ± 0.1
$[SbF_6]$	**Pd945**	2.94 ± 0.2*	3.54 ± 0.1‡	1.54 ± 0.1‡	0.79 ± 0.02‡
$[PF_3(C_2F_5)_3]$	**Pd1154**	4.91 ± 0.4*	5.16 ± 2	2.28 ± 0.4	1.17 ± 0.5
$[B(C_6F_5)_4]$	**Pd1388**	4.78 ± 0.4	6.58 ± 0.8	2.35 ± 0.4	1.70 ± 0.2

* Only one measurement of the rate constant k_H was taken. The error is quoted as that for **Pd1388**, which was determined to be ± 8%.

‡ Only one set of monomer consumption data was obtained. The error quoted is that for the fit of the data to equation 3.3.

The rates of hydride loss measured for **Pd796**, **Pd1154** and **Pd1388** (X = $[BF_4]$, $[PF_3(C_2F_5)_3]$ and $[B(C_6F_5)_4)]$) were found to be similar within the error limits of the experiment, which was determined to ± 8%. The rate measured for the $[SbF_6]$ salt, **Pd945** is lower, however it is unclear why the rate should differ in this instance. The first-order rate constants k_1 are similar for initiators in which X = $[BF_4]$, and $[SbF_6]$ (**Pd796** and **Pd945**, respectively) within the error limits of the experiment, however both initiators show lower polymerisation activity than **Pd1388** (X = $[B(C_6F_5)_4)]$). The rate constants of **Pd1154** (X = $[PF_3(C_2F_5)_3]$) are more comparable to those of **Pd1388** however the error in the average k_1 values obtained is fairly large and also covers the range of values determined for both the $[BF_4]$ and $[SbF_6]$ analogues.

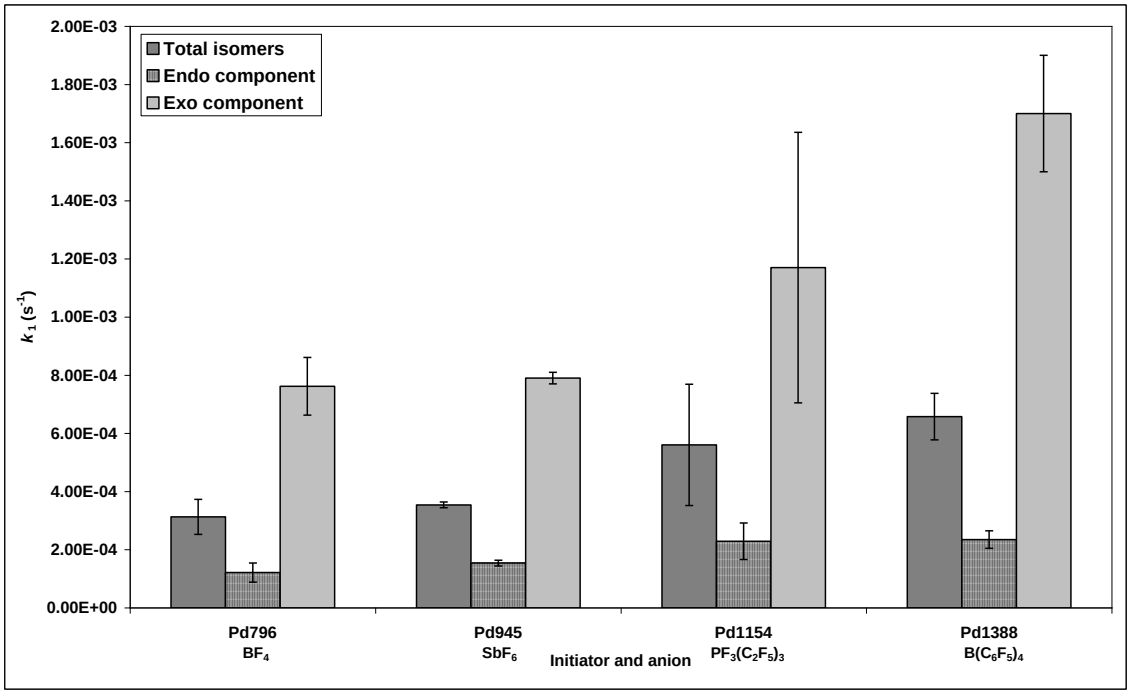

Figure 5.10 Comparison (with errors) of first-order rate constants of propagation, k_1, for the polymerisation of **SXN4** initiated using a selection if palladium-hydride pro-initiators of the type $[Pd(H)(MeCN)(PCy_3)_2][X]$ at 70 ºC in d_2-TCE.

Table 5.10 Second-order rate constants of propagation, k_2, for the polymerisation of **SXN4** initiated using a selection if palladium-hydride pro-initiators of the type $[Pd(H)(MeCN)(PCy_3)_2][X]$ at 70 ºC in d_2-TCE

Anion, X	**Initiator**	k_{2total} (10^{-3} $Mol^{-1}dm^3s^{-1}$)	k_{2endo} (10^{-3} $Mol^{-1}dm^3s^{-1}$)	k_{2exo} (10^{-2} $Mol^{-1}dm^3s^{-1}$)
$[BF_4]$	**Pd796**	1.93 ± 0.5	1.46 ± 0.5	0.73 ± 0.5
$[SbF_6]$	**Pd945**	2.86 ± 0.1*	3.09 ± 0.3*	1.21 ± 0.04*
$[PF_3(C_2F_5)_3]$	**Pd1154**	3.68 ± 1	3.35 ± 1	1.78 ± 0.7
$[B(C_6F_5)_4]$	**Pd1388**	4.77 ± 0.5	3.09 ± 0.7	2.60 ± 0.3

* Only one set of monomer consumption data was obtained. The error quoted is that for the fit of the data to equation 3.3.

5.2.6.3 Molecular weight and PDI analysis of poly(*endo*-/*exo*-NBCH$_2$C(CF$_3$)$_2$OH) (SXN4) prepared using palladium-hydride pro-initiators in TCE

Polymerisation reactions were carried out using **SXN4**, initiated by **Pd796**, **Pd945**, **Pd1154** and **Pd1388** for 3 hours at 70 °C in d_2-TCE. The extent of conversion was determined using ^{1}H NMR spectroscopy and the polymers isolated as discussed previously. The molecular weight, PDI and overall conversion data are summarised in Table 5.11.

Table 5.11 Experimentally-determined molecular weight, PDI and conversion data for the polymerisation of **SXN4** using palladium-hydride initiators, after 3 hours at 70 °C in d_2-TCE

Anion, X	Conversion (%)	M_n (Daltons)*		M_w (Daltons)*		M_p (Daltons)*		PDI
[BF_4]	40	8300		12300		13600		1.5
[SbF_6]	35	8500		11400		11400		1.3
[$PF_3(C_2F_5)_3$]	34	10500		13600		13100		1.3
[$B(C_6F_5)_4$]	49	30300	10500	32200	12600	29700	16500	-

* All molecular weights are quoted relative to polystyrene standards

The percentage conversion ranges from 35 – 49% depending upon the initiator used, with **Pd1388** (X = [$B(C_6F_5)_4$]) showing the highest conversion after 3 hours at 70 °C. The polymers obtained are of similar molecular weight and PDI, irrespective of the initiator used, however the polymer obtained using **Pd1388** shows biomodal character. It is unclear why the **Pd1388** system behaves in a different manner to those using initiators with other anions. Given the reasonable similarities in overall conversion between the initiator systems, coupled with the molecular weights and relatively low PDIs of the polymers obtained, the initiators **Pd796**, **Pd945** and **Pd1154** with counter anions [BF_4], [SbF_6] and [$PF_3(C_2F_5)_3$] could provide a viable, cheaper alternative to **Pd1388** in the polymerisation of **SXN4** and other HFP-functionalised norbornenes.

5.2.6.4 Polymerisation of SXN4 using palladium-hydride pro-initiators in toluene:fluorobenzene

The polymerisation of **SXN4** was also carried out in a 5:1 mixture of toluene:fluorobenzene using **Pd1388** and **Pd796**. The kinetics of polymerisation were measured along with the extent of conversion, and the polymers isolated as discussed previously. A summary of the rate constants, k_1 and k_2 are given in Table 5.12. Conversion, copolymer composition molecular weight and PDI data are given in Table 5.13.

Table 5.12 First- and second-order rate constants of propagation, k_1 and k_2 for the polymerisation of **SXN4** initiated using **Pd1388** and **Pd796** at 70 ºC in a 5:1 mixture of toluene:fluorobenzene[†]

Anion, X	Initiator	k_{1total} (10^{-5} s^{-1})	k_{1endo} (10^{-5} s^{-1})	k_{1exo} (10^{-5} s^{-1})	k_{2total} (10^{-4} $Mol^{-1}dm^3s^{-1}$)	k_{2endo} (10^{-4} $Mol^{-1}dm^3s^{-1}$)	k_{2exo} (10^{-3} $Mol^{-1}dm^3s^{-1}$)
$[BF_4]$	**Pd796**	7.42 ± 0.1	5.33 ± 0.1	11.1 ± 0.2	7.02 ± 0.2	9.58 ± 0.3	2.77 ± 0.8
$[B(C_6F_5)_4]$	**Pd1388**	3.11 ± 0.1	1.36 ± 0.07	6.31 ± 0.2	4.69 ± 0.3	5.85 ± 0.5	1.93 ± 0.1

[†]The polymerisation reactions were only carried out once. The errors quoted are those in the fit of monomer consumption data to equation 3.3

Table 5.13 Copolymer composition, molecular weight and PDI data for the polymerisation of **SXN4** initiated using **Pd1388** and **Pd796** after 3 hours at 70 ºC in a 5:1 mixture of toluene:fluorobenzene

Anion, X	Initiator	Copolymer composition (%)		Conversion (%)			M_n (Daltons)*	M_w (Daltons)*	PDI
		endo	*exo*	*endo*	*exo*	*Total*			
$[BF_4]$	**Pd796**	63	37	21	43	26	5000	8100	1.6
$[B(C_6F_5)_4]$	**Pd1388**	46	54	7	31	13	10400	14600	1.4

* All molecular weights are quoted relative to polystyrene standards

When **SXN4** is polymerised in a 5:1 mixture of toluene:fluorobenzene, the reaction proceeds more quickly and to higher conversion using the initiator **Pd796** (X = $[BF_4]$) than using **Pd1388** (X = $[B(C_6F_5)_4]$). This observation is in contrast to the effect seen in TCE, for which **Pd1388** gives higher conversion and more rapid polymerisation. Interestingly, the molecular weight of polymer obtained using **Pd1388** (X = $[B(C_6F_5)_4]$) is double that obtained using **Pd796** (X = $[BF_4]$) suggesting that in toluene:fluorobenzene, faster polymerisation kinetics and higher conversion do not necessarily lead to polymers of higher molecular weight.

5.3 Conclusions

For the series of *endo*/*exo* monomers of the type $NB(CH_2)_nOCH_2C(CF_3)_2OH$ and $NB(CH_2)_nC(CF_3)_2OH$, in general an increase in the number of methylene groups, n, spacing the HFP functionality away from the norbornene skeleton leads to a corresponding enhancement in polymerisation rate and overall conversion. A similar increase in the rate of hydride consumption (related to initiation) is also observed as chain length is increased. The observed increase in polymerisation rate with increasing chain length for HFP-functionalised monomers is in contrast to observations involving both pure *exo and* pure *endo* alkyl-functionalised norbornenes, for which polymerisation rate was found to be independent of chain length (*exo*) and decrease with increasing chain length (*endo*). [4, 18-19]

For the majority of the monomers studied, uptake of the *exo* isomer within a mixture is preferred over the corresponding *endo* component, which is in agreement with the known preference for polymerisation of *exo* monomers, highlighted in other studies.[4, 18-19, 54-61] The exception to this trend is for polymerisation of *endo*-/*exo*-$NBOCH_2C(CF_3)_2OH$ which shows preferential uptake of the *endo* isomer. Similar rates of uptake of *endo*/*exo* isomers have been reported for neutral initiator systems,[50-53] however a satisfactory explanation for the low *exo* reactivity observed for of **ZXN2** with **Pd1388** in this work has not, to date, been established.

In contrast to the series of pure *exo* HFP-functionalised monomers studied in Chapter IV (**ZX2**, **SX1**, **SX2**, **DX2** and **TX2**, respectively), for which an increase in n leads to a corresponding increase in polymer molecular weight, for *endo*/*exo* mixtures no particular trend is observed in M_p as a function of n, with the peak molecular weights of the polymers obtained ranging between 8000 (**DXN2**) and 21000 Daltons (**HXN1**). The PDIs of the polymers obtained vary between 1.3 and 2 and, in general, are narrower for polymers with $n \geq 3$ methylene units.

The monomer **SXN4** can be polymerised using a series of palladium-hydride pro-initiators of the type [Pd(H)(MeCN)(PCy_3)$_2$][X], where X is a weakly-coordinating anion ([BF_4], [SbF_6], [$PF_3(C_2F_5)_3$] or [$B(C_6F_5)_4$]). In TCE, **Pd1388** (X = [$B(C_6F_5)_4$]) shows the most rapid polymerisation kinetics along with overall higher conversion (49%), however the extent of conversion for the other initiators studied is only slightly lower (34-40%). The molecular weights of the polymers obtained using different anions are similar, however the character of the polymer obtained using **Pd1388** (X = [$B(C_6F_5)_4$) is bimodal. In a 5:1 mixture of toluene fluorobenzene, the polymerisation kinetics are faster with overall higher conversion when X = [BF_4] (**Pd796**), however the molecular weight of the final polymer obtained is higher using **Pd1388** than using **Pd796**.

5.4 References

1. P. Mayo, G. Orlova, J.D. Goddard and W. Tam, *J. Org. Chem.*, 2001, **66**, 5182-5191
2. S.J. Cristol, T.C. Morrill and R.A. Sanchez, *J. Org. Chem*. 1966, **31**, 2719-2725
3. W. Oppolzer, C. Chapuis, D. Dupuis and M. Guo, *Helvetica Chimica Acta*, 1985, **68**, 2100-1114
4. A.T. Cooper, Ph.D Thesis, Durham University, 2008
5. A.E. Feiring, M.K. Crawford, W.B. Farnham, J. Feldman, R.H. French, K.W. Leffew, V.A. Petrov, F.L. Schadt III, R.C. Wheland and F.C. Zumsteg, *J. Fluorine Chem.*, 2003, **122**, 11-16
6. A.E. Feiring, V.A. Petrov and F.L. Schadt III, US 2005/00588932 A1,2005
7. A.E. Feiring, V.A. Petrov and F.L. Schadt III, US 2005/6875555 B1, 2005
8. A.E. Feiring, J. Feldman, F.L. Schadt III, G. Newton Taylor, US 2005/6884564 B2, 2005
9. H.V. Tran, R.J. Hung, T. Chiba, S. Yamada, T. Mrozec, T-Y. Hsieh, C.R. Chambers, B.P. Osborn, B.C. Trinque, J.P. Matthew, S.A. MacDonald and C.G. Willson, *Macromolecules*, 2002, **35**, 6539-6549
10. A.J. Pasquale, A.R. Fornot and T.E. Long, *Macromol. Chem. Phys.* 2004, **205**, 621-627
11. E.G. Mamedov and E.I. Klabunovakii, *Russ. J. Chem.*, 2008, 44, 1097-1120
12. H. Ito, H.D. Truong, L.F. Rhodes, C. Chang, L.J. Langdorf, H.A. Sidaway, K. Maeda and S. Sumida, *Journal of Photopolymer Science and Technology*, 2004, **17**, 609-620

13. C. Chang, J. Lipian, D.A. Barnes, L. Seger, C. Burns, B. Bennett, L. Bonney, L.F. Rhodes, G. M. Benedikt, R. Lattimer, S.S. Huang and V.W. Day, *Macromol. Chem. Phys.*, 2005, **206**, 1988-2000
14. S. Breunig and W. Risse, *Makromol. Chem.*, 1992, **193**, 2915-2927
15. J. Melia, E. Connor, S. Rush, S. Breunig, C. Mehler and W. Risse, *Macrol. Symp.* 1995, **89**, 433-442
16. J.P. Mathew, A. Reinmuth, W. Risse, W. Melia and N. Swords, *Macromolecules*, 1996, **29**, 2755-2763
17. B.S. Heinz, F.P. Alt and W. Heitz, *Macromol. Rapid Commun.*, 1998, **19**, 251-256
18. A.D. Hennis, J.D. Polley, G.S. Long, A. Sen, D. Yandulov, J. Lipian, G.M. Benedikt, L.F. Rhodes and J. Huffman, *Organometallics,* 2001, **20**, 2802-2812
19. J.K. Funk, C. Andes and A. Sen, *Organometallics,* 2004, **23**, 1680-1683
20. J.M.G. Cowie, *Polymers: Chemistry and Physics of Modern Materials*, 2nd Edition, Blackie Academic and Professional, London, 1993, p104-122
21. C. Andes, L. Fischetti, A. Hennis and A. Sen, *Polymer Preprints*, 2002, **43**, 963-964
22. J.K. Funk, C. Andes and A. Sen, *Polymer Preprints*, 2003, **44**, 681-682
23. C.M. Dettmer, M.K. Gray, J.M Torkelson and S.T. Nguyen, *Macromolecules*, 2004, **37**, 5504-5512
24. M. Finemann and S.D. Ross, *J. Polym. Sci*, 1950, **5**, 259-265
25. H. Dostal, *Monatsh. Chem.* 1936, **69**, 424-426
26. F.R. Mayo and F.M.J. Lewis, *J. Am. Chem Soc.*, 1944, **66**, 1594-1601
27. T. Alfrey Jr. and G.J. Goldfinger, *Chem. Phys.*, 1944, **12**, 115
28. F.T.J. Wall, *J. Am. Chem. Soc.*, 1944, **66**, 2050-2057
29. L.M. Morris, T.P. Davies and R.P. Chaplin, *Polymer*, 2000, **42**, 941-952
30. P.J. Flory, *Principles of Polymer Chemistry*, Cornell University Press, Ithaca and London, 1953, p178-203
31. M.L. Coote and T.P. Davis, *Prog. Polym. Sci*, 2000, **24**, 1217-1251
32. D.W. Cywar and D.A. Tirrell, *J. Am. Chem. Soc*., 1989, **111**, 7544-7553
33. H. Tanaka, K. Sasai, T. Sato and T. Ota, *Macromolecules*, 1988, **21**, 3534-3536
34. D.J.T. Hill, A.P. Lang, H.H. O'Donnell and P.W. O'Sullivan, *Eur. Polym. J.* 1989, **25**, 911-915
35. E. Merz, T. Alfrey and G.J. Goldfinger, *J. Polym. Sci.*, 1946, **1**, 75-82
36. W.G.J. Barb, *J. Polym. Sci.*, 1953, **11**, 117-126

37. E.G. Ham, *J. Polm. Sci.*, 1954, **14**, 87-93
38. J. Guillot, J. Vialle and A. Guyot, *Macromol. Sci. Chem.*, 1971, A5, 735
39. R. Van Der Meer, J.M. Alberti, A.L. German and H.N.J. Linssen, *J. Polym. Sci. A: Polym. Chem.*, 1979, **17**, 3349-3364
40. D.J.T. Hill, J.H. O'Donnell and P.W. O'Sullivan, *Macromolecules*, 1985, **18**, 9-17
41. T. Fukuda, Y.D. Ma and H. Inagaki, *Macromolecules*, 1985, **18**, 17-26
42. I. Tritto, L. Boggioni, J.C. Jansen, K. Thorshaug, M.C. Sacchi and D.R. Ferro, *Macromolecules*, 2002, **35**, 616-623
43. I. Tritto, C. Marestin, L. Bogoioni, A. Provasoli and D.R. Ferro, *Macromolecules*, 2000, **33**, 8931-8944
44. C.T. Zhao, M. do Rosario Riberio, M. Farinha Portela, S. Pereira and T. Nunes, *Europ. Polym. J.*, 2001, **37**, 45-54
45. S. Y. Park, K.Y. Choi, K. H. Song and B.G. Jeong, *Macromolecules*, 2003, **36**, 4216-4225
46. I. Tritto, L. Boggioni, and D.R. Ferro, *Coord. Chem. Rev.*, 2006, **250**, 212-241
47. A.M. van Herk, *J. Chem. Edu*, 1995, **72**, 138
48. A.M. van Herk and T. Dröge, *Macromol. Theory Simul*, 1997, **6**, 1263-1276
49. S.V. Arehart and K. Matyjaszewski, *Macromolecules*, 1999, **32**, 2221-2231
50. M. Kang and A. Sen, *Organometallics*, 2004, **23**, 5396-5398
51. I. Takamiya, M. Yamashita and K. Nozaki, *Organometallics*, 2008, **27**, 5347-5352
52. C. Shikada, S. Kaita, Y. Maruyama, M. Takei and Y. Watatsuki, *Macromol. Rapid Commun.*, 2008, **29**, 219-223
53. A. Michalak and T. Ziegler, *Organometallics*, 2001, **20**, 1521-1532
54. A. Sen, *Acc. Chem. Res.* 1993, **26**, 303-310
55. B.A. Markies, D. Kruis, M.H.P. Rietveld, K.A.N. Verkerk, J. Boersma, H. Kooijman, T.M. Lakin, A.L. Spek and G. van Koten, *J. Am. Chem. Soc.* 1995, **117**, 5263-5274
56. R. van Asselt, E.E.C.G. Gielens, R.E. Rülke, K. Vrieze and C.J. Elsevier *J. Am. Chem. Soc.* 1994, **116**, 977-985
57. M. Zocchi and G. Tieghi, *J. Chem. Soc., Dalton Trans.*, 1979, 944-947
58. N. Carr, D.J. Dunne, A.G. Orpen and J.L. Spencer, *J. Chem. Soc., Chem. Commun.*, 1988, 926-928

59. J.G.P. Delis, P.B. Aubel, D. Vrieze, P.W.N.M. van Leeuwen, N. Veldman and A.L. Spek, *Organometallics*, 1997, **16**, 4150-4160

60. C.S. Li, D.C. Jou and C.H. Cheng, *Organometallics*, 1993, **12**, 3945-3954

61. R.P Hughes and J. Powell, *J. Organomet. Chem.* 1973, **60**, 427-441

Chapter VI

Summary and future work

Chapter VI

Summary and Future Work

6.1 Introduction

The polymerisation of cyclic olefins such as norbornene has attracted a great deal of interest over the past two decades, primarily due to the attractive properties of the resulting polymeric materials. Norbornene can be polymerised using a number of different mechanisms by suitable choice of a polymerisation initiator, each resulting in a different class of polymer.[1] Of particular interest to this current work is the vinyl polymerisation of norbornene to yield saturated polymeric materials, which retain the rigid fused ring system within the backbone chain. Such polymers have a number of advantageous properties (compared to those obtained *via* ROMP) that include excellent thermal stability (T_g > 370 ºC), low dielectric constant and low birefringence, something which coupled with high optical transparency and excellent etch resistance make functionalised poly(norbornene) derivatives a suitable choice for use in binder resins for use deep UV photolithography.[2-9] Work within this thesis has focused on the in depth study of the vinyl polymerisation behaviour of hexafluoropropanol-(HFP) functionalised norbornenes using palladium hydride initiators, of commercial interest to Promerus for use in 157 nm photolithography.

6.2 Summary Chapter II

In Chapter II, the synthesis of a series of HFP-functionalised monomers is described, which differ in the number of methylene units (n) separating the HFP-functionality from the norbornene skeleton (Figure 6.1). Spacing of a functional group from the norbornene skeleton has previously been shown to have an effect on polymerisation rate.[10] The synthesis of monomers of the type $NB(CH_2)_nC(CF_3)_2OH$ (Figure 6.1 **a**, n = 1, **SN3**) and $NB(CH_2)_nOCH_2C(CF_3)_2OH$ (Figure 6.1 **a**, n = 0, **ZXN**, **ZX3**; n = 2, **DXN2** and n = 3, **TX3** and **TXN3**) are reported with a view to the subsequent determination of the effect of n on polymerisation rate. A summary of the HFP-functionalised norbornene monomers used within this thesis is provided on page XV and as a pull out sheet for easy reference.

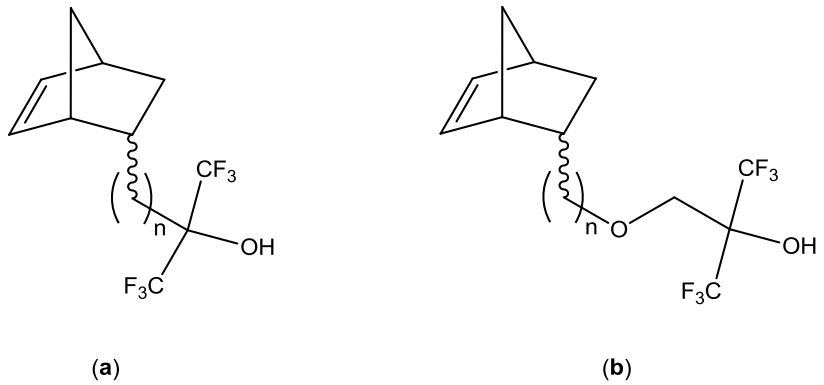

(**a**) (**b**)

Figure 6.1 Structures of HFP-functionalised norbornenes: (**a**) $NB(CH_2)_nC(CF_3)_2OH$) and (**b**) $NB(CH_2)_nOCH_2C(CF_3)_2OH$

Commercially, the polymerisation of HFP-functionalised norbornenes is carried out using a variety of different initiators, one of which is the palladium hydride complex $[Pd(H)(MeCN)(PCy_3)_2][B(C_6F_5)_4]$ (**Pd1388**). However, the weakly coordinated counter anion of **Pd1388** is expensive and hence cheaper alternatives, with comparable activity to **Pd1388** were sought. In Chapter II, the series of palladium hydride complexes $[Pd(H)(MeCN)(PCy_3)_2][X]$ (anion X = BF_4, PF_6, SbF_6, I and $B(C_6F_5)_4$) were prepared with a view to determining the effect of the anion on polymerisation rate. The syntheses of similar complexes of the type $[PdH(X)(PCy_3)_2]$ (anion X = Cl, I and OTf) in which the anion is bound to the palladium centre are also described, generating the desired palladium hydride complexes in reasonable yield (>50%).

6.3 Summary Chapter III

Polymerisation of HFP-functionalised monomers is traditionally carried out in halogenated polar solvents such as chlorobenzene or 1,1,2,2-teterachloroethane (TCE), which serve to solubilise the palladium hydride initiator as well as allowing the reaction to be carried out at elevated temperatures (~50-70 °C). However, although the desired HFP-functionalised poly(norbornenes) are obtained, the stability of palladium hydride initiators in halogenated solvents, in particular at elevated temperatures, remained unknown.

In Chapter III the stability of the discrete complex $[PdH(MeCN)(PCy_3)_2][B(C_6F_5)_4]$ (**Pd1388**) was examined and found to be unstable in TCE at a temperature of 70 °C decomposing to form $PdCl_2(PCy_3)_2$ and two further species, **b** and **c** that, despite extensive efforts, could not be identified. However, in

contrast, **Pd1388** was found to be stable upon prolonged heating to 70 °C in a 5:1 (v/v) mixture of toluene:fluorobenzene.

In TCE both **Pd1388** itself and **Pd1388** in its decomposed form (*i.e.* a mixture of $PdCl_2(PCy_3)_2$, **b** and **c**) are able to act as pro-initiator systems in the polymerisation of *exo*-$NBCH_2OCH_2C(CF_3)_2OH$ (**SX1**). The rate of palladium hydride decomposition (k_d) was examined for **Pd1388** in TCE at 70 °C using ^1H NMR spectroscopy in the presence and absence of monomer (**SX1**). In the presence of monomer, the rate of hydride consumption measured experimentally, k_H, is related to the rate of initiation of the polymerisation reaction. However, as the initiation process relies upon a complex series of equilibria involving the dissociation of ligands and *cis*/*trans* isomerism the rate constants of initiation and hydride consumption are not necessarily equivalent. Hydride consumption *via* a decomposition pathway to form the decomposition products $PdCl_2(PCy_3)_2$, **b** and **c** (k_d) is an order of magnitude slower than consumption of hydride during the polymerisation of **SX1**. This observation leads us to conclude that decomposition of **Pd1388** during the polymerisation of **SX1** is likely to contribute little to the observed rate of hydride consumption, the majority of the palladium hydride being consumed during initiation of the polymerisation process.

In order to understand the polymerisation of **SX1** initiated by **Pd1388** in detail, the kinetics of its polymerisation (propagation) were examined. Previous reports that have considered the polymerisation kinetics for functionalised norbornenes have analysed monomer consumption data using *pseudo* first-order kinetics.[10-12] However, consideration of the possible mechanism of polymerisation suggests that approximation of polymerisation rate to a *pseudo* first-order process may be an oversimplification and hence not provide an accurate description of polymerisation kinetics. Data corresponding to monomer (**SX1**) consumption (as a function of time were analysed according using *pseudo*-first order kinetics and unsurprisingly the resulting logarithmic plots of $\ln([M]/[M]_0)$ (where $[M]_0$ is initial monomer concentration at time = 0) did not produce a linear relationship. Clearly a more rigorous model for the treatment of these data was required, which requires consideration of the possible mechanism of polymerisation.

The first step in the polymerisation of norbornene (NB) will involve insertion of a monomer unit into a palladium hydride bond. It is therefore reasonable to assume that such an insertion will demonstrate a first order dependence upon both initiator and monomer concentration. However, subsequent insertion steps will involve insertion of monomer into a palladium alkyl (palladium norbornene) bond and the nature of this

bond will change throughout the course of the reaction (Pd-NB dimer, Pd-NB trimer, *etc*.). Consequently, the kinetics of the propagation process could be considered to be time dependent, with a different value of *k* for each insertion step. It is also possible that additional monomer units are involved in the transition state, and that polymerisation rate is influenced by the changing viscosity of the system as the reaction progresses, resulting in kinetic behaviour which is considerably more complex than that expected for a *pseudo*-first order system. It is not practical (or even necessarily possible) to measure the rate of each insertion step independently; instead it is more useful to have a model that accurately describes the monomer consumption data obtained as a function of time, which gives an approximation of the polymerisation rate over the course of the reaction.

In order to determine an overall rate constant of polymerisation, it is necessary to consider the amount of monomer consumed, as well as the concentration of monomer remaining in solution at any given time. The concentration of free monomer as a function of time is readily measured and hence a known value, [M]. The concentration of monomer at the start of the reaction is also a known value hence the amount of monomer consumed is given by ($[M]_0 - [M]$), which can be linked to conversion {($[M]_0 - [M]$)/$[M]_0$)}. It is now possible to define a second rate constant, k_2, which considers both ($[M]_0 - [M]$) and free monomer concentration [M].

Combining the processes described by k_1 and k_2, a kinetic model has been proposed for the polymerisation of norbornene monomers *via* a step-wise addition mechanism, which provides an appropriate means of fitting monomer concentration data as a function of time and an indication of overall polymerisation rate. The model is given in equation 3.2 and its integrated form in equation 3.3 and describes the propagation stage of the polymerisation reaction. The value of $[M]_0$ at the start of the propagation process cannot be measured directly and hence is approximated *via* extrapolation of monomer consumption data relating to propagation (*i.e.* once all of the palladium hydride pro-initiator has been consumed) to time = 0. To avoid confusion, this quantity determined *via* extrapolation, is denoted $[M]_0$'.

$$\frac{d[M]}{dt} = -((k_1 - k_2([M]_0' - [M]))[M] \qquad \text{Equation 3.2}$$

$$[M] = \frac{[M]_0'(k_1 - [M]_0' k_2)e^{-(k_1 - [M]_0' k_2)t}}{k_1 - [M]_0' k_2 e^{-(k_1 - [M]_0' k_2)t}} \qquad \text{Equation 3.3}$$

Values of k_1, k_2 and $[M]_0$' are obtained *via* non-linear curve fitting of experimentally-determined monomer consumption data to equation 3.3 using Origin 8.1. The model was shown to provide an excellent fit to the data for polymerisation of **SX1** using **Pd1388** and its decomposed form in both TCE and a 5:1 (v/v) mixture of toluene:fluorobenzene with R^2 values of 0.993 or greater. For polymerisation of **SX1**, both k_1 and k_2 are highest using **Pd1388** in polar solvents such as TCE and these rapid polymerisation kinetics correlate well with the high degree of conversion (94%) observed. The polymerisation reaction proceeds more slowly using decomposed **Pd1388** and conversion is approximately half that achieved using **Pd1388** itself in the same time frame, resulting in a HFP-functionalised poly(norbornene) of lower molecular weight and higher polydispersity. **Pd1388** will also act as a pro-initiator in a 5:1 (v/v) mixture of toluene:fluorobenzene, however conversion and polymerisation rate are significantly lower than in the more polar solvent TCE, resulting in a HFP-functionalised poly(norbornene) of lower molecular weight, relative to that obtained in TCE. High conversion is of vital importance industrially to generate the maximum yield of polymer in the shortest possible time frame.

6.4 Summary Chapter IV

In Chapter IV, the kinetic model given by equation 3.3, developed to describe the polymerisation of the model system **SX1** using **Pd1388**, was extended to the study of the pure *exo* and pure *endo* HFP-functionalised monomers whose preparation was described in Chapter II. Such a study was necessary to examine the general applicability of the polymerisation model to other HFP-functionalised monomers and also to provide a means to study the effect of the methylene spacer group (n) on polymerisation rate.

For the series of *exo* HFP-functionalised monomers $NB(CH_2)_nOCH_2C(CF_3)_2OH$ (n = 0-3, Figure 6.1, **b**) an increase in the value of n, which spaces the HFP-functionality away from the norbornene skeleton, leads to an corresponding enhancement in polymerisation rate and overall conversion. An increase in the rate of hydride consumption (related to the initiation process) is also observed with increasing chain length, n. For the two examples studied, pure *exo*-functionalised norbornenes (**SX1** and **SN2**) were found to polymerise much more quickly than their *endo* counterparts (**SX2** and **SN3**), respectively, which is consistent with previous studies.[10-11,14-27] An increase in the number of methylene units, n, in the monomer structure leads to a corresponding increase in the molecular weight of the resulting HFP-functionalised polymeric material obtained after a 3 hour reaction time. The HFP-functionalised

poly(norbornenes) obtained are characterised by relatively narrow polydispersities, with values ranging between 1.2 and 1.4 irrespective of the value of n.

The polymerisations of a selection of HFP-functionalised norbornenes (**SX1**, **SX2** and **SN2**) using **Pd1388** were also studied using GPC to monitor the molecular weight of the polymers as a function of time. A number of interesting effects were observed, including the formation of high molecular weight material at relatively low monomer conversion (<35%). In addition, during the early stages of the polymerisation reaction (<30 minutes) a reduction in the molecular weight of the polymer is observed as a function of time. For the polymerisation of **SX1** in TCE, a polymer of trimodal character (M_p = 4000, 21000 and 70,000 Daltons, respectively) was obtained after 1 minute at 70 °C, however over the course of the reaction, loss of both the high and low molecular weight species is observed to yield a final polymer (3 hours at 70 °C) of M_p = 22,000 Daltons and moderately low polydispersity of 1.4.

An identical effect is observed during the polymerisation of **SX1** in a 17:1 (v/v) mixture of toluene:fluorobenzene. The low molecular weight species was attributed to oligomers of around ten monomer units and its' disappearance as a function of time is expected with continued growth of the polymer chain. Loss of the high molecular weight species, which is complete within 25 minutes, is more unusual and consequently more difficult to explain.

The polymerisation of **SX2** using **Pd1388** in TCE shows similar behaviour to that observed for **SX1**, with a reduction in peak average molecular weight of approximately 15,000 Daltons over the course of the 3 hour reaction, however all of the polymers obtained show monomodal character with polydispersities of 1.3 or less. Loss or molecular weight reduction of high molecular weight species, with retention of low PDI is extremely difficult to rationalise in terms of either thermal or metal-mediated processes, both of which would be expected to be random in nature hence resulting in a broadening of the molecular weight distribution. However, one explanation could relate to the ceiling temperature of the polymerisation reaction and its possible proximity to the reaction temperature of 70 °C, however further work is needed to confirm whether this is indeed the case.

6.5 Summary Chapter V

In Chapter V the polymerisation kinetic model was extended to the study of *endo*/*exo* mixtures of HFP-functionalised norbornenes. For the series of *endo*/*exo* monomers of the type $NB(CH_2)_nOCH_2C(CF_3)_2OH$ and $NB(CH_2)_nC(CF_3)_2OH$, in general an increase in the number of methylene groups, n, spacing the HFP functionality away from the norbornene skeleton, leads to a corresponding enhancement in polymerisation rate and overall conversion. For the majority of the monomers studied, uptake of the *exo* isomer within a mixture is preferred over the corresponding *endo* component, which is in agreement with the known preference for polymerisation of *exo* monomers, highlighted in other studies.[11-24] In contrast, the polymerisation of *endo*-/*exo*-$NBOCH_2C(CF_3)_2OH$ (**ZXN2**) that shows preferential uptake of the *endo* isomer. To the best of our knowledge, this effect has not previously been observed for the polymerisation of substituted norbornenes with cationic palladium initiators. Similar rates of uptake of *endo*/*exo* isomers have been reported for neutral initiator systems, which are rationalised in terms of the weaker interaction between a metal centre and a functionality for neutral complexes,[13,28-29] however a satisfactory explanation for the low *exo* reactivity observed for of **ZXN2** with **Pd1388** in this work has not, to date, been established.

In contrast to the series of pure *exo* HFP-functionalised monomers studied in Chapter IV (**ZX2**, **SX1**, **SX2**, **DX2** and **TX2**, respectively), for which an increase in n leads to a corresponding increase polymer molecular weight, for *endo*/*exo* mixtures no particular trend is observed in M_p as a function of n, with the peak molecular weights of the polymers obtained ranging between 8000 (**DXN2**) and 21000 Daltons (**HXN1**). The PDIs of the polymers obtained vary between 1.3 and 2 and, in general, are narrower for polymers with $n \geq 3$ methylene units.

Finally, the effect of the anion of the initiator on polymerisation rate was examined for the polymerisation of *endo*-/*exo*-$NBCH_2C(CF_3)_2OH$ (**SXN4**) using palladium hydride initiators of the type $[PdH(MeCN)(PCy_3)_2][X]$, where X is a weakly-coordinating anion (BF_4, SbF_6, $PF_3(C_2F_5)_3$ or $B(C_6F_5)_4$). In TCE, **Pd1388** (X = $B(C_6F_5)_4$) shows the most rapid polymerisation kinetics along with the best overall conversion (49%), although the extent of conversion obtained using the other initiators studied is only slightly lower (34-40%). The molecular weights of the polymers obtained using initiators with different counter anions are similar, however the character of the polymer obtained using **Pd1388** (X = $[B(C_6F_5)_4]$) is bimodal, whereas a monomodal distribution is observed using initiators with alternate counter anions. The bimodal character is completely reproducible and is also observed for the pure *endo*

isomer (*endo*-$NBCH_2C(CF_3)_2OH$, **SN3**), however to date, a satisfactory explanation for this bimodal character has not been established.

When the polymerisation of *endo*-/*exo*-$NBCH_2C(CF_3)_2OH$ **SXN4** is carried out in a 5:1 (v/v) mixture of toluene:fluorobenzene, the polymerisation kinetics are faster with overall higher conversion when X = $[BF_4]$ (**Pd796**) than when X = $[B(C_6F_5)_4]$ (**Pd1388**), however the molecular weight of the final polymer obtained is higher using **Pd1388** than that obtained using **Pd796**. In less polar solvents such as toluene:fluorobenzene, faster polymerisation kinetics and higher conversion do not necessarily generate polymers of higher molecular weight.

6.6 Future Work

Studies within this thesis have examined in detail the polymerisation kinetics of HFP-functionalised norbornenes containing methylene spacer groups (n). However, the performance of the HFP-functionalised polynorbornenes obtained to function in the desired application of these polymeric materials (photolithographic imaging) has yet to be explored. It would be interesting to study the effect of n on the dissolution rate of these polymers in basic developer solution and hence, the quality of the lithographic images obtained. It would be also be interesting to study the dissolution rates of *endo*- and *exo*-HFP poly(norbornenes) independently and a mixtures of isomers to determine the *endo*/*exo* effect on lithographic performance.

In Chapter V it was noted that during the polymerisation of *endo*/*exo* mixtures, increasing the value of n above four did not lead to any further enhancement in the rate of polymerisation of the *exo* component within the mixture. However, an increase was observed for the *endo* component. An interesting future addition to this study would be to consider monomers with n>6 to explore whether increasing the number of methylene units further eventually leads to a point where steric interactions overcome electronic donor effects and results in an overall reduction in polymerisation rate for the *endo*-component within mixtures of HFP-functionalised monomers. An increase in the steric bulk of substituents in both the *endo* and *exo*-positions has been shown to reduce polymerisation rate in certain instances and was discussed in Chapter IV.

Given the availability of sufficient quantities of pure isomer, coupled with adequate spectrometer time, it would be very interesting to examine the reactivity ratios of *endo* and *exo* HFP-functionalised norbornenes using a non-linear least squares approach. Reactivity ratios give an indication of the relative rates of self- versus cross-propagation and provide an insight into the structure of the copolymer obtained (*e.g.*

random, blocky etc.).[30] A similar study of reactivity ratios using the Finemann Ross method is reported in Chapter V, however proved to be unsuccessful in the generation of reliable values of r_{endo} and r_{exo} due to the large errors associated with this model and the fact that it assumes terminal kinetics, which have been shown not to be appropriate for the study of vinyl type HFP-functionalised norbornene polymerisations.

The changes in the molecular weight of HFP-functionalised polynorbornenes, with retention of low PDI as function of time (discussed in Chapter IV) are extremely unusual and worthy of further investigation. It would be interesting to examine the polymerisation of norbornene monomer bearing groups other than HFP with **Pd1388** to see if the effects observed are specific to these particular monomers or applicable to vinyl norbornene polymerisations in general. It would also be worthwhile to consider the polymerisation of HFP-functionalised norbornenes with other, non-palladium hydride based initiators to examine if the hydride is key to the reduction in molecular weight. A detailed study of the polymerisation thermodynamics of functionalised-norbornenes would be extremely useful given the lack of current literature in this area, especially if the ceiling temperatures of such reactions could be determined.

Pd1388 is an extremely effective polymerisation initiator, however it does have a drawback that is related to the phosphines substituents. The HFP-functionalised norbornenes used in photolithography need to be of extremely high purity requiring the removal of residual palladium, phosphorus and other contaminants to parts per billion levels. It is not possible to avoid the use transition metals however the development of phophine-free initiators, with activity comparable to that of **Pd1388** would be extremely advantageous.

6.7 References

1. C. Janiak and P.G. Lassahn, *J. Mol. Catal. A: Chem.*, 2001, **166**, 193-209
2. E. Reichmanis, O. Nalamasu and F.M. Houlihan, *Acc. Chem Res.*, 1999, **32**, 659-667
3. A.E. Feiring, V.A. Petrov and F.L. Schadt III, US 2005/00588932 A1, 2005
4. A.E. Feiring, V.A. Petrov and F.L. Schadt III, US 2005/6875555 B1, 2005
5. A.E. Feiring, J. Feldman, F.L. Schadt III, G. Newton Taylor, US 2005/6884564 B2, 2005
6. H.V. Tran, R.J. Hung, T. Chiba, S. Yamada, T. Mrozec, T-Y. Hsieh, C.R. Chambers, B.P. Osborn, B.C. Trinque, J.P. Matthew, S.A. MacDonald, C.G.

Willson, D.P Sanders, E.F. Connor, R.H. Grubbs and W. Conley *Macromolecules,* 2002, **35**, 6539-6549

7. A.E. Feiring, M.K. Crawford, W.B. Farnham, J. Feldman, R.H. French, K.W. Leffew, V.A. Petrov, F.L. Schadt III, R.C. Wheland and F.C. Zumsteg, *J. Fluorine Chem.*, 2003, **122**, 11-16

8. H. Ito, H.D. Truong, L.F. Rhodes, C. Chang, L.J. Langdorf, H.A. Sidaway, K. Maeda and S. Sumida, *Journal of Photopolymer Science and Technology,* 2004, **17**, 609-620

9. C. Chang, J. Lipian, D.A. Barnes, L. Seger, C. Burns, B. Bennett, L. Bonney, L.F. Rhodes, G. M. Benedikt, R. Lattimer, S.S. Huang and V.W. Day, *Macromol. Chem. Phys.*, 2005, **206**, 1988-2000

10. A.T. Cooper, Ph.D Thesis, Durham University, 2008

11. C. Andes, L. Fischetti, A. Hennis and A. Sen, *Polymer Preprints*, 2002, **43**, 963-964

12. J.K. Funk, C. Andes and A. Sen, *Polymer Preprints*, 2003, **44**, 681-682

13. I. Takamiya, M. Yamashita and K. Nozaki, *Organometallics,* 2008, **27**, 5347-5352

14. J. Melia, E. Connor, S. Rush, S. Breunig, C. Mehler and W. Risse, *Makromol. Chem. Macrol. Symp.* 1995, **89**, 433-442

15. S. Breunig and W. Risse, *Makromol. Chem.*, 1992, **193**, 2915-2927

16. B.S. Heinz, F.P. Alt and W. Heitz, *Macromol. Rapid Commun.*, 1998, **19**, 251-256

17. A. Reinmuth, J.P. Mathew, J. Melina and W. Risse, *Macromol. Rapid. Commun.,* 1996, **17**, 173-180

18. J.P. Mathew, A. Reinmuth, W. Risse, W. Melia and N. Swords, *Macromolecules*, 1996, **29**, 2755-2763

19. A.D. Hennis, J.D. Polley, G.S. Long, A. Sen, D. Yandulov, J. Lipian, G.M. Benedikt, L.F. Rhodes and J. Huffman, *Organometallics,* 2001, **20**, 2802-2812

20. J.K. Funk, C.E. Andes and A. Sen, *Organometallics,* 2004, **23**, 1680-1683

21. M. Kang and A. Sen, *Organometallics,* 2004, **23**, 5396-5398

22. A. Sen, *Acc. Chem. Res.* 1993, **26**, 303-310

23. B.A. Markies, D. Kruis, M.H.P. Rietveld, K.A.N. Verkerk, J. Boersma, H. Kooijman, T.M. Lakin, A.L. Spek and G. van Koten, *J. Am. Chem. Soc.* 1995, **117**, 5263-5274

24. R. van Asselt, E.E.C.G. Gielens, R.E. Rülke, K. Vrieze and C.J. Elsevier *J. Am. Chem. Soc.* 1994, **116**, 977-985

25. M. Zocchi and G. Tieghi, *J. Chem. Soc., Dalton Trans.*, 1979, 944-947

26. N. Carr, D.J. Dunne, A.G. Orpen and J.L. Spencer, *J. Chem. Soc., Chem. Commun.*, 1988, 926-928

27. J.G.P. Delis, P.B. Aubel, D. Vrieze, P.W.N.M. van Leeuwen, N. Veldman and A.L. Spek, *Organometallics*, 1997, **16**, 4150-4160

28. C. Shikada, S. Kaita, Y. Maruyama, M. Takei and Y. Watatsuki, *Macromol. Rapid Commun.*, 2008, **29**, 219-223

29. A. Michalak and T. Ziegler, *Organometallics*, 2001, **20**, 1521-1532

30. J.M.G. Cowie, *Polymers: Chemistry and Physics of Modern Materials*, 2nd Edition, Blackie Academic and Professional, London, 1993, p104-122

Chapter VII

Experimental procedures and preparations

Chapter VII

Experimental procedures and preparations

7.1 General Considerations

All operations were conducted under an atmosphere of dry nitrogen or argon using standard Schlenk and cannula techniques or in a nitrogen-filled glove box (Braun) unless stated otherwise. All NMR-scale reactions were conducted using NMR tubes fitted with Young's tap valves. Bulk solvents were purified using an Innovative Technologies Purification System and degassed prior to use. NMR solvents ($CDCl_3$, C_6D_6, C_7D_8, $C_2D_2Cl_4$) were dried over P_2O_5 or CaH_2, distilled and degassed prior to use.

Solution phase NMR spectroscopy

Routine solution phase NMR spectra were collected on a Varian Unity 300, a Varian Mercury 200 or 400, a Bruker Avance 400, a Varian Inova 500 and a Varian VNMRS 700 MHz spectrometer at ambient probe temperatures (~20 °C) unless stated otherwise. Chemical shifts were referenced to residual protio impurities in the deuterated solvent (^1H), ^{13}C shift of the solvent (^{13}C) or to external aqueous 85% H_3PO_4 (^{31}P). Solvent proton shifts (ppm): $CDCl_3$, 7.26 (s); C_6D_6, 7.15 (s), $C_6D_5CD_3$, 2.09 (s) 6.98 (m) 7.00 (m), 7.09 (m); $C_2D_2Cl_4$, 5.91(s). Solvent carbon shifts (ppm): $CDCl_3$ 77.36 (t), $C_2D_2Cl_4$ 73.78 (t). ^1H and ^{13}C spectra were assigned with the aid of COSY, HSQC, HMBC and DEPT 135 and an example of assigned spectra is given in Appendix 2. For the purpose of notation in ^1H NMR spectral assignments, *endo* is abbreviated to N and *exo* to X. # denotes an unseparated mixture of *endo* and *exo* isomers, however the proton and carbon resonances corresponding to each isomer in the mixture have been assigned and are reported separately. ^{13}C-NMR spectra (2000 scans) were recorded using continuous broad band proton decoupling and a 3 s recycle delay and therefore are not quantitative. All chemical shifts are reported in ppm with coupling constants in Hz.

Mass Spectrometry

Mass spectra were recorded by the Chemistry Department Mass Spectrometry Service, Durham University (EI^+ GCMS: Thermo-Finnigan Trace, Accurate mass EI^+: Waters Xevo QTOF) and are reported in (*m/z*). The isotope distributions were verified *via* comparison with the theoretical isotope pattern. Retention times (RT) are given in minutes.

Elemental Analysis

Elemental analyses were performed by the Chemistry Analytical Services Department, Durham University.

Infrared Spectroscopy

Infrared spectra were recorded on a Perkin Elmer 1600 series FT-IR spectrometer fitted with a Golden Gate ATR device. Spectra were run on neat solid and neat liquid samples. Values are quoted in cm^{-1}.

Size exclusion chromatography (GPC)

Polymer molecular weight analysis was carried out by size exclusion chromatography (SEC) on a Viscotek TDA 302 with triple detectors (refractive index, viscosity and light scattering). A value of 0.185 (obtained from Viscotek) was used for the dn/dc of polystyrene. PLgel 2 x 300 mm 5 μm mixed C columns (with a linear range of molecular weight from 200 – 2000,000 g mol^{-1}) were employed; THF was used as the eluent with a flow rate of 1.0 mL/min at a temperature of 303 K. All molecular weights are reported relative to polystyrene standards.

Materials

$PdMe_2$(TMEDA) was prepared according to literature procedures.[1-2] Monomers received from Promerus (**ZX1**, **SX1**, **SX2**, **SN2**, **SXN1**, **SXN3**, **SXN4**, **DX1**, **DX2**, **DXN3**, **DXN5**, **QXN1** and **HXN1**) were fully characterised prior to use. Monomers for use in polymerisation kinetic studies were dried and degassed prior to use unless otherwise stated. All other chemicals were obtained commercially and used as received unless otherwise stated.

7.2 Experimental procedures and monomer characterisation – Chapter II

Characterisation of *endo*-/*exo*-NBOH (ZXN1) (unseparated mixture of isomers)#

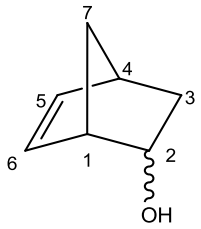

^{1}H NMR (699.7 MHz, $CDCl_3$):

***endo* component** (74%) δ 6.42 (dd, $J_{H5\text{-}H6}$ = 5.7 Hz $J_{H4\text{-}H5}$ = 3.1 Hz, 1H, H^5), 6.03 (dd, $J_{H5\text{-}H6}$ = 5.7 Hz, $J_{H1\text{-}H6}$ = 2.9 Hz, 1H, H^6), 4.44 (m, 1H, H^2), 2.97 (m, 1H, H^1), 2.79 (m, 1H, H^4), 2.08 (ddd, $J_{H3X\text{-}H3N}$ = 12.1 Hz, J = 8.1, 3.8 Hz, 1H, H^{3X}), 1.45 (m, 1H, H^{7syn}), 1.40 (br, s, 1H, OH), 1.24 (m, 1H, H^{7anti}), 0.74 (ddd, $J_{H3X\text{-}H3N}$ = 12.3 Hz, $J_{H3N\text{-}H4,\ H2}$ = 3.2 Hz, 1H, H^{3N})

***exo* component** (26%) δ 6.14 (dd, $J_{H5\text{-}H6}$ = 5.7 Hz $J_{H1\text{-}H6}$ = 2.8 Hz, 1H, H^6), 5.92 (dd, $J_{H5\text{-}H6}$ = 5.7 Hz $J_{H4\text{-}H5}$ = 3.2 Hz, 1H, H^5), 3.86 (m, 1H, H^2), 2.97 (m, 1H, H^4), 2.68 (m, 1H, H^1), 1.71 (m, 1H, H^7), 1.61 (m, 1H, H^{3X}), 1.60 (br, s, 1H, OH), 1.54 (m, 1H, H^7), 1.24 (m, 1H, H^{3N})

^{13}C{^{1}H} NMR (175.9 MHz, $CDCl_3$):

***endo* component** δ 140.8 (C^5), 131.2 (C^6), 72.9 (C^2), 48.7 (C^7), 48.5 (C^1), 43.3 (C^4), 38.2 (C^3)

***exo* component** δ 139.6 (C^6), 132.7 (C^5), 71.9 (C^2), 49.6 (C^1), 44.9 (C^7), 40.0 (C^4), 36.6 (C^3)

Accurate Mass MS: Found: 111.0809 ($M\text{-}H^+$) Calculated for $C_7H_{11}O$: 111.0810

GCMS EI$^+$: RT = 6.50, 110.0 ($C_7H_{10}O$, M^+, *endo*) 6.59, 110.0 ($C_7H_{10}O$, M^+, *exo*)

IR: 3600-3200 (O-H), 2965 (saturated C-H)

Synthesis and characterisation of *endo*-/*exo*-NBOCH$_2$C(CF$_3$)$_2$OH (ZXN2)#

A 3-necked round bottomed flask fitted with a nitrogen inlet, CO_2/acetone condenser and magnetic fly was charged with sodium hydride (95%, 2.61 g, 109 mmol) and THF (35 mL). The resulting slurry was cooled to -20 ºC and a solution of *endo*-/*exo*- NBOH (**ZXN1**) (10 g, 91 mmol) in THF (15 mL) added drop-wise over 20 minutes with vigorous stirring. The cooling bath was removed and the mixture warmed to ambient temperature overnight with vigorous stirring to yield a dark brown slurry. The mixture was cooled to -20 ºC and chilled HFIBO (14 mL, 109 mmol) added drop-wise with vigorous stirring. The mixture was stirred overnight at ambient temperature to yield a dark brown solution.

The solution was cooled to ~1 ºC and distilled water (50 mL) added drop-wise over 30 minutes. Concentrated hydrochloric acid (2 mL) was added drop-wise to bring the pH between 1 and 2 and the resulting layers separated. The aqueous phase was extracted with diethyl ether (2 x 20 mL) and the combined organic portions washed with brine (7 x 20 mL) until the last washing gave pH 6. The extracts were dried over $MgSO_4$, filtered and the solvent removed *in vacuo* to yield a dark brown liquid. The crude product was distilled using a column packed with 0.15 mm Propak beads to yield a yellow oil (15.07 g, 51%, bp 58-60 °C, 0.4 mbar.) ^{1}H NMR spectroscopic analysis of the oil showed the presence of unreacted **ZXN1** starting material, which was removed using column chromatography (90:10 hexane:ethyl acetate eluent) to give **ZXN2** as a colourless oil (2.8 g, 36% yield relative to crude material columned, 10% overall).

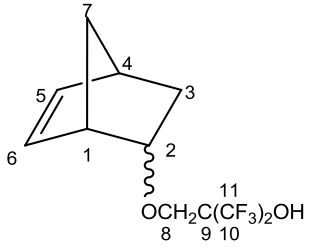

Unseparated mixture of isomers

^{1}H NMR (699.7 MHz, CDCl$_3$):

***endo* component** (70%) δ 6.34 (dd, $J_{H5\text{-}H6}$ = 5.6 Hz $J_{H1\text{-}H6}$ = 3.0 Hz, 1H, H^6), 5.93 (dd, $J_{H5\text{-}H6}$ = 5.6 Hz $J_{H4\text{-}H5}$ = 2.7 Hz, 1H, H^5), 4.30 (m, 1H, H^2), 4.00 (bs s, 1H, OH), 3.78 (d, $J_{H8\text{-}H8'}$ = 10.0 Hz, 1H, H^8), 3.72 (d, $J_{H8\text{-}H8'}$ = 10.0 Hz, 1H, $H^{8'}$), 3.12 (m,1H, H^4), 2.85 (m, 1H, H^1), 2.01 (ddd, $J_{H3X\text{-}H3N}$ = 12.3 Hz, $J_{H3X,\ H2,\ H4}$ = 7.9, 3.1 Hz, H^{3X}), 1.49 (m, 1H, H^7), 1.40 (m, 1H, H^7), 0.95 (ddd, $J_{H3N\text{-}H3X}$ = 12.3 Hz, $J_{H3N,\ H2,\ H4}$ = 6.2, 3.0 Hz, H^{3N})

***exo* component** (30%) δ 6.24 (dd, J_{H5-H6} = 5.7 Hz J_{H4-H5} = 2.9 Hz, 1H, H^5), 5.91 (dd, J_{H5-H6} = 5.7 Hz J_{H1-H6} = 3.3 Hz, 1H, H^6), 4.04 (br s 1H, OH), 3.85 (d, $J_{H8-H8'}$ = 10.3 Hz, 1H, H^8), 3.78 (d, $J_{H8-H8'}$ = 10.3 Hz, 1H, $H^{8'}$), 3.62 (m, 1H, H^2) 2.92 (m, 1H, H^1), 2.85 (m, 1H, H^4), 1.67-1.59 (m, 3H, H^{3X} and H^7), 1.39 (m, 1H, H^{3N})

$^{13}C\{^1H\}$ NMR (175.9 MHz, $CDCl_3$):

***endo* component** 139.2 (C^6), 130.9 (C^5), 122.8 (q, J_{C-F} = 285 Hz, C^{10}, C^{11}), 82.2 (C^2), 74.6 (sept, J_{C-F} = 28.9 Hz, C^9), 63.9 (C^8), 47.6 (C^7), 45.7 (C^4), 42.6 (C^1), 34.5 (C^3)

***exo* component** δ 141.7 (C^5), 132.7 (C^6), 122.8 (q, J_{C-F} = 285 Hz, C^{10}, C^{11}), 82.9 (C^2), 74.7 (sept, J_{C-F} = 28.9 Hz, C^9), 64.4 (C^8), 46.7 (C^1), 46.2 (C^7), 40.7 (C^4), 34.8 (C^3)

$^{19}F[^1H]$ NMR (376.3 MHz, $C_2D_2Cl_4$): δ -77.2 (m, 6F, $2CF_3$, *exo*), -77.3 (m, 6F, $2CF_3$, *endo*)

Accurate mass MS: Found: 291.0808 ($M-H^+$) Calculated for $C_{11}H_{13}O_2F_6$: 291.0820

GCMS EI^+: RT = 9.41, 291.1 ($C_{11}H_{13}O_2F_6$, $M-H^+$, *endo*), 9.58, 291.1 ($C_{11}H_{13}O_2F_6$, $M-H^+$, *exo*)

IR: 3600-3300 (O-H), 2975 (saturated C-H)

Characterisation of *exo*-NBOAc (ZX1)

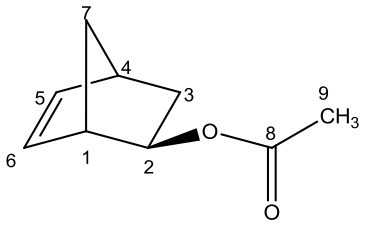

^{1}H NMR (699.7 MHz, $CDCl_3$): δ 6.21 (dd, $J_{H5\text{-}H6}$ = 5.7 Hz $J_{H4\text{-}H5}$ = 2.9 Hz, 1H, H^5), 5.95 (dd, $J_{H5\text{-}H6}$ = 5.7 Hz, $J_{H1\text{-}H6}$ = 3.3 Hz, 1H, H^6), 4.63 (m, 1H, H^2), 2.86 (m, 1H, H^1), 2.83 (m, 1H, H^4), 2.02 (s, 3H, H^9), 1.68 (ddd, $J_{H3X\text{-}H3N}$ = 12.5 Hz, $J_{H3X\text{-}H2,\,H4}$ = 9.6, 2.7Hz 1H, H^{3X}), 1.62 (m, 1H, H^7), 1.55 (m, 1H, H^7), 1.38 (ddd, $J_{H3X\text{-}H3N}$ = 12.5 Hz, $J_{H3X\text{-}H2,\,H4}$ = 2.7 Hz, 1H, H^{3N})

^{13}C{^{1}H} NMR (175.9 MHz, $CDCl_3$): δ 171.4 (C^8), 141.3 (C^5), 132.9 (C^6), 75.5 (C^2), 47.6 (C^1), 46.5 (C^7), 40.9 (C^4), 34.9 (C^3), 21.7 (C^9)

Accurate Mass MS: Found: 153.0912 ($M\text{-}H^+$) Calculated for $C_9H_{13}O_2$: 153.0916

GCMS EI$^+$: RT = 8.86, 152.0 ($C_9H_{12}O_2$, M^+)

IR: 2976 (saturated C-H), 1732 (C=O)

Synthesis and characterisation of *exo*-NB-OH (ZX2)

A 3 necked round bottomed flask, fitted with a nitrogen inlet and reflux condenser was charged with sodium hydroxide pellets (36 g, 0.9 mol), methanol (3.5 mL) and degassed, distilled water (50 mL). The solution was heated to 80 ºC with vigorous stirring and *exo*-NBOAc (**ZX1**) (35 g, 0.23 mol) added drop-wise. The solution was cooled to room temperature with stirring overnight, resulting in a brown solid precipitate. The precipitate was filtered, washed with water, dissolved in diethyl ether (100 mL) and treated with 10% aqueous HCl (17.5 mL). The ether layer was separated and washed with dilute sodium bicarbonate and brine. The ether solution was dried over $MgSO_4$, filtered and the solvent removed *in vacuo* to yield an off white solid. Pure **ZX2** was obtained in good yield (21.5 g, 85%) upon recrystallisation from hexane.

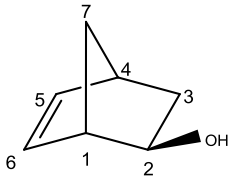

^{1}H NMR (699.7 MHz, $CDCl_3$): δ 6.17 (dd, J_{H5-H6} = 5.7 Hz J_{H1-H6} = 2.8 Hz, 1H, H^6), 5.95 (dd, J_{H5-H6} = 5.7 Hz J_{H4-H5} = 3.2 Hz, 1H, H^5), 3.89 (m, 1H, H^2), 2.81 (m, 1H, H^4), 2.71 (m, 1H, H^1), 1.72 (m, 1H, H^7), 1.64 (m, 1H, H^{3X}), 1.60 (br, s, 1H, OH), 1.56 (m, 1H, H^7), 1.27 (m, 1H, H^{3N})

^{13}C{^{1}H} NMR (175.9 MHz, $CDCl_3$): δ 139.6 (C^6), 132.7 (C^5), 71.9 (C^2), 49.6 (C^1), 44.9 (C^7), 40.0 (C^4), 36.6 (C^3)

Accurate Mass MS: Found: 111.0813 ($M-H^+$) Calculated for $C_7H_{11}O$: 111.0810

GCMS EI$^+$: RT = 6.56, 110.0 ($C_7H_{10}O$, M^+)

IR: 3600-3000 (O-H), 3000-2800 (saturated C-H)

Synthesis and characterisation of *exo*-NBOCH$_2$C(CF$_3$)$_2$OH (ZX3)

A 3-necked round bottomed flask fitted with a nitrogen inlet, CO_2/acetone condenser and magnetic fly was charged with sodium hydride (95%, 2.61 g, 109 mmol) and THF (35 mL). The resulting slurry was cooled to -20 ^{o}C and a solution of *exo* NBOH (10 g, 91mmol) in THF (15 mL) added drop-wise over 20 minutes with vigorous stirring. The cooling bath was removed and the mixture warmed to ambient temperature overnight with vigorous stirring to yield a dark brown slurry. The mixture was cooled to -20 ^{o}C and chilled HFIBO (14 mL, 109 mmol) added drop-wise with vigorous stirring. The mixture was stirred overnight at ambient temperature to yield a dark brown solution.

The solution was cooled to ~1 ^{o}C and distilled water (50 mL) added drop-wise over 30 minutes. Concentrated hydrochloric acid (~2 mL) was added drop-wise to bring the pH between 1 and 2 and the resulting layers separated. The aqueous phase was extracted with diethyl ether (2 x 20 mL) and the combined organic portions washed with brine (~6 x 20 mL) until the last washing gave pH 6.The extracts were dried over

$MgSO_4$, filtered and the solvent removed *in vacuo* to yield a dark brown liquid. The crude product was distilled using a column packed with Propak beads to yield a yellow oil (10.35 g, 39%, bp 56-58 ^oC, 0.4 mbar.) The oil was purified using column chromatography (90:10 hexane:ethyl acetate) to give **ZX3** as a colourless oil (0.8 g, 3%)

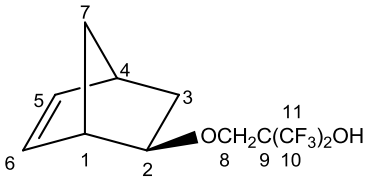

^{1}H NMR (699.7 MHz, $CDCl_3$): δ 6.24 (dd, J_{H5-H6} = 5.7 Hz J_{H4-H5} = 2.9 Hz, 1H, H^5), 5.91 (dd, J_{H5-H6} = 5.7 Hz J_{H1-H6} = 3.3 Hz, 1H, H^6), 4.03 (br s 1H, OH), 3.85 (d, $J_{H8-H8'}$=10.3Hz, 1H, H^8), 3.78 (d, $J_{H8-H8'}$=10.3 Hz, 1H, $H^{8'}$), 3.62 (m, 1H, H^2) 2.92 (m, 1H, H^1), 2.85 (m, 1H, H^4), 1.61 (m, 3H, H^{3x} and H^7), 1.39 (m, 1H, H^{3N})

^{13}C{^{1}H} NMR (175.9 MHz, $CDCl_3$): δ 141.7 (C^5), 132.7 (C^6), 122.8 (q, J_{C-F} =285 Hz, C^{10}, C^{11}), 82.9 (C^2), 74.7 (sept, J_{C-F} =28.9 Hz, C^9), 64.4 (C^8), 46.7 (C^1), 46.2 (C^7), 40.7 (C^4), 34.8 (C^3)

^{19}F[^{1}H] NMR (188.2 MHz, $CDCl_3$): δ -77.5 (m, 6F, $2CF_3$)

Accurate mass MS: Found: 291.0830 ($M\text{-}H^+$) Calculated for $C_{11}H_{13}O_2F_6$: 291.0820

GCMS EI$^+$: RT= 9.44, 291.2 ($C_{11}H_{13}O_2F_6$, $M\text{-}H^+$)

IR: 3600-3000 (O-H), 2978 (saturated C-H)

Synthesis and characterisation of norbornenone (ZNO)

All reagents were purchased as anhydrous or pre-dried dried prior to use. Triethylamine was distilled from KOH. *endo*/*exo*-NBOH (**ZXN1**) was dissolved in anhydrous DCM, dried over activated molecular sieves and the solvent removed *in vacuo* to yield a waxy solid.

To a 3-necked round bottomed flask equipped with a magnetic fly, nitrogen inlet and addition funnel was added a solution of oxalyl chloride (2.0 M in DCM, 136 mL, 272 mmol) in DCM (250 mL). The solution was cooled to -78 °C and a solution of dimethyl sulfoxide (40 mL) in DCM (40 mL) added drop-wise over 30 minutes.[3] A solution of **ZXN1** (24.0 g, 218 mmol) was added drop-wise and the solution stirred for 10 minutes. Triethylamine (150 mL) was added drop-wise over 40 minutes and the mixture stirred for 10 minutes at -78 ºC and then allowed to warm to 0 ºC over 1 hour. Water (250 mL) was added and the organic layer separated and washed with HCl (2 M, 4 x 160 mL) and brine (2 x 200 mL). The combined organic portions were dried over $MgSO_4$, filtered and the solvent removed *in vacuo* to yield a dark brown liquid. The crude product was distilled under reduced pressure to yield a mixture of the **ZNO** product and 7% residual DMSO (22.39 g, 88%, 56-58 ºC 18 mbar.) Pure **ZNO** can be isolated *via* column chromatography however this process is extremely time-consuming on a multi-gram scale. Pure **ZNO** is isolated as a yellow low melting point solid (39%).

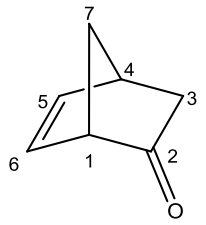

^{1}H NMR (699.7 MHz, $CDCl_3$): δ 6.52 (dd, $J_{H5\text{-}H6}$ = 5.6 Hz, $J_{H1\text{-}H6}$ = 2.8 Hz, 1H, H^6), 6.06 (m, 1H, H^5), 3.14 (m, 1H, H^1), 2.95 (m, 1H, H^4), 2.15 (m, J = 9.2 Hz, 1H, H^7), 1.96–1.88 (m, $J_{H3X\text{-}H3N}$ = 16.5 Hz, J = 9.2, 2H, H^7 and H^{3X}), 1.79 (dd, $J_{H3X\text{-}H3N}$ = 16.5 Hz , $J_{H3N\text{-}H4}$ = 4.5 Hz, 1H, H^{3N}).

^{13}C{^{1}H} NMR (175.9 MHz, $CDCl_3$): δ 215.8 (C^2), 143.3 (C^6), 130.8 (C^5), 56.1 (C^4), 51.1 (C^7), 40.3 (C^1), 37.4 (C^3).

GCMS EI$^+$: RT = 7.12, 109.1 (C_7H_9O, M-H^+)

IR: 3060-2860 (saturated C-H), 1740 (C=O)

Synthesis and characterisation of *endo*-NBOH (ZN1)

Route 1: A solution of pure **NBO** (5.81 g, 53.2 mmol) in methanol (400 mL) was cooled to 0 ºC and sodium borohydride (2.01 g, 53.2 mmol) added portion wise down a condenser with vigorous stirring.[4-5] The solution was warmed to ambient temperature and stirred over night. The reaction was quenched with 2M HCl (50 mL) and the methanol removed under reduced pressure. The remaining aqueous phase was extracted with diethyl ether (4 x 100 mL) and the combined organic portions washed with brine to pH 6 (2 x 100 mL). The organic fractions were dried over $MgSO_4$, filtered and the solvent removed to give a yellow oil. **ZN1** was isolated by sublimation under reduced pressure to yield a waxy white solid (150 mg, 3%). The majority of the **ZN1** product was found to be inseparable from the methanol solvent, either by distillation or removal of solvent under reduced pressure.

Route 2: A mixture of **NBO** and 7% residual DMSO (22.39 g, 191 mmol **NBO**) in ethanol (800 mL) was cooled to 0 ºC and excess sodium borohydride (38.86 g, 1.03 mol) added portion wise down a condenser with vigorous stirring. The procedure for route 1 was then followed and **ZN1** isolated *via* sublimation (800 mg, 4%). As was the case using methanol, it was not possible to isolate the majority of the **ZN1** product from the alcohol solvent.

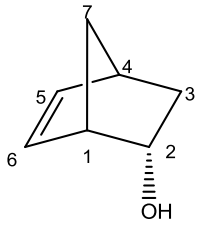

^{1}H NMR (699.7 MHz, $CDCl_3$): δ 6.45 (dd, $J_{H5\text{-}H6}$ = 5.7 Hz $J_{H4\text{-}H5}$ = 3.1 Hz, 1H, H^5), 6.06 (dd, $J_{H5\text{-}H6}$ = 5.7 Hz, $J_{H1\text{-}H6}$ = 2.9 Hz, 1H, H^6), 4.47 (m, 1H, H^2), 2.99 (m, 1H, H^1), 2.81 (m, 1H, H^4), 2.10 (ddd, $J_{H3X\text{-}H3N}$ = 12.1 Hz, $J_{H3X\text{-}H2,\ H4}$ = 8.1, 3.8 Hz, 1H, H^{3X}), 1.47 (m, 1H, H^{7syn}), 1.28 (m, 1H, H^{7anti}), 1.17 (d, 1H, OH), 0.76 (ddd, $J_{H3X\text{-}H3N}$ = 12.3 Hz, $J_{H3N\text{-}H4,\ H2}$ = 3.2 Hz, 1H, H^{3N})

^{13}C{^{1}H} NMR (175.9 MHz, $CDCl_3$): δ 140.8 (C^5), 131.2 (C^6), 72.9 (C^2), 48.7 (C^7), 48.5 (C^1), 43.3 (C^4), 38.2 (C^3).

Accurate Mass MS: Found: 111.0809 ($M\text{-}H^+$) Calculated for $C_7H_{11}O$: 111.0810

GCMS EI$^+$: RT = 6.67, 109.9 ($C_7H_{10}O$, M^+)

IR: 3600-3000 (O-H), 3000-2800 (saturated C-H)

Attempted synthesis of *endo*-NBOCH$_2$C(CF$_3$)$_2$OH (ZN2)

A slurry of sodium hydride (95%, 0.29 g, 11.4 mmol) in THF (10 mL) was cooled to -20 ºC and treated drop wise with a solution of **ZN1** (0.8 g, 7.26 mmol) in THF (10 mL). The solution was warmed to ambient temperature and stirred overnight. The mixture was cooled to -20 ºC, treated with chilled HFIBO (1.31 g, 1.0 mL, 7.26 mmol) and warmed to ambient temperature with stirring overnight.

The reaction was cooled in an ice bath and quenched using water (10 mL). The solution was acidified to pH 1 and the layers separated. The aqueous phase was extracted with diethyl ether, washed with brine to pH 6, dried over $MgSO_4$, filtered and the solvent removed to yield a brown oil. Kugelrohr distillation (60 ºC) gave a colourless oil, however analysis by ^{1}H and ^{19}F NMR spectroscopies and GCMS analysis showed the oil to be a mixture of products including **ZN2**. Purification of the oil was attempted using B10 distillation through a Vigreux column and column chromatography, however both proved to be unsuccessful.

Characterisation of *endo*-$NBCH_2OCH_2C(CF_3)_2OH$ (SN2)

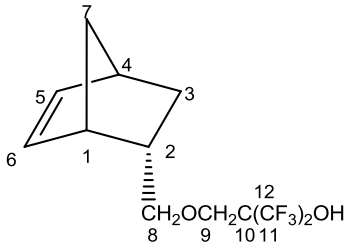

^{1}H NMR (699.7 MHz, $CDCl_3$): δ 6.14 (dd, J_{H5-H6} = 5.6 Hz J_{H4-H5} = 3.1 Hz, 1H, H^5), 5.89 (dd, J_{H5-H6} = 5.6 Hz J_{H1-H6} = 2.8 Hz, 1H, H^6), 4.13 (br s, 1H, OH), 3.70-3.76 (m, J = 10.4 Hz, 2H, H^9), 3.32 (m, 1H, H^8), 3.19 (m, 1H, $H^{8'}$), 2.87 (m, 1H, H^1), 2.81 (m, 1H, H^4), 2.37 (m, 1H, H^2), 1.81 (ddd, $J_{H3X-H3N}$ = 11.9 Hz, J = 9.4, 3.8 Hz 1H, H^{3X}), 1.44 (m, 1H, H^7) 1.24 (m, 1H, H^7), 0.49 (m,1H, H^{3N})

^{13}C{^{1}H} NMR (175.9 MHz, $CDCl_3$): δ 141.2 (C^5), 135.5 (C^6), 126.0 (q, J_{C-F} = 288 Hz, C^{11}, C^{12}) 79.6 (C^9), 77.9 (sept, J_{C-F} = 29.5 Hz, C^{10}), 69.0 (C^8), 52.9 (C^7), 47.3 (C^1), 45.6 (C^4), 41.9 (C^2), 32.2 (C^3)

^{19}F[^{1}H] NMR (376.3 MHz, $C_2D_2Cl_4$): δ -77.2 (m, 6F, $2CF_3$)

Accurate mass MS: Found: 305.0972 ($M-H^+$) Calculated for $C_{12}H_{15}O_2F_6$: 305.0976

GCMS EI$^+$: RT = 11.09, 305.1 ($C_{12}H_{15}O_2F_6$ $M-H^+$)

IR: 3600-3300 (OH), 2970-2870 (saturated C-H)

Characterisation of exo-NBCH$_2$OCH$_2$C(CF$_3$)$_2$OH (SX1)

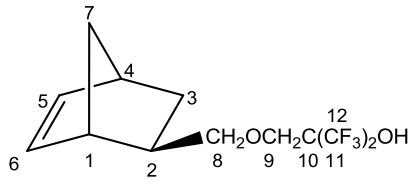

^{1}H NMR (499.8 MHz, $C_2D_2Cl_4$): δ 6.04 – 6.00 (m, 2H, H^5, H^6), 4.05 (s, 1H, OH), 3.73 (s, 2H, H^9), 3.54 (m, 1H, H^8), 3.44 (m, 1H, H^8), 2.76 (m, 1H, H^4), 2.71 (m, 1H, H^1), 1.64 (m, 1H, H^2), 1.27 (m, 1H, H^7), 1.19 (m, 2H, H^7 and H^{3X}), 1.04 (ddd, $J_{H3X-H3N}$ = 11.8 Hz, $J_{H3N-H4,\ H2}$ = 3.7 Hz 1H, H^{3N})

^{13}C{^{1}H} NMR (125.7 MHz, $C_2D_2Cl_4$): δ 136.9 (C^6), 136.1 (C^5), 124.6 (q, J_{C-F} = 287 Hz, C^{11}, C^{12}) 76.9 (C^8), 74.0 (sept, J_{C-F} = 29.5 Hz, C^{10}), 65.2 (C^9), 44.9 (C^7), 43.4 (C^1), 41.5 (C^4), 38.4 (C^2), 29.3 (C^3)

^{19}F[^{1}H] NMR (188.2 MHz, $C_2D_2Cl_4$): δ -77.2 (m, 6F, 2CF$_3$)

Accurate mass MS: Found: 305.0978 (M-H$^+$) Calculated for $C_{12}H_{15}O_2F_6$: 305.0976

GCMS EI$^+$: RT = 11.12, 305.1 ($C_{12}H_{15}O_2F_6$ M-H$^+$)

IR: 3600-3300 (O-H), 2969-2871 (saturated C-H)

Characterisation of *endo*-/*exo*-NBCH$_2$OCH$_2$C(CF$_3$)$_2$OH (SXN3)#

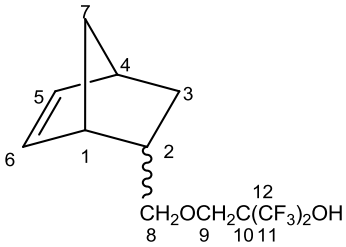

Unseparated mixture of isomers

^{1}H NMR (499.8 MHz, CDCl$_3$):

***endo* component** (80%) δ 6.15 (dd, J_{H5-H6} = 5.6 Hz J_{H4-H5} = 3.1 Hz, 1H, H^5), 5.91 (dd, J_{H5-H6} = 5.6 Hz J_{H1-H6} = 2.8 Hz, 1H, H^6), 4.08 (br s, 1H, OH) 3.78-3.71 (m, J = 10.4 Hz, 2H, H^9), 3.33 (m, 1H, H^8), 3.21 (m, 1H, $H^{8'}$), 2.89 (m, 1H, H^1), 2.82 (m, 1H, H^4), 2.39 (m, 1H, H^2), 1.82 (ddd, $J_{H3X-H3N}$ = 11.9 Hz, J = 9.4, 3.8 Hz 1H, H^{3X}), 1.45 (m, 1H, H^7) 1.25 (m, 1H, H^7), 0.50 (m,1H, H^{3N})

***exo* component** (20%) δ 6.11 – 6.07 (m, 2H, H^5, H^6), 4.06 (s, 1H, OH), 3.71 (s, 2H, H^9), 3.62 (m, 1H, H^8), 3.52 (m, 1H, $H^{8'}$), 2.89 (m, 1H, H^4), 2.70 (m, 1H, H^1), 1.72 (m, 1H, H^2), 1.35 (m, 1H, H^7), 1.25 (m, 2H, H^7 and H^{3X}), 1.12 (ddd, $J_{H3X-H3N}$ = 11.8 Hz, $J_{H3N-H4,\ H2}$ = 3.7 Hz, 1H, H^{3N})

^{13}C{^{1}H} NMR (125.7 MHz, CDCl$_3$):

***endo* component** δ 138.0 (C^5), 132.4 (C^6), 122.8 (q, J_{C-F} = 288 Hz, C^{11}, C^{12}) 76.4 (C^9), 74.7 (sept, J_{C-F} = 29.5 Hz, C^{10}), 65.8 (C^8), 49.8 (C^7), 44.1 (C^1), 42.5 (C^4), 38.7 (C^2), 29.0 (C^3)

***exo* component:** δ 137.3 (C^6), 136.6 (C^5), 122.8 (q, J_{C-F} = 287 Hz, C^{11}, C^{12}), 76.4 (C^8), 74.7 (sept, J_{C-F} = 29.5 Hz, C^{10}), 65.9 (C^9), 45.4 (C^7), 43.8 (C^1), 41.9 (C^4), 38.9 (C^2), 29.8 (C^3)

^{19}F[^{1}H] NMR (376.3 MHz, C$_2$D$_2$Cl$_4$): δ -77.2 (m, 6F, 2CF$_3$, *exo*), -77.3 (m, 6F, 2CF$_3$ *endo*)

Accurate mass MS: Found: 305.0978 (M-H$^+$) Calculated for $C_{12}H_{15}O_2F_6$: 305.0976

GCMS EI$^+$: RT = 11.01, 305.1 ($C_{12}H_{15}O_2F_6$ M-H$^+$), 11.07, 305.1 ($C_{12}H_{15}O_2F_6$ M-H$^+$)

IR: 3600-3300 (O-H), 2970-2871 (saturated C-H)

Characterisation of *exo*-NBCH$_2$C(CF$_3$)$_2$OH (SX2)

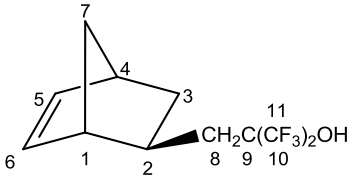

^{1}H NMR (499.8 MHz, $C_2D_2Cl_4$): δ 6.04 (dd, J_{H5-H6} = 5.6 Hz, J_{H4-H5} = 3.0 Hz, 1H, H^5), 5.99 (dd, J_{H5-H6} = 5.6 Hz, J_{H1-H6} = 2.9 Hz, 1H, H^6), 2.79 (m, 1H, H^1), 2.71 (s, 1H, OH), 2.55 (m, 1H, H^4), 2.02 (dd, $J_{H8-H8'}$ = 15.2 Hz, J_{H6-H8} = 5.3 Hz, 1H, H^8), 1.95 (dd, $J_{H8-H8'}$ = 15.2 Hz, J_{H6-H8} = 8.0Hz, 1H, $H^{8'}$), 1.61 (m, 1H, H^2), 1.35 (m, 1H, H^{3X}), 1.30 – 1.25 (m, 2H, H^7), 1.20 (ddd, $J_{H3X-H3N}$ = 11.7 Hz, $J_{H3N-H4,\,H2}$ = 3.7 Hz, 1H, H^{3N})

^{13}C{^{1}H} NMR (125.7 MHz, $C_2D_2Cl_4$): δ 136.7 (C^6), 136.2 (C^5), 122.9 (q, J_{C-F} = 288 Hz, C^{10}, C^{11}), 76.4 (sept, J_{C-F} = 28.8 Hz, C^9), 48.2 (C^4), 45.1 (C^7), 42.1 (C^1), 36.1 (C^8), 34.3 (C^3), 32.0 (C^2)

^{19}F[^{1}H] NMR (188.2 MHz, $C_2D_2Cl_4$): δ -77.0 (m, 6F, 2CF_3)

Accurate mass MS: Found: 275.0863 (M-H^+) Calculated for $C_{11}H_{13}OF_6$: 275.0871

IR: 3600-3300 (O-H), 2969 (saturated C-H)

Isolation and characterisation of *endo*-NBCH$_2$C(CF$_3$)$_2$OH (SN3)

A solution of *endo*-/*exo*-NBCH$_2$C(CF$_3$)$_2$OH (**SXN4**) (19.75 g, 72.0 mmol) in TCE (14 mL) was heated to 70 °C and treated with a solution of **Pd1388** (100 mg, 7.2 x 10^{-5} mol) in TCE (1 mL) with vigorous mechanical stirring. After 2 hours, a further 20 mL of TCE was added to reduce the viscosity of the solution. The solution was heated for a further 2 hours at 70 °C, cooled to ambient temperature and left overnight with vigorous stirring. Residual TCE was decanted off and set aside leaving the polymer as a gelatinous yellow solid. The polymer was dissolved in THF (50 mL) and precipitated into an excess of hexane (3 x 600 mL portions.) poly(endo-/exo-NBCH$_2$C(CF$_3$)$_2$OH) was isolated as a yellow white solid, washed twice with hexane and discarded. The

hexane portions were combined and the solution concentrated on a rotary evaporator to yield a yellow oil. The oil was combined with the isolated TCE and residual solvent removed *in vacuo*. Hexane was added to precipitate any remaining polymer and the hexane portion concentrated to yield a yellow oil. The oil was distilled under reduced pressure and *endo*-$NBCH_2C(CF_3)_2OH$ (**SN3**) isolated as a colourless oil (0.4 g, 3%, bp 22-24 °C, 0.1 mbar). Analysis by ^1H NMR spectroscopy and GCMS analysis shows only the presence of the *endo* isomer.

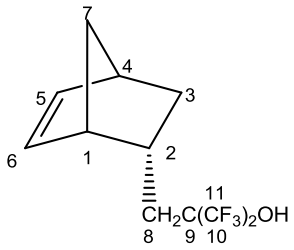

^1H NMR (499.8 MHz, $CDCl_3$): δ 6.21 (dd, J_{H5-H6} = 5.7 Hz, J_{H4-H5} = 3.0 Hz 1H, H^5), 5.97 (dd, J_{H5-H6} = 5.7 Hz, J_{H1-H6} = 2.9 Hz, 1H, H^6), 2.91 (m, 1H, H^1), 2.80 (m, 1H, H^4), 2.74 (s, 1H, OH), 2.37 (m, 1H, H^2), 2.01 (ddd, $J_{H3X-H3N}$ = 11.8 Hz, $J_{H3X-H4,\ H2}$ = 9.0, 3.8 Hz, 1H, H^{3X}), 1.85 (dd, $J_{H8-H8'}$ = 15.3 Hz, J_{H6-H8} = 6.6 Hz, 1H, H^8) 1.68 (dd, $J_{H8-H8'}$ = 15.3 Hz, J_{H6-H8} = 7.4 Hz, 1H, $H^{8'}$), 1.44 (m, 1H, H^7), 1.27 (m, 1H, H^7), 0.65 (ddd, $J_{H3X-H3N}$ = 11.8, $J_{H3N-H4,\ H2}$ = 6.7, 2.8 Hz, 1H, H^{3N})

$^{13}C\{^1H\}$ NMR (125.7 MHz, $CDCl_3$): δ 138.6 (C^5), 132.3 (C^6), 123.5 (q, J_{C-F} = 287 Hz, C^{10}, C^{11}), 77.3 (sept, J_{C-F} = 28.8 Hz, C^9), 49.9 (C^7), 47.4 (C^1), 42.0 (C^4), 34.9 (C^8), 34.2 (C^3), 32.7 (C^2)

$^{19}F[^1H]$ NMR (376.3 MHz, $C_2D_2Cl_4$): δ -76.5 (m, 3F, CF_3) -77.5 (m, 3F, CF_3)

Accurate mass MS: Found: 275.0858 ($M\text{-}H^+$) Calculated for $C_{11}H_{12}OF_6$: 275.0871

GCMS EI^+: RT = 8.61, 275.1 ($C_{11}H_{12}OF_6$ $M\text{-}H^+$)

IR: 3600-3300 (O-H), 2967 (saturated C-H)

Characterisation of *endo*-/*exo*-NBCH$_2$C(CF$_3$)$_2$OH (SXN4)#

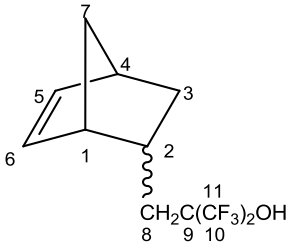

Unseparated mixture of isomers

^{1}H NMR (499.8 MHz, $C_2D_2Cl_4$):

***endo* component** (76%) δ 6.13 (dd, J_{H5-H6} = 5.7 Hz, J_{H4-H5} = 3.0 Hz 1H, H^5), 5.89 (dd, J_{H5-H6} = 5.7 Hz, J_{H1-H6} = 2.9 Hz, 1H, H^6), 2.81 (m, 1H, H^1), 2.84 (m, 1H, H^4), 2.77 (s, 1H, OH), 2.25 (m, 1H, H^2), 1.92 (ddd, $J_{H3X-H3N}$ = 11.8 Hz, $J_{H3X-H4,\ H2}$ = 9.0, 3.8 Hz, 1H, H^{3X}), 1.74 (dd, $J_{H8-H8'}$ = 15.3 Hz, J_{H6-H8} = 6.6 Hz, 1H, H^8) 1.56 (dd, $J_{H8-H8'}$ = 15.3 Hz, J_{H6-H8} = 7.4 Hz, 1H, $H^{8'}$), 1.35 (m, 1H, H^7), 1.23 (m, 1H, H^7), 0.55 (ddd, $J_{H3X-H3N}$ = 11.8, $J_{H3N-H4,\ H2}$ = 6.7, 2.8 Hz, 1H, H^{3N})

***exo* component** (24%) δ 6.03 (dd, J_{H5-H6} = 5.6 Hz, J_{H4-H5} = 3.0 Hz, 1H, H^5), 5.99 (dd, J_{H5-H6} = 5.6 Hz, J_{H1-H6} = 2.9 Hz, 1H, H^6), 2.77 (m, 1H, H^1), 2.71 (s, 1H, OH), 2.54 (m, 1H, H^4), 2.00 (dd, $J_{H8-H8'}$ = 15.2 Hz, J_{H6-H8} = 5.3Hz, 1H, H^8), 1.93 (dd, $J_{H8-H8'}$ = 15.2 Hz, J_{H6-H8} = 8.0 Hz, 1H, $H^{8'}$), 1.61 (m, 1H, H^2), 1.35 (m, 1H, H^{3X}), 1.30 – 1.25 (m, 2H, H^7), 1.20 (dt, $J_{H3X-H3N}$ = 11.7 Hz, $J_{H3N-H4,\ H2}$ = 3.7 Hz, 1H, H^{3N})

^{13}C{^{1}H} NMR (125.7 MHz, $C_2D_2Cl_4$):

***endo* component** δ 138.2 (C^5), 131.8 (C^6), 123.0 (q, J_{C-F} = 287 Hz, C^{10}, C^{11}), 76.5 (sept, J_{C-F} = 28.8 Hz, C^9), 49.5 (C^7), 46.9 (C^1), 42.1 (C^4), 34.5 (C^8), 34.3 (C^3), 32.1 (C^2)

***exo* component** δ 136.8 (C^6), 136.2 (C^5), 123.0 (q, J_{C-F} = 288 Hz, C^{10}, C^{11}), 76.4 (sept, J_{C-F} = 28.8 Hz, C^9), 48.2 (C^4), 45.1 (C^7), 42.1 (C^1), 36.1 (C^8), 34.3 (C^3), 32.0 (C^2)

^{19}F[^{1}H] NMR (376.3 MHz, $C_2D_2Cl_4$): δ -76.5 (m, 3F, CF_3, *endo*), -77.0 (m, 6F, $2CF_3$, *exo*), -77.5 (m, 3F, CF_3, *endo*)

Accurate mass MS: Found: 275.0854 (M-H$^+$) Calculated for $C_{11}H_{12}OF_6$: 275.0871

IR: 3600-3300 (O-H), 2967 (saturated C-H)

Synthesis and characterisation of *endo/exo*-NB$(CH_2)_2$OH (DXN1)#

Small scale Carius tube reaction

A 60 cm^3 Carius tube was charged with high purity (>99%) dicyclopentadiene (3.23 g, 24 mmol) and 3-buteneol (17 mL, 199 mmol) (dried, over $MgSO_4$ overnight). The resulting mixture was degassed and the tube evacuated and sealed. The tube was heated to 220 ºC (493 K) for 6 hours and allowed to cool. The resulting colourless liquid was distilled under reduced pressure to yield **DXN1** as a colourless oil (4.2 g, 72%, bp 78-82 ^oC, 0.6 mbar).

Scale up of DXN1 synthesis

A 0.5 L stainless steel pressure vessel was charged with high purity (>99%) dicyclopentadiene (18.9 g, 0.143 mol) and 3-butenol (150 mL, 1.754 mol) (dried, over $MgSO_4$ overnight). The vessel was heated to 220 ºC (493 K) over ~3 hours, followed by reaction at 220 ºC for 12 hours with vigorous agitation *via* a rocking mechanism. The resulting yellow brown solution was distilled under reduced pressure through a short Vigreux column to remove the majority of the alcohol. Further purification was achieved *via* distillation under reduced pressure through a column packed with Propac beads to yield **DXN1** as a colourless oil (12.3 g, 62%, bp 48-52 ^oC, 0.1 mbar).

Further scale up of DXN1 synthesis

A 2 L stainless steel pressure vessel was charged with high purity (>99%) dicyclopentadiene (48.0 g, 0.363 mol) and 3-butenol (375 mL, 4.384 mol) (dried, over $MgSO_4$ overnight). The vessel was heated to 220 ºC (493 K) over ~3 hours, followed by reaction at 220 ºC for 12 hours with vigorous agitation *via* a rocking mechanism. The resulting yellow brown solution was distilled under reduced pressure through a short vigreux column to remove the majority of the alcohol. Further purification was achieved *via* distillation under reduced pressure through a column packed with Propak beads to yield a colourless oil (36.11 g, 38%, bp 64-66 ºC, 0.2 mbar).

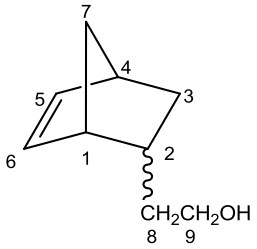

Unseparated mixture of isomers

^{1}H NMR (499.8 MHz, $CDCl_3$):

***endo* component** (70%) δ 6.13 (dd, $J_{H5\text{-}H6}$ = 5.5 Hz, $J_{H4\text{-}H5}$ = 3.0 Hz, 1H, H^5), 5.92 (dd, $J_{H5\text{-}H6}$ = 5.5 Hz, $J_{H1\text{-}H6}$ = 2.6 Hz, 1H, H^6), 3.63 (m, 2H, H^9), 2.76 (m, 2H, H^1, H^4), 2.03 (m, 1H, H^2), 1.86 (ddd, $J_{H3X\text{-}H3N}$ = 11.4 Hz, $J_{H3N\text{-}H2,\ H4}$ = 9.3, 3.8 Hz, 1H, H^{3X}), 1.50 (s, 1H, OH), 1.39 (m, 2H, H^7, H^8), 1.32 (m, 1H, H^8), 1.22 (m, 1H, H^7), 0.53 (ddd, $J_{H3X\text{-}H3N}$ = 11.4 Hz, $J_{H3N\text{-}H2,\ H4}$ = 6.8, 4.2 Hz, 1H, H^{3N})

***exo* component** (30 %) δ 6.08 (dd, $J_{H5\text{-}H6}$ = 5.5 Hz, $J_{H4\text{-}H5}$ = 3.0 Hz, 1H, H^5), 6.01 (dd, $J_{H5\text{-}H6}$ = 5.5 Hz, $J_{H1\text{-}H6}$ = 3.0 Hz, 1H, H^6), 3.60 (m, 2H, H^9), 2.80 (m, 1H, H^1), 2.53 (m, 1H, H^4), 2.09 (m, 1H, H^2), 1.68 (m, 1H ,H^{3N}), 1.50 (s, 1H, OH), 1.39 (m, 2H, H^8), 1.33 (m, 1H , H^7), 1.22 (m, 1H , H^7), 1.13 (ddd, $J_{H3X\text{-}H3N}$ = 7.5 Hz, 1H ,H^{3N})

^{13}C{^{1}H} NMR (125.7 MHz, $CDCl_3$): ***endo* component** δ 137.4 (C^6), 132.5 (C^5), 62.3 (C^9), 49.8 (C^7), 45.7 (C^1), 42.7 (C^4), 38.0 (C^8), 35.2 (C^2), 32.4 (C^3)

***exo* component** δ 136.9, (C^3) 136.5 (C^2), 62.4 (C^9), 46.6 (C^1), 45.5 (C^7), 42.1 (C^4), 39.7 (C^8), 35.2 (C^6), 33.1 (C^5)

GCMS EI$^+$ RT = 11.06, 138.0 ($C_9H_{14}O$, M^+, *endo)*, 11.27, 138.0 ($C_9H_{14}O$, M^+, *exo*)

Accurate mass MS: Found: 139.1127 (M-H^+) Calculated for $C_9H_{15}O$: 139.1123

IR: 3600-3100 (O-H), 3000-2800 (saturated C-H)

Characterisation of *exo*-NB$(CH_2)_2OCH_2C(CF_3)_2OH$ (DX2)

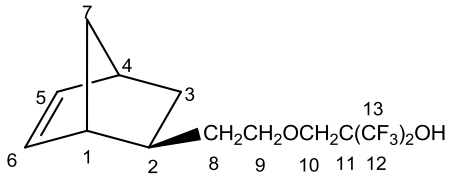

^{1}H NMR (499.8 MHz, $CDCl_3$): δ 6.08 (dd, J_{H5-H6} = 5.7 Hz, J_{H1-H6} = 3.1 Hz, 1H, H^6), 6.03 (dd, J_{H5-H6} = 5.7 Hz, J_{H4-H5} = 2.9 Hz, 1H, H^5), 4.04 (s, 1H, OH), 3.79 (s, 2H, H^{10}), 3.65 (m, 2H, H^9), 2.82 (m, 1H, H^4), 2.52 (m, 1H, H^1), 1.79-1.65 (m, 2H, H^8), 1.41 (m, 1H, H^2), 1.32-1.28 (m, 3H, H^{3X}, H^7), 1.12 (ddd, $J_{H3X-H3N}$ = 11.3 Hz, $J_{H3N-H2,\ H4}$ = 3.7 Hz, 1H, H^{3N})

^{13}C{^{1}H} NMR (125.7 MHz, $CDCl_3$): δ 136.9 (C^6), 136.8 (C^5), 122.8 (q, J_{C-F} = 288 Hz, C^{12}, C^{13}), 74.7 (sept, J_{C-F} = 29.6 Hz, C^{11}), 72.5 (C^9), 62.9 (C^{10}), 46.7 (C^1), 45.5 (C^7), 42.3 (C^4), 36.2 (C^8), 35.5 (C^2), 33.2 (C^3)

^{19}F[^{1}H] (376.3 MHz, $CDCl_3$): δ -77.6 (m, 6F, $2CF_3$)

Accurate mass MS: Found: 319.1126 ($M\text{-}H^+$) Calculated for $C_{13}H_{17}O_2F_6$: 318.1133

GCMS EI$^+$: RT = 12.46, 319.1 ($C_{13}H_{17}O_2F_6$, $M\text{-}H^+$)

IR: 3600-3300 (O-H), 2958 (saturated C-H)

Synthesis and characterisation of *endo-/exo*-NB$(CH_2)_2OCH_2C(CF_3)_2OH$ (DXN2)#

A slurry of sodium hydride (95%, 7.52 g, 313 mmol) in THF (75 mL) was cooled to -20 ºC and treated drop wise with a solution of **DXN1** (36.11 g, 261 mmol) in THF (40 mL). The solution was warmed to ambient temperature and stirred overnight. The mixture was cooled to -20 ºC, treated with chilled HFIBO (47.0 g, 33 mL, 297 mmol) and warmed to ambient temperature with stirring overnight. The yellow-brown reaction mixture was cooled to -20 ºC and water (75 mL) added drop-wise over 10 minutes. Concentrated hydrochloric acid was added to bring the pH between 1 and 2. The resulting layers were separated and the aqueous phase extracted with diethyl ether (2 x 75 ml.) The combined organic phases were washed with brine until the last washing gave pH 6. The extracts were dried over $MgSO_4$, filtered and the solvent removed in *vacuo* to give a yellow–brown liquid. The crude product was distilled under reduced pressure, using a column packed with Propak beads to yield a colourless oil (31.85 g, 38%, bp 52-64 ^oC, 0.4 mbar). However, analysis of the oil by ^1H and ^{19}F NMR spectroscopy showed the oil to contain several impurities.

The majority of the oil (30.4 g, 95 mmol) was dissolved in heptane (33 mL) and treated with aqueous sodium hydroxide (25 wt%, 18 mL). The resulting milky suspension was rotary evaporated to yield a yellow oil which could not be solidified. The oil was dissolved in heptane and acidified with concentrated HCl. The aqueous phase was removed and the heptane portion treated with aqueous sodium hydroxide (25 wt%, 19 mL) until the formation of a small aqueous NaOH layer was observed. The aqueous layer was removed and the heptane phase concentrated to a yellow oil which was chilled in a methanol-ice bath to yield *endo-/exo*-NB$(CH_2)_2OCH_2C(CF_3)_2ONa$ as a wax.

The wax was slurried in heptane and heated to dissolve. Upon settling, a small aqueous phase was formed and removed leaving a clear heptane solution. The heptane phase was cooled in a methanol-ice bath to induce crystallisation and the crystals isolated and washed with heptane. The crystals were dispersed in distilled water, treated with concentrated HCl to bring the pH between 1 and 2 and the phases separated. The organic phase was washed with brine to pH 6, dried over $MgSO_4$, filtered and the solvent removed *in vacuo* to yield a yellow oil. The oil was distilled under reduced pressure to yield pure (>99% by GC analysis) **DXN1** was a colourless oil (1.03 g, 3% of treated oil, 1% overall). Despite numerous attempts at recrystallisation of the sodium salt, all further batches of isolated *endo-/exo*-NB$(CH_2)_2OCH_2C(CF_3)_2OH$ contained residual impurities and were unsuitable for use in kinetics experiments.

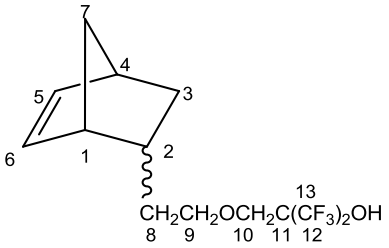

Unseparated mixture of isomers

^{1}H NMR (499.8 MHz, $CDCl_3$):

***endo* component** (68%) δ 6.15 (dd, J_{H5-H6} = 5.7 Hz, J_{H4-H5} = 3.0 Hz, 1H, H^5), 5.91 (dd, J_{H5-H6} = 5.7 Hz, J_{H1-H6} = 2.8 Hz, 1H, H^6), 3.99 (s, 1H, OH), 3.75 (s, 2H, H^{10}), 3.57 (m, 2H, H^9), 2.78 (m, 1H, H^4), 2.75 (m, 1H, H^1), 2.06 (m, 1H, H^2), 1.86 (m, 1H, H^{3X}), 1.50-1.32 (m, 2H, H^8), 1.41 (m, 1H, H^7), 1.22 (m, 1H, H^7), 0.53 (ddd, $J_{H3N-H3X}$ = 11.3 Hz, $J_{H3N-H2,\ H4}$ = 6.9, 2.7 Hz 1H, H^{3N})

***exo* component** (32%) δ 6.08 (dd, J_{H5-H6} = 5.7 Hz, J_{H1-H6} = 3.1 Hz, 1H, H^6), 6.03 (dd, J_{H5-H6} = 5.7 Hz, J_{H4-H5} = 2.9 Hz, 1H, H^5), 4.04 (s, 1H, OH), 3.79 (s, 2H, H^{10}), 3.65 (m, 2H, H^9), 2.82 (m, 1H, H_4), 2.52 (m, 1H, H^1), 1.79-1.65 (m, 2H, H^8), 1.41 (m, 1H, H^2), 1.32-1.28 (m, 3H, H^{3X}, H^7), 1.12 (ddd, $J_{H3X-H3N}$ = 11.3 Hz, $J_{H3N-H2,\ H4}$ = 3.7 Hz, 1H, H^{3N})

^{13}C{^{1}H} NMR (125.7 MHz, $CDCl_3$):

***endo* component** δ 137.8 (C^5), 132.4 (C^6), 122.8 (q, J_{C-F} = 288 Hz, C^{12}, C^{13}), 74.7 (sept, J_{C-F} = 29.6 Hz, C^{11}), 72.5 (C^9), 65.8 (C^{10}), 49.9 (C^7), 45.9 (C^1), 42.8 (C^4), 35.2 (C^2), 34.5 (C^8), 32.3 (C^3)

***exo* component** δ 136.9 (C^6), 136.8 (C^5), 122.8 (q, J_{C-F} = 288 Hz, C^{12}, C^{13}), 74.7 (sept, J_{C-F} = 29.6 Hz, C^{11}), 72.5 (C^9), 62.9 (C^{10}), 46.7 (C^1), 45.5 (C^7), 42.3 (C^4), 36.2 (C^8), 35.5 (C^2), 33.2 (C^3)

^{19}F[^{1}H] NMR (376.34 MHz, $CDCl_3$): δ -77.6 (m, 6F, $2CF_3$)

Accurate mass MS: Found: 319.1126 ($M\text{-}H^+$) Calculated for $C_{13}H_{17}O_2F_6$: 319.1133

GCMS EI$^+$: RT = 13.38, 319.2 ($C_{13}H_{17}O_2F_6$, ($M\text{-}H^+$, *endo*), 13.44, 319.2 ($C_{13}H_{17}O_2F_6$, ($M\text{-}H^+$, *exo*)

IR: 3600-3300 (O-H), 2947-2869 (saturated C-H stretching)

Characterisation of *endo*-/*exo*-NBCH$_2$CO$_2$TMS (SXN1)#

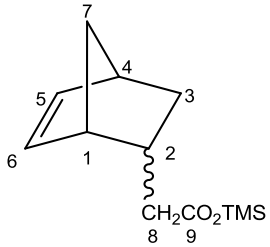

Unseparated mixture of isomers

^{1}H NMR (400.0 MHz, CDCl$_3$):

***endo* component** (84%) δ 6.13 (dd, J_{H5-H6} = 5.7 Hz, J_{H4-H5} = 3.0 Hz, 1H. H^5), 5.91 (dd, J_{H5-H6} = 5.7 Hz, J_{H1-H6} = 2.9 Hz, 1H, H^6), 2.78 (m, 1H, H^1), 2.74 (m, 1H, H^4), 2.38 (m, 1H, H^2), 2.11 (dd, $J_{H8-H8'}$ = 15.3 Hz, J_{H8-H2} = 7.4 Hz,1H, H^8) 2.02 (dd, $J_{H8-H8'}$ = 15.3 Hz, J_{H8-H2} = 8.4 Hz, 1H, H^8), 1.90 (m, 1H, H^{3X}), 1.40 (m, 1H, H^7), 1.25 (m, 1H, H^7), 0.54 (m, 1H, H^{3N}), 0 (s, 12H, $SiMe_3$)

***exo* component** (16%) δ 6.07 (dd, J_{H5-H6} = 5.7 Hz, J_{H1-H6} = 3.1 Hz,1H, H^6), 6.02 (dd, J_{H5-H6} = 5.7 Hz, J_{H4-H5} = 2.9 Hz, 1H, H^5), 2.74 (m, 1H, H^1), 2.51 (m, 1H, H^4), 2.41-2.34 (m, 2H, H^8), 1.80-1.73 (m, 1H, H^2), 1.37-1.29 (m, 3H, H^{3X}, H^7), 1.13 (m, 1H, H^{3N}), 0 (s, 12H, $SiMe_3$)

^{13}C{^{1}H} NMR (125.7 MHz, CDCl$_3$):

***endo* component** δ 174.4 (C=O), 137.9 (C^5), 132.5 (C^6), 49.9 (C^7), 46.0 (C^1), 42.9 (C^4), 41.3 (C^8), 35.3 (C^2), 32.3 (C^3), 0.08 ($SiMe_3$)

***exo* component** δ 174.1 (C=O), 136.7 (C^6, C^5), 46.6 (^{C4}), 45.3 (C^7), 42.8 (C^1), 42.3 (C^8), 35.2 (C^2), 32.8 (C^3), 0.08 ($SiMe_3$)

IR: 2960 (saturated C-H), 1705 (C=O)

Synthesis of *endo*-/*exo*-NBCH$_2$CO$_2$H (SXN2)#

endo/exo NB(CH$_2$)CO$_2$TMS (**SXN1**) (40 g, 178 mmol) was treated with distilled water (16 mL, 891 mmol) and concentrated hydrochloric acid (1 mL) with stirring overnight. The resulting aqueous and organic layers were separated and the aqueous phase extracted with diethyl ether (2 x 20 mL). The combined organic portions were dried over MgSO$_4$, filtered and the solvent removed in *vacuo* to yield a pale yellow oil in quantitative yield (26.4 g).

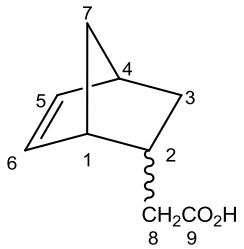

Unseparated mixture of isomers

^{1}H NMR (499.8 MHz, CDCl$_3$):

***endo* component** (84%) δ 11.98 (br s 1H OH), 6.16 (dd, $J_{H5\text{-}H6}$ = 5.7 Hz, $J_{H4\text{-}H5}$ = 3.0 Hz, 1H. H^5), 5.94 (dd, $J_{H5\text{-}H6}$ = 5.7 Hz, $J_{H1\text{-}H6}$ = 2.9 Hz, 1H, H^6), 2.84 (m, 1H, H^1), 2.78 (m, 1H, H^4), 2.47-2.41 (m, 1H, H^2), 2.17 (dd, $J_{H8\text{-}H8'}$ = 15.5 Hz, $J_{H8\text{-}H2}$ = 7.6 Hz, 1H, H^8) 2.08 (dd, $J_{H8\text{-}H8'}$ = 15.5 Hz, $J_{H8\text{-}H2}$ = 7.9 Hz, 1H, $H^{8'}$), 1.94 (m, 1H, H^{3X}), 1.43 (m, 1H, H^7), 1.26 (m, 1H, H^7), 0.57 (m, 1H, H^{3N})

***exo* component** (16%) δ 11.98 (br s 1H OH), 6.09 (dd, $J_{H5\text{-}H6}$ = 5.7 Hz, $J_{H1\text{-}H6}$ = 3.1 Hz, 1H, H^6), 6.03 (dd, $J_{H5\text{-}H6}$ = 5.7 Hz, $J_{H4\text{-}H5}$ = 2.9 Hz, 1H, H^5), 2.81(m, 1H, H^1), 2.58 (m, 1H, H^4), 2.47-2.41 (m, 2H, H^8), 1.84-1.78 (m, 1H, H^2), 1.37 (m, 1H, H^7), 1.36 (m, 1H, H^{3X}), 1.30 (m, 1H, H^7), 1.16 (m, 1H, H^{3N})

^{13}C{^{1}H} NMR (125.7 MHz, CDCl$_3$):

***endo* component** δ 180.7 (C=O), 138.1 (C^5), 132.3 (C^6), 49.9 (C^7), 45.9 (C^1), 42.9 (C^4), 39.4 (C^8), 34.9 (C^2), 32.3 (C^3)

***exo* component** δ 180.5 (C=O), 136.8 (C^6), 136.6 (C^5), 46.6 (C^4), 45.3 (C^7), 42.4 (C^1), 41.0 (C^8), 34.9 (C^2), 32.9 (C^3)

Accurate mass MS: Found: 153.0907 (M-H$^+$) Calculated for $C_9H_{13}O_2$: 153.0916

IR: 3600-2500 (O-H), 2960-2864 (saturated C-H), 1702 (C=O)

Synthesis of 6-*endo*-hydroxy-5-*exo*-iodonorbornan-2-*endo*-2ylacetic acid δ-lactone (I1)

A solution of iodine (45.18 g, 178 mmol) and potassium iodide (177.62 g, 1.07 mol) in water (410 mL) was prepared with protection from light. The iodine solution was treated with an aqueous solution of *endo/exo* $NB(CH_2)CO_2H$ (**SXN2**, 26.4g, 178 mmol) and sodium bicarbonate (0.5 M, 1.07 L) at 10 ^oC (ice/water bath.) The mixture was warmed to room temperature overnight with vigorous mechanical stirring.[6]

The resulting solution was treated with 0.1 M sodium thiosulphate (2 x 500 mL) and extracted with chloroform (3 x 500 mL). The combined extracts were washed with aqueous sodium bicarbonate (5%, 2 x 500 mL) and water (2 x 500 mL). The extracts were dried over $MgSO_4$, filtered and the solvent removed *in vacuo* to give a yellow white solid in quantitative yield. The solid was recrystallised from chloroform to yield the iodolactone, **I1**, as colourless needles (30.82 g, 83%)

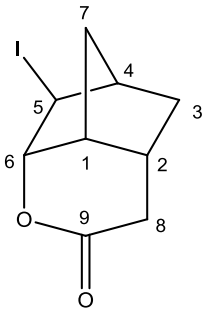

^{1}H NMR (699.7 MHz, $CDCl_3$): δ 5.24 (m, 1H, H^6), 3.81 (m, 1H, H^1), 2.61 (m, 2H, H^8), 2.55 (m, 1H, H^4), 2.42-2.37 (m, 2H, H_2, H^5), 2.24 (m, 1H, H^7), 2.18-2.14 (m, J_{H3N-3X} = 6.8, 1H, H^{3X}), 1.77 (m, 1H, H^7), 1.12 (ddd, J_{H3N-3X} = 6.8, $J_{H3N-H2,\ H4}$ = 4.4, 2.4 Hz, 1H, H^{3N})

^{13}C{^{1}H} NMR (175.9 MHz, $CDCl_3$): δ 168.4 (C=O), 91.7 (C^6), 47.2 (C^4), 39.3 (C^5), 38.6 (C^7), 36.1 (C^3), 33.5 (C^8) 33.4 (C^1) 30.5 (C^2)

Accurate mass MS: Found: 278.9883 ($M-H^+$) Calculated for $C_9H_{12}O_2{}^{127}I$: 278.9882

GCMS EI$^+$: RT = 18.71, 279.0 ($C_9H_{12}O_2{}^{127}I$, $M-H^+$)

IR: 2980-2860 (saturated C-H), 1717 (C=O)

Anal. Found: C, 38.89 H, 3.97 Calc: C: 38.72 H: 4.34% O 1.47 I: 45.47

Synthesis of *endo*-NBCH$_2$CO$_2$H (SN1)

Iodolactone (**I1**) (50.81 g, 183 mmol) was treated with zinc powder (179.2 g, 2.74 mol) and copper(I) bromide (58.97 g, 411 mmol) in methanol (1.2 L) and stirred vigorously for 2 hours at room temperature. The reaction is slightly exothermic and although the flask warms a little, a condenser was not necessary. The mixture was filtered through Celite to yield a colourless solution. Removal of the solvent in *vacuo* gave a yellow-oil which was treated with a mixture of distilled water (250 mL) and concentrated HCl (25 mL). The aqueous solution was extracted with diethyl ether (5 x 100 mL) and the combined organics dried over $MgSO_4$, filtered and the solvent removed *in vacuo* to yield the crude **SN1** carboxylic acid as a sticky pale brown liquid (42.43 g, > 100 % crude yield). Attempts were made to purify the crude carboxylic acid *via* distillation under reduced pressure. However, the **SN1** product proved impossible to distil so was used in the next synthetic step without further purification.

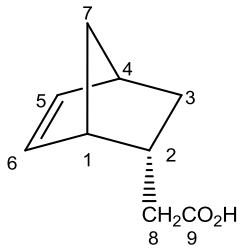

^{1}H NMR (499.77 MHz, CDCl$_3$): δ 11.0 (br s 1H OH), 6.17 (dd, $J_{H5\text{-}H6}$ = 5.7 Hz, $J_{H4\text{-}H5}$ = 3.0 Hz, 1H. H^5), 5.94 (dd, $J_{H5\text{-}H6}$ = 5.7 Hz, $J_{H1\text{-}H6}$ = 2.9 Hz, 1H, H^6), 2.84 (m, 1H, H^1), 2.78 (m, 1H, H^4), 2.47-2.41 (m, 1H, H^2), 2.17 (dd, $J_{H8\text{-}H8'}$ = 15.5 Hz, $J_{H8\text{-}H2}$ = 7.6 Hz, 1H, H^8) 2.08 (dd, $J_{H8\text{-}H8'}$ = 15.5 Hz, $J_{H8\text{-}H2}$ = 7.9 Hz, 1H, H^8), 1.94 (m, 1H, H^{3X}), 1.43 (m, 1H, H^7), 1.26 (m, 1H, H^7), 0.57 (m, 1H, H^{3N})

^{13}C{^{1}H} NMR (125.67 MHz, CDCl$_3$): δ 180.6 (C=O), 138.2 (C^5), 132.3 (C^6), 49.9 (C^7), 45.9 (C^1), 42.9 (C^4), 39.4 (C^8), 34.9 (C^2), 32.3 (C^3)

Accurate mass MS: Found: 153.0907 (M-H$^+$) Calculated for $C_9H_{13}O_2$: 153.0916

GCMS EI$^+$: RT = 12.70, 152.0 ($C_9H_{12}O$, M^+)

IR: 3600-2500 (O-H), 2960-2864 (saturated C-H stretching), 1702 (C=O)

Synthesis of *endo*-NB$(CH_2)_2$OH (DN1)

A two-necked round bottomed flask fitted with a magnetic fly, reflux condenser and nitrogen inlet was charged with a solution of *endo* $NBCH_2CO_2H$ (42.43 g, impure) in diethyl ether (200 mL). The solution was cooled to -78 ^oC and $LiAlH_4$ (1.0 M, diethyl ether, 400 mL, 400 mmol) added drop-wise with vigorous stirring. The mixture was stirred overnight at ambient temperature followed by a 4 hour reflux. The mixture was cooled to 0 ºC and isopropanol (100 mL) added drop-wise. The solution was treated with distilled water (250 mL) followed by concentrated HCl (30 mL) to pH 6, leaving a milky aqueous suspension and a clear diethyl ether layer. The organic layer was isolated and the aqueous layer washed with diethyl ether (3 x 100 mL). The combined organic portions were washed with brine, dried over $MgSO_4$, filtered and the solvent removed *in vacuo* to yield a yellow-brown oil. The crude oil was distilled to yield **DN1** as a colourless oil (11.39 g, 45%, bp 60-62 ºC, 0.8 mbar).

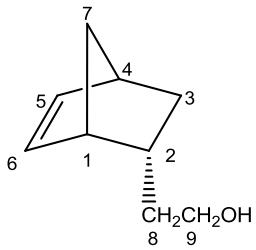

^{1}H NMR (699.7 MHz, $CDCl_3$): δ 6.11 (dd, J_{H5-H6} = 5.5 Hz, J_{H4-H5} = 3.0 Hz, 1H, H^5), 5.92 (dd, J_{H5-H6} = 5.5 Hz, J_{H1-H6} = 2.6 Hz, 1H, H^6), 3.61 (m, 2H, H^9), 2.76 (m, 2H, H^1, H^4), 2.09 (m, 1H, H^2) 1.85 (ddd, $J_{H3X-H3N}$ = 11.4 Hz, $J_{H3N-H2,\ H4}$ = 9.3, 3.8 Hz, 1H, H^{3X}) 1.50 (s, 1H, OH), 1.40 (m, 2H, H^7, H^8), 1.30 (m, 1H, $H^{8'}$) 1.21 (m, 1H, H^7), 0.52 (ddd, $J_{H3X-H3N}$ = 11.4 Hz, $J_{H3N-H2,\ H4}$ = 6.8, 4.2 Hz, 1H, H^{3N})

^{13}C{^{1}H} NMR (175.9 MHz, $CDCl_3$): δ 137.5 (C^6), 132.6 (C^5), 62.6 (C^9), 49.9 (C^7), 45.9 (C^1), 42.8 (C^4), 38.2 (C^8), 35.3 (C^2), 32.5 (C^3)

Accurate mass MS: Found: 139.1109 ($M\text{-}H^+$) Calculated for $C_9H_{15}O$: 139.1123

GCMS EI$^+$: RT = 11.05, 138.0 ($C_9H_{14}O$, M^+)

IR: 3600-3100 (O-H), 3000-2800 (saturated C-H)

Attempted synthesis of *endo*-NB(CH_2)$_2$OCH_2C(CF_3)$_2$OH (DN2)

A slurry of sodium hydride (95%, 0.685 g, 28.6 mmol) in THF (30 mL) was cooled to -20 ºC and treated drop wise with a solution of **DN1** (3.00 g, 21.7 mmol) in THF (15 mL). The solution was warmed to ambient temperature and stirred overnight. The mixture was cooled to -20 ºC, treated with chilled HFIBO (4.68 g, 3.3 mL, 26 mmol) and warmed to ambient temperature with stirring overnight to yield a yellow brown slurry. Analysis of the reaction mixture by GCMS analysis showed that conversion of the alcohol to the hexafluoropropanol product was low (<30%), resulting in a mixture of **DN1**, **DN2** and several other species. Addition of further portions of HFIBO (2.7 ml, 21.1 mmol), additional reaction time (1 month) or heating to 40 ºC did not improve the conversion. Efforts were made to isolate pure **DN2** by distillation, column chromatography and formation of the sodium salt followed by recrystallisation and work up (as discussed in the synthesis of **DXN2**) however all proved to be unsuccessful.

Synthesis of *endo*-NBCH$_2$CH$_2$OMs (DN3)

A solution of *endo*-NB(CH$_2$)$_2$OH (3.00 g 19.7 mmol, DN1) in DCM (20 mL) was treated with methane sulfonoyl chloride (2.37 g, 1.6 mL, 20.7 mmol) and the mixture cooled to -12.5 ºC in a methanol-ice bath. Triethylamine (2.39 g, 3.3 mL, 23.6 mmol) was added drop-wise, keeping the temperature below -1 ºC, resulting in a white precipitate. The mixture was warmed to 14 ºC over 40 minutes, treated with water (200 mL) and the phases separated. The organic phase was treated with 1M HCl and washed with brine to pH 6. The combined organic portions were dried over MgSO$_4$, filtered and the solvent removed under reduced pressure to yield the **DN3** product isolated as a yellow oil (3.58 g, 84%).

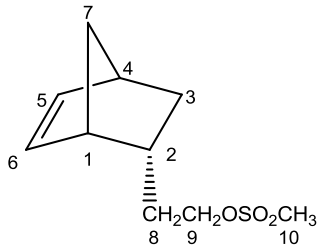

^{1}H NMR (699.7 MHz, CDCl$_3$): δ 6.15 (dd, $J_{H5\text{-}H6}$ = 5.6 Hz, $J_{H4\text{-}H5}$ = 3.0 Hz, 1H, H^5), 5.92 (dd, $J_{H5\text{-}H6}$ = 5.6 Hz, $J_{H1\text{-}H6}$ = 2.7 Hz, 1H, H^6), 4.20 (m, 2H, H^9), 2.99 (s, 3H, H^{10}), 2.79 (m, 2H, H^1, H^4), 2.12 (m, 1H, H^2) 1.89 (ddd, $J_{H3X\text{-}H3N}$ = 11.4 Hz, $J_{H3N\text{-}H2,\ H4}$ = 9.2, 3.8 Hz, 1H, H^{3X}), 1.60 (m, 1H, H^8), 1.49 (m, 1H, H$^{8'}$), 1.42 (m, 1H, H^7), 1.23 (m, 1H, H^7), 0.55 (dt, $J_{H3X\text{-}H3N}$ = 11.4 Hz, $J_{H3N\text{-}H2,\ H4}$ = 2.9 Hz, 1H, H^{3N})

^{13}C{^{1}H}NMR (175.9 MHz, CDCl$_3$): δ 138.0 (C^5), 132.2 (C^6), 69.9 (C^9), 49.9 (C^7), 45.7 (C^1), 42.8 (C^4), 37.7 (C^{10}), 35.1 (C^2), 34.3 (C^8), 32.3 (C^3)

GCMS EI$^+$: RT = 17.10, 216.0 ($C_{10}H_{16}SO_3$, M^+)

Characterisation of *endo*-/*exo*-NB$(CH_2)_2C(CF_3)_2OH$ (DXN5)#

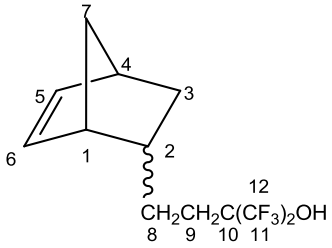

Unseparated mixture of isomers

^{1}H NMR (499.8 MHz, $C_2D_2Cl_4$):

***endo* component** (79%) δ 6.09 (dd, J_{H5-H6} = 5.7 Hz, J_{H4-H5} = 3.0 Hz, 1H, H^5), 5.84 (dd, J_{H5-H6} = 5.7 Hz, J_{H1-H6} = 2.7 Hz, 1H, H^6), 2.71 (m, 2H, H^1), 2.69 (m, 1H, H^4), 2.10 (br, s 1H, OH), 1.87 (m, 3H, H^2, H^9), 1.35 (m, 1H, H^{3X}), 1.27 – 1.15 (m, 4H, H^7, H^8), 0.44 (ddd, $J_{H3N-H3X}$ = 11.0 Hz, $J_{H3N-H2,\ H4}$ = 6.5, 2.8 Hz, 1H, H^{3N})

***exo* component** (21%) δ 6.01 (dd, J_{H5-H6} = 5.7 Hz J_{H1-H6} = 3.0 Hz, 1H, H^6) 5.98 (dd, J_{H5-H6} = 5.7 Hz, J_{H4-H5} = 2.9 Hz, 1H, H^5), 2.75 (m, 1H, H^1), 2.47 (m, 1H, H^4), 2.10 (br, s, 1H, OH), 1.87 (m, 1H, H^2), 1.52 (m, 2H, H^9), 1.27 – 1.15 (m, 5H, H^{3X}, H^7, H^8), 1.02 (ddd, $J_{H3N-H3X}$ = 10.6 Hz, $J_{H3N-H2,\ H4}$ = 3.4, 6.9 Hz, 1H, H^{3N})

^{13}C{^{1}H} NMR (125.7 MHz, $C_2D_2Cl_4$):

***endo* component** δ 137.7 (C^5), 131.6 (C^6), 122.9 (q, J_{C-F} = 287 Hz, C^{11}, C^{12}), 76.0 (sept, J_{C-F} = 28.9 Hz, C^{10}), 49.4 (C^7), 45.0 (C^1), 42.4 (C^4), 38.7 (C^2), 32.1 (C^9), 29.3 (C^3), 26.3 (C^8)

***exo* component** δ 136.5 (C^5, C^6), 122.9 (q, J_{C-F} = 287 Hz, C^{11}, C^{12}), 76.0 (sept, J_{C-F} = 28.9 Hz, C^{10}), 46.1 (C^4), 45.1 (C^7), 41.8 (C^1), 39.0 (C^2), 32.8 (C^9), 29.6 (C^3), 28.1 (C^8)

^{19}F[^{1}H] NMR (376.3 MHz, $C_2D_2Cl_4$): δ -76.5 (m, 3F, CF_3, *endo*) -76.6 (s, 6F, $2CF_3$, *exo*), -77.8 (m, 3F, CF_3, *endo*)

Accurate mass MS: Found: 289.1030 ($M\text{-}H^+$) Calculated for $C_{12}H_{15}OF_6$: 289.1027

GCMS EI$^+$: RT= 10.21, 288.0 ($C_{12}H_{14}OF_6$ M^+, *endo*), RT= 10.24, 288.0 ($C_{12}H_{14}OF_6$ M^+, *exo*)

IR: 3600-3300 (O-H), 2966-2868 (saturated C-H)

Attempted synthesis of *endo/exo*-NB$(CH_2)_3$OH (TXN1)

Small scale Carius tube reaction

A 60 cm^3 Carius tube was charged with high purity (>99%) dicyclopentadiene (2.79 g, 21 mmol) and 4-pentenol (14 mL, 166 mmol) (dried over $MgSO_4$ overnight). The resulting mixture was degassed and the tube evacuated and sealed. The tube was heated to 220 ºC (493 K) for 6 hours and allowed to cool. The resulting colourless liquid was distilled under reduced pressure to yield a colourless oil which was shown by ^{1}H NMR spectroscopic and GCMS analyses to be a mixture of **TXN1** and residual 4-pentenol.

Scale up of TXN1 synthesis

A 2 L stainless steel pressure vessel was charged with high purity (>99%) dicyclopentadiene (45.0 g, 0.340 mol) and 4-pentenol (dried over $MgSO_4$ overnight, 385 mL, 3.782 mol). The vessel was heated to 220 ºC (493 K) over ~3 hours, followed by reaction at 220 ºC for 12 hours with vigorous agitation *via* a rocking mechanism. The resulting yellow brown solution was distilled under reduced pressure through a short Vigreux column to remove the majority of the alcohol.

Further purification was attempted using Kügelrohr distillation (at a variety of temperatures and pressures), and distillation through a column packed with Propak beads (again under various conditions), however, removal of all of the residual alkenol proved to be impossible. In all cases, the **TXN1** product was contaminated with ~ 7% residual pentenol. Separation of **TXN1** and 4-pentenol was also attempted using column chromatography using a variety of solvent combinations however proved unsuccessful in all cases due to the similarity in the Rf values of the two compounds.

Attempted synthesis and characterisation of *endo*-/exo-NB$(CH_2)_3$OAc (TXN2) and separation from and $CH_2CH(CH_2)_3$OAc

A mixture of **TXN1** and 7% residual 4-pentenol (15.0 g) was dissolved in diethyl ether (25 mL) and treated with triethylamine (20.5 mL, 148 mmol). The solution was cooled to 0 ºC and treated drop wise with a solution of acetyl chloride (10.5 mL, 148 mmol) in diethyl ether (10 mL) with vigorous stirring. The solution was stirred for 1 hour at 0 ºC and warmed to ambient temperature overnight to yield an orange-brown slurry. The slurry was filtered and washed with diethyl ether (50 mL). The organic portions were concentrated to yield an orange-brown oil, which was distilled under reduced pressure to yield a colourless oil. Analysis of the oil by ^{1}H NMR spectroscopic and GCMS

analyses showed the oil to be a mixture of the desired TXN2 product and $C=C(CH_2)_3OAc$ (7%) which could not be separated chromatographically or using distillation techniques.

Attempted synthesis and characterisation of *endo-/exo*-NB$(CH_2)_3OCH_2C(CF_3)_2OH$ (TXN3)

A slurry of sodium hydride (95%, 1.186 g, 49.4 mmol) in THF (15 mL) was cooled to -20 ºC and treated drop wise with a mixture of **TXN1** and 7% residual 4-pentenol (6.45 g) as a solution in THF (7 mL). The solution was warmed to ambient temperature and stirred overnight. The mixture was cooled to -20 ºC, treated with chilled HFIBO (9.84 g, 7.0 mL, 54.6 mmol) and warmed to ambient temperature with stirring overnight.

The reaction was cooled in an ice bath and quenched using water (15 mL). The solution was acidified to pH 1 and the layers separated. The aqueous phase was extracted with diethyl ether, washed with brine to pH 6, dried over $MgSO_4$, filtered and the solvent removed to yield a yellow-brown oil. The crude product was distilled under reduced pressure, using a short Vigreux column to yield a colourless oil (5.62 g, 39%). Analysis of the oil using ^{1}H NMR spectroscopic and GCMS analyses confirmed the oil to be a mixture of the desired **TXN3** product (69% of the mixture) as well as numerous other impurities, which could not be removed chromatographically or using distillation techniques.

Attempted synthesis of *endo-/exo*-NB$(CH_2)_2CO_2H$

A 60 cm^3 Carius tube was charged with dicyclopentadiene (1.94 g, 14.7 mmol) and pentenoic acid (18 mL, 176 mmol).[7] The reaction mixture was degassed and the tube sealed under vacuum. The tube was heated to 220 ^{o}C for 17 hours and after cooling a yellow oil was obtained. ^{1}H NMR spectroscopy of the crude reaction mixture showed that the desired product was not obtained. The reaction was repeated using a different heating cycle (185 ^{o}C, 30 h), however again the desired product was not obtained.

Characterisation of *endo*-/*exo*-NB$(CH_2)_2CO_2Et$ (DXN3)#

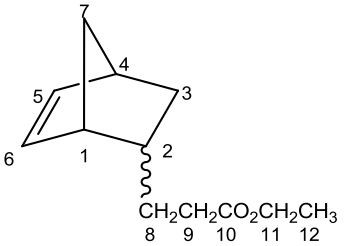

Unseparated mixture of isomers

^{1}H NMR (499.8 MHz, $CDCl_3$):

***endo* component** (80.7%) δ 6.12 (dd, J_{H5-H6} = 5.7 Hz, J_{H4-H5} = 3.0 Hz, 1H, H^5), 5.92 (dd, J_{H5-H6} = 5.7 Hz, J_{H1-H6} = 2.8 Hz, 1H, H^6), 4.11 (q, J = 7.1 Hz, 2H, H^{11}), 2.76 (m, 2H, H^1, H^4), 2.70 (m, 2H, H^9), 1.96 (m, 1H, H^2), 1.86 (m, 1H, H^{3X}), 1.4 – 1.20 (m, 4H, H^8, H^7), 1.25 (t, $J_{H11-H12}$ = 7.1 Hz, 3H, H^{12}), 0.50 (ddd, $J_{H3N-H3X}$ = 11.3 Hz, $J_{H3N-H2,\ H4}$ = 6.9, 2.7 Hz, 1H, H^{3N})

***exo* component** (19.3%) δ 6.06 (dd, J_{H5-H6} = 5.4 Hz, J_{H1-H6} = 3.0 Hz, 1H, H^6) 6.02 (dd, J_{H5-H6} = 5.4 Hz, J_{H4-H5} = 2.9 Hz, 1H, H^5), 4.11 (q, J = 7.1 Hz, 2H, H^{11}), 2.79 (m, 1H, H^1), 2.52 (m, 1H, H^4), 2.34 (m, 2H, H^9), 1.77-1.63 (m, 2H, H^8), 1.43-1.20 (m, 4H, H^7, H^{3X}, H^2), 1.25 (t, $J_{H11-H12}$ = 7.1 Hz, 3H, H^{12}), 1.10 (m,1H, H^{3N})

$^{13}C\{^1H\}$ NMR (125.7 MHz, $CDCl_3$):

***endo* component** δ 174.3 (C=O), 137.6 (C^5), 132.4 (C^6), 60.5 (C^{11}), 49.9 (C^7), 45.5 (C^1), 42.8 (C^4), 38.7 (C^2), 33.9 (C^9), 32.5 (C^3), 30.2 (C^8), 14.6 (C^{12})

***exo* component** δ 174.2 (C=O), 137.0 (C^6), 136.7 (C^5), 60.5 (C^{11}), 46.4 (C^4), 45.5 (C^7), 42.2 (C^1), 38.8 (C^2), 34.1 (C^9), 33.2 (C^3), 31.9 (C^8), 14.6 (C^{12})

Accurate mass MS: Found: 195.1375 ($M-H^+$) Calculated for $C_{12}H_{19}O_2$: 195.1385

IR: 3000-2800 (saturated C-H stretching), 1732 (C=O)

Characterisation of *exo*-NB$(CH_2)_2CO_2H$ (DX1)

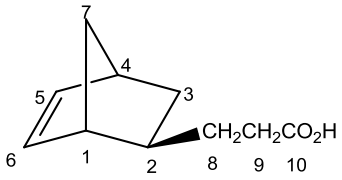

^{1}H NMR (499.8 MHz, $CDCl_3$): δ 9.4 (br s, 1H, OH), 6.08 (dd, J_{H5-H6} = 5.5 Hz J_{H1-H6} = 3.1 Hz, 1H, H^6) 6.03 (dd, J_{H5-H6} = 5.5 Hz, J_{H4-H5} = 2.9 Hz, 1H, H^5) 2.81 (m, 1H, H^1), 2.53 (m, 1H, H^4), 2.41 (m, 2H, H^9), 1.80-1.65 (m, 2H, H^8), 1.37-1.28 (m, 4H, H^7, H^{3X}, H^2), 1.10 (m, 1H, H^{3N})

^{13}C{^{1}H} NMR (125.7 MHz, $CDCl_3$): δ 180.1 (C=O), 137.0 (C^6), 136.8 (C^5), 46.4 (C^4), 45.5 (C^7), 42.2 (C^1), 38.7 (C^2), 33.7 (C^9), 33.2 (C^3), 31.6 (C^8)

Accurate mass MS: Found: 167.1064 ($M-H^+$) Calculated for $C_{10}H_{15}O_2$: 167.1072

IR: 3100-2800 (OH and saturated C-H), 1703 (C=O)

Synthesis of *endo-/exo*-NB$(CH_2)_2$COOH (DXN4)#

A round bottomed flask was charged with sodium hydroxide (5.00 g, 125 mmol), and distilled water (50 mL) to give a 10 wt% solution. *endo/exo*-NB$(CH_2)_2CO_2$Et (5.73 g, 29.5 mmol) was added and the mixture heated to reflux for 2 hours to give a homogeneous solution.

The solution was cooled and concentrated HCl added to bring the pH between 1 and 2. The aqueous phase was extracted with diethyl ether (2 x 20 mL) and the combined organic portions dried over $MgSO_4$, filtered and the solvent removed *in vacuo* to yield the product, **DXN4**, as a colourless oil (3.56 g, 73%).

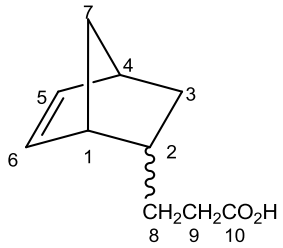

Unseparated mixture of isomers

^{1}H NMR (499.8 MHz, $CDCl_3$):

***endo* component** (82%) δ 9.4 (br s 1H OH), (dd, $J_{H5\text{-}H6}$ = 5.6 Hz $J_{H4\text{-}H5}$ = 3.0 Hz, 1H, H^5) (dd, $J_{H5\text{-}H6}$ = 5.6 Hz $J_{H1\text{-}H6}$ = 2.7 Hz, 1H, H^6), 2.77 (m, 2H, H^1, H^4), 2.32 (m, 2H, H^9), 2.00 (m, 1H, H^2), 1.86 (m, 1H, H^{3X}), 1.45 – 1.21 (m, 4H, H^8, H^7), 0.50 (m, 1H, H^{3N})

***exo* component** (18%) δ 9.4 (br s, 1H, OH), 6.08 (dd, $J_{H5\text{-}H6}$ = 5.5 Hz $J_{H1\text{-}H6}$ = 3.1 Hz, 1H, H^6) 6.03 (dd, $J_{H5\text{-}H6}$ = 5.5 Hz $J_{H4\text{-}H5}$ = 2.9 Hz, 1H, H^5) 2.81 (m, 1H, H^1), 2.53 (m, 1H, H^4), 2.41 (m, 2H, H^9), 1.80-1.65 (m, 2H, H^8), 1.37-1.28 (m, 4H, H^7, H^{3X}, H^2), 1.10 (m, 1H, H^{3N})

^{13}C{^{1}H} NMR (125.7 MHz, $CDCl_3$):

***endo* component** δ 180.7 (C=O), 137.8 (C^5), 132.3 (C^6), 49.4 (C^7), 45.5 (C^1), 42.9 (C^4), 38.5 (C^2), 33.6 (C^9), 32.5 (C^3), 29.9 (C^8)

***exo* component** δ 180.5 (C=O), 137.0 (C^6), 136.8 (C^5), 46.4 (C^4), 45.5 (C^7), 42.2 (C^1), 38.7 (C^2), 33.7 (C^9), 33.2 (C^3), 31.6 (C^8)

Accurate mass MS: Found: 167.1064 ($M\text{-}H^+$) Calculated for $C_{10}H_{15}O_2$: 167.1072

IR: 3100-2800 (OH and saturated C-H), 1701 (C=O)

Synthesis of 3-(2-endo-hydroxy-7-anti-iodonorbornan-2-exo-yl)propionic acid γ-lactone (I2)

A solution of iodine (5.43 g, 21.4 mmol) and potassium iodide (21.3 g, 1.28 mol) in water (56 mL) was prepared with protection from light. The iodine solution was treated with an aqueous solution of *endo-/exo*-NB$(CH_2)_2CO_2H$ (**DXN4**, 3.56 g, 21.4 mmol) and sodium bicarbonate (0.5 M, 128 mL) at 10 ^oC (ice/water bath.) The mixture was warmed to room temperature overnight with vigorous mechanical stirring.[7]

The resulting solution was treated with 0.1 M sodium thiosulphate (100 mL) and extracted with chloroform (6 x 100 mL). The combined extracts were washed with aqueous sodium hydrogen carbonate (5%, 2 x 100 mL) and water (2 x 100 mL). The extracts were dried over $MgSO_4$, filtered and the solvent removed *in vacuo* to yield a yellow oil which quickly turned brown upon standing. The oil was purified using column chromatography (diethyl ether as eluent) to give a white solid (390 mg, 8%), which was recrystallised from diethyl ether to yield the product as colourless needles (241 mg, 5%).

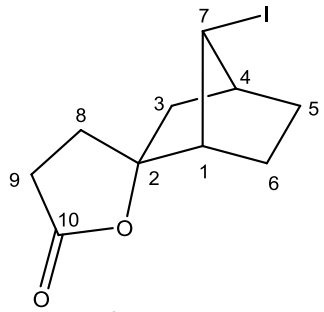

^{1}H NMR (699.7 MHz, $CDCl_3$): δ 3.90 (m, 1H, H^7), 2.53 (m, 2H, H^9), 2.39 (m, 1H, H^4), 2.31 (m, 1H, H^1), 2.25 (m, 1H, H^8), 2.06 (m, 1H, $H^{8'}$), 2.01 (m, 2H, H^5, H^6), 1.87 (m, 3H, H^3, H^6), 1.44 (m, 1H, H^5)

^{13}C{^{1}H} NMR (175.9 MHz, $CDCl_3$): δ 176.5 (C=O), 88.0 (C^2), 54.1 (C^1), 44.8 (C^4), 43.4 (C^3), 36.6 (C^8), 30.7 (C^7), 29.4 (C^9), 27.1 (C^5), 21.6 (C^6)

Accurate mass MS: Found: 293.0042 ($M\text{-}H^+$) Calculated for $C_{10}H_{14}O_2{}^{127}I$: 293.0039

GCMS EI$^+$: RT = 18.74, 292.9 ($C_{10}H_{14}O_2{}^{127}I$, $M\text{-}H^+$)

IR: 2943-2869 (saturated C-H), 1775 (C=O)

Anal. Found: C, 41.06 H, 4.40%, Calc: C, 41.11 H, 4.49%

Synthesis of *endo/exo*-NB$(CH_2)_3$OH (TXN1)#

A two-necked round bottomed flask fitted with a magnetic fly, reflux condenser and nitrogen inlet was charged with a solution of *endo-/exo*-NB$(CH_2)_3CO_2$Et (**DXN3**, 5.15 g, 26.5 mmol) in diethyl ether (40 mL). The solution was cooled to -78 ºC and $LiAlH_4$ (1.0 M, diethyl ether, 60 mL, 60 mmol) added drop-wise with vigorous stirring over 5 minutes. The mixture was allowed to warm to room temperature overnight followed by a 4 hour reflux.

The solution was cooled to 0 °C and isopropanol (40 mL) added drop-wise over 30 minutes followed by water (40 mL), also drop-wise over 30 minutes. A grey white precipitate was observed. The mixture was warmed to room temperature and acidified with concentrated hydrochloric acid to pH 6. The mixture was filtered, the resulting solution treated with saturated brine (100 mL) and the organic phase isolated. The aqueous phase was washed with diethyl ether (2 x 50 mL) and the combined organics dried over $MgSO_4$, filtered and the solvent removed *in vacuo* to yield the pure **TXN1** product as a colourless oil (3.08 g, 76%).

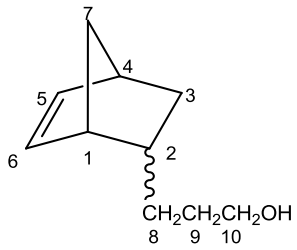

Unseparated mixture of isomers

^{1}H NMR (699.7 MHz, $CDCl_3$):

***endo* component** (80%) δ 6.06 (dd, $J_{H5\text{-}H6}$ = 5.7 Hz, $J_{H4\text{-}H5}$ = 3.0 Hz, 1H, H^5), 5.87 (dd, $J_{H5\text{-}H6}$ = 5.7 Hz, $J_{H1\text{-}H6}$ = 2.9 Hz, 1H, H^6), 3.52 (t, $J_{H9\text{-}H10}$ = 6.8 Hz, 2H, H^{10}), 2.72 (m, 1H, H^1), 2.71 (m, 1H, H^4), 2.63 (br, s 1H, OH), 1.93 (m, 1H, H^2), 1.80 (ddd, $J_{H3X\text{-}H3N}$ =11.4 Hz, $J_{H3X\text{-}H2,\ H4}$ = 8.7, 3.9 Hz, 1H, H^{3X}), 1.54-1.45 (m, 2H, H^9), 1.34 (m, 1H, H^7), 1.17 (m, 1H, H^7), 1.12-1.03 (m, 2H, H^8), 0.46 (ddd, $J_{H3N\text{-}H3X}$ =11.4 Hz, $J_{H3N\text{-}H2,\ H4}$ = 4.2, 2.7 Hz, 1H, H^{3N})

***exo* component** (20%) δ 6.03 (dd, $J_{H5\text{-}H6}$ = 5.6 Hz $J_{H1\text{-}H6}$ = 3.1 Hz, 1H, H^6) 5.97 (dd, $J_{H5\text{-}H6}$ = 5.6 Hz $J_{H4\text{-}H5}$ = 2.9 Hz, 1H, H^5), 3.56 (t, $J_{H9\text{-}H10}$ = 6.0 Hz, 2H, H^{10}), 2.74 (m, 1H, H^4), 2.63 (br, s 1H, OH), 2.47 (m, 1H, H^1), 1.58-1.53 (m, 2H, H^9), 1.40 (m, 2H, H^8), 1.27 (m, 4H, H^2, H^{3X}, H^7), 1.05 (ddd, $J_{H3X\text{-}H3N}$ = 11.1Hz, $J_{H3N\text{-}H2,\ H4}$ = 3.6 Hz, 1H, H^{3N})

$^{13}C\{^1H\}$ NMR (175.9 MHz, $CDCl_3$):

***endo* component** 137.3 (C^5), 132.5 (C^6), 63.1 (C^{10}), 49.8 (C^7), 45.6 (C^1), 42.8 (C^4), 38.8 (C^2), 32.6 (C^3), 32.0 (C^9), 31.0 (C^8)

***exo* component** δ 137.0 (C^6), 136.4 (C^5), 63.0 (C^{10}), 46.5 (C^1), 45.4 (C^2), 42.1 (C^4), 38.8 (C^7), 33.3 (C^3), 32.8 (C^8), 32.2 (C^9)

Accurate mass MS: Found: 153.1284 ($M\text{-}H^+$) Calculated for $C_{10}H_{17}O$: 153.1279

GCMS EI^+: RT = 12.52, 153.1 ($C_{10}H_{17}O$, $M\text{-}H^+$, *endo*), 12.57, 153.1 ($C_{10}H_{17}O$, $M\text{-}H^+$, *exo*)

IR: 3300-3000 (O-H), 3000-2800 (saturated C-H)

Synthesis of *exo*-NB $(CH_2)_3OH$ (TX1)

A two-necked round bottomed flask fitted with a magnetic fly, reflux condenser and nitrogen inlet was charged with a solution of *exo*-$NB(CH_2)_2CO_2H$ (**DX1**, 2.8 g, 16.8 mmol) in diethyl ether (30 mL). The solution was cooled to -78 ºC and $LiAlH_4$ (1.0 M, diethyl ether, 30 mL, 30 mmol) added drop-wise with vigorous stirring over 5 minutes. The mixture was allowed to warm to room temperature overnight followed by a 10 hour reflux.

The solution was cooled to 0 ºC and isopropanol (30 mL) added drop-wise over 20 minutes followed by water (30 mL), also drop-wise over 20 minutes. A grey white precipitate was observed. The mixture was warmed to room temperature and acidified with concentrated hydrochloric acid to pH 6. Saturated brine (100 mL) was added and the organic phase isolated. The aqueous phase was washed with diethyl ether (2 x 50 mL) and the combined organic portions dried over $MgSO_4$, filtered and the solvent removed *in vacuo* to give the product, **TX1**, as a colourless oil (1.05 g, 41 %).

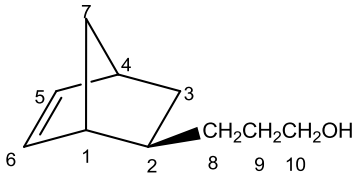

^{1}H NMR (699.7 MHz, $CDCl_3$): δ 6.07 (dd, J_{H5-H6} = 5.6 Hz, J_{H1-H6} = 3.1 Hz, 1H, H^6) 6.01 (dd, J_{H5-H6} = 5.6 Hz, J_{H4-H5} = 2.9 Hz, 1H, H^5) 3.63 (t, J_{H9-H10} = 6.0 Hz, 2H, H^{10}), 2.78 (m, 1H, H^4), 2.51 (m, 1H, H^1), 1.62 (m, 2H, H^9), 1.54 (s, 1H, OH), 1.47-1.37 (m, 2H, H^8), 1.34-1.26 (m, 4H, H^2, H^{3X}, H^7), 1.09 (ddd, $J_{H3X-H3N}$ = 11.1 Hz, $J_{H3N-H2,\ H4}$ = 3.6 Hz, 1H, H^{3N})

^{13}C{^{1}H} NMR (175.9 MHz, $CDCl_3$): δ 137.1 (C^6), 136.6 (C^5), 63.5 (C^{10}), 46.7 (C^1), 45.5 (C^2), 42.2 (C^4), 38.9 (C^7), 33.4 (C^3), 32.9 (C^8), 32.4 (C^9)

GCMS EI$^+$: RT = 12.40, 153.1 ($C_{10}H_{17}O$, M-H^+)

Synthesis of *endo/exo*-NB$(CH_2)_3OCH_2C(CF_3)_2OH$ (TXN2)#

A slurry of sodium hydride (95%, 0.64 g, 26.6 mmol) in THF (13 mL) was cooled to -20 ºC and treated drop wise with a solution of **TXN1** (3.08 g, 20.2 mmol) in THF (5 mL). The solution was warmed to ambient temperature and stirred overnight. The mixture was cooled to -20 ºC, treated with chilled HFIBO (3.64 g, 2.6 mL, 20.2 mmol) and warmed to ambient temperature with stirring overnight.

The reaction was cooled in an ice bath and quenched using water (10 mL). The solution was acidified to pH 1 using concentrated HCl and the resulting layers separated. The aqueous phase was extracted with diethyl ether (2 x 15 mL), washed with brine to pH 6 (6 x 15 mL), dried over $MgSO_4$, filtered and the solvent removed to yield a yellow-brown oil. The crude product was distilled using a column packed with Propak beads to yield a colourless oil (2.43 g, 36%, bp 60-62 °C, 0.4 mbar). However, analysis of the oil by ^{19}F NMR spectroscopic and GCMS analysis indicated the presence of ~7% of a fluorinated impurity. A portion of the oil (2.0 g) was purified using column chromatography followed by distillation under reduced to yield pure **TXN2** as a colourless oil (0.59 g, 30% of purified oil, 7% overall, bp 58-60 °C, 0.1 mbar).

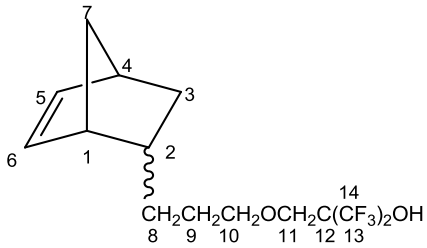

Unseparated mixture of isomers

^{1}H NMR (699.7 MHz, $CDCl_3$):

***endo* component** (81%) δ 6.13 (dd, J_{H5-H6} = 5.7 Hz, J_{H4-H5} = 3.2 Hz, 1H, H^5), 5.90 (dd, J_{H5-H6} = 5.7 Hz, J_{H1-H6} = 2.6 Hz, 1H, H^6), 4.04 (s, 1H, OH), 3.76 (s, 2H, H^{11}), 3.56 (t, $J_{H10-H11}$ = 6.6 Hz, 2H, H^{10}), 2.76 (m, 2H, H^1, H^4), 1.98 (m, 1H, H^2), 1.85 (ddd, $J_{H3X-H3N}$ =11.4 Hz, $J_{H3X-H2,\ H4}$ = 9.1, 3.9 Hz, 1H, H^{3X}), 1.60 (m, 2H, H^9), 1.40 (m, 1H, H^7), 1.23 (m, 1H, H^7), 1.11 (m, 2H, H^8), 0.49 (ddd, $J_{H3N-H3X}$ =11.4 Hz, $J_{H3N-H2,\ H4}$ = 4.0, 2.6 Hz, 1H, H^{3N})

***exo* component** (19%) δ 6.08 (dd, J_{H5-H6} = 5.7 Hz J_{H1-H6} = 3.1 Hz, 1H, H^6) 6.03 (dd, J_{H5-H6} = 5.7 Hz, J_{H4-H5} = 2.8 Hz, 1H, H^5) 4.04 (s, 1H, OH), 3.78 (s, 2H, H^{11}), 3.60 (t, J_{H9-H10} = 6.6 Hz, 2H, H^{10}), 2.80 (m, 1H, H^4), 2.51 (m, 1H, H^1), 1.68 (m, J_{H9-H10} = 6.6 Hz, 2H, H^9), 1.47-1.37 (m, 2H, H^8), 1.32-1.27 (m, 4H, H^2, H^{3X}, H^7), 0.86 (ddd, $J_{H3X-H3N}$ = 10.6 Hz, $J_{H3N-H2,\ H4}$ = 3.3 Hz, 1H, H^{3N})

^{13}C{^{1}H} NMR (175.9 MHz, $CDCl_3$):

***endo* component** δ 137.6 (C^5), 132.4 (C^6), 124.4 (q, J_{C-F} = 285 Hz, C^{13}, C^{14}), 74.7 (sept, J_{C-F} = 29.6 Hz, C^{12}), 73.3 (C^{10}), 65.8 (C^{11}), 50.0 (C^7), 45.7 (C^1), 42.2 (C^4), 38.8 (C^2), 32.7 (C^3), 31.2 (C^8), 28.7 (C^9)

***exo* component** δ 137.1 (C^6), 136.7 (C^5), 124.4 (q, J_{C-F} = 285 Hz, C^{13}, C^{14}), 74.7 (sept, J_{C-F} = 29.6 Hz, C^{12}), 73.2 (C^{10}), 65.8 (C^{11}), 46.6 (C^4), 45.5 (C^7), 42.2 (C^1), 38.9 (C^2), 33.4 (C^3), 32.9 (C^8), 28.9 (C^9)

^{19}F[^{1}H] NMR (376.3 MHz, $C_2D_2Cl_4$): δ -77.2 (m, 6F, $2CF_3$)

Accurate mass MS: Found: 333.1283 ($M\text{-}H^+$) Calculated for $C_{14}H_{19}O_2F_6$: 333.1289

GCMS EI$^+$: RT = 13.75, 333.1 ($C_{14}H_{19}O_2F_6$, $M\text{-}H^+$, *endo*), RT = 13.79, 333.1 ($C_{14}H_{19}O_2F_6$, $M\text{-}H^+$, *exo*)

Synthesis of *exo*-NB(CH_2)$_3$OCH_2C(CF_3)$_2$OH (TX2)

A slurry of sodium hydride (95%, 0.22 g, 9.07 mmol) in THF (5 mL) was cooled to -20 ºC and treated drop-wise with a solution of **TX1** (1.05 g, 6.90 mmol) in THF (5 mL). The solution was warmed to ambient temperature and stirred overnight. The mixture was cooled to -20 ºC, treated with chilled HFIBO (1.24 g, 0.9 mL, 6.90 mmol) and warmed to ambient temperature with stirring overnight.

The reaction was cooled in an ice bath and quenched using water (10 mL). The solution was acidified to pH 1 using concentrated HCl and the resulting layers separated. The aqueous phase was extracted with diethyl ether (2 x 15 mL), washed with brine to pH 6 (6 x 15 mL), dried over $MgSO_4$, filtered and the solvent removed to yield a yellow-brown oil. The crude product was distilled using Kugelröhr apparatus to yield a colourless oil (1.05 g, 46%, pot temperature 104 °C, 0.8 mbar.) However, analysis of the oil by ^{19}F NMR spectroscopic and GCMS analysis indicated the presence of ~7% of a fluorinated impurity. The oil was purified using column chromatography followed by Kugelröhr distillation under reduced pressure to yield pure **TX2** as a colourless oil (69 mg, 3%).

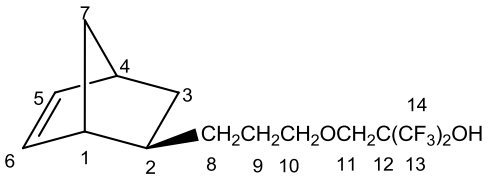

^{1}H NMR (499.8 MHz, $CDCl_3$): δ 6.08 (dd, J_{H5-H6} = 5.7 Hz J_{H1-H6} = 3.1 Hz, 1H, H^6) 6.02 (dd, J_{H5-H6} = 5.7 Hz, J_{H4-H5} = 2.8 Hz, 1H, H^5) 4.13 (s, 1H, OH), 3.78 (s, 2H, H^{11}), 3.60 (t, J_{H9-H10} = 6.6 Hz, 2H, H^{10}), 2.80 (m, 1H, H^4), 2.51 (m, 1H, H^1), 1.68 (m, J_{H9-H10} = 6.6 Hz, 2H, H_9), 1.47-1.37 (m, 2H, H^8), 1.32-1.27 (m, 4H, H^2, H^{3X}, H^7), 1.08 (ddd, $J_{H3X-H3N}$ = 10.6 Hz, $J_{H3N-H2,\,H4}$ = 3.3 Hz, 1H, H^{3N})

^{13}C{^{1}H} NMR (125.7 MHz, $CDCl_3$): δ 136.9 (C^6), 136.5 (C^5), 122.7 (q, J_{C-F} = 285 Hz, C^{13}, C^{14}), 74.6 (sept, J_{C-F} = 29.6 Hz, C^{12}), 73.1 (C^{10}), 65.7 (C^{11}), 46.5 (C^4), 45.4 (C^7), 42.1 (C^1), 38.7 (C^2), 33.2 (C^3), 32.8 (C^8), 28.8 (C^9)

^{19}F[^{1}H] NMR (376.3 MHz, $C_2D_2Cl_4$): δ -77.2 (m, 6F, $2CF_3$)

Accurate mass MS: Found: 333.1301 ($M\text{-}H^+$) Calculated for $C_{14}H_{19}O_2F_6$: 333.1289

GCMS EI$^+$: RT = 13.74, 333.1 ($C_{14}H_{19}O_2F_6$, $M\text{-}H^+$)

IR: 3600-3300 (O-H), 3000–2800 (saturated C-H)

Characterisation of *endo*-/*exo*-NB$(CH_2)_4OCH_2C(CF_3)_2OH$ (QXN1)#

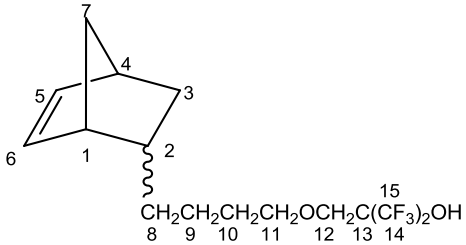

Unseparated mixture of isomers

^{1}H NMR (699.7 MHz, $C_2D_2Cl_4$):

***endo* component** (77%) δ 6.05 (dd, J_{H5-H6} = 5.5 Hz, J_{H4-H5} = 2.8 Hz, 1H, H^5), 5.84 (dd, J_{H5-H6} = 5.5 Hz, J_{H1-H6} = 2.7 Hz, 1H, H^6), 4.03 (s, 1H, OH), 3.69 (s, 2H, H^{12}), 3.50 (t, $J_{H10-H11}$ = 6.6 Hz, 2H, H^{11}), 2.68 (m, 2H, H^1, H^4), 1.89 (m, 1H, H^2), 1.77 (m, 1H, H^{3X}), 1.53 (m, 2H, H^{10}), 1.31 (m, 1H, H^7), 1.23 (m, 2H, H^9), 1.15 (m, 1H, H^7), 1.02 (m, 2H, H^8), 0.40 (ddd, $J_{H3N-H3X}$ =11.3 Hz, 1H, H^{3N})

***exo* component** (23%) δ 6.02 (dd, J_{H5-H6} = 5.5 Hz, J_{H1-H6} = 3.0 Hz, 1H, H^6), 5.96 (dd, J_{H5-H6} = 5.5 Hz, J_{H4-H5} = 2.8 Hz, 1H, H^5), 4.03 (s, 1H, OH), 3.69 (s, 2H, H^{12}), 3.51 (t, $J_{H10-H11}$ = 6.8 Hz, 2H, H^{11}), 2.71 (m, 1H, H^4), 2.43 (m, 1H, H^1), 1.89, 1.77, 1.53, 1.31, 1.23, 1.15, 1.02 (series of multiplets (signals masked by *endo* isomer), 11H, H^2, H^3, H^7, H^8, H^9, H^{10})

^{13}C{^{1}H} NMR (125.7 MHz, $C_2D_2Cl_4$): *endo* component δ 137.0 (C^5), 132.2 (C^6), 122.3 (q, J_{C-F} = 285 Hz, C^{14}, C^{15}), 73.9 (sept, J_{C-F} = 29.6 Hz, C^{13}), 72.6 (C^{11}), 65.1 (C^{12}), 49.5 (C^7), 45.2 (C^1), 42.4 (C^4), 38.5 (C^2), 34.3 (C^8), 32.32 (C^3), 29.3 (C^9), 24.6 (C^{10})

***exo* comp** δ 136.8 (C^6), 136.2 (C^5), 122.3 (q, J_{C-F} = 285 Hz, C^{14}, C^{15}), 73.9 (sept, J_{C-F} = 29.6 Hz, C^{13}), 72.6 (C^{11}), 65.1 (C^{12}), 46.2 (C^4), 45.1 (C^7), 41.8 (C^1), 38.5 (C^2), 36.0 (C^8), 32.9 (C^3), 29.3 (C^9), 24.9 (C^{10})

^{19}F NMR[^{1}H] (376.3 MHz, $C_2D_2Cl_4$): δ -77.2 (m, 6F, $2CF_3$)

Accurate mass MS: Found: 347.1154 ($M\text{-}H^+$) Calculated for $C_{15}H_{21}O_2F_6$: 347.1446

GCMS EI$^+$: RT = 14.89, 347.1 ($C_{15}H_{21}O_2F_6$, $M\text{-}H^+$, *endo*), RT = 14.69, 347.1 ($C_{15}H_{21}O_2F_6$, $M\text{-}H^+$, *exo*)

IR: 3600-3300 (O-H), 3000-2800 (saturated C-H)

Characterisation of *endo*-/*exo*-NB$(CH_2)_6OCH_2C(CF_3)_2OH$ (HXN1)#

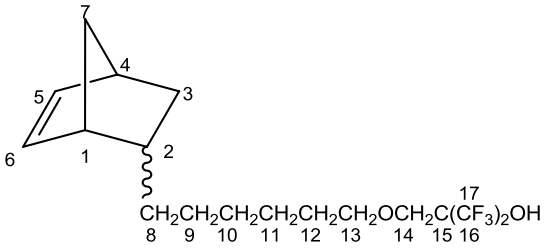

Unseparated mixture of isomers

^{1}H NMR (699.7 MHz, $C_2D_2Cl_4$):[§]

***endo* component** (80%) δ 6.03 (dd, $J_{H5\text{-}H6}$ = 5.7 Hz, $J_{H4\text{-}H5}$ = 3.0 Hz, 1H, H^5), 5.84 (dd, $J_{H5\text{-}H6}$ = 5.7 Hz, $J_{H1\text{-}H6}$ = 2.8 Hz, 1H, H^6), 4.03 (s, 1H, OH), 3.69 (s, 2H, H^{14}), 3.50 (t, $J_{H12\text{-}H13}$ = 6.6 Hz, 2H, H^{13}), 2.67 (m, 2H, H^1, H^4), 1.88 (m, 1H, H^2), 1.75 (ddd, $J_{H3X\text{-}H3N}$ = 11.3 Hz, 1H, H^{3X}), 1.52 (m, 2H, H^{12}), 1.29 (m, 1H, H^7), 1.20 (m, 6H, H^9, H^{10}, H^{11}), 1.13 (m, 1H, H^7), 0.98 (m, 2H, H^8), 0.40 (ddd, $J_{H3N\text{-}H3X}$ = 11.3 Hz, $J_{H3N\text{-}H2,\ H4}$ = 3.9, 6.8 Hz, 1H, H^{3N})

***exo* component** (20%) δ 6.01 (dd, $J_{H5\text{-}H6}$ = 5.7 Hz, $J_{H1\text{-}H6}$ = 3.0 Hz, 1H, H^6), 5.94 (dd, $J_{H5\text{-}H6}$ = 5.7 Hz, $J_{H4\text{-}H5}$ = 2.9 Hz, 1H, H^5), 4.03 (s, 1H, OH), 3.69 (s, 2H, H^{14}), 3.51 (t, $J_{H12\text{-}H13}$ = 6.6 Hz, 2H, H^{13}), 2.67 (m, 1H, H^4), 2.42 (m, 1H, H^1), 1.88, 1.75, 1.52, 1.29, 1.20, 1.13, 0.98, 0.79 (series of multiplets (signals masked by *endo* isomer), 15H, H^2, H^3, H^7, H^8, H^9, H^{10}, H^{11}, H^{12})

^{13}C{^{1}H} NMR (125.7 MHz, $C_2D_2Cl_4$**):[§]**

***endo* component** δ 136.8 (C^5), 132.3 (C^6), 122.4 (q, $J_{C\text{-}F}$ = 285 Hz, C^{16}, C^{17}), 74.2 (sept, $J_{C\text{-}F}$ = 29.6 Hz, C^{15}), 72.6 (C^{13}), 65.1 (C^{14}), 49.5 (C^7), 45.3 (C^1), 42.4 (C^4), 36.6 (C^2), 34.6 (C^8), 32.3 (C^3), 29.4, 29.1, 28.4 (C^{12}), 25.7

***exo* component** δ 136.1 (C^5, C^6), 122.4 (q, $J_{C\text{-}F}$ = 285 Hz, C^{16}, C^{17}), 74.2 (sept, $J_{C\text{-}F}$ = 29.6 Hz, C^{15}), 72.6 (C^{13}), 65.1 (C^{14}), 46.3 (C^4), 45.1 (C^7), 41.8 (C^1), 38.6 (C^2), 36.4 (C^8), 32.9 (C^3) 29.4, 29.1, 28.6 (C^{12}), 25.7

^{19}F[^{1}H] NMR (376.3 MHz, $C_2D_2Cl_4$): δ -77.3 (m, 6F, $2CF_3$)

[§] Due to the overlapping nature of both the proton and carbon resonances it was not possible to conclusively assign all of the peaks in either spectrum.

Accurate mass MS: Found: 375.1771 ($M\text{-}H^+$) Calculated for $C_{17}H_{25}O_2F_6$: 375.1759

GCMS EI$^+$: RT = 17.17, 375.1 ($C_{17}H_{25}O_2F_6$, $M\text{-}H^+$, *endo*), RT = 17.22, 375.1 ($C_{17}H_{25}O_2F_6$, $M\text{-}H^+$, *exo*)

IR: 3600-3300 (O-H), 3000-2800 (saturated C-H)

7.2.1 Synthesis and characterisation of palladium hydride pro-initiators

Synthesis of $Pd(PCy_3)_2$

To a pale yellow solution of $PdMe_2(TMEDA)$ (1.00 g 3.99 mmol) in toluene (10 mL) was added a solution of PCy_3 (2.227 g, 7.97 mmol) in toluene (10 mL), to give a transparent yellow solution.[8] After stirring overnight at ambient temperature the solvent was removed *in vacuo* to yield a yellow-white solid. Washing with methanol gave **$Pd(PCy_3)_2$** as a white solid, which was isolated by filtration and dried *in vacuo* (2.27 g, 85%).

$^{31}P\{^1H\}$ NMR (161.91 MHz, C_7D_8): δ 40.2 (s)

Synthesis of *trans*-$[Pd(H)(MeCN)(PCy_3)_2][B(C_6F_5)_4]$ (Pd1388)

$Pd(PCy_3)_2$ (0.5015 g, 0.752 mmol) was suspended in toluene (2 mL) and a solution of $[HNMe_2Ph][B(C_6F_5)_4]$ (0.6022 g, 0.752 mmol) in acetonitrile (2 mL) added dropwise over 5 minutes.[9] The yellow suspension cleared at the end of the addition. The solution was stirred for 2 hours at ambient temperature and then reduced to dryness leaving a yellow-brown foam. Toluene (0.6 mL) was added to re-dissolve the foam, followed by hexane (2.5 mL) to give an oily mixture which gradually deposited solids. Sonication for 5 minutes afforded more solids which were stirred for a further 5 minutes then isolated *via* cannula filtration. The solids were washed with hexane (3 x 2.5 mL) and dried in *vacuo* to yield the product as an off white powder (0.98 g, 95%).

^{1}H NMR (400.0 MHz, $C_2D_2Cl_4$): δ 2.27 (s, 3H, **Me**CN), 1.79-1.69, 1.29-1.15 (m, 66H, (P**Cy$_3$**)$_2$), -15.44 (t, $^{2}J_{P-H}$ = 8.0 Hz, 1H, Pd(**H**))

^{31}P{^{1}H} NMR (161.9 MHz, $C_2D_2Cl_4$): δ 44.2 (s)

Anal. Found: C, 54.26 H, 5.10 N, 1.45%, Calc: C, 53.63, H 5.09, N 1.01%

Synthesis of [HNMe$_2$Ph][BF$_4$]

To a stirred solution of N,N-dimethylaniline (2 mL, 15.8 mmol, 1.2 mol excess) in diethyl ether (50 mL), HBF_4 (50 wt%, H_2O, 1.5 mL, 13.2 mmol) was added drop wise to give a cloudy solution.[10] After stirring for 10 minutes the aqueous layer was isolated and the water removed in *vacuo* to yield a white semi-solid, which was washed with diethyl ether to yield the product as a white semi-solid (0.56 g, 20%.) The low yield may be attributed to problems in isolating the product from the aqueous layer.

^{1}H NMR (400 MHz, $CDCl_3$): δ 3.23 (s, 6H, C**H$_3$**), 7.37-7.51 (m, 5H, C$_6$**H$_5$**), 9.10 (s, 1H, N**H**)

^{13}C{^{1}H} NMR (125.7 MHz, $CDCl_3$): δ 47.7 (**C**H$_3$), 120.2 (*o*- **C**$_6$H$_5$), 130.8 (*p*- **C**$_6$H$_5$), 130.8 (*m*- **C**$_6$H$_5$), 142.1 (*i*- **C**$_6$H$_5$)

MS ES$^+$:122.0 ($C_8H_{12}N$, M^+)

Synthesis of *trans*-[Pd(H)(MeCN)(PCy$_3$)$_2$]BF$_4$ (Pd796)

To a stirred, white suspension, of Pd(PCy$_3$)$_2$ (300 mg, 0.54 mmol) in acetonitrile (20 mL), HBF_4 (48 wt%, H_2O, 60 μL, 0.54 mmol) was added drop wise using a micro-syringe to give a transparent yellow solution. After stirring for 1 hour at ambient temperature, the solvent was removed *in vacuo* to yield a yellow solid. Washing with cold diethyl ether, isolation by filtration and drying in *vacuo* gave the **Pd796** product as a pale yellow-brown solid (208 mg, 69%).

^{1}H NMR (400.0 MHz, $C_2D_2Cl_4$): δ 2.26 (s, 3H, **Me**CN), 1.95-1.80, 1.51-1.27 (m, 66H, (P**Cy$_3$**)$_2$), -15.47 (t, 1H, $^{2}J_{P-H}$ = 6.8 Hz, [Pd(**H**)(MeCN)(PCy$_3$)$_2$]BF_4)

^{31}P{^{1}H} NMR (161.9 MHz, $C_2D_2Cl_4$): δ 44.3 (s)

Anal. Found: C, 54.48 H, 8.66 N, 2.02%, Calc: C, 57.32, H 8.66, N 1.76%

Synthesis of *trans*-[Pd(H)(MeCN)(PCy$_3$)$_2$]PF_6 (Pd854)

To a stirred, white suspension, of Pd(PCy$_3$)$_2$ (200 mg, 0.3 mmol) in acetonitrile (20 mL), HPF_6 (60.24 wt%, H_2O, 44 μL, 0.3 mmol) was added drop wise using a micro-syringe to give a transparent yellow solution. After stirring for 1 hour at ambient temperature, the solvent was removed *in vacuo* to yield a sticky yellow-brown solid. Washing with cold diethyl ether (20 mL), isolation by filtration and drying *in vacuo* gave **Pd854** as a pale orange-brown solid (138.3 mg, 54%)

^{1}H NMR (400.0 MHz, $C_2D_2Cl_4$): δ 2.27 (s, 3H, **Me**CN), 1.94-1.64, 1.35-1.10 (m, 66H, (P**Cy$_3$**)$_2$), -15.47 (t, 1H, [Pd(**H**)(MeCN)(PCy$_3$)$_2$]PF_6)

^{31}P{^{1}H} NMR (161.9 MHz, $C_2D_2Cl_4$): δ 44.3 (s), δ -143.5 (septet, J_{P-F} = 714 Hz)

Anal. Found: C, 47.83 H, 7.88 N, 1.68%, Calc: C, 53.39, H 8.27, N 1.64%

Synthesis of *trans*-[Pd(Cl)(H)(PCy$_3$)$_2$] (Pd704)

To a stirred, pale green solution of Pd(PCy$_3$)$_2$ (400 mg, 0.6 mmol) in toluene (20 mL) HCl (1 M, Et_2O, 0.6 mL, 0.6 mmol) was added drop wise to give a transparent yellow-brown solution.[11] After stirring for 1 hour at ambient temperature the solvent was removed *in vacuo* to yield a sand coloured solid (0.35 g, 83%). Several attempts to scale up this reaction resulted in the immediate formation of a brown solution upon addition of HCl to a solution of Pd(PCy$_3$)$_2$ which, despite containing 70-80% of the desired **Pd704** product was impossible to separate from the impurities.

^{1}H NMR (499.8 MHz, $C_6D_5CD_3$): δ 2.26-2.15, 1.80-1.67, 1.34-1.23 (m, 66H, (P**Cy$_3$**)$_2$), -14.29 (1H, t, $^{2}J_{P\text{-}H}$ = 4.5Hz [Pd(Cl)(**H**)(PCy$_3$)$_2$])

^{31}P{^{1}H} NMR (161.9 MHz, $C_6D_5CD_3$): δ 42.3 (s)

***Anal*. Found:** C, 60.91 H, 9.51 %, **Calc:** C, 61.43, H 9.61 %

Synthesis of *trans*-[Pd(H)(MeCN)(PCy$_3$)$_2$]SbF$_6$

To a stirred yellow-brown solution of [Pd(Cl)(H)(PCy$_3$)$_2$] (**Pd704**, 100 mg, 0.15 mmol) in toluene (10 mL) was added a solution of NaSbF$_6$ (38.5 mg, 0.15 mmol) in acetonitrile (1.5 mL). A reddy-brown solution was formed along with formation of a white precipitate over the space of 1 hour. The precipitate was removed *via* cannula filtration to yield a reddy-brown liquid. The solvent was removed *in vacuo* to yield **Pd945** as a pinky-brown solid (91.5 mg, 68%).

^{1}H NMR (400.0 MHz, $C_2D_2Cl_4$): δ 2.25 (s, 3H, **Me**CN), 1.90-1.80, 1.39-1.22 (m, 66H, (P**Cy$_3$**)$_2$), -15.38 (t, 1H, $^{2}J_{P\text{-}H}$ = 6.8 Hz [Pd(**H**)(MeCN)(PCy$_3$)$_2$]SbF$_6$)

^{31}P{^{1}H} NMR (161.9 MHz, $C_2D_2Cl_4$): δ 44.3 (s)

Synthesis of [Pd(H)(OTf)(PCy$_3$)$_2$] (Pd817)

To a stirred yellow-brown solution of [Pd(Cl)(H)(PCy$_3$)$_2$] (**Pd704**,100 mg, 0.15 mmol) in toluene (10 mL) was added a solution of AgOTf (37 mg, 0.15 mmol) in toluene (1 mL) and acetonitrile (1 mL), to give a green/black solution. A grey-white precipitate formed initially, which turned black over the space of 1 hour. The precipitate was removed *via* cannula filtration to yield a bright yellow liquid. The solvent was removed *in vacuo* to yield a yellow solid (55 mg, 55%).

^{1}H NMR (400.0 MHz, $C_2D_2Cl_4$): δ 2.01-1.55, 1.45-1.18 (m, 66H, (P**Cy$_3$**)$_2$), -19.61 (m, 1H, [Pd(**H**)(OTf)(PCy$_3$)$_2$])

^{31}P{^{1}H}(161.9 MHz, $C_2D_2Cl_4$): δ 42.9 (s)

^{19}F[^{1}H] (376.3 MHz, $C_2D_2Cl_4$) δ -77.6 (s)

Anal. Found: C, 52.87 H, 8.18 %, Calc: C, 54.29, H 8.39 %

Reaction of [Pd(Cl)(H)(MeCN)(PCy$_3$)$_2$] with ^{t}Bu$_4$NI – preparation of *trans*-[Pd(H)(MeCN)(PCy$_3$)$_2$]I (Pd836) and *trans*-[Pd(H)(I)(MeCN)(PCy$_3$)$_2$] (Pd795)

A yellow-brown solution of [Pd(Cl)(H)(PCy$_3$)$_2$] (**Pd704**) (10 mg, 1.4 x 10^{-5} mol) in d_2-TCE (0.6 mL) was treated with ^{t}Bu$_4$NI (5.3 mg, 1.4 x 10^{-5} mol) and acetonitrile (0.7 μL, 1.4 x 10^{-5} mol) and the resulting solution transferred to a Young's NMR tube. A mixture of two palladium-hydride containing-products are formed, characterised by triplet resonances at δ -12.2 and δ -15.4 ppm in approximately a 1:1 ratio by ^{1}H NMR spectroscopic analysis. The resonances are assigned to the complexes *trans*-[Pd(H)(I)(PCy$_3$)$_2$] (**Pd795**) and *trans*-[Pd(H)(MeCN)(PCy$_3$)$_2$]I (**Pd836**) respectively. The ratio between **Pd836** and **Pd795** is influenced by addition of tetrabutylammonium iodide (0.5 equivalents) or MeCN (1 equivalent), both of which lead to an increase in the proportion of **Pd795** within the mixture (30:70 and 35:65 **Pd836:Pd795** respectively).

^{1}H NMR (400.0 MHz, $C_2D_2Cl_4$): δ 0.5 – 2 (m, (P**Cy$_3$**)$_2$, **Me**CN (bound and free)), -12.16 (t, $^{2}J_{P\text{-}H}$ = 8.4 Hz, 1H, [Pd(**H**)(I)(PCy$_3$)$_2$]), -15.35 (t, $^{2}J_{P\text{-}H}$ = 4.4 Hz, 1H, [Pd(**H**)(MeCN)(PCy$_3$)$_2$]I)

^{31}P{^{1}H} NMR (161.9 MHz $C_2D_2Cl_4$): δ 41.6 (s, **Pd836**) δ 42.2 (s, **Pd795**)

7.3 Experimental procedures and analysis of polymerisation kinetics data - Chapter III

Stability of Pd1388 at 70 °C

Separate solutions of **Pd1388** (5 mg, 3.6 x 10^{-6} mol) in TCE, chlorobenzene and a 5:1 mixture of toluene:fluorobenzene (0.6 mL) were prepared in Young's tap NMR tubes. A further tube was prepared containing **Pd1388** (25.1 mg, 1.8 x 10^{-5} mol), TCE (1.91 µL, 1.8 x 10^{-5} mol) and a 5:1 mix of toluene:fluorobenzene (0.6 mL). A sealed lock tube containing $O=PH(OH)_2$ in d_6-benzene was added to each NMR tube as an internal standard. The tubes were heated to 70 °C and monitored using ^{31}P NMR spectroscopy. Please see Chapter III for further details.

Stability of PCy_3 at 70 °C

Separate solutions of PCy_3 (25.0 mg, 8.9 x 10^{-5} mol) in TCE, and a 5:1 mixture of toluene:fluorobenzene (0.6 mL) were prepared in Young's tap NMR tubes. A further tube was prepared containing PCy_3 (25.4 mg, 9.1 x 10^{-5} mol), TCE (9.6 µL, 9.1 x 10^{-5} mol) and a 5:1 mix of toluene:fluorobenzene (0.6 mL). A sealed lock tube containing $O=PH(OH)_2$ in d_6-benzene was added to each NMR tube as a non-reactive internal standard. The tubes were heated to 70 °C and monitored using ^{31}P NMR spectroscopy. Please see Chapter III for further details.

Polymerisation kinetics – general procedures and comments

A monomer concentration of 0.3 M and a **Pd1388** concentration of 6 mM in a total solvent volume of 0.6 mL was used for all experiments, giving a monomer:initiator ratio of 50:1. Polymerisations were carried out in Young's tap NMR tubes prepared in a glove box. Tubes were quickly removed from the glove box and frozen in liquid nitrogen during transport to the spectrometer. Polymerisation reactions were monitored using ^1H NMR spectroscopy recorded on a Varian Inova spectrometer at 70 °C. The temperature of the probe was stabilised for at least 30 minutes prior to beginning any experiments. A solution of an appropriate hexafluoropropanol-functionalised norbornene monomer (1.8 x 10^{-4} mol) in the appropriate solvent (0.6 mL, usually d_2-TCE) was used to preliminarily lock and shim the spectrometer. In addition, it is necessary to fine tune the shimming of the spectrometer and equilibrate the reaction solution to 70 ºC prior to commencement of the NMR experiment, a process which was minimised to approximately 60 seconds.

Spectra were recorded using arrayed experiments with integrals referenced relative to the preceding spectrum to prevent the need for an internal standard. An acquisition duration of 4.1 seconds and a delay between pulses of 1 second were used. Ideally a longer delay would have been employed, (larger than the longest T_1 relaxation value for a particular monomer) to allow all centres to fully relax prior to application of the next pulse. However, many of the polymerisation reactions were too fast for this to be feasible and for this reason a consistent values was chosen to allow reliable comparison between data for different monomers. The number of transients recorded per spectrum was dependent upon the speed of the polymerisation, ranging from 4 through to 16. A wide spectral window (δ + 12 to -20 ppm) was used to ensure visibility of both the hydride resonance of the pro-initiator (δ -15 ppm) and the vinylic resonances of the norbornene monomer (δ + 6 ppm)

Polymerisation of *exo*-NBCH$_2$OCH$_2$C(CF$_3$)$_2$OH (SX1) using Pd1388 and its decomposition products

Separate solutions of **Pd1388** (5 mg, 3.6 x 10^{-6} mol) were prepared in d_2-TCE (**a**) and fluorobenzene (**b**) (0.1 mL) in Young's tap NMR tubes. A third solution was prepared in d_2-TCE (0.3 mL) and heated overnight at 70 °C (**c**). Separate solutions of **SX1** (54.8 mg, 1.8 x 10^{-4} mol) were prepared in d_2-TCE (**a**) (0.5 mL), d_8-toluene (**b**) (0.5 mL) and d_2-TCE (**c**) (0.3 mL) and added to the corresponding tubes containing **Pd1388**. The reactions were monitored over a period of 4 hours using ^{1}H NMR spectroscopy, as described previously. Please see Chapter III for discussion of polymerisation kinetics.

Isolation of polymers from reactions a, b and c

Upon completion of the polymerisation reactions (4 hours at 70 °C), each reaction was quenched with an excess of methanol. The solution was reduced to dryness *in vacuo* and the solid polymer dissolved in the minimum of THF. The solution was passed through Celite to remove residual palladium and the resulting polymers isolated as pale yellow solids *via* precipitation into hexane. The isolated polymers were dried overnight under vacuum at 40 °C and subsequently analysed by GPC (THF), the data for which is given in Chapter III.

7.4 Experimental procedures - Chapter IV

Polymerisation reactions for the determination of kinetics data

Polymerisation reactions were carried out as discussed previously and monitored using ^{1}H NMR spectroscopy at 70 °C in d_2-TCE. The amounts of monomer used to prepare stock solutions are summarised in table 6.1. In each case, 0.5 mL of monomer solution was treated with 0.1 mL of a freshly prepared stock solution of **Pd1388** (50 mg/mL). Each reaction was repeated 3 times. The kinetics data (rate constants and R^2 values) obtained for each individual run are given in Appendix 3.

Table 7.1 Summary of amounts of monomer required to prepare stock solutions for polymerisation kinetics reactions

Monomer	Code	Mass of monomer per 0.5 mL solvent (mg)
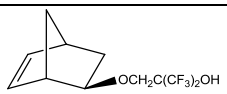	**ZX3**	52.2
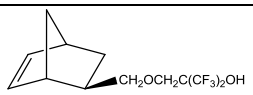	**SX1**	54.8
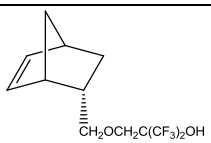	**SN2**	54.8
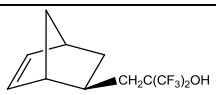	**SX2**	49.4
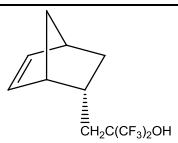	**SN3**	49.4
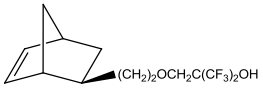	**DX2**	57.3
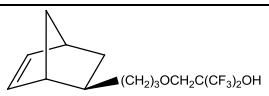	**TX2**	59.8

Determination of the extent of conversion of monomer to polymer

A sample of stock solution (0.5 mL) of each monomer was treated with mesitylene (3 µL) and analysed by ^{1}H NMR spectroscopy to determine the mesitylene:norbornene ratio. Mesitylene was used as an internal standard for a combination of high temperature stability, non reactivity and the suitable position of the resonances within the ^{1}H NMR spectrum. The monomer solutions were treated with a freshly prepared stock solution of **Pd1388** (1 mL, 50 mg/mL), heated to 70 °C and reanalysed by ^{1}H NMR spectroscopy to determine the extent of conversion. The polymers were then isolated as discussed in section 6.3 and analysed using GPC (THF). Molecular weight, PDI and conversion data are given in chapter IV.

Solution polymerisation of *exo*-NBCH$_2$OCH$_2$C(CF$_3$)$_2$OH (SX1) in TCE

A solution of **SX1** (4.165g, 137 mmol) in TCE (40 mL) containing nonane (1 mL) as an internal standard was prepared and an aliquot removed for analysis by GC. (1 mL) The remaining solution was pre-heated to 70 ^{o}C and treated with a solution of **Pd1388** (0.375 g, 2.7 x 10^{-4} mol) in TCE (5 mL) with vigorous stirring. Samples were taken at intervals throughout the polymerisation reaction (~5 mL during the first 10 minutes, ~2 mL thereafter) using a pre-warmed, glass syringe fitted with a wide bore needle. Samples were quenched using a ten-fold excess of methanol and a sample of the solution removed for submission for GC analysis. The remainder of each solution was reduced to dryness and dissolved in the minimum of THF. The THF solution was passed through Celite and precipitated in to hexane. The isolated pale-yellow polymers were dried *in vacuo* (40 °C) and analysed by GPC (THF). At the end of the reaction period (3 hours) the reaction vessel was quenched with methanol and the resulting polymer isolated. GPC and GC data are summarised in Chapter IV.

Solution polymerisation of *exo*-NBCH$_2$OCH$_2$C(CF$_3$)$_2$OH (SX1) in toluene:fluorobenzene

The polymerisation of **SX1** was repeated on a slightly smaller scale using a toluene:fluorobenzene mixture as the reaction solvent. **SX1** (1.644 g, 5.40 mmol) was dissolved in toluene (17 mL) and treated with a solution of **Pd1388** (150 mg, 1.8 x 10^{-4} mol) in fluorobenzene (1 mL) at 70 °C. In this case, the reaction was not examined using GC hence nonane was not included. Samples were isolated over a period of 3 hours as discussed previously and analysed by GPC. GPC data are summarised in Chapter IV

Solution polymerisation of *endo*-$NBCH_2OCH_2C(CF_3)_2OH$ (SN2) in TCE

SN2 (1.644 g, 5.40 mmol) was dissolved in TCE containing nonane internal standard (17 mL) and treated with a solution of **Pd1388** (150 mg, 1.8 x 10^{-4} mol) in TCE (1 mL) at 70 °C. Samples were isolated and analysed as discussed for the polymerisation of **SX1** in TCE. GPC and GC data are summarised in Chapter IV.

Solution polymerisation of *exo*-$NBCH_2C(CF_3)_2OH$ (SX2) in TCE

SX2 (1.482 g, 5.40 mmol) was dissolved in TCE containing nonane internal standard (17 mL) and treated with a solution of **Pd1388** (150 mg, 1.8 x 10^{-4}) in TCE (1 mL) at 70 °C. Samples were isolated and analysed as discussed for the polymerisation of **SX1** in TCE. GPC and GC data are summarised in Chapter IV.

Reaction of poly(*exo*-$NBCH_2OCH_2C(CF_3)_2OH$) with Pd1388

A sample of poly(*exo*-$NBCH_2OCH_2C(CF_3)_2OH$) of known molecular weight (trimodal distribution, M_p = 70,000, 21,000 and 4000) (35 mg) was treated with a solution of **Pd1388** (3 mg) in TCE (0.6 mL) in a Young's tap NMR tube. The polymer did not dissolve into solution at ambient temperature. The mixture was heated to 70 °C for 30 minutes. The polymer showed swelling behaviour however did not dissolve. The tube was treated with methanol (0.6 mL) to quench the reaction and the solution isolated. The tube was washed with THF to dissolve the remaining polymer and the washings combined with the TCE/methanol mixture. The solution was reduced to dryness and the resulting polymer dissolved in the minimum of THF, passed through Celite and precipitated into hexane. The polymer was reanalysed using GPC (THF). GPC analysis confirms that the polymer retains a trimodal distribution, however the high molecular weight species shows a reduction in peak average molecular weight of approximately 10,000 Daltons (M_p = 60,000, 11,000 and 8000 Daltons, respectively.)

Thermal stability of poly(*exo*-$NBCH_2OCH_2C(CF_3)_2OH$) in TCE

A sample of poly(*exo*-$NBCH_2OCH_2C(CF_3)_2OH$) of known molecular weight was treated with TCE (0.6 mL) and heated overnight at 70 °C. The polymer was isolated *via* precipitation into hexane and analysed by GPC (THF).

7.5 Experimental procedures Chapter V

Determination of reactivity ratios using the Finemann Ross Method

Monomer solutions (50 equivalents) were prepared in Young's tap NMR tubes containing 0.5 mL TCE. Solutions ranged between 100% *endo* and 100% *exo* isomers with the exact *endo*:*exo* ratio determined *via* careful integration of the vinylic resonances relative to a mesitylene internal standard (5 µL per mL of TCE) to determine the mole fractions (f). Solutions were then treated with 1 equivalent of **Pd1388** in TCE (0.1 mL) and heated to 70 °C for ~ 1 minute, keeping the extent of conversion below 10%. The mole fractions of the *endo* and *exo* isomera in the resulting copolymer (F) were calculated by consideration of free monomer in solution. Reactivity ratios were determined *via* plots of f vs F as discussed in Chapter V.

Polymerisation reactions for the determination of kinetics data

Stock solutions of monomer and **Pd1388** were prepared in d_2-TCE, as described in section 6.4. The amounts of monomer used to prepare stock solutions are summarised in Table 6.2. Polymerisation kinetics were carried out as described previously, with full kinetics data for each individual run given in appendix 3.

Polymerisation of *endo*-/exo-$NBCH_2C(CF_3)_2OH$ (SNX4) using palladium-hydride pro-initiators

Stock solutions of **SXN4** (0.5 mL, 1.8 x 10^{-4} mol) were treated with initiator solutions (Table 6.3, 0.1 mL, 3.6 x 10^{-6} mol) in Young's tap NMR tubes and analysed by ^1H NMR spectroscopy. The tubes were heated to 70 °C for 1 hour and the resulting mixtures reanalysed. Of the palladium complexes studied, only **Pd796**, **Pd945** and **Pd1154** were active in the polymerisation of **SXN4**. Please see Chapter V for further discussion.

Table 7.2 Summary of amounts of monomer required to prepare stock solutions for polymerisation kinetics reactions

Monomer	Code	Mass of monomer per 0.5 mL solvent (mg)
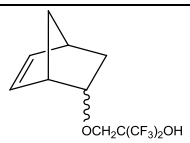	**ZXN**	52.2
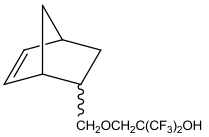	**SXN3**	54.8
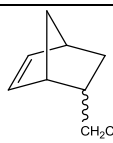	**SXN4**	49.4
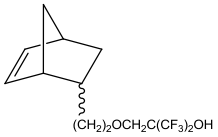	**DXN2**	57.3
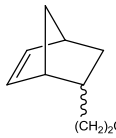	**DXN5**	51.9
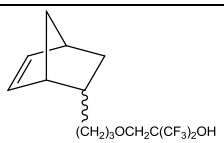	**TXN3**	59.8
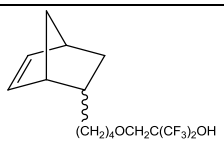	**QXN1**	62.3
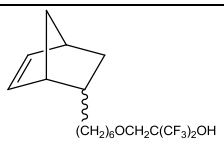	**HXN1**	67.4

Table 7.3 Mass of initiator used to prepare stock solutions for polymerisation of SXN4

Initiator	Code	Anion	Mass initiator per 0.1 mL TCE solvent (mg)
$[Pd(Cl)(H)(MeCN)(PCy_3)_2]$	**Pd704**	Cl	2.5
$[Pd(H)(MeCN)(PCy_3)_2]I$/ $[Pd(H)(I)(MeCN)(PCy_3)_2]$	**Pd836/Pd795**	I	*
$[Pd(H)(OTf)(MeCN)(PCy_3)_2]$	**Pd817**	OTf	2.9
$[Pd(H)(MeCN)(PCy_3)_2][BF_4]$	**Pd796**	BF_4	2.9
$[Pd(H)(MeCN)(PCy_3)_2][PF_6]$	**Pd854**	PF_6	3.1
$[Pd(H)(MeCN)(PCy_3)_2][SbF_6]$	**Pd945**	SbF_6	3.4
$[Pd(H)(MeCN)(PCy_3)_2][PF_3(C_2F_5)_3]$	**Pd1154**	$PF_3(C_2F_5)_3$	4.2

* The mixture of $[Pd(H)(MeCN)(PCy_3)_2]I$ / $[Pd(H)(I)(MeCN)(PCy_3)_2]$ was prepared on an NMR scale (10 mg of $[Pd(Cl)(H)(MeCN)(PCy_3)_2]$ starting material, described in section 6.2) and was simply combined with 50 mg of neat monomer.

7.6 References

1. J. Boersma, W. de Graff; D. Grove, G. van Koten and A.L. Spek, *Rec. Trav. Chim.*, 1988, **107**, 299-301
2. J. Boersma, W. de Graff, G. van Koten, J.J. Smeets and A.L. Spek, *Organometallics*, 1989, **8**, 2907-2917
3. P. Mayo, G. Orlova, J.D. Goddard and W. Tam, *J. Org. Chem.*, 2001, **66**, 5182-5191
4. C. Le Drian and A.E. Greene, *J. Am. Chem. Soc.* 1982, **104**, 5473-5483; H. Kreiger, Suom. Kemistil. B. 1963, **36**, 68; P.K. Freeman, D.M. Balls and D.J. Brown, *J. Org. Chem.* 1968, **33**, 2211-2214
5. A.T. Cooper, Ph.D Thesis, Durham University, 2008
6. D.I. Davies and M.D. Dowle, J. *Chem. Soc. Perkin Trans. 1*, 1976, 2267-2270
7. D.I. Davies and M.D. Dowle, J. *Chem. Soc. Perkin Trans. 1*, 1978, 227-231
8. M. Tanabe, N. Ishikawa and K. Osakada, *Organometallics*, 2006, **25**, 796-798
9. N. Thirupathi, D. Amoroso, A. Bell and J.D. Protasiewicz, *J. Polym. Sci. A: Polym. Chem.* 2009, **47**, 103-110

10. M. Sommovigo; M. Pasquali; P. Leoni; P. Sabatio; D. Braga, *J. Organometal. Chem,*. 1991, **418**, 119-126

11. D. Nguyen; G. Laurenczy; M. Urrutigoïty; P. Kalck, *Eur. J. Inorg. Chem.*, 2005, 4215-4225

12. M. Haufe; R.D. Köhn; R. Weimann; G. Seifert; D. Zeigan, *J. Organometal. Chem.* 1996, **520**, 121-129

Appendices

Appendix 1 – Crystallographic data

All X-ray diffraction experiment data collections were conducted using graphite-monochromated Mo-Kα radiation (λ = 0.71073 Å) on a Bruker Smart 1K or a 6K CCD area diffractometer at 120K. Cell parameters were determined and refined using SMART[1] software and raw frame data were integrated using SAINT[2] programs. Structures were refined using SHELXL-97.[3]

Parameters from X-Ray Diffraction Experiments

Complex	Iodolactone (**I1**)	Iodolactone (**I2**)
Empirical formula	$C_9 H_{11} I O_2$	$C_{10} H_{13} I O_2$
Formula weight	278.08	292.10
Temperature/K	120(2)	120(2)
Crystal system	Monoclinic	Orthorhombic
Space group	$P2_1/c$	Pccn
a/Å	6.3104(10)	15.669(3)
b/Å	9.1301(14)	20.017(4)
c/Å	15.948(2)	15.948(2)
α/°	90.00	90.00
β/°	91.66(2)	90.00
γ/°	90.00	90.00
Volume/Å^3	918.4(2)	2020.5(7)
Z	4	8
ρ_{calc}mg/mm^3	2.011	1.921
m/mm^{-1}		
F(000)	536	1136
Crystal size	0.75 x 0.56 x 0.50 mm^3	0.36 x 0.16 x 0.12 mm^3
Theta range for data collection	2.23-30.02	2.60-29.97
Index ranges		
Reflections collected	12367	26477
Independent reflections	2615	2921
Data/restraints/parameters	2551 reflections, 154 parameters, 0 restraints	2487 reflections, 171 parameters, 0 restraints
Goodness-of-fit on F^2	1.189	1.061
Final R indexes [I>2σ (I)]	0.0214	0.0323
Final R indexes [all data]	0.0210	0.0178
Largest diff. peak/hole	1.773	0.772

[1] SMART – NT, Data Collection Software, version 6.1. Bruker Analytical X-ray Instruments Inc, Madison, WI, USA, 2000.

[2] SAINT – NT, Data Collection Software, version 6.1. Bruker Analytical X-ray Instruments Inc, Madison, WI, USA, 2000.

[3] SHELX – G.M. Sheldrick, *Acta Crysta.*, 2008, **A64**, 112.

Appendix 2 – Assignment of ^{1}H and ^{13}C NMR spectra of HFP-functionalised norbornenes

Proton and carbon NMR spectra of functionalised norbornenes were assigned with the aid of COSY, HSQC, HMBC and DEPT 135 experiments. Examples of assigned ^{1}H and $^{13}C\{^{1}H\}$ spectra for *endo*-/*exo*-$NBOCH_2C(CF_3)_2OH$ (**ZXN2**) are given in Figures 1 and 2, respectively. The corresponding COSY and HSQC spectra are given in Figures 3 and 4, respectively.

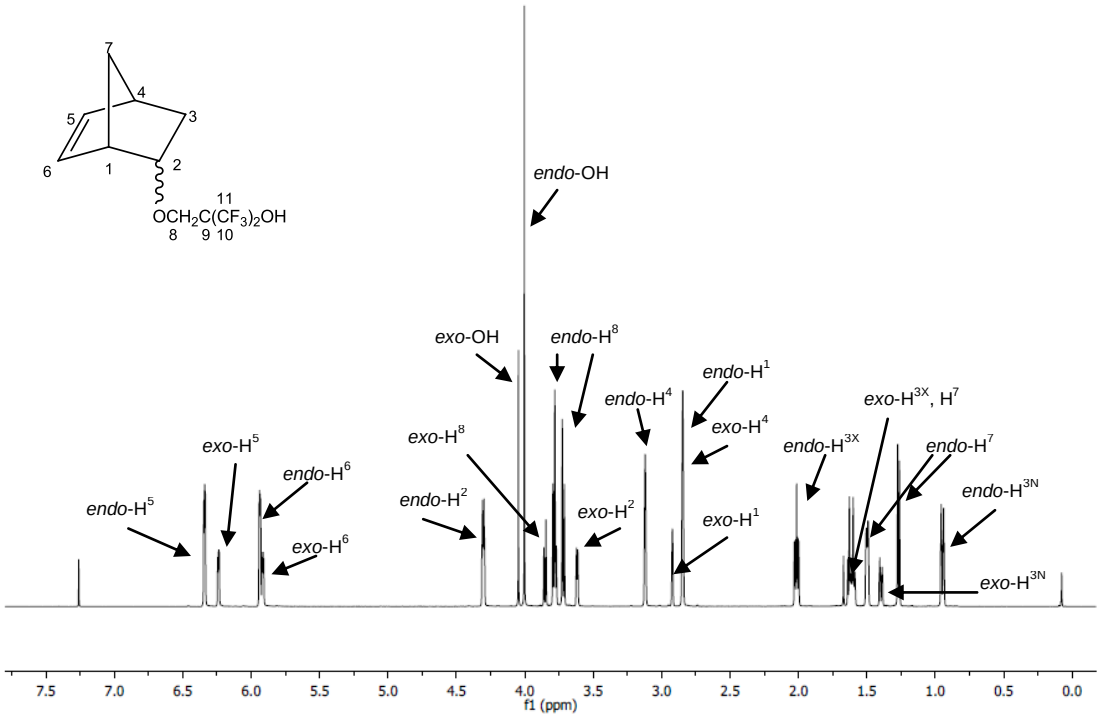

Figure 1 700 MHz $CDCl_3$ ^{1}H NMR spectrum of *endo*-/*exo*-$NBOCH_2C(CF_3)_2OH$ (**ZXN2**)

The assignment of ^{1}H NMR spectra of functionalised norbornene derivatives is often a tricky and time consuming process, due to the fact that non of the protons are equivalent. In order to correctly identify each resonance, extensive use of correlation spectroscopy is required.

Taking the ^{1}H and $^{13}C\{^{1}H\}$ spectra of *endo*-/*exo*-$NBOCH_2C(CF_3)_2OH$ (**ZXN2**) as an example, the vinylic resonances of the monomer are immediately apparent based upon their chemical shift of ~ δ 6 ppm (^{1}H spectrum) and 130-140 ppm ($^{13}C\{^{1}H\}$ spectrum) hence are assigned as protons 5 and 6, with the larger resonances corresponding to the *endo* isomer, which makes up the majority of the mixture). The proton-carbon connectivity (*i.e.* which proton resonance correlates with which carbon

resonance) is determined using the HSQC spectrum which shows directly bonded protons and carbons (Figure 4). Protons 5 and 6 show a 'doublet of doublets' (dd) splitting pattern with coupling to each other (J = 5.6 Hz for the *endo* isomer and 5.7 Hz for the *exo* isomer) and also to the bridgehead protons, 1 and 4. Protons 1 and 4 can be assigned based upon the COSY spectrum (off-diagonal peaks indicate positive correlations with protons 5 and 6), and the corresponding carbon resonances assigned using the HSQC spectrum.

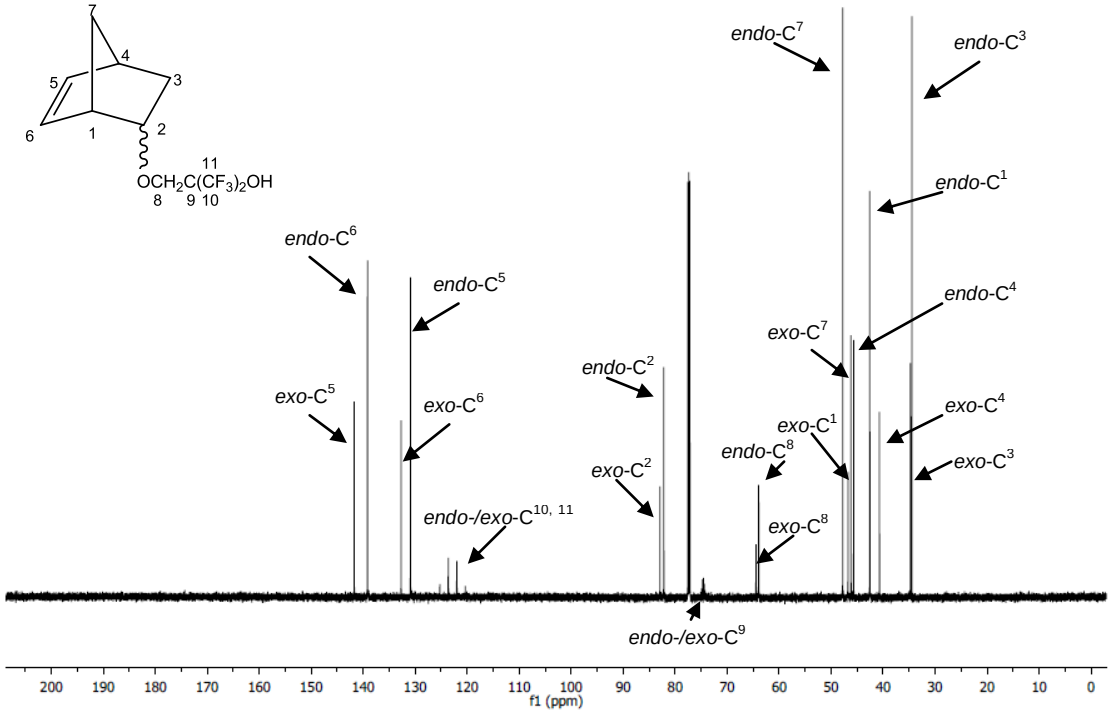

Figure 2 176 MHz $CDCl_3$ $^{13}C\{^1H\}$ NMR spectrum of *endo*-/*exo*-$NBOCH_2C(CF_3)_2OH$ (**ZXN2**)

The OH resonances are easily assigned by means of a D_2O shake, or by the fact that they show no proton-proton or proton carbon correlations in the COSY or HSQC spectra, respectively. Protons 8 and 8' show doublet slitting, with coupling only to one another (J = 10 Hz) and hence are straightforward to identify from the COSY spectrum. Carbons 9, 10 and 11 are also easily assigned based upon their septet and quartet splitting patterns, respectively.

The remaining resonances to be assigned correspond to proton and carbons 2, 3 and 7. Proton 2 is readily identified from the HSCQ spectrum as it is a CH resonance (hence shows only one proton-carbon correlation), whereas both 3 and 7 are CH_2s (showing two proton correlations with a single carbon). Now that proton 2 has been

confirmed, protons 3 and 1 can be assigned *via* positive correlations in the COSY spectrum. Knowing the assignment of proton 1, it is then possible to conclusively assign the vinylic resonances as 5 or 6, respectively and the remaining bridgehead proton as 4. This leaves protons 3^N and 3^X (*i.e.* hydrogens in the *endo* (N) and *exo* (X) positions) which are assigned based upon their coupling to protons 2, 4 and to each other. Finally, the resonances corresponding to proton 7 are assigned.

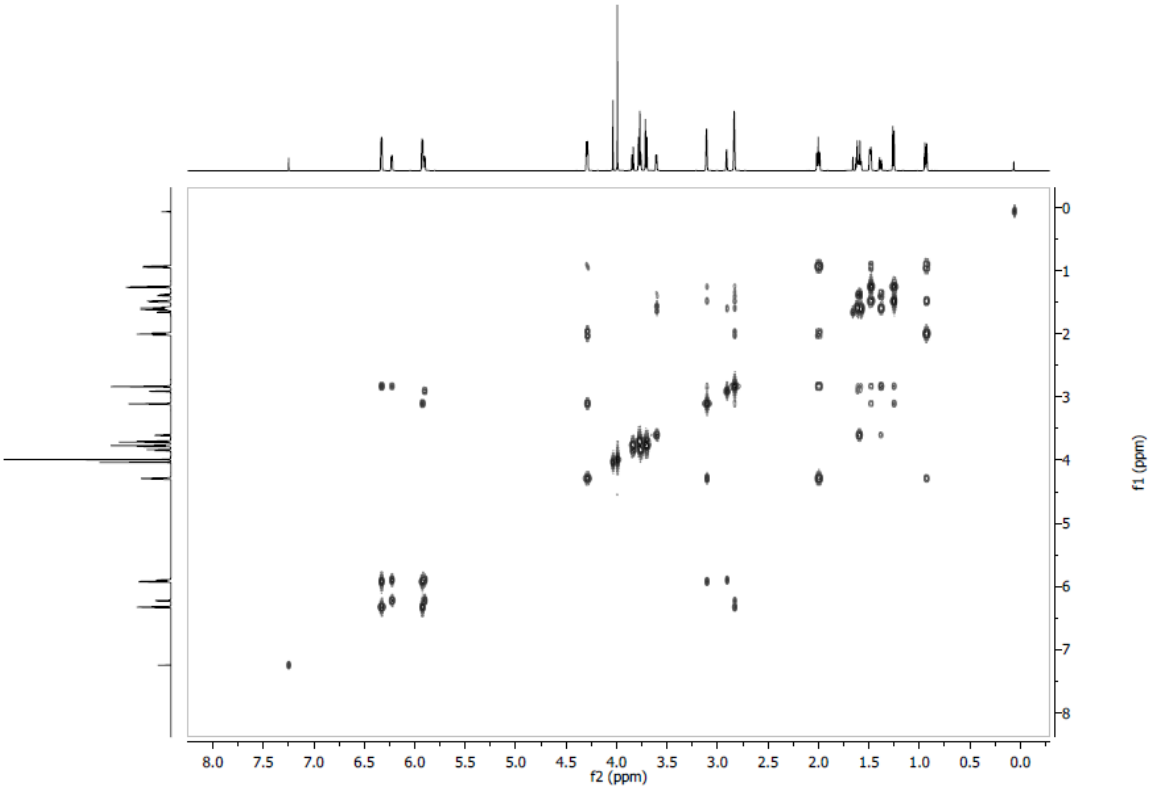

Figure 3 700 MHz $CDCl_3$ COSY spectrum of *endo*-/*exo*-$NBOCH_2C(CF_3)_2OH$ (**ZXN2**)

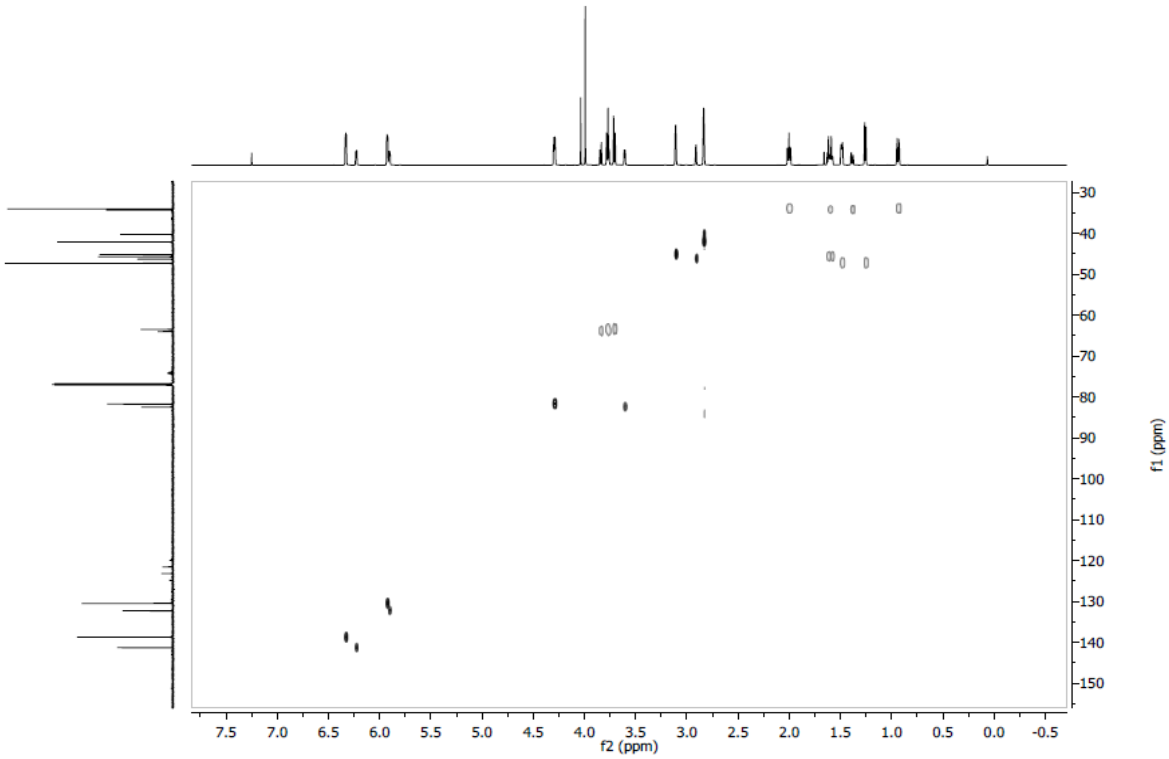

Figure 4 700 MHz $CDCl_3$ HSQC spectrum of *endo*-/*exo*-$NBOCH_2C(CF_3)_2OH$ (**ZXN2**)

Appendix 3 Kinetics Data

Data for the polymerisation of the various functionalised norbornenes utilised in this thesis initiated by **Pd1388** were fitted to equation 3.3 using the non-linear curve fitting function of *Origin 8.1* software, as discussed in Chapters III-V. The resulting rate constants, k_1 and k_2, are given for each individual kinetics run, and are quoted with their associated 'goodness of fit' to the model. For mixtures of *endo*/*exo* isomers, individual rate constants are quoted for the overall polymerisation rate (total) and individually for the *endo* and *exo* components, respectively. Where data from one individual kinetic run is significantly different to the others, only the two concurrent data sets were used. Due to the unreliability of the errors obtained from non-linear curve fitting, mean values (3 runs) are quoted in the main body of this manuscript along with their associated standard deviation. For this reason, the errors quoted in Chapters III – V do not necessarily match exactly with those for each individual run quoted here.

A3.1 Kinetics data for pure *exo*-monomers

ZX3[§]

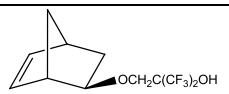	k_{1exo} (10^{-4} s^{-1})	k_{2exo} (10^{-3} $Mol^{-1}dm^3s^{-1}$)	R^2
1	1.16 ± 0.2	3.60 ± 0.4	0.999
2	1.20 ± 0.2	3.59 ± 0.4	0.999
3	1.11 ± 0.2	3.33 ± 0.5	0.998

[§] Monomer contains 2% of the *endo* isomer

SX1

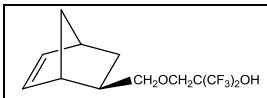	k_{1exo} (10^{-3} s^{-1})	k_{2exo} (10^{-3} $Mol^{-1}dm^3s^{-1}$)	R^2
1	2.22 ± 0.05	7.91 ± 0.09	0.995
2	2.24 ± 0.05	6.92 ± 0.2	0.999
3	2.25 ± 0.02	6.81 ± 0.09	0.999

SX2

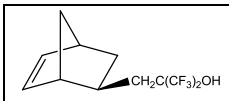	k_{1exo} (10^{-3} s^{-1})	k_{2exo} (10^{-3} $Mol^{-1}dm^3s^{-1}$)	R^2
1	2.37 ± 0.03	7.83± 0.09	0.999
2	3.97 ± 0.04	10.2 ± 0.1	0.999
3	2.65 ± 0.02	8.65 ± 0.06	0.999

DX2

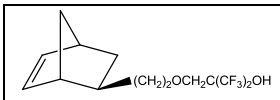	k_{1exo} (10^{-2} s^{-1})	k_{2exo} (10^{-3} $Mol^{-1}dm^3s^{-1}$)	R^2
1	1.19 ± 0.007	31.8 ± 2	0.999
2	1.20 ± 0.4	28.1 ± 2	0.999
3	120 ± 0.3	29.7 ± 1	0.999

TX2

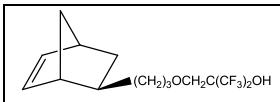	k_{1exo} (10^{-2} s^{-1})	k_{2exo} (10^{-2} $Mol^{-1}dm^3s^{-1}$)	R^2
1	2.70 ± 0.01	4.43 ± 0.06	0.999
2	2.83 ± 0.08	6.04 ± 0.3	0.999
3	2.53 ± 0.08	4.62 ± 0.04	0.999

A3.2 Kinetics data for pure *endo*-monomers

SN2

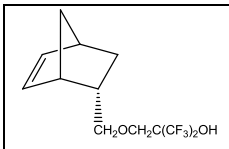	k_{1endo} (10^{-5} s^{-1})	k_{2endo} (10^{-4} $Mol^{-1}dm^3s^{-1}$)	R^2
1	4.01 ± 0.3	6.34 ± 0.5	0.994
2	4.03 ± 0.3	6.36 ± 0.4	0.996
3	3.94 ± 0.3	6.23 ± 0.5	0.995

SN2

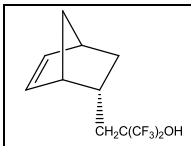	k_{1endo} (10^{-5} s^{-1})	k_{2endo} (10^{-3} $Mol^{-1}dm^3s^{-1}$)	R^2
1	7.63 ± 0.9	1.85 ± 0.3	0.999
2	7.44 ± 0.6	1.44 ± 0.1	0.993

For the polymerisation of monomer **SN2** only two sets of data were of sufficient quality for analysis.

A3.3 Kinetics data for un-separated mixtures of *endo*/*exo* monomers

ZXN3

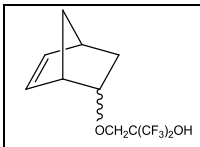	k_{1total} (10^{-4} s^{-1})	k_{2total} ($Mol^{-1}dm^3s^{-1}$)	R^2
1	0.49 ± 0.3	0	0.990
2	1.76 ± 0.5	0	0.999
3	1.07 ± 0.6	0	0.999

Overall consumption of monomer in the **ZX3** mixture shows a rate constant, k_2, of zero within the error limits of the experiment, *i.e.* the system obeys *pseudo*-first order kinetics.

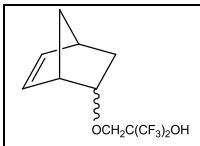	k_{1endo} (10^{-4} s^{-1})	k_{2endo} (10^{-3} $Mol^{-1}dm^3s^{-1}$)	R^2
1	1.39 ± 0.3	2.98 ± 0.8	0.999
2	1.07 ± 0.2	1.75 ± 0.7	0.999
3	1.54 ± 0.5	2.72 ± 1	0.997

It was not possible to extract rate constants relating to the *exo* component of the mixture. Overall consumption of monomer is predominately related to uptake of the *endo* isomer, with the change in the concentration of the *exo* isomer being extremely small.

SXN3

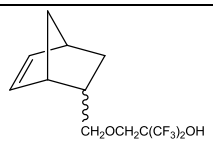	k_{1total} (10^{-4} s^{-1})	k_{2total} (10^{-3} $Mol^{-1}dm^3s^{-1}$)	R^2
1	3.04 ± 0.3	4.44 ± 0.5	0.999
2	2.32 ± 0.2	3.74 ± 0.5	0.999
3	9.76 ± 1	12.7 ± 0.7	0.999

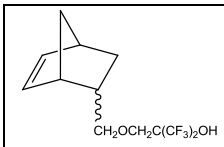	k_{1endo} (10^{-4} s^{-1})	k_{2endo} (10^{-1} $Mol^{-1}dm^3s^{-1}$)	R^2
1	2.13 ± 0.2	6.04 ± 0.7	0.999
2	1.45 ± 0.2	4.22 ± 1	0.998
3	7.30 ± 0.9	15.8 ± 1	0.999

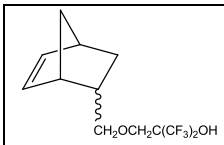	k_{1exo} (10^{-4} s^{-1})	k_{2exo} (10^{-2} $Mol^{-1}dm^3s^{-1}$)	R^2
1	8.16 ± 1	1.61 ± 1	0.999
2	7.63 ± 0.8	1.97 ± 0.3	0.999
3	28.5 ± 0.5	7.93 ± 0.7	0.999

SXN4

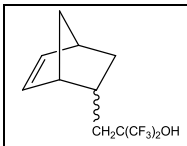	k_{1total} (10^{-4} s^{-1})	k_{2total} (10^{-3} $Mol^{-1}dm^3s^{-1}$)	R^2
1	6.31 ± 0.3	4.69 ± 0.3	0.999
2	5.96 ± 0.4	4.34 ± 0.5	0.999
3	7.47 ± 0.3	5.29 ± 0.3	0.999

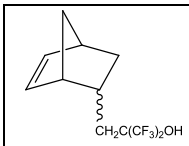	k_{1endo} (10^{-4} s^{-1})	k_{2endo} (10^{-3} $Mol^{-1}dm^3s^{-1}$)	R^2
1	1.97 ± 0.1	2.47 ± 0.6	0.999
2	2.28 ± 0.2	2.95 ± 0.9	0.998
3	2.80 ± 0.2	3.84 ± 0.5	0.999

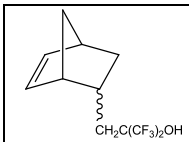	k_{1exo} (10^{-3} s^{-1})	k_{2exo} (10^{-2} $Mol^{-1}dm^3s^{-1}$)	R^2
1	1.64 ± 0.07	2.62 ± 0.1	0.999
2	1.54 ± 0.1	2.25 ± 0.3	0.999
3	1.92 ± 0.09	2.93 ± 0.2	0.999

DXN2

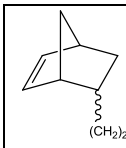	k_{1total} (10^{-3} s^{-1})	k_{2total} (10^{-3} $Mol^{-1}dm^3s^{-1}$)	R^2
1	2.15 ± 0.06	9.79 ± 0.4	0.999
2	2.04 ± 0.06	9.51 ± 0.4	0.999
3	2.09 ± 0.07	9.25 ± 0.5	0.999

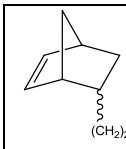	k_{1endo} (10^{-3} s^{-1})	k_{2endo} (10^{-3} $Mol^{-1}dm^3s^{-1}$)	R^2
1	1.26 ± 0.04	9.26 ± 0.6	0.999
2	1.20 ± 0.04	8.73 ± 0.6	0.998
3	1.30 ± 0.05	8.81 ± 0.7	0.998

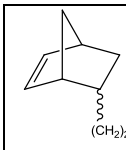	k_{1exo} (10^{-3} s^{-1})	k_{2exo} (10^{-2} $Mol^{-1}dm^3s^{-1}$)	R^2
1	5.15 ± 0.05	3.32 ± 0.07	0.999
2	5.26 ± 0.07	4.05 ± 0.09	0.999
3	5.30 ± 0.2	3.00 ± 0.2	0.999

DXN5

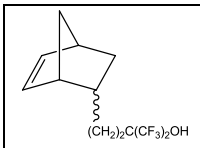	k_{1total} (10^{-3} s^{-1})	k_{2total} (10^{-3} $Mol^{-1}dm^3s^{-1}$)	R^2
1	1.90 ± 0.09	9.81 ± 0.7	0.997
2	1.57 ± 0.1	7.42 ± 0.8	0.995
3	2.37± 0.2	17.6 ± 1	0.998

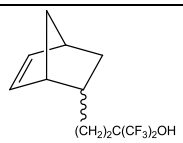	k_{1endo} (10^{-3} s^{-1})	k_{2endo} (10^{-3} $Mol^{-1}dm^3s^{-1}$)	R^2
1	1.48 ± 0.09	10.7 ± 0.9	0.996
2	1.25 ± 0.09	7.90 ± 1	0.994
3	1.91 ± 0.2	21.0 ± 2	0.997

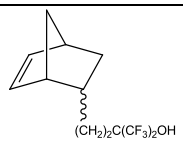	k_{1exo} (10^{-3} s^{-1})	k_{2exo} (10^{-2} $Mol^{-1}dm^3s^{-1}$)	R^2
1	3.95 ± 0.08	5.83 ± 0.2	0.999
2	3.38 ± 0.1	4.78 ± 0.3	0.999
3	4.04 ± 0.1	7.15 ± 0.4	0.999

TXN3

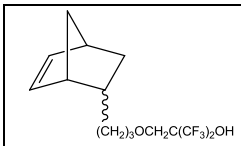	k_{1total} (10^{-3} s^{-1})	k_{2total} (10^{-2} $Mol^{-1}dm^3s^{-1}$)	R^2
1	5.12 ± 0.2	2.58 ± 0.1	0.998
2	4.91 ± 0.2	2.45 ± 0.1	0.998
3	4.83 ± 0.04	2.28 ± 0.02	0.999

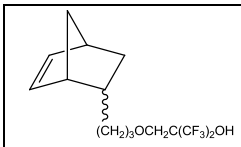	k_{1endo} (10^{-3} s^{-1})	k_{2endo} (10^{-2} $Mol^{-1}dm^3s^{-1}$)	R^2
1	3.95 ± 0.2	2.67 ± 0.2	0.997
2	3.74 ± 0.2	2.54 ± 0.2	0.997
3	3.71 ± 0.08	2.38 ± 0.07	0.999

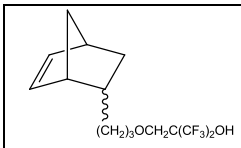	k_{1exo} (10^{-2} s^{-1})	k_{2exo} (10^{-1} $Mol^{-1}dm^3s^{-1}$)	R^2
1	1.37 ± 0.06	1.93 ± 0.1	0.999
2	1.16 ± 0.03	1.35 ± 0.07	0.999
3	0.98 ± 0.08	0.84 ± 0.2	0.996

QXN1

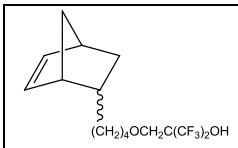	k_{1total} (10^{-3} s^{-1})	k_{2total} (10^{-2} $Mol^{-1}dm^3s^{-1}$)	R^2
1	6.70 ± 0.1	2.12 ± 0.03	0.999
2	5.80 ± 0.08	1.77 ± 0.03	0.999
3	4.97 ± 0.1	1.62 ± 0.04	0.999

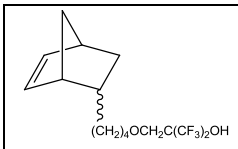	k_{1endo} (10^{-3} s^{-1})	k_{2endo} (10^{-2} $Mol^{-1}dm^3s^{-1}$)	R^2
1	4.82 ± 0.1	1.86 ± 0.05	0.999
2	4.52 ± 0.07	1.68 ± 0.04	0.999
3	4.35 ± 0.1	1.80 ± 0.06	0.999

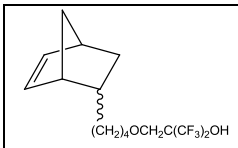	k_{1exo} (10^{-2} s^{-1})	k_{2exo} (10^{-1} $Mol^{-1}dm^3s^{-1}$)	R^2
1	1.90 ± 0.08	1.41 ± 0.02	0.999
2	1.72 ± 0.05	1.15 ± 0.01	0.999
3	1.68 ± 0.1	1.06 ± 0.02	0.999

HXN1

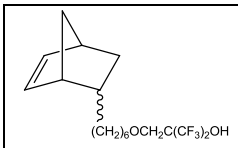	k_{1total} (10^{-3} s^{-1})	k_{2total} (10^{-2} $Mol^{-1}dm^3s^{-1}$)	R^2
1	7.77 ± 0.2	1.16 ± 0.08	0.999
2	7.69 ± 0.1	1.12 ± 0.07	0.999
3	7.31 ± 0.2	0.97 ± 0.08	0.999

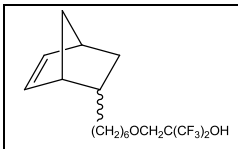	k_{1endo} (10^{-3} s^{-1})	k_{2endo} (10^{-3} $Mol^{-1}dm^3s^{-1}$)	R^2
1	6.81 ± 0.1	9.81 ± 0.9	0.999
2	6.86 ± 0.1	9.95 ± 0.8	0.999
3	6.44 ± 0.1	7.77 ± 0.9	0.999

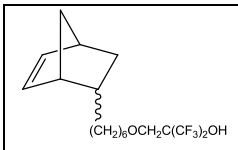	k_{1exo} (10^{-2} s^{-1})	k_{2exo} (10^{-1} $Mol^{-1}dm^3s^{-1}$)	R^2
1	1.55 ± 0.2	0	0.999
2	1.57 ± 0.2	0	0.998
3	2.08 ± 0.2	0	0.998

A3.4 Kinetics data for polymerisation of SXN4 using different palladium-hydride initiators

$[Pd(H)(MeCN)(PCy_3)_2][BF_4]$ (Pd796)

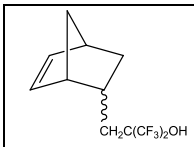	k_{1total} (10^{-4} s^{-1})	k_{2total} (10^{-3} $Mol^{-1}dm^3s^{-1}$)	R^2
1	3.80 ± 0.3	1.75 ± 0.5	0.999
2	2.70 ± 0.2	1.96 ± 0.2	0.998
3	2.90 ± 0.1	2.07 ± 0.1	0.999

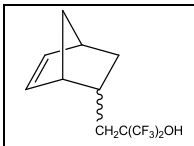	k_{1endo} (10^{-4} s^{-1})	k_{2endo} (10^{-3} $Mol^{-1}dm^3s^{-1}$)	R^2
1	1.56 ± 0.2	1.14 ± 0.8	0.999
2	1.18 ± 0.1	1.99 ± 0.3	0.996
3	0.90 ± 0.1	1.24 ± 0.4	0.991

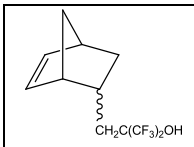	k_{1exo} (10^{-3} s^{-1})	k_{2exo} (10^{-2} $Mol^{-1}dm^3s^{-1}$)	R^2
1	0.82 ± 0.06	0.37 ± 0.2	0.999
2	0.65 ± 0.01	0.87 0.3	0.995
3	0.81 ± 0.03	0.97 ± 0.4	0.999

$[Pd(H)(MeCN)(PCy_3)_2][SF_6]$ (Pd945)

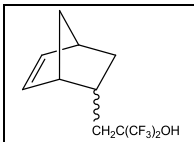	k_{1total} (10^{-4} s^{-1})	k_{2total} (10^{-3} $Mol^{-1}dm^3s^{-1}$)	R^2
1	3.54 ± 0.1	2.86 ± 0.1	0.999

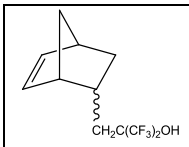	k_{1endo} (10^{-4} s^{-1})	k_{2endo} (10^{-3} $Mol^{-1}dm^3s^{-1}$)	R^2
1	1.54 ± 0.1	3.09 ± 0.3	0.997

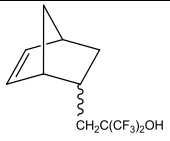	k_{1exo} (10^{-3} s^{-1})	k_{2exo} (10^{-2} $Mol^{-1}dm^3s^{-1}$)	R^2
1	0.79 ± 0.02	1.21 ± 0.04	0.999

$[Pd(H)(MeCN)(PCy_3)_2][PF_3(C_2F_5)_3]$ (Pd1154)

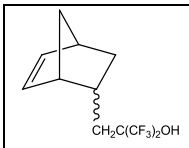	k_{1total} (10^{-4} s^{-1})	k_{2total} (10^{-3} $Mol^{-1}dm^3s^{-1}$)	R^2
1	6.79 ± 0.5	5.13 ± 0.5	0.999
2	3.52 ± 0.3	2.23 ± 0.3	0.997

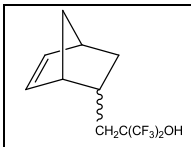	k_{1endo} (10^{-4} s^{-1})	k_{2endo} (10^{-3} $Mol^{-1}dm^3s^{-1}$)	R^2
1	2.66 ± 0.3	4.45 ± 1	0.998
2	1.91 ± 0.2	2.24 ± 0.4	0.992

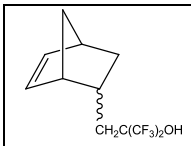	k_{1exo} (10^{-3} s^{-1})	k_{2exo} (10^{-2} $Mol^{-1}dm^3s^{-1}$)	R^2
1	1.63 ± 0.1	2.50 ± 0.2	0.999
2	0.70 ± 0.3	1.05 ± 0.06	0.999

Appendix 4 - Attendance at Postgraduate Seminars 2006-2009

Date	Speaker	Title of Talk
18/10/06	Dr Stuart Warren	Asymmetric Synthesis with Sulfur Migration
25/10/06	Prof. Harry Anderson	Some Recent Experiments with Molecular Wires – Organic Synthesis to Photophysics
01/11/06	Prof. John Kelly	Photochemical and Photophysical probes for DNA
15/11/06	Prof. Michael Bruce	Carbon-rich Complexes—Some Recent Results
	Prof. Odile Eisenstein	Simple Ideas for d(0) Olefin Metathesis Catalyst Design from a DFT Perspective
06/12/06	Prof. Victor Snieckus	Flatland Metalation: In Search of New Synthetic Aromatic Chemistry
17/01/07	Prof. Guy Lloyd-Jones	Mechanistic studies of metal-mediated processes
24/01/07	Prof. Dame Louise Johnson	The Diamond Light Source: Implications for UK research and some recent results on structural studies on cell cycle regulatory proteins
14/02/07	Dr Michael Whittlesey	N-heterocyclic carbenes: far from inert ligands
21/02/07	Prof. Samir Z. Zard	Adventures with Radicals: A Matter of Lifetime
	Prof. Richard Catlow	Computer Modelling and Synchrotron Radiation Studies of Complex Materials
24/04/07	Prof. Keith Pannell	Recent advances in the transition metal organometallic chemistry of tin, germanium and silicon
24/05/07	Dr Sebastien Perrier	RAFTing in Leeds: a Radical Route for Molecular Engineering
30/05/07	Prof. Ian Manners	Functional metallized supramolecular materials via block copolymer self-assembly and living supramolecular polymerisations

	Prof. Guy Bertrand	New Families of Stable Cyclic Carbenes for the Preparation of Low Ligated Transition Metals, and Highly Active Catalysts. Can a Carbene do the Job of a Metal?
24/10/07	Prof. David McMillin	Acids, Bases and the Photochemistry of Platinum(II) Polypyridines
31/10/07	Prof. Malcolm Chisholm	Linking MM Quadruple Bonds (M = Mo or W) with Organic π-Systems: Studies of Mixed Valency and $M_2\delta$-π Conjugation
14/11/07	Dr. Richard Layfield	Organometallic Chemistry with Manganese(II): a Transition Metal Masquerading as a Main Group Element
21/11/07	Prof. Peter Bernath	Molecular Astronomy
28/11/07	Dr. Stuart Mackenzie	Shining Light on the Effects of Geometrical Structure on the Reactivity of Small Transition Metal Clusters
05/12/07	Prof. Kalman Szabo	One-Pot Transformations Involving Catalytic Generation of Allyl Boronates
25/01/08	Prof. Trygve U. Helgaker	The Application of Quantum Chemistry to Large Systems
30/01/08	Prof. Martin Schröder,	Functional Porous Coordination Framework Materials: Gas Adsorption and Selectivity
05/02/08	Prof. Steven Nolan	The Use of N-Heterocyclic Carbenes in Homogeneous Catalysis
06/02/08	Dr. Polly Arnold	Controlled Reduction and Activation Reactions in Organometallic f-block Complexes
20/02/08	Dr. Julie Macpherson	Carbon Nanotube Networks for Chemical Sensing
27/03-28/03/08		Structure, Property and Function Across The Periodic Table' Mini-symposium
18/04/08	Prof. Jack Passmore	Homopoly atomic Cations of Groups 16 and 17: Structure, Energetics and Chemistry

	Prof. Deryn Fogg	Shining Light Inside the Black Box: Perspectives on Transformations in Catalysis
09/05/08	Prof. Penny Brothers	Diboron Porphyrins and Corroles: Unexpected Chemistry for Both Boron and the Ligands
	Prof. T. Don Tilley	New Bond Activations at Transition Metal Centres: Fundamental Studies and Applications to Catalysis
19/05/08	Prof Mark Dadmun	Tuning Interfaces in Multi-Component Polymer Systems: Surface Segregation and Non-covalent Interactions
17/06/08	Prof. Dr. Martin Broering	Chemical Communications: How Molecules Talk
23/06/08	Prof. Bill Henderson	Chemistry by mass spectrometry: Studies of the reactivity of the metalloligands $Pt_2(m\text{-}E)_2(PPh_3)_4$ (E = S or Se)
22/07/08	Prof. Zhenfeng Xi	Cooperative Effect: Discovery and Development of Organo-bi-Metallic Reagents
	Prof. Hiroto Nakano	Design of Chiral Ligands and their Applications to Pd-Catalyzed Asymmetric Reactions
	Dr. Ian J.S. Fairlamb	Cross-coupling Processes: Mechanism, Reactivity and Application
06/08/08	Prof. Heinrich Lang	Homogeneous Catalysis: Carbon-Carbon Bond Forming Reactions
22/10/08	Prof. Mike Ward	Self-assembly and host-guest chemistry of polyhedral coordination cages
29/10/08	Prof. Naokazu Kano	Development of organic fluorescent materials by taking advantage of N-B interaction
05/11/08	Prof. Paul Beer	Anion templated assembly of interlocked structures and ion-pair recognition
04/02/09	Prof. Todd Marder	Metal Catalysed Synthesis of Retinoids for Stem Cell Differentiation Including

		Applications of Novel C-H Bond Functionalisation Processes
06/05/09	Prof. Erick Carreira	Discovery and Surprises with Small Molecules
08/05/09	Prof. Christo Jossifoy	Carbonyl Olefin Metathesis
02/07/09	Prof. Manfred Scheer	Complexed Main group-Congeners of Hydrocarbons in Molecular and Supramolecular Environments
07/07/09	Prof. Tim Swager	Electronic Polymers for Chemical Sensing

4.1 Conference and Meeting Attendance

RSC Catalysis Meeting - October 2006

IRC Polymer Science and Technology Modular Course, Sheffield - 31/10 - 01/11/06

European Polymer Congress, Slovenia - 02/07 - 06/07/07

Scottish Dalton Meeting, Herriot Watt University, Edinburgh - 09/04/08

Symposium on Catalysis & Creative Synthesis, University of Newcastle - 01/07/08

ICOMC, Rennes - 12/07 – 16/07/08

IRC Polymer Showcase, Sheffield - September 2009. Poster presented ('Kinetic Studies on the Polymerisation of Functionalised Norbornenes')

Macro 2010 - 12/07-16/07/10 Poster presented ('Kinetic Studies on the Polymerisation of Functionalised Norbornenes')